Targeting B non-Hodgkin lymphoma and tumor-supportive follicular helper T cells with anti-CXCR5 CAR T cells

D i s s e r t a t i o n

zur Erlangung des akademischen Grades

doctor rerum naturalium

(Dr. rer. nat.)

im Fach Biologie

eingereicht an der

Lebenswissenschaftlichen Fakultät

der Humboldt-Universität zu Berlin

von

Master of Science

Janina Pfeilschifter

Präsidentin der Humboldt-Universität zu Berlin
Prof. Dr.-Ing. Dr. Sabine Kunst

Dekan der Lebenswissenschaftlichen Fakultät
Prof. Dr. Dr. Christian Ulrichs

Gutachter/innen: 1. Prof. Dr. Thomas Sommer

2. PD Dr. Uta Höpken

3. Prof. Dr. Birgit Sawitzki

Tag der mündlichen Prüfung: 29.6.2021

Table of Contents

I Abbreviations

7-AAD	7-aminoactinomycin D
ABC	Activated B-cell-like
AITL	Angioimmunoblastic T cell lymphoma
ALL	Acute lymphoblastic leukemia
ALT	Alanine transaminase
APC	Antigen presenting cell
APC	Allophycocyanin
APC/Cy	Allophycocyanin/cyanin
AST	Aspartate transaminase
ATT	Adoptive T cell transfer
BAFF	B cell activating factor
BAFF-R	BAFF receptor
BCL	B cell lymphoma
BCMA	B cell maturation antigen
BCR	B cell receptor
BL	Burkitt's lymphoma
BLIMP-1	B lymphocyte-induced maturation protein 1
BMSC	Bone marrow stromal cell
B-NHL	B non-Hodgkin lymphoma
bp	Base pair
BSA	Bovine serum albumin
BV	Brilliant violet
CAR	Chimeric antigen receptor
CCL	CC-chemokine ligand
CCR	CC-chemokine receptor
CD	Cluster of differentiation
CD40L	CD40 ligand
cDNA	Complementary DNA
CLL	Chronic lymphocytic leukemia
CRE	Creatinine
cTEC	Cortical thymic epithelial cell
CTLA-4	Cytotoxic T lymphocyte-associated protein 4
DC	Dendritic cell
DLBCL	Diffuse large B-cell lymphoma
DMEM	Dulbecco's Modified Eagle's Medium
DMSO	Dimethyl sulfoxide
DN	Double negative
DNA	Deoxyribonucleic acid
dNTP	Deoxynucleotide
DSMZ	Deutsche Sammlung von Mikroorganismen und Zellkulturen GmbH
eGFP	Enhanced green fluorescent protein
ELISA	Enzyme-linked immunosorbent assay
EMA	European Medicine Agency
Et al.	Et alii
FACS	Fluorescence-activated cell sorting
FCS	Fetal calf serum
FDA	U.S. Food and Drug Administration
FDC	Follicular dendritic cells
FITC	Fluorescein isothiocyanate
FL	Follicular lymphoma
FO B cells	Follicular B cells
FRC	Fibroblastic reticular cell
FSC	Forward scatter

GaIV	Gibbon ape leukemia virus
GAPDH	Glyceraldehyde 3-phosphate dehydrogenase
GC	Germinal center
GCB	Germinal center B-cell-like
gMFI	Geo mean fluorescence intensity
GMP	Good manufacturing practice
GvHD	Graft-versus-host disease
h	Hour
HA	Human astrocytes
HCerEpic	Human cervical epithelium cells
HCoEpiC	Human colonic epithelial cells
HEV	High endothelial venule
HIV	Human immunodeficiency virus
HLA	Human leukocyte antigen
HN	Human neurons
HPNC	Human perineurial Cells
HUAEC	Human umbilical artery endothelial cells
HUC	Human urothelial cells
HUVEC	Human umbilical vein endothelial cells
ICAM-1	Intracellular adhesion molecule 1
ICOS	Inducible T cell co-stimulator
IFN	Interferon
Ig	Immunoglobulin
IL	Interleukin
ITAM	Immunoreceptor tyrosine-based activation motif
IVIS	In vivo imaging system
L	Linker
LAG-3	Lymphocyte-activation gene 3
LDH	Lactate dehydrogenase
LFA-1	Lymphocyte-function-associated protein 1
LT	Lymphotoxin
LTR	Lymphotoxin receptor
mAB	Monoclonal Antibody
MAGE	Melanoma antigen
MALT	Mucosa-associated lymphoid tissue
MCL	Mantle cell lymphoma
MHC	Major histocompatibility complex
min	Minutes
MM	Multiple Myeloma
MRC	Marginal reticular cell
MZ	Marginal zone
MZL	Marginal zone lymphoma
NF-κB	Nuclear factor kappa-light-chain-enhancer of activated B cells
NK cell	Natural killer cell
NOD	Non-Obese Diabetic
NSG	NOD.Cg-Prkdc^{scid} Il2rg^{tm1Wjl}/SzJ
PALS	Periarteriolar lymphoid sheaths
PAMP	Pathogen-associated molecular pattern
PB	Pacific Blue
PBMC	Peripheral blood mononuclear cell
PBS	Phosphate buffered saline
PCR	Polymerase chain reaction
PD-1	Programmed death protein 1
PD-L1	Programmed death ligand 1

PDX	Patient-derived xenograft
PE	Phycoerythrin
PerCP/Cy	Peridinin chlorophyll protein complex/cyanin
pH	Potential of hydrogen
PMA	Phorbol 12-myristate 13-acetate
R-CHOP	Rituximab, Cyclophosphamide, Doxorubicin, Vincristine and Prednisone
rh	Recombinant human
RPMI 1640	Roswell Park Memorial Institute 1640
RT	Room temperature
sBCMA	Soluble BCMA
scFV	Single chain variable fragment
SCID	Severe combined immunodeficiency
SEM	Standard error of the mean
SLO	Secondary lymphoid organ
TAA	Tumor-associated antigen
T_{CM} cell	Central memory T cell
TCR	T cell receptor
T_{EM} cell	Effector memory T cell
T_{FH} cell	Follicular helper T cell
T_{FR} cell	Follicular regulatory T cell
T_{H} cell	T helper cell
TIL	Tumor-infiltrating lymphocyte
TIM	Tumor-infiltrating myeloid cell
TIM-3	T-cell immunoglobulin and mucin-domain containing-3
TME	Tumor microenvironment
TNF	Tumor necrosis factor
TNFRSF	Tumor necrosis factor receptor superfamily
TNFSF	Tumor necrosis factor ligand superfamily
T_{REG} cell	Regulatory T cell
TRUCK	T cell redirected for universal cytokine killing
TSA	Tumor-specific antigen
T_{SCM} cell	Stem memory T cell
UT	Untransduced
VH	Variable heavy chain
VL	Variable light chain

II Tables

III Figures

IV Abstract

B non-Hodgkin lymphomas (NHLs) are a highly diverse group of lymphoid tumors characterized by the expansion of malignant B cells. Depending on the subtype, the disease ranges from indolent to aggressive. For aggressive B-NHLs, combination therapy of chemotherapy and rituximab is indicated. Despite advances in treatment options, survival is still poor for these patients, especially if they relapse or become refractory. The recent introduction of anti-CD19 CAR T cell therapy succeeded in drastically improving survival. In CAR T cell therapy, patient-derived T cells are genetically modified to express a chimeric receptor commonly directed towards a surface antigen expressed by neoplastic cells. However, anti-CD19 CAR T cells can lack anti-tumor efficiency due to CD19 antigen loss or downregulation. In this thesis, anti-CXCR5 CAR T cell therapy was investigated as an alternative to anti-CD19 CAR T cell therapy for the treatment of mature B-NHLs. CXCR5 is a B cell homing receptor expressed by mature B cells and a subset of T cells in the B cell follicle, which are termed follicular helper T (T_{FH}) cells. These cells were described to support the tumor cells in chronic lymphocytic leukemia (CLL) and follicular lymphoma (FL). This expression pattern allows simultaneous targeting of the malignant cells as well as the tumor-supporting microenvironment by CAR T cell therapy against a chemokine receptor in an unprecedented manner. Main findings included that (1) anti-CXCR5 CAR T cells targeted specifically CXCR5 expressing mature B-NHL cell lines and patient samples *in vitro* and showed strong *in vivo* anti-tumor reactivity in an immunodeficient xenograft mouse model, (2) anti-CXCR5 CAR T cells targeted tumor-supportive T_{FH} cells derived from CLL and FL patient samples *in vitro* and (3) CXCR5 showed a safe expression profile. CXCR5 was strongly and frequently expressed by B-NHLs and its expression on healthy tissue was restricted to lymphoid cells. In summary, anti-CXCR5 CAR T cell therapy presents a novel treatment option for patients suffering from mature B-NHLs by eliminating the tumor and part of the tumor-supportive microenvironment.

The second part of the project was focused on understanding the influence of tumor progression on the CXCR5 expressing T cell compartment and in particular T_{FH} cells. For CLL patients, lymphomagenesis is described to alter T_{FH} cells. The *Eμ-Tcl1* murine lymphoma model, which mimics human CLL, was used to study the impact of lymphomagenesis on $CXCR5^+$ T cells. Single cell RNA sequencing was the method of choice to obtain RNA expression profiles at single cell resolution. A profound influence of lymphoma growth on the T cell compartment in *Eμ-Tcl1* tumor-challenged mice could be shown. In these mice, the fraction of T_{FH} cells was expanded and they upregulated tumor-supportive factors.

V Zusammenfassung

B-Zell Non-Hodgkin-Lymphome sind eine hochdiverse Gruppe von lymphoiden Tumoren, die sich durch die Vermehrung von malignen B Zellen auszeichnen. Abhängig vom Subtyp kann die Erkrankung einen indolenten oder aggressiven Verlauf nehmen. Bei aggressiven B-NHL ist eine Kombinationstherapie mit Chemotherapeutika und Rituximab notwendig. Trotz Fortschritten in den Behandlungsmöglichkeiten ist die Prognose für diese Patienten schlecht, vor allem wenn sie nicht auf die Therapie ansprechen oder es zu einem Rezidiv kommt. Mit der Einführung der CAR-T-Zell-Therapie, gerichtet gegen CD19, konnte die Überlebensrate drastisch verbessert werden. In der CAR-T-Zell-Therapie werden T Zellen des Patienten derart genetisch verändert, dass sie einen chimären Rezeptor exprimieren, der üblicherweise gegen ein Oberflächenantigen, das von neoplastischen Zellen exprimiert wird, gerichtet ist. Dennoch kann die anti-Tumor Wirksamkeit der anti-CD19 CAR-T-Zellen aufgrund von CD19 Antigenverlust oder Downregulation eingeschränkt sein. In dieser Arbeit wurde die anti-CXCR5 CAR-T-Zell-Therapie als Alternative zur anti-CD19 CAR-T-Zell-Therapie für die Behandlung von reifen B-NHLs untersucht. CXCR5 ist ein B-Zell-homing Rezeptor, der von reifen B Zellen und einer Subpopulation von T Zellen im B-Zell-Follikel, den follikulären T-Helferzellen (T_{FH} Zellen), exprimiert wird. Diese Zellen wurden als tumor-unterstützend in chronisch lymphatischer Leukämie (CLL) und im follikulären Lymphom (FL) beschrieben. Dieses Expressionsmuster erlaubt es, auf einzigartige Weise zeitgleich die malignen Zellen und die tumorunterstützende Mikroumgebung mithilfe von CAR-T-Zell-Therapie gerichtet gegen einen Chemokinrezeptor anzugreifen. Die wichtigsten Ergebnisse dieser Arbeit waren, dass (1) die anti-CXCR5 CAR T-Zellen zielgerichtet CXCR5 positive reife B-NHL Zelllinien und Patientenproben *in vitro* eliminierten und eine starke anti-Tumor Reaktivität in einem immundefizienten Xenotransplantationsmausmodell zeigten, (2) die anti-CXCR5 CAR T-Zellen zielgerichtet die tumorunterstützenden T_{FH} Zellen in CLL und FL Patientenproben *in vitro* erkannten und dass (3) CXCR5 ein sicheres Expressionsprofil zeigte. CXCR5 war stark und häufig auf B-NHL exprimiert und die Expression auf gesundem Gewebe war auf lymphoide Zellen beschränkt. Zusammenfassend lässt sich sagen, dass die anti-CXCR5 CAR-T-Zell-Therapie eine neue Behandlungsmöglichkeit für Patienten mit reifen B-NHL darstellt, indem durch die anti-CXCR5 CAR-T Zellen sowohl der Tumor als auch ein Anteil der tumorunterstützende Mikroumgebung eliminiert werden.
Im zweiten Teil der Arbeit wurde der Fokus darauf gelegt, den Einfluss des Tumorwachstums auf das CXCR5 exprimierende T Zell-Kompartiment, insbesondere auf die T_{FH} Zellen, besser zu verstehen. Für CLL Patienten sind Veränderungen der T_{FH} Zellen beschrieben worden. Das *Eμ-Tcl1* murine Lymphommodell, das humane CLL nachahmt, wurde genutzt um die Auswirkung der Lymphomentwicklung auf die $CXCR5^+$ T Zellen zu untersuchen. RNA-Einzelzell-Sequenzierung war die Methode der Wahl um RNA Expressionsprofile in Einzelzell-Auflösung

zu erhalten. Ein profunder Einfluss des Lymphomwachstums auf das T Zell-Kompartiment in Mäusen, denen *Eμ-Tcl1* Zellen gespritzt wurden, konnte gezeigt werden. In den Mäusen war der Anteil an T_{FH} Zellen erhöht und diese zeigten eine Hochregulierung von Tumor-unterstützenden Faktoren.

1 Introduction

We are exposed to countless pathogens daily, but rarely get sick. Our immune system is capable of tirelessly repelling attacks of disease-causing bacteria, viruses and other microorganisms. Threats also come from within. Genetic alterations, caused by environmental factors or spontaneous occurrence, modify the cellular protein machinery and can result in neoplastic growth. Foreign structures of various origins must therefore be distinguished from the body's own tissues in a timely manner. In more detail, the immune system depends on two types of immune responses, the innate and the adaptive response (Alberts et al., 2002).

The innate response has developed earlier during evolution and is not only present in vertebrates, but also in invertebrates. The first line of defense are the epithelium, the skin and the linings of lung and gut, which serve as a physical barrier and prevent the entry of pathogens. Inner surfaces are equipped with mucus, which contains anti-microbial peptides, most importantly defensins, and facilitates clearance by cilia movements. If microorganisms succeed in invading the body, the innate response starts fighting them within the first hours after infection. This fast response is credited to the ability to recognize certain structures, pathogen-associated molecular patterns (PAMPs), which are prevalent on pathogens, but absent in humans. Bacterial and fungal cell wall components, bacterial DNA pieces and viral double-stranded RNA are examples for PAMPs. This mechanism allows a quick reaction, even if the host has never been infected with the pathogen before.

PAMPs trigger the inflammatory response, which includes the reactivity of the complement system, as well as phagocytosis. The complement system comprises more than 20 soluble proteins, mostly secreted by the liver, which are present in an inactive state in the blood and the extracellular fluid. Upon activation, they initiate a proteolytic cascade, leading to an enhanced antibody and phagocyte function. The phagocytic cells of the innate response are macrophages and neutrophils. Upon pathogen encounter, they engulf the invader and degrade it. Macrophages are long-lived, tissue-resident and enriched in the lung and gut, areas with a higher likelihood of infection. As they are present in the tissues, they are usually the first cells to encounter a pathogen. Neutrophils are short-lived phagocytes prevalent in the blood, which are subsequently recruited to infection sites by macrophages and molecules produces by the intruders themselves. Apart from neutrophils, lymphocytes as part of the adaptive response, monocytes, tissue-resident macrophages and dendritic cells are attracted to the site of infection. Chemoattractive cytokines secreted by macrophages, which are called chemokines, play a role in this recruitment. The innate response is also engaged in viral infection. Cells infected with viruses secrete interferons, which act in an autocrine and paracrine manner. In stimulated cells, viral replication is hampered and natural killer (NK) cells, which are innate cells that can induce apoptosis in infected cells, are activated.

In vertebrates, the innate immune response acts in close collaboration with the adaptive immune response. The adaptive immune system can elicit strong and, upon repeated encounter, fast responses to pathogens. As opposed to the innate response, it is able to establish long-term protection after infection. However, in order to eliminate invaders and toxic substances produced by them, the adaptive response first has to learn to discriminate self from foreign. For that, mechanisms are in place to ensure the selection of non-self reactive cells. If this fails, the immune cells attack the body's own tissues, resulting in autoimmune diseases. The adaptive immune system provides two main modes of action, a humoral response and a cell-mediated response.

The humoral response is mediated by antibody-producing B cells. B cells, as opposed to the other antigen-presenting cells (APCs), only present antigen specific to its B cell receptor. The antigen is bound, internalized, degraded and presented on the B cell's surface. To support B cells, naive helper T cells are first activated by APCs, the most efficient being dendritic cells. They become effector helper T cells (T_H2), which secrete cytokines and express costimulatory molecules, and can subsequently activate a B cell that presents an antigen matching their T cell receptor. Memory B cells or antibody-producing plasma cells can develop from activated B cells. Antibodies are immunoglobulins prevalent in the blood and other fluids, which specifically bind to the antigen that triggered their production. Antigen binding can neutralize viruses and toxins or tag a pathogen for phagocytosis by innate cells. Help from T cells is also crucial for the induction of B cell proliferation or antibody class switch.

Cytotoxic $CD8^+$ T cells are the main actors in the cell-mediated response. Their mode of action is direct killing of cells infected with viruses, intracellular bacteria or parasites. In order to become effector cells, they first have to be activated by an infected antigen-presenting cell, which presents the T cell receptor specific antigen. This activation is only possible if it is supported by a helper T cell. In order to support cytotoxic T cells, $CD4^+$ helper T cells have to be activated by APCs and become T_H1 effector cells. Effector T cells promote expression of certain APC proteins, which induces a positive feedback loop and enhances the T cell response. Cytotoxic T cells kill their target cells by inducing apoptosis. This can be achieved by secretion of perforin, a pore-forming protein, or Fas ligand binding, which induces a caspase cascade. $CD8^+$ and some $CD4^+$ T cells show an additional anti-viral function by secreting interferon γ, which inhibits viral replication and makes infected cells more visible to cytotoxic T cells.

In summary, both the innate and the adaptive immune response are crucial in the fight against pathogens. The innate system is able to initiate a very fast, unspecific response against intruders and plays an important role in the first hours and days after infection. The adaptive system needs longer to establish an immune response after primary infection. However, it has the

unique ability to generate long-term memory and can elicit a very fast and strong response upon re-exposure with a pathogen (Alberts et al., 2002).

1.1 T cell immunity

T cells are crucial in the adaptive immune response. Various subtypes fulfill distinct functions and ensure immune maintenance in health and disease. Opposed to B cells, they only recognize processed antigens presented in an MHC complex. T cells express a large variety of T cell receptors, which are generated by gene rearrangements and allow targeting of cells diseased from infection or malignant transformation. Due to this capability, they attracted attention in the search of novel strategies for the fight against cancer.

1.1.1 T cell development in the thymus

The thymus, the site of T cell development, is supplied with hematopoietic progenitor cells from the bone marrow. The progenitor cells are mobilized from their niche and travel via the blood to the thymus, which they enter near the cortico-medullary junction. Upon entry, the cells are double-negative (DN1) and do not express CD4 or CD8. As the T cells mature, they migrate towards the subcapsular epithelium. T cell receptor (TCR) rearrangement takes place and α/β and γ/δ lineages develop (Starr et al., 2003). The majority of T cells carry TCRs composed of α/β subunit chains, which recognize peptide antigens. Less frequently, T cells express the γ/δ TCR and react to phosphoantigens. They are associated with the γ, δ, ε, and ζ subunits, which form the CD3 complex. This complex is responsible for signal transduction into the cells (Morath and Schamel, 2020). The large variety of TCRs, which ultimately allows an effective adaptive immune response, is based on the somatic assembly of TCR gene regions. During T cell development in the thymus, variable (V), diversity (D) and joining (J) gene segments are rearranged by recombination-activating gene (RAG1/2) recombinases, which act by inducing double-strand breaks at recombination signal sequences adjacent to the gene segments and non-homologous end joining. After recombination of the TCRβ chain gene, the β chain first forms a pre-TCR together with a surrogate pre-α chain. Signaling through the pre-TCR induces recombinase downregulation, proliferation, differentiation and entry into the double positive state, in which T cells express both CD4 and CD8 (Krangel, 2009). CD4 and CD8 are coreceptors of the TCR required for T cell activation (Li et al., 2013). Double positive thymocytes subsequently reexpress the recombinases and the TCRα chain gene is recombined (Krangel, 2009).

1.1.2 T cell maturation and differentiation

Subsequent positive and negative selection steps ensure that the T cells released into the periphery are equipped with a functional, non-self reactive TCR. Positive selection is closely connected to successful rearrangement of the TCRα chain. Recombination of the TCRα chain

is terminated once an MHC-restricted receptor together with the TCRβ chain is formed. MHC molecules present peptides to the immune system. MHC class I molecules are expressed by virtually all cells and present endogenously synthesized peptide antigens to $CD8^+$ cytotoxic T cells. MHC class II molecules are found on antigen-presenting cells (macrophages, dendritic cells and B cells) and present antigens after endocytic ingestion to $CD4^+$ helper T cells (Rock et al., 2016). As successful TCR generation is an infrequent event, the majority of cells at this stage stays undifferentiated and expresses high levels of RAG enzymes (Starr et al., 2003). Over 90% of double positive thymocytes experience death by neglect and do not succeed in generating a useful TCR. Positive selection is granted to thymocytes that are capable of engaging in interaction with cortical thymic epithelial cells (cTECs), a self-antigen presenting stromal cell type. cTECs present MHC class I and II molecules on their surface. Interaction of double-positive cells with MHC class I molecules results in CD8 lineage commitment, interaction with MHC class II molecules results in CD4 lineage commitment. After committing to the lineages, thymocytes migrate to the medulla. The single-positive cells undergo negative selection there by interacting with medullary thymic epithelial cells (mTECs) (Klein et al., 2014). In mTECs, the autoimmune regulator (AIRE) gene mediates the expression of peripheral tissue self-antigens on MHC class I molecules (Nagamine et al., 1997; Passos et al., 2018). The expression on MHC class II molecules is achieved by mTEC autophagy. Dendritic cells are additionally involved in self-antigen presentation on MHC class II molecules. Thymocytes interact with several hundred antigen-presenting cells during their stay in the medulla. Single-positive cells that show strong binding to these self-antigens are eliminated and undergo apoptosis (Klein et al., 2014). Negative selection ensures central tolerance and defects result in severe autoimmune disorders (Cheng and Anderson, 2018). Ultimately, non-self reactive, single-positive naïve T cells, which express either CD8 or CD4, leave the thymus.

$CD8^+$ T cells directly kill their target cells and are termed cytotoxic T cells. $CD4^+$ T cells, which are also termed helper T cells, assist other immune cells. Cytokines further influence the differentiation of naïve T cells into various effector types. The effector types serve distinct function in the immune response. IL12 and IFNγ induce T_H1 differentiation, which is required for antiviral, antimicrobial and cell-mediated immunity. IL4 stimulation results in T_H2 differentiation, which mediates the immune reaction against extracellular parasites. Certain cytokine combinations initiate T_H17 differentiation. T_H17 cells provide immunity at mucocutaneous sites. Follicular helper T (T_{FH}) cells are differentiated by IL6, IL21 and/or IL27, and IL12 stimulation and support B cell activation, differentiation and generate long-term antibody responses (Tangye et al., 2013). The immunological tolerance towards self-tissues can only be maintained by an opponent $CD4^+$ T cell type, the regulatory T (T_{REG}) cells. Their main function lays in the oppression of potentially destructive activities of other T cells and prevent autoimmune disorders

(Corthay, 2009). T cells can also differentiate into memory T cells, which provide long-term protection against pathogens and stay present decades after antigen exposure (Farber et al., 2014).

1.1.3 T cell activation

Activation of a helper T cell or a cytotoxic T cell requires two signals in order to induce proliferation and differentiation into an effector cell. These signals are provided by antigen-presenting cells. Signal 1 is induced by a peptide-MHC complex interacting with the T cell receptor and signaling through connected proteins. Signal 2 is provided by costimulatory proteins. Most importantly, CD28 on T cells engages with the B7 proteins (CD80 and CD86) on antigen-presenting cells, which are upregulated by the innate response upon infection. T cells lacking signal 2 undergo apoptosis or cannot get activated anymore. T cell engagement with an antigen-presenting cells results in induction of lymphocyte-function-associated protein 1 (LFA-1) on the T cells, which in turn binds to intracellular adhesion molecule 1 (ICAM-1) on the antigen-presenting cells. This enhanced binding elongates the duration of the cell interaction and enables T cell activation. A negative feedback signal is provided by the inhibitory molecule CTLA-4 expressed by T cells. It is similar to CD28, but allows B7 binding with higher affinity and represses T cell activation (Alberts et al., 2002).

1.2 B cell immunity and malignancies

1.2.1 B cell development and activation

Conventional B cells (B2 B cells) originate from common lymphoid progenitor cells in the bone marrow. The early development stages depend on the status of the B cell receptor (BCR). The BCR consists of heavy and light chains, which require prior rearrangement of their immunoglobulin gene segments. In pro-B cells, the heavy chain rearrangement takes place. The rearranged heavy chain is expressed on the cell surface with a surrogate light chain (pre-BCR) and the cell enters the pre-B cell state (Mårtensson and Ceredig, 2000). Signaling through the pre-BCR terminates heavy chain rearrangement and initiates rearrangement of the light chain. After rearrangement of the κ or λ light chain, the immature B cells exit from the bone marrow to the periphery. Only non-self reactive B cells can exit the bone marrow. Self-reactive B cells are retained and can edit their receptor again by light-chain rearrangement (Hoffman et al., 2016).

Immature B cells leaving the bone marrow are called transitional T1 B cells. Primarily within the spleen, they acquire the T2 phenotype and further differentiate into marginal zone (MZ) or follicular (FO) B cells (Chung et al., 2003). The B cell fate depends on the signaling strength

through the BCR. Low signaling strength favors MZ differentiation and high signal strength favors FO B cell differentiation.

Marginal zone B cells reside in the marginal zone of the spleen and within structures of the lymph nodes and mucosa-associated lymphoid tissue. They directly interact with blood-borne antigen and transport it to the follicular dendritic cells (FDCs) in the follicles, which present antigens to B cells. FO B cells are enriched in primary follicles, but also represent the majority of mature B cells in the blood, bone marrow and other lymphoid organs. They interact with T cells and initiate germinal center (GC) responses (Cyster et al., 2000; Yam-Puc et al., 2018).

Another subclass of B cells are B1 cells, which are not part of the adaptive immune system, but nevertheless take part in the humoral response. They produce natural immunoglobulins against conserved pathogen patterns (Prieto and Felippe, 2017).

The BCR is crucial for B cell activation. Upon antigen binding to the BCR, internalization is initiated. The antigen is degraded and subsequently presented on the B cell surface in an MHC class II molecule. Activation can occur in a thymus-dependent or in a thymus-independent way. Protein antigens are thymus-dependent and require T cell help in order to elicit B cell activation. Helper T cells can recognize their specific antigen in an MHC class II complex. The T cell provides the B cell with the costimulatory molecule CD40L and cytokines, inducing B cell proliferation and differentiation in memory B cells and plasma cells, which secrete antibodies. Bacterial antigens are thymus-independent and do not require T cell help in order to enable a B cell response. Thymus-independent type 1 antigens, like lipopolysaccharides, can directly induce B cell proliferation. Thymus-independent type 2 antigens, such as polysaccharides of encapsulated bacteria, likely stimulate B cells by inducing crosslinking of B cell receptors and require costimulation by macrophages and dendritic cells (Murphy et al., 2008). FO B cells are preferably stimulated by thymus-dependent antigens, whereas marginal B cells and B1 B cells respond to thymus-independent antigens (Nutt et al., 2015).

1.2.2 Lymphoid organs

Lymphoid organs are classified as primary or secondary. Primary lymphoid organs are the bone marrow and the thymus, sites of lymphopoiesis and lymphocyte selection. The bone marrow in adults is located in the bone cavities of the central skeleton, the pelvis and parts of the long bones. Its main components are hematopoietic tissue islands, stem cells, adipocytes, stromal cells and vasculature (Nombela-Arrieta and Manz, 2017). B and T progenitor cells are produced in the bone marrow. B cells also mature in the bone marrow, but T cells travel to the thymus, where they undergo differentiation and maturation (Pearse, 2006). Secondary lymphoid organs, which include the spleen, lymph nodes and mucosa-associated lymphoid tissue (MALT), are responsible for initiating an adaptive immune response by antigenic activation of lymphocytes. The spleen is divided in red and white pulp. The red pulp removes deformed

erythrocytes; the white pulp hosts cells of the immune system. The marginal zone separates the white pulp from the red pulp. In the marginal zone, blood-borne antigen is collected by antigen-presenting cells, for instance marginal zone B cells. Rodents and primates show their greatest difference in lymphoid structure in the architecture of the marginal zone. In humans, the marginal zone is divided in an inner and outer zone, surrounded by the perifollicular zone, which hosts blood vessels endings wrapped by macrophages. Periarteriolar lymphoid sheaths (PALS) are regions of T cell accumulations around small vessels and B cells are located in adjacent follicles (Mebius and Kraal, 2005). Lymphocytes enter the lymph node and other SLOs, but not the spleen, via high endothelial venules (HEVs) from the blood (Indrasingh et al., 2002). Coming from tissues, antigens (mostly carried by dendritic cells) and leukocytes enter the lymph node via the afferent lymphatics (Braun et al., 2011). T cells are mostly located in the paracortex supported by a fibroblastic reticular cell (FRC) network, whereas B cells reside in follicles in the cortex supported by follicular dendritic cells (FDCs) (Bajénoff and Germain, 2009). The structure of mucosa-associated lymphoid tissues (MALT), which are diffuse SLOs associated with the digestive tract (tonsils, Peyer‘s patches, appendix), is comparable concerning the T cell zones and B cell follicles (Cesta, 2006). Upon antigen contact, B cells initiate a germinal center (GC) reaction (Nieuwenhuis and Opstelten, 1984). In the GCs, B cells undergo B cell receptor (BCR) affinity maturation and class switch. Affinity maturation by somatic hypermutation of variable region genes is needed to achieve high antibody affinity (Victora and Nussenzweig, 2012).

1.2.3 Lymphocyte migration and homing

A functional immune response requires lymphocytes in certain places at certain times. B and T cells mature in primary lymphoid organs, travel in the blood to peripheral lymphoid tissues and migrate within lymphoid tissues. Lymphocytes continually circulate between peripheral lymphoid tissues, the blood and the lymph until they encounter antigen or eventually die. Key factors regulating entry into lymphoid organs from the blood and the lymph, and movements within these organs are chemokines.

Chemokines are chemoattractive signaling proteins. Four subgroups were determined based on the location of the structurally critical cysteine residues closest to the N terminus: CC, CXC, CX_3C and XC. They are the ligands for G protein-coupled heptahelical chemokine receptors. In most cases, the interaction between a chemokine and a receptor is promiscuous. Many chemokines bind to various receptors and many receptors can bind more than one chemokine (Hughes and Nibbs, 2018). Chemokine receptors are classified as homeostatic or inflammatory. Homeostatic receptors are required for the shaping of lymphoid organs during development and basal trafficking. Inflammatory receptors orchestrate leukocytes to sites of infection or injury. Chemokine receptors can also have a dual function and play a role in homeostasis

and inflammation (Bachelerie et al., 2014). The chemokine receptors CXCR4, CXCR5 and CCR7 are essential in homeostatic trafficking and maintaining the architecture of lymphoid structures (Förster et al., 1996, 1999; Ma et al., 1998). CXCR4 and its only ligand CXCL12 are highly conserved between species and crucial in embryonic development (D'Apuzzo et al., 1997; DeVries et al., 2006). Most prominently, CXCL12 is expressed by stromal cells in the bone marrow and mediates the retention of stem cells and progenitor cells. CXCL12 is also expressed in high endothelial venules, the lymph node medulla, the red pulp of the spleen and in germinal center reactions, especially in the dark zone. Thus, the CXCR4/CXCL12 axis regulates the entry to the bone marrow and secondary lymphoid organs and is required for germinal center organization (Allen et al., 2004; Nie et al., 2004). CXCR5 is another chemokine receptor that plays a crucial role in maintaining lymphoid function and architecture. CXCL13, the only ligand for CXCR5, is produced by follicular dendritic cells (FDCs) and attracts $CXCR5^+$ cells, leading to the formation of a B cell zone in secondary lymphoid organs (Cyster et al., 2000). It is also indispensable for germinal center organization (Allen et al., 2004). CCR7 is another important chemokine receptor. In homeostasis, fibroblastic reticular cells (FRCs) secrete CCL19 and CCL21, the ligands for CCR7, and strongly attract $CCR7^+$ cells, thus B cells, dendritic cells and naïve, regulatory and central memory T cells. In the lymph node for instance, the CCL19/21 gradient guides $CCR7^+$ T cells to the T cell zone and CXCL13 leads $CXCR5^+$ B cells to the B cell follicle. Upon activation, B cells downregulate CXCR5 and upregulate CCR7, resulting in a transient movement of follicular B cells to the T cell border, where they receive stimuli from helper T cells. A small subpopulation of T cells expresses only low levels of CCR7, but is $CXCR5^+$. This chemokine expression profile enables these follicular helper T cells to provide B cell help for class switch and antibody production within the B cell follicle (Förster et al., 2008). Apart from the conventional chemokine receptors, atypical chemokine receptors have been identified, which fulfill other functions than the conventional receptors and usually do not activate signal transduction pathways. Instead, they regulate chemokine location and abundance by acting as chemokine shuttles or scavengers (Hughes and Nibbs, 2018).

Adhesion molecules, especially integrins and selectins, also play a major role in the migration and homing of lymphocytes. Immune cells frequently travel via the blood and have to reach tissues to fulfill their functions. At their destination, they extravasate in order to migrate into the tissue. This process is called leukocyte extravasation cascade. First, the immune cells tether and slowly roll on the endothelium. The adhesion slows down the leukocyte movement and allows contact initiation between the vascular surface and the immune cell (Butcher and Picker, 1996; Schnoor et al., 2015). Selectins are the initiators of leukocyte adhesion and mediate rolling on endothelial surfaces. They are transmembrane molecules with an N-terminal calcium-dependent lectin domain and an epidermal growth factor-like module (McEver, 2015).

Lymphocytes express L-selectin (CD62L), whereas P-selectin and E-selectin are expressed by the endothelium. L-selectin guides naïve lymphocytes into secondary lymphoid organs via high endothelial venules (HEVs) by binding to CD34 and GlyCAM-1 on the vasculature. P-selectin and E-selectin mediate adhesion of mature lymphocytes at sites of infection (Murphy et al., 2008). The cells subsequently firmly adhere to the vascular wall, crawl and form the transmigratory cup. Ultimately, the lymphocytes perform paracellular or transcellular diapedesis and cross the basement membrane (Butcher and Picker, 1996; Schnoor et al., 2015). These steps, as well as the previous rolling, are dependent on various integrins, most prominently, LFA-1 and VLA-4 (Murphy et al., 2008). These integrins bind to ICAM-1 and VCAM-1 on endothelial cells. Integrins are transmembrane αβ heterodimers, which link the cytoskeleton of the cells to the surrounding extracellular matrix. While rolling slowly, lymphocytes approach the endothelium and are activated by chemokines on the surface of endothelial cells. Chemokine receptors on the lymphocytes engage with the chemokines and subsequently, lymphocyte integrins change their inactive confirmation and become activated (Muller, 2013). For instance, CCL21 is expressed by vascular HEVs, lymphoid tissue stromal cells and DCs in the T cell zones. The chemokine receptor CCR7, most prominently expressed on naïve T cells, recognizes CCL21 on the endothelial cells and LFA-1 is subsequently activated, enhancing affinity for ICAM-1/2. ICAM-1 is found on HEVs on lymphoid organs, whereas ICAM-2 is ubiquitously expressed on endothelium. Upon entry into the T cell zone, naïve T cells are retained there by CCL19 and CCL21 and scan DC-MHC complexes for their TCR specific antigen (Murphy et al., 2008). Altogether, chemokines and adhesion molecules orchestrate the movement of leukocytes in homeostasis and inflammation.

1.2.4 The homeostatic chemokine receptor CXCR5

The chemokine receptor CXCR5, also called CD185, was first identified in 1992. Originally detected in Burkitt's lymphoma, it was named Burkitt's lymphoma receptor 1 (BLR1). It was shown to be a novel member of the G protein-coupled receptor family with a limited expression pattern, which was indicative of a potential role in homeostatic trafficking and B cell activation in lymphoid tissues (Dobner et al., 1992). Flow cytometry analysis further revealed that CXCR5 expression is restricted to B cells and subsets of $CD4^+$ (14%) and $CD8^+$ (2%) T cells in peripheral blood, and B and $CD4^+$ T cells in secondary lymphoid organs, but is absent on B cells in the bone marrow, indicating that it marks mature B cells (Förster et al., 1994) (Figure 1). The expression profile for CXCR5 on B cells is therefore more stringent than for CD19, which is additionally expressed on B cells at earlier development stages (Vale and Schroeder, 2010).

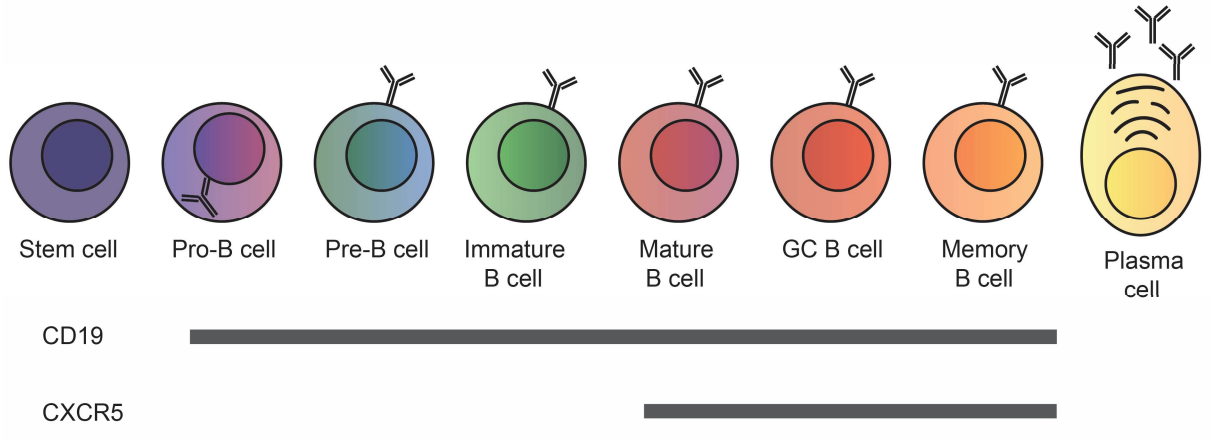

Figure 1: CXCR5 expression in B cell development. CXCR5 is expressed on mature B cells, GC B cells and memory B cells, whereas CD19 is also detected on Pro-/Pre-B cells and immature B cells. Stem cells and plasma cells do not express CXCR5 or CD19. The figure was adapted from Vale and Schroeder, 2010.

Years of research showed that CXCR5 is indispensable in sustaining immune functions and lymphoid architecture. The quest for the ligand of CXCR5 ultimately revealed CXCL13 (originally termed B-cell attracting chemokine 1, BCA-1) as the only CXCR5-binding chemokine. CXCL13 is expressed at high levels in the follicles of the spleen, lymph nodes and Peyer's patches. Analysis of the chemoattraction showed that it uniquely acts on mature B cells (Gunn et al., 1998; Legler et al., 1998). Follicular dendritic cells (FDCs) are a main source of CXCL13. FDCs are stromal cells in the follicle of SLOs, with the ability to trap immune complexes and presenting antigen to B cells. CXCL13 production allows them to gather CXCR5 expressing B cells in close proximity (Cyster et al., 2000). Later on, another mesenchymal cell type, marginal reticular cells (MRCs), which are located at the margin of SLOs, was identified as a producer of CXCL13. MRCs express MAdCAM-1 and CXCL13 at high levels in resting follicles, in which CXCL13 production by FDCs is limited (Katakai, 2012; Katakai et al., 2008).

In order to study the function of CXCR5 in great detail, CXCR5 knock-out mice were generated. The mice were viable, fertile and showed structural abnormalities restricted to lymphoid tissues. Structural abnormalities were only observed in $CXCR5^{-/-}$, but not in $CXCR5^{+/-}$ mice. In $CXCR5^{-/-}$ mice, CXCR5 was virtually absent on B cells. Due to impaired lymphocyte migration, the structure of splenic follicles was disrupted. The formation of germinal centers was hampered and activated B cells in the T cell areas could not enter the splenic B cell follicles. However, the humoral response to T cell-dependent antigens was not impaired and an antibody response was detected upon antigenic challenge. Moreover, the mutant mice lacked inguinal lymph nodes and Peyer's patches were absent or structurally altered. Transfer experiments of B cells derived from $CXCR5^{-/-}$ mice into wild-type mice further showed that the mutant cells do not migrate into the B cell follicle of the spleen and Peyer's patches. However, migration into

the lymph nodes was not impaired. These knock-out experiments provided the first evidence that CXCR5 is involved in microenvironmental homing of lymphocytes and guides B cells to defined lymphoid structures (Förster et al., 1996).

CXCR5 is, like the knock-out mouse model showed, involved in the organogenesis of secondary lymphoid organs. Together with other homeostatic chemokine receptors, especially CCR7, CXCR5 orchestrates the development of lymph nodes, mesenteric lymph nodes excluded, and Peyer's patches. CXCR5 guides $CD3^-CD4^+$ hematopoietic precursor cells, which are attracted by mesenchymal cells, to these prospective lymphoid development sites. The precursor cells further express lymphotoxin (LT)α1β2, IL-7Rα and α4β7 integrin (Ohl et al., 2003). They eventually develop into antigen-presenting dendritic cells, macrophages or NK cells. Lymph node organogenesis is initiated by the formation of lymph sacs by budding of endothelial cells. Connective tissue follows and gives rise to lymph node anlagen. The lymphatic vasculature subsequently develops from the lymph sacs. Early in formation, the lymph node anlagen are populated by the CXCR5 expressing precursor cells. They signal through their IL-7Rα, inducing lymphotoxin expression, which is indispensable in lymphoid organogenesis. Mutant mice with LTβR, LTα or LTβ deficiency do not develop lymph nodes (Mebius, 2003). The $LT\beta R^+$ mesenchymal cells are stimulated to produce chemokines and adhesion molecules (Ohl et al., 2003). As lymphotoxin signaling pathways are also crucial in the development of Peyer's patches, the mutant mice lacked those lymphoid structures as well. The development of Peyer's patches starts at the adhesion molecules VCAM-1 and ICAM-1 expressing spots. Subsequently, the $CD3^-CD4^+$ hematopoietic precursor cells are recruited. In the last development phase, mature B and T cells populate the Peyer's patch anlagen (Mebius, 2003). The organogenesis of the mesenteric lymph nodes and the spleen is not hampered in CXCR5-deficient mice and other mechanisms are in place to attract hematopoietic precursors; however, the structure of primary B cell follicles is severely disrupted (Ohl et al., 2003). The development of splenic B cell follicles requires a positive feedback loop involving the CXCR5/CXCL13 axis and lymphotoxin signaling. Follicular dendritic cells express CXCL13 and attract $CXCR5^+$ B cells. CXCR5 signaling initiates LTα1β2 expression on the B cells, resulting in LTβR signaling on FDCs, which in turn induces CXCL13 expression (Ansel et al., 2000; Ngo et al., 1999).

In 2000, a $CXCR5^+$ T cell subset was identified with the unique feature to home to the B cell follicles of secondary lymphoid organs. These cells were shown to promote the production of isotype switched antibodies in tonsillar B cells and termed follicular helper T (T_{FH}) cells. Their expression profile showed that they are a subtype of memory T cells. In the blood, they coexpress CD45RO, the T cell homing receptor CCR7 and the adhesion molecule CD62L. Interestingly, around 10% of $CXCR5^+$ cells in the blood are $CD8^+$, whereas almost all $CXCR5^+$ cells in tonsils are $CD4^+$. In secondary lymphoid organs, they downregulate CCR7, granting them

access to B cell follicles and germinal centers. In germinal centers, they highly express CD40 ligand (CD40L) and the inducible costimulator (ICOS), which promote B cell activation and differentiation. In comparison with their $CXCR5^-$ counterparts, $CD4^+CD45RO^+$ T_{FH} cells strongly support immunoglobulin A and G production. $CXCR5^+$ T cells in the peripheral blood are however in a resting state and do not express costimulatory molecules (ICOS, CD40L, OX40) (Breitfeld et al., 2000; Schaerli et al., 2000a).

Expression studies of lymphoma and leukemia cells revealed that CXCR5 is abundant on numerous B cell malignancies, such as follicular lymphoma, mantle cell lymphoma, chronic lymphocytic leukemia; thus, on neoplasms derived from mature B cells. It is absent on precursor B-ALL and multiple myeloma, derived from immature B cells and plasma cells respectively (Dürig et al., 2001).

1.2.5 Cellular origin and pathogenesis of B-NHLs

Originating from malignant B cells, B non-Hodgkin lymphomas (NHL) are a highly diverse group of tumors. The lymphoma classification was provided by the World Health Organization. The classification of subtypes is based on morphologic, immunologic, genetic and histologic features of the malignant cells and clinical characteristics of the disease (Harris et al., 1994). It is frequently updated in order to include new entities and diagnosis criteria to facilitate treatment decisions for clinicians (Swerdlow et al., 2016). Around 17.000 non-Hodgkin lymphoma patients are newly diagnosed every year in Germany (Robert Koch institute, 2018). It is largely a disease of the elderly with a median age of 69 years at diagnosis, with males having an earlier diagnosis and higher incident rates (Smith et al., 2015). The overall 5-year relative survival for these patients is 63%, decreasing in old age and highly dependent on the lymphoma entity. The most common entities, follicular lymphoma and diffuse B cell lymphoma, have survival rates of 78% and 57% respectively (Pulte et al., 2013). Acquired or congenital immunodeficiency, treatment for certain types of cancer, the exposure to solvents and infection with Epstein-Barr virus or Helicobacter pylori are considered to be risk factors for developing certain non-Hodgkin lymphomas (Cocco et al., 2010; Ekström Smedby et al., 2008; Goedert et al., 1998; Henle et al., 1968; Kaldor et al., 1987; Wotherspoon et al., 1991). Figure 2 gives an overview of the cellular origins of the presented types of B cell neoplasms (Küppers et al., 1999).

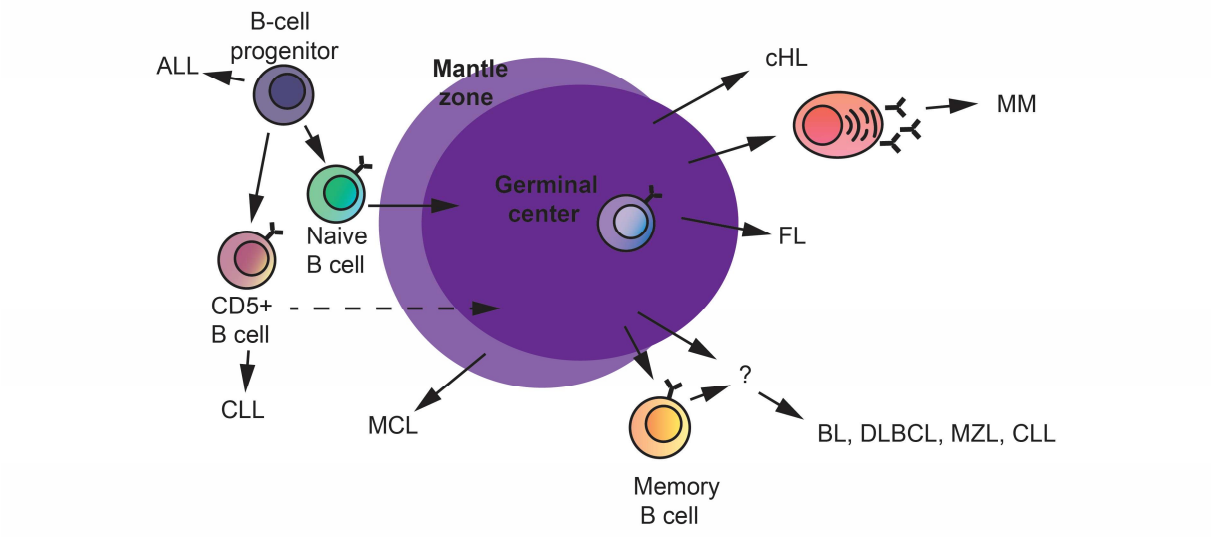

Figure 2: The cellular origin of B cell lymphomas. ALL (Acute lymphoblastic leukemia) is a B cell progenitor neoplasm. CLL (Chronic lymphocytic leukemia) is either derived from pre-germinal center (GC) CD5+ B cells or GC B cells. MCL (Mantle cell lymphoma) is derived from pre-GC mantle zone B cells. cHL (Classical Hodgkin's lymphoma), FL (Follicular lymphoma), BL (Burkitt's lymphoma), DLBCL (Diffuse large B cell lymphoma) and MZL (Marginal zone lymphoma) have their origin in GC/post-GC B cells. MM (Multiple myeloma) originates from plasma cells. Pre-GC-derived neoplasms do not harbor mutations in variable-region genes; GC/post-GC-derived malignancies show somatic mutations in variable-region genes. Figure was adapted from Küppers et al., 1999.

Diffuse large B cell lymphoma (DLBCL) is the most frequent type with 31% of NHL cases (The Non-Hodgkin's Lymphoma Classification Project, 1997). Mutated variable region genes indicate that DLBCL is derived from (post) germinal center B cells. They accumulate a particularly high number of mutations due to prolonged residence in the germinal center (Küppers et al., 1997). Therapeutic outcome shows great heterogeneity due to previously unrecognized subclassifications. (Alizadeh et al., 2000; Choi et al., 2009).

With 22% of NHL patients, follicular lymphoma (FL) is the second most frequent type (The Non-Hodgkin's Lymphoma Classification Project, 1997). Considered incurable, FL is however an indolent disease with a medium survival of over 10 years (Vidal et al., 2017). Most patients carry a t(14;18) translocation that juxtaposes the antiapoptotic gene *BCL2* with the immunoglobulin heavy chain locus (McDonnell et al., 1989; Tsujimoto et al., 1985; Vaux et al., 1988). Follicular lymphoma cells show somatic mutations in variable chain genes, which indicate their origin in germinal center B cells (Bahler et al., 1991; Oprea and Perelson, 1997).

Marginal zone lymphoma is the third most common subtype of NHL with 9% of patients (The Non-Hodgkin's Lymphoma Classification Project, 1997). The cells of origin are marginal zone B cells that show somatic mutations in variable region genes (Tierens et al., 1998). Most patients show extranodal involvement of mucosa-associated lymphoid tissue (MALT); nodal and splenic MZL are less common (Olszewski and Castillo, 2013; Swerdlow et al., 2016). In gastric MALT lymphoma, disease development is strongly associated with Helicobacter pylori

infection (Wotherspoon et al., 1991). The overall 5-year survival for MZL patients is around 80%, with differences depending on the site of origin (Olszewski and Castillo, 2013).

7% of non-Hodgkin lymphoma patients suffer from mantle cell lymphoma (MCL) (The Non-Hodgkin's Lymphoma Classification Project, 1997). MCL is derived from pre-germinal center B cells and somatic mutations are absent or very rare (Hummel et al., 1994). It is an aggressive disease with a five-year overall survival rate between 34% and 83%, depending on the risk classification (Hoster et al., 2014). At the time of diagnosis, patients present with advanced disease with involvement of lymph nodes, bone marrow and in some cases with lymphocytosis and gastrointestinal disease. Most cases show t(11;14) translocation with *Bcl1* rearrangement and cyclin D1 deregulation, which disrupts cell cycle regulation (Baldin et al., 1993; Samaha et al., 1998; Shui et al., 2003).

Chronic lymphocytic leukemia (CLL) cases account for 7% of all NHL diagnoses (The Non-Hodgkin's Lymphoma Classification Project, 1997). It is characterized by expansion of mature lymphocytes in the blood and possibly in the lymph nodes, bone marrow and spleen (Cheson et al., 1996). Small lymphocytic leukemia is identical to CLL, with CLL patients showing a higher count of lymphocytes in the peripheral blood (Tsimberidou et al., 2007). Somatic mutations are found in more than half the cases, indicating their origin in (post) GC B cells. A large fraction of CLL patients does not show any mutations, indicating that the origin of their disease is germinal center independent (Fais et al., 1998). The unmutated form is associated with a more aggressive disease progression (Hamblin et al., 1999). The neoplastic B cells show distinctive CD5 expression and a particularly low amount of surface immunoglobulin (Marti et al., 1992; Ternynck et al., 1974). Many patients do not require immediate treatment and the progression of their disease is only monitored (CLL Trialists' Collaborative Group, 1999).

Burkitt lymphoma (BL) is a rare subtype with less than 1% of NHL patients suffering from this disease (The Non-Hodgkin's Lymphoma Classification Project, 1997). Unlike in the other subtypes of B non-Hodgkin lymphoma described, around half the patients are under 40 years old, with a 5-year relative survival of 56% among all age groups and a worse survival in the older age groups (Costa et al., 2013). It was the first cancer that could be associated with viral infection (Epstein et al., 1964). The hallmark translocation t(8;14) leads to myc deregulation (Taub et al., 1982; Zech et al., 1976). It can be further classified as sporadic, endemic (Epstein-Barr virus and malaria associated) or immunodeficiency-related (HIV associated) (Jaffe et al., 1999; Mutalima et al., 2008).

1.2.6 Dissemination and localization of B-NHLs

The migration and homing of lymphocytes to lymphoid organs is strongly regulated by chemokines. Expression of chemokine receptors on lymphoma and leukemic cells allows them to benefit from entry to survival niches intended for the proliferation and maturation of healthy

lymphocytes. CXCR4 is broadly expressed in B cell malignancies. It is found on precursor B-ALL, but also on neoplasms originating from mature B cells, such as chronic lymphocytic leukemia, follicular lymphoma, mantle cell lymphoma, and plasma cell-derived multiple myeloma (Dürig et al., 2001). CXCR5 shows a smaller expression profile and is absent on precursor B-ALL and multiple myeloma, but expressed by diffuse large B cell lymphoma (DLBCL), marginal zone lymphoma (MZL), CLL, FL and MCL. CCR7 expression was described for DLBCL, CLL and MCL. Especially CLL cells express high levels of the three chemokine receptors CXCR4, CXCR5 and CCR7. Generally, the chemokine receptor profile of lymphoma and leukemia cells parallels that of their cells of origin. The neoplastic receptor combination determines to which anatomical sites within the body the malignant cells migrate (Du et al., 2019; López-Giral et al., 2004; Middle et al., 2015a). In secondary lymphoid organs, follicular lymphoma and diffuse large B cell lymphoma are frequently found, whereas this location is less common for marginal zone lymphoma and mantle cell lymphoma. The majority of lymphomas in the extranodal site of the ocular adnexa are extranodal marginal zone lymphomas. Blood involvement is most often described for follicular lymphoma and mantle cell lymphoma. Certain molecules orchestrate lymphoma dissemination into the distinct anatomical locations. CCR7, CCL21 and LFA-1 regulate the entry into secondary lymphoid organs for healthy lymphocytes. However, in malignancy, only CCL21 is highly upregulated in lymphomas with SLO involvement and facilitates lymph node dissemination. Healthy lymphocytes require CXCR4, CXCL12 and VLA-4 to access extranodal tissues. Analysis of lymphoma cells showed that CXCR4 and VLA-4 are expressed at higher levels and play a role in the migration of malignant cells to extranodal sites like the ocular adnexa (Middle et al., 2015a). The CXCR4/CXCL12 axis is especially crucial in bone marrow homing. Bone marrow stromal cells produce CXCL12 and attract CXCR4 expressing lymphoma cells, allowing them access to survival niches (Burger, 2011; Panayiotidis et al., 1996). CXCR4 expression was shown to promote tumor cell proliferation and reduce apoptosis (Huang et al., 2019). The axis can be inhibited by CXCR4 antagonists, resulting in the release of lymphoma cells into the blood, which makes them more accessible to treatments like chemotherapy or B cell antibodies (Burger, 2011; Hu et al., 2012). Factors that regulate tissue retention are CXCR5, CXCL13 and the lipid signaling receptor S1PR2. In lymphoma, CXCR5 is upregulated in malignancies involving SLO and extranodal sites, whereas S1PR2 is only expressed at higher levels in SLOs (Middle et al., 2015b). Lymphoma cells expressing CXCR5 are activated and attracted by CXCL13 (Burger, 2011). The egress receptor S1PR1 is highly upregulated in leukemic lymphomas, which is surprising as S1PR1 on healthy lymphocytes is rapidly internalized upon ligand binding and they only express S1PR1 at very low levels (Middle et al., 2015b).

1.3 The tumor microenvironment

Tumorigenesis is a multistep process. Cells gradually gain capabilities, termed the six hallmarks of cancer, which turn them malignant (Hanahan and Weinberg, 2000, 2011). Most importantly, cancer cells maintain proliferative signaling. Genetic alterations cause continuous activation of signaling pathways or dysfunctions in negative-feedback loops. Also, tumor cells learn to escape growth suppressors, mainly dependent on the function of tumor-suppressor genes, which act as gatekeepers. Malfunction results in constitutive proliferation (Feitelson et al., 2015). Another hallmark is cell death inhibition. Benign cells undergo apoptosis under certain circumstances, but this mechanism is disrupted in malignant cells. Also, as cancer cells evade apoptosis and senescence, they achieve replicative immortality (Lowe and Lin, 2000; Voutsadakis, 2000). As tumor cells grow, they increasingly require access to nutrients and oxygen. Thus, inducing angiogenesis is another hallmark of cancer (Hanahan and Folkman, 1996; Ruan et al., 2009). It is also characteristic of malignant cells to metastasize and invade tissues. Cancerous cells metastasize by altering their shape and the expression of molecules that attach them to neighboring cells and the extracellular matrix (Cavallaro and Christofori, 2004). A recently added hallmark considers the altered energy metabolism in tumor cells. Tumorigenic growth and proliferation require reprogramming of metabolic processes. Most prominently, a metabolic switch that allows aerobic glycolysis is frequently found in neoplastic cells (DeBerardinis et al., 2008). In short, the hallmarks of cancer are acquired functional capabilities that allow survival, proliferation and dissemination of tumor cells. Their acquisition is driven by two enabling characteristics. First, a lack of genomic stability in cancer cells causes random mutations, which can equip them with the hallmark capabilities (Negrini et al., 2010). A fraction of mutant cells gains selective advantages, achieving outgrowth and dominance. Secondly, in recent years, immune cells were recognized as active contributors to tumorigenesis in the inflammatory environment of premalignant and malignant lesions. Tumors have long been known to be abundantly infiltrated with cells of the innate and adaptive immune system, creating an environment similar to inflammation in non-neoplastic tissues (Grivennikov et al., 2010; Pagès et al., 2010). In the past, the involvement of the immune system was considered exclusively an anti-tumor response. Mouse models showed that tumor incidence or progression is increased in animals with T cell, NK cell or macrophage deficiencies; similarly, in humans, immunodeficient and immunosuppressed individuals also show significantly higher susceptibility to cancer (Ostroumov et al., 2018). Cancer is indeed pressured to avoid destruction by the immune system, but recent research surprisingly indicates that tumor-associated inflammation promotes tumorigenesis. Inflammatory processes were shown to provide factors for all hallmark capabilities, such as survival factors, growth factors, and enzymes that modify the extracellular matrix and contribute to metastasis and angiogenesis (Iijima et al., 2011; Wu and

Zhou, 2009). Interestingly, the immune system is already involved at the very early stages of tumorigenesis and even contributes to mutagenesis by releasing mutagenic reactive oxygen species (Hussain et al., 2003). The tumor microenvironment contributes in a previously unexpected manner to the accumulation of hallmark traits and promotes tumorigenesis (Hanahan and Weinberg, 2011).

1.3.1 The tumor microenvironment in B cell lymphoma and leukemia

B cell neoplasms are a highly diverse group of cancers; the composition and inflammatory status of their tumor microenvironment differs greatly depending on the subtype. Three major patterns of tumor microenvironments in lymphoma can be distinguished. The first is the "re-education" pattern, which occurs for instance in follicular lymphoma. In this pattern, the lymphoma cells are strongly dependent on survival and proliferation stimuli from their environment. The microenvironment is largely similar to healthy lymphoid tissue. The second pattern, "recruitment", is found in classical Hodgkin's lymphoma and provides a microenvironment that differs from normal tissue, but strongly supports the lymphoma cells. "Effacement" is the third pattern, which occurs in Burkitt's lymphoma. In this pattern, genetic alterations provide the tumor cells with strong autonomy from their surroundings. The microenvironment in these lymphomas is minor and effaced by tumor cells (Scott and Gascoyne, 2014). The malignant cells in lymphoma and leukemia benefit to a smaller or larger extend from the environment intended for the maturation and proliferation of normal B cells. In the development of healthy lymphocytes, proliferation stimuli in the bone marrow give rise to B cells with a functional B cell receptor. The B cells migrate to secondary lymphoid organs and mature in germinal centers with help from $CD4^+$ T cells and stromal cells. Cells of the microenvironment provide support at all development stages for non-transformed B cells. Lymphoma cells do not only take advantage of these mechanisms, but also manipulate their surrounding in order to support tumorigenesis.

1.3.2 Tumor-stroma interaction and microenvironment remodeling in B cell neoplasms

In the microenvironment of B cell lymphoma and leukemia, stromal cells, conventional and regulatory T cells, and tumor-infiltrating myeloid cells (TIMs) derived from bone marrow hematopoietic stem cells were shown to be closely involved in pathogenesis. Interestingly, the tumor cells are engaged in reciprocal interactions with the cells of the microenvironment and remodel their surroundings to meet their needs (Höpken and Rehm, 2019).

Stromal cells in lymphoma include mesenchymal cells and vascular endothelial cells. Mesenchymal cells in the bone marrow support normal hematopoiesis by providing growth factors and attachment sites and can be accessed by the CXCR4/CXCL12 axis. Fibroblastic reticular cells, which provide the cytokines CCL19 and CCL21, and follicular dendritic cells, which secrete CXCL13, are cells of mesenchymal origin that provide a supportive environment for the

proliferation of B cells in SLOs. Lymphoma cells benefit from stimulation by chemokines and other factors secreted by mesenchymal cells in lymphoid organs (Burger, 2011; Höpken and Rehm, 2019). The importance of bone marrow stromal cells (BMSCs), which are obtained from human bone marrow donations, was shown in numerous coculture experiments with lymphoma cells. First demonstrated for CLL cells, BMSCs activate the tumor cells *in vitro* and provide them with drug resistance (Panayiotidis et al., 1996). Cocultures of primary mantle cell lymphoma with bone marrow-derived stromal cells showed correspondingly that the tumor cells are able to expand long-term and are also provided with increased drug resistance. The mesenchymal cells produce BAFF (B cell activating factor), which binds to BAFF-R on MCL cells and constitutively activates the nuclear factor-κB (NF-κB) pathway. NF-κB signaling induces MCL chemotaxis towards CXCL12/CXCL13 and upregulates anti-apoptotic proteins like BCL2 (Medina et al., 2012). BMSCs additionally induce oncogenic signaling pathways, for instance by β-catenin stabilization in the Wnt pathway in CLL or acute lymphoblastic leukemia (ALL), which induces constitutive activation (Mangolini et al., 2018; Yang et al., 2013). Enhanced proliferation activity of lymphoma cells requires them to fulfill their need for increased uptake of nutrients. The required changes in the neoplastic metabolism can be induced by mesenchymal cells. BMSCs were described to promote mitochondrial oxidative phosphorylation and glycolysis in multiple myeloma (Marlein et al., 2019).

FRCs and FDCs, which are mesenchymal cells in secondary lymphoid organs, cannot be easily obtained from humans and their function was mainly studied in mouse models. Access to follicular FDCs was shown to be crucial in the pathogenesis of murine chronic lymphocytic leukemia. As mentioned earlier, access to FDCs is CXCR5-dependent and induces proliferation in leukemic cells. Correspondingly, access to the FRC network within T cell zones is CCR7-regulated and can provide murine lymphoma cells with survival stimuli. The interaction between leukemic cells and FRCs/FDCs was shown to be reciprocal and establishes a positive feedback loop. Chemokine receptor-mediated signaling induces LTα1β2 expression on the malignant B cells, leading to LTβR signaling on FRCs and FDCs, which in turn triggers chemokine expression (Heinig et al., 2014; Rehm et al., 2011). Numerous mechanisms for reciprocal interactions were not only described for mesenchymal cells in the SLOs, but also in the bone marrow. In B acute lymphoblastic leukemia, leukemic cell adhesion via VCAM-1/VLA-4 was shown to induce NF-κB signaling in BMSCs, which provided a pro-inflammatory environment and chemoresistance for the malignant cells (Jacamo et al., 2014). Reciprocal interactions were also described to induce metabolic alterations in BMSCs. CLL cells require cysteine, which is however limited due to poor uptake ability of the oxidized form. BMSCs are able to take up the oxidized cysteine and convert it to the usable form of cysteine for the lymphoma cell (Zhang et al., 2012).

Summing up, mesenchymal cells were shown to establish three of the hallmarks of cancer in lymphoma cells. They promote apoptosis evasion by inducing anti-apoptotic proteins in the malignant cells; they induce constitutive proliferation upon induction of oncogenic signaling pathways and make changes to the lymphoma metabolism. The interaction between leukemic cells and mesenchymal cells is reciprocal and the tumor cells have the capability to remodel their mesenchymal neighbor cells. Most importantly, lymphoma cells alter the gene expression following the induction of signaling pathways and change the metabolism of mesenchymal cells. These alterations result in the production of pro-inflammatory chemokines and activation markers in mesenchymal cells, which creates a pro-inflammatory tumor microenvironment (Mangolini and Ringshausen, 2020).

Endothelial cells of the vasculature are another stromal cell subtype in lymphoma and leukemia. Lymphoma cells can induce angiogenesis by expressing vascular endothelial growth factors (Gloger et al., 2020). Vascularization is especially prominent in aggressive lymphoma and an angiogenesis-related expression profile was shown to be associated with poor prognosis for DLBCL (Ribatti et al., 2013).

Tumor-infiltrating myeloid cells, which include macrophages, dendritic cells, neutrophils and myeloid-derived suppressor cells, strongly hamper the adaptive and innate anti-tumor response. They differentiate from hematopoietic stem cells upon long-term stimulation with substances released from the tumor, but tumor-associated macrophages also develop from tissue-resident macrophages. As they are tumor-induced, they provide an example for tumor microenvironment remodeling. Lymphoma infiltration with TIMs is associated with therapy failure (Awad et al., 2018).

T cells and NK cells are lymphoid cells that play a role in lymphoma/leukemia progression, for instance by lymphoma stimulation or reduced killing capacities. $CD4^+$ helper T cells were described to stimulate lymphoma cell proliferation in various B-NHL entities. For example, they were shown to engage with CLL cells in proliferation centers or pseudofollicles located in the white pulp of the spleen, the bone marrow and the lymph nodes. There, they activate CLL tumor cells by CD40L signaling (Ghia et al., 2002; Patten et al., 2008). CD40-mediated stimulation was equally important for follicular lymphoma and IL4 provided by follicular helper T cells was shown to induce proliferation (Scott and Gascoyne, 2014). T cell activities are closely related to the interactions that contribute to the lymphoma's ability to escape the antitumor response of the immune system. Three main mechanisms contribute to this immune evasion. First, the tumor cells alter expression of surface molecules, which allows them to minimize their immunogenicity. Secondly, lymphoma cells directly weaken the function of immune cells and thirdly, they engage immunosuppressive cells at the site of lymphoma progression. As the tumor originates from B cells, which are MHC II expressing antigen-presenting cells, MHC II

loss is prevalent in malignant cells. Lymphoma cells lose MHC II expression by homozygous gene deletions, translocation of the CIITA MHC II master regulator or partial plasma cell differentiation. MHC II downregulation contributes to invisibility from the immune system, most likely by preventing tumor antigen presentation to helper T cells, which in turn hampers cytotoxic T cell activation. Additionally, mutations in a subunit of the MHC I molecule, the β2-microglobulin, were shown to be very common in DLBCL, which allows immune escape from cytotoxic T cells as it prevents successful tumor antigen presentation. MHC I loss makes the tumor cells vulnerable to NK cells, which recognize MHC I downregulation; however, the malignant cells also lack CD58, a ligand required for cell elimination by NK cells and cytotoxic T cells. Some lymphomas express PD-L1 and PD-L2, which are the ligands for programmed cell death 1 (PD-1), and induce exhaustion in cytotoxic T cells and T helper cells. In the tumor microenvironment of FL and classical Hodgkin's lymphoma, recruitment of immunosuppressive immune cells was described. These lymphomas are especially enriched in regulatory T cells, which were shown to hamper the proliferation and cytotoxic activity of $CD8^+$ T cells (Scott and Gascoyne, 2014). The mechanisms of lymphoma immune escape also present a challenge in adoptive T cell therapy in lymphoma treatment, which has to be addressed and overcome.

1.3.3 B non-Hodgkin lymphoma mouse models

Various mouse models make it possible to study the onset and progression of B cell neoplasms. They further allow investigation of migration pattern of malignant cells and testing of novel treatment options. Murine models are either spontaneous and occur in genetically modified animals or induced by implantation of malignant cells (Donnou et al., 2012). A very commonly used mouse model is the *Eμ-myc* model. In these transgenic mice, *c-myc* is expressed under the IgH enhancer (Adams et al., 1985). MYC is highly expressed in proliferating cells and deregulated in many types of cancer. Most prominently, it is translocated in Burkitt's lymphoma, but it is also rearranged in diffuse large B cell lymphoma (Nesbit et al., 1999). The *Eμ-myc* model recapitulates the pathogenesis of these two lymphomas. At an early time of tumor onset, the malignant cells show features similar to tumor cells in Burkitt's lymphoma. After day 400, neoplastic mature B cells are detected, which resemble DLBCL (Donnou et al., 2012; Mori et al., 2008). Bichi et al. generated and described the *Eμ-Tcl1* model, in which mice develop expansion of $CD5^+$ B cells. *Tcl1* is involved in chromosomal translocation and inversion in mature T cell leukemias, but it is also highly expressed in some B cell lines derived from human tumors and B cell malignancies. Double-negative T cells and B cells at several development stages, ranging from pre-B cells to GC B cells, are healthy cells expressing *Tcl1*. In *Eμ-Tcl1* mice, the human *Tcl1* transgene was introduced under the control of the immunoglobulin heavy chain Eμ-enhancer, targeting expression of *Tcl1* in immature and mature B cells. Malignant cells are found in transgenic mice older than seven months. The mice present

with pathogenesis corresponding to chronic lymphocytic leukemia (CLL) in humans. Their spleens and livers are enlarged, the cellularity in the peritoneal cave and the number of circulating lymphocytes is increased and they suffer from advanced lymphadenopathy. Human CLL cells show low proliferative activity, which was resembled by the *Eμ-Tcl1* tumor cells as they do not actively divide (Bichi et al., 2002). The *Eμ-Tcl1* tumor cells strongly express CXCR5, CXCR4 and CCR7. In our group, it was shown that the leukemic cells require CXCR5 to access the follicular dendritic cells in the B cell follicle, which provide them with proliferation stimuli. CLL cells that lack CXCR5 are denied access to their survival niche and disease progression was delayed in these mice (Heinig et al., 2014).

Oftentimes, immunodeficient mouse models are used in leukemia/lymphoma research, as they allow engraftment of human tumor cells. They bridge the gap between humans and rodent models (Shultz et al., 2012). NSG (NOD.Cg-Prkdc^{scid} Il2rg^{tm1Wjl}/SzJ) mice harbor genetic mutations causing immunodeficiency. A severe combined immunodeficiency (*scid*) mutation in the DNA repair protein *Prkdc* induces B and T cell deficiency. The null allele of the IL2 receptor common gamma chain (IL2rg^{null}) inhibits cytokine signaling and results in NK cell deficiency. The mutations were crossed onto the NOD strain background, which is intrinsically defective in innate immune functions. Due to the lack of lymphocytes, lymphoid structures are severely affected. The splenic follicular structure is lost and lymph nodes are hypocellular and strongly diminished in size (Shultz et al., 2005). The development of immunodeficient mice allowed studying human cells and tissues *in vivo*. NSG mice engrafted with human patient-derived xenografts (PDX) or cell lines are used to study carcinogenesis, metastasis and the efficacy of drugs or immunotherapeutic treatments (Shultz et al., 2007).

1.4 Pharmacological and immunological targeting of B-NHLs

1.4.1 Pharmacological treatment of B-NHLs

Indolent types of for B non-Hodgkin lymphomas are frequently monitored and might not need treatment. In early stages, radiation treatment of affected and adjacent lymph nodes is an option (Ahmed et al., 2013; Ott et al., 2003). Often, treatment of slowly progressing low-grade lymphoma is not advantageous and is usually only initiated upon disease aggravation (CLL Trialists' Collaborative Group, 1999).

For aggressive B-NHL entities, intensive chemotherapy is indicated. Combinatorial therapy has been long shown to be beneficial for patient survival (Habermann et al., 2006). Chemotherapy is therefore administered in combination with immunotherapy. In more detail, the standard first-line treatment for B non-Hodgkin lymphomas has been R-CHOP (Rituximab, Cyclophosphamide, Doxorubicin, Vincristine and Prednisone) (Watanabe et al., 2011). The cytostatic chemotherapeutics Cyclophosphamide, Doxorubicin and Vincristine are combined with

the anti-inflammatory glucocorticoid Prednisone (CHOP) (Below and M Das, 2020; Johnson-Arbor and Dubey, 2020; Ogino and Tadi, 2020; Puckett et al., 2020). CHOP is often supplemented with Rituximab, a B cell specific monoclonal CD20 antibody, which was shown to be superior to CHOP-only treatment (Habermann et al., 2006; Reff et al., 1994; Tariq et al., 2018). Monoclonal antibodies can hamper tumor growth and destroy lymphoma cells in various ways. For instance, Fc receptor expressing effector cells mediate antibody-dependent cytotoxicity and the complement system induces lysis by complement-dependent cytotoxicity upon antibody opsonization of tumor cells (Harjunpää et al., 2000; Manches et al., 2003). Pathway inhibitors are another addition to targeted therapy. These small molecules inhibit for instance BCR signaling and hamper neoplastic growth (Advani et al., 2013; Herman et al., 2014). Ibrutinib is an oral BCR inhibitor that works by inhibiting Brutin tyrosine kinase, which acts downstream of the BCR (Crisci et al., 2019). Moreover, checkpoint inhibitors are used to unleash the anti-tumor potency of the immune system. PD-1 and CTLA-4 are co-inhibitory receptors that downregulate T cell activity (Blank et al., 2004; Freeman et al., 2000; Krummel and Allison, 1995). Monoclonal antibodies can inhibit the activation of these receptors and potentiate the T cell anti-tumor response. Nivolumab, directed towards PD-1, and Ipilimumab, directed towards CTLA-4, are antibodies used in clinical application (Ansell et al., 2009; Lesokhin et al., 2016).

1.4.2 Adoptive T cell transfer

Despite improvements in the therapy options for B non-Hodgkin lymphoma patients, such as monoclonal antibodies, pathway inhibitors and checkpoint inhibitors, many patients still relapse (Coiffier et al., 2010; Kluin-Nelemans et al., 2012). These relapsed patients can be further treated with adoptive T cell transfer (ATT). ATT is the treatment of patients with autologous or allogenic T cells, thus patient-derived or donor-derived cells.

For many decades, stem cell transplantation has been the treatment of choice. Autologous transplantation, using patient-derived blood or bone marrow, is more common and shows less toxicity (Ali et al., 2015; Buadi et al., 2006; Philip et al., 1995; Smith et al., 2018). In allogenic transplantation, the donor cells can remove residual tumor cells in the patient in a graft-versus-leukemia effect, however, in these patients, the graft-versus-host effect is extremely pronounced and has to be clinically managed (Barnes et al., 1956; Weiden et al., 1979). Patients that relapse after allogenic transplantation can be further treated with donor lymphocyte infusion. They receive blood from the original marrow donor and take advantage of the graft-versus-leukemia effect by the donor immune cells. The challenge in this treatment is again the induction of a severe graft-versus-host effect (Kolb et al., 1990, 1995).

In recent years, adoptive T cell transfer has advanced and T cell receptor (TCR) therapy, tumor-infiltrating lymphocytes (TILs) and chimeric antigen receptor (CAR) therapy are applied in clinical application. In these treatments, commonly autologous T cells are treated outside of

the patient's body and modified in order to improve anti-tumor efficacy before reinjection. The use of patient-derived cells is safer for the patient as adverse effects, for instance graft-versus-host disease by donor T cells or transplant rejection by the host immune system can be avoided (Jeon et al., 2019; Murphy et al., 1987; Storb et al., 1983). Antigens for targeted T cell mediated therapies can be divided in two groups. Antigens that are exclusively expressed in malignant cells are called tumor-specific antigens (TSAs) or neoantigens. They are absent in healthy cells and provide an ideal target in therapy, as non-neoplastic tissue is not recognized by the targeted T cells. TSAs occur upon nonsynonymous mutations. Tumor-associated antigens (TAAs) are highly expressed by tumor cells, but also, although often at low levels, expressed by healthy cells. Naturally occurring high-affinity TCRs against TAAs are usually removed during thymic selection and targeting TAAs can result in severe tissue damages by off tumor/on target effects (Jiang et al., 2019).

Tumor-infiltrating lymphocytes can be extracted from a patient's tumor, expanded and activated *ex vivo*, and reinjected into the patient (Rosenberg et al., 1988; Topalian et al., 1988). TILs within the tumor microenvironment are strongly suppressed and their anti-tumor efficacy is disturbed (Holmes, 1985). Reactivation outside of the hostile milieu reconstitutes their capacities and enables tumor reduction in patients (Dudley et al., 2003). TILs have been administered, among others, for the treatment of melanoma and ovarian cancer (Aoki et al., 1991; Rosenberg et al., 2011).

In T cell receptor therapy, autologous T cells are equipped with a TCR specific for an antigen. The α and β chains genes of the TCR are transferred into T cells and redirect them towards the antigen (Clay et al., 1999). *Ex vivo* culture allows the generation of sufficient numbers of T cells for the treatment of patients (Petersen et al., 2018; Tumeh et al., 2010). Antigen-specific TCRs can be derived by various ways. For instance, they can be isolated from tumor-infiltrating T cells of patients that showed a strong anti-tumor response or using a screening system with a HLA transgenic mouse (Hughes et al., 2005; Obenaus et al., 2015). A clinical study was pioneered with a TCR against the melanoma-associated antigen MART-1 (Morgan et al., 2006). TCRs are mostly used in the treatment of solid tumors, but can also target hematopoietic malignancies (Rapoport et al., 2015; Robbins et al., 2011). TCR therapy still faces numerous challenges. TCR antigen recognition is MHC restricted and thus only possible for antigens that are successfully presented by MHC (Garboczi et al., 1996; Katz et al., 1973; Zinkernagel and Doherty, 1974). Also, on-target toxicity by T cells attacking healthy tissue and autoreactivity after mispairing of transferred TCR chains with the endogenous TCR, resulting in unpredicted epitope recognition, are safety concerns (Bendle et al., 2010; Johnson et al., 2009; van Loenen et al., 2010).

A milestone in adoptive T cell transfer was the approval of Kymriah and Yescarta by the US food and drug administration in 2017. Those were the first chimeric antigen receptor (CAR) products directed against certain $CD19^+$ B-NHL malignancies administered to patients (Jain et al., 2018; Liu et al., 2017). Patient-derived T cells are genetically modified in order to express a chimeric antigen receptor that targets an epitope expressed by tumor cells (Vormittag et al., 2018). Opposed to TCRs, they allow MHC-independent antigen recognition (Mezzanzanica et al., 1998). A CAR binds its antigen with single-chain variable fragments (scFv) derived from an antibody sequence. The scFvs are composed of a variable heavy (VH) and a variable light (VL) chain connected via a linker sequence (Bird et al., 1988). A commonly IgG-derived spacer (hinge region) joins the variable fragments to the transmembrane domain and allows flexibility to improve target recognition. The ideal spacer length is antigen dependent (Guest et al., 2005; Hudecek et al., 2015). The transmembrane domain anchors the CAR in the T cell membrane and can be derived from CD3ζ, CD4, CD8α or CD28 (Alabanza et al., 2017; Bridgeman et al., 2010; Fitzer-Attas et al., 1998). The CAR endodomains are the costimulatory domain and the activation domain. The costimulatory domain originates from the tumor necrosis factor receptor family (4-1BB, CD27, OX40) or the CD28 family (CD28, ICOS) (Finney et al., 2004; Guedan et al., 2014; Song et al., 2012). The activation domain is based on CD3ζ of the TCR complex (Finney et al., 2004). T cell activation is transmitted by phosphorylation of the CD3ζ immunoreceptor tyrosine-based activation motifs (ITAMs) (Irving and Weiss, 1991; Ramello et al., 2019).

CARs were first developed by Kuwana et al. and Gross et al. (Gross et al., 1989; Kuwana et al., 1987). Ever since the advent of CAR T cell therapy, efforts have been made to improve the constructs. It appeared that these first generation CARs without costimulatory domain benefited from additional costimulation to establish a stable cytokine response (Gong et al., 1999). Thus, second generation CARs equipped with a costimulatory domain were developed. T cells endowed with a second generation CAR showed superior expansion and persistence compared with first generation CARs (Maher et al., 2002; Savoldo et al., 2011). CD28 and 4-1BB are the most commonly used costimulatory domains (Chavez et al., 2019; Weinkove et al., 2019). The CD28 costimulatory domain is derived from a costimulatory T cell protein which, upon ligand binding by B7.1 and B7.2 on antigen-presenting cells, provides a proliferative signal in combination with TCR/CD3 activation (Linsley et al., 1990; Stein et al., 1994; Turka et al., 1990). The T cell activation receptor 4-1BB (CD137) from the tumor necrosis factor superfamily, which is also involved in T cell proliferation, was the basis for the second widely used costimulatory domain (DeBenedette et al., 1995; Pollok et al., 1993). In more detail, the CD28 costimulatory domain allows a rapid anti-tumor effect and the 4-1BB costimulatory domain allows longer T cell persistence (Milone et al., 2009; Zhao et al., 2015). The reason for these

differences could lay in the distinct metabolic regulation. T cells with CD28 costimulatory domains formed an effector memory compartment with enhanced glycolysis, whereas 4-1BB yielded an increase in $CD8^+$ central memory cells and upregulation of mitochondrial biogenesis and fatty acid metabolism (Kawalekar et al., 2016).

In an effort to combine the benefits of the CD28 and the 4-1BB costimulatory domain of second generations CARs, third generation CARs, which combine two costimulatory domains, were developed (Zhong et al., 2010). However, it is not clear if these have any advantage over second generation CAR constructs (Guedan et al., 2018; Haso et al., 2013; Yi et al., 2018).

2 Aim of this thesis

Anti-CD19 CAR T cell therapy improved the prognosis for patients suffering from relapsed and refractory aggressive B non-Hodgkin lymphomas; however, many patients do not respond to treatment or relapse (Crump et al., 2017; Locke et al., 2019; Maziarz et al., 2020). Therefore, there is a high demand for treatment alternatives. The chemokine receptor CXCR5, which guides B cells to the B cell zones of secondary lymphoid organs, was identified as a novel target for immunotherapy (Heinig et al., 2014; Panjideh et al., 2014). CXCR5 is not only expressed on mature B cells and their neoplastic counterparts, but also on follicular helper T cells (Breitfeld et al., 2000; Schaerli et al., 2000a). This T cell subset is described to have a tumor-supportive function in follicular lymphoma and chronic lymphocytic leukemia (Ahearne et al., 2013; Pangault et al., 2010). Previously in the group, an anti-CXCR5 CAR construct based on a monoclonal antibody was designed. In this thesis, the anti-CXCR5 CAR product was functionally characterized and the safety of anti-CXCR5 treatment was assessed.

In detail, the following questions were addressed in this thesis:

(1) Do anti-CXCR5 CAR T cells exhibit a specific and efficient anti-tumor effect against CXCR5 expressing B non-Hodgkin lymphoma *in vitro* and *in vivo*?

(2) Do anti-CXCR5 CAR T cells target tumor-supportive T_{FH} cells in follicular lymphoma and chronic lymphocytic leukemia?

(3) Does CXCR5 show a safe expression profile and can on-target/off-tumor toxicity be avoided?

As anti-CXCR5 CAR T cells target subsets of CXCR5 expressing T cells, it is of interest to study the $CXCR5^+$ T cell compartment in closer detail, especially upon lymphoma challenge. Therefore, the influence of lymphomagenesis on the splenic $CXCR5^+$ T cells was studied in the syngeneic *Eμ-Tcl1* mouse model by means of single cell RNA sequencing.

Additional questions addressed in the second part of the thesis were:

(4) Is the composition of $CXCR5^+$ T cell subsets changed upon lymphomagenesis?

(5) Which transcriptional changes are induced in T_{FH} cells upon tumor challenge? In particular, are tumor-supportive genes upregulated?

3 Material and Methods

3.1 Material

3.1.1 Chemicals and consumables

Abbott Laboratories: Isoflurane

BD Biosciences: 7-AAD, TMB Substrate Reagent Set

Biolegend: Human TruStain FcX, TruStain Monocyte Blocker

Carl Roth: Phosphate-buffered formaldehyde (PFA)

Gibco: DMEM high glucose, fetal calf serum (FCS), Non-Essential Amino Acid Solution 100x, Penicillin/Streptomycin, RPMI 1640, Sodium Pyruvate 100mM, Trypsin/EDTA

Merck: Biocoll, Polybrene

Miltenyi Biotec: rhIL2, rhIL7, rhIL15

PeproTech: hIFNγ

PromoCell: Accutase-Solution

Sigma-Aldrich: Dimethyl sulfoxide (DMSO), Poly-L-lysine solution

TaKaRa: RetroNectin

ThermoFisher Scientific: LIVE/DEAD™ Fixable Aqua Dead Cell Stain Kit, O'RangeRuler 100bp, Phusion High-Fidelity DNA Polymerase

3.1.2 Primary cells and media

Table 1: Primary cells and media

Cell type	Medium
HUAEC (PromoCell)	Endothelial cell growth medium and supplements (PromoCell)
Human astrocytes (ScienCell)	HA medium and supplements (ScienCell)
Human colonic epithelial cells (ScienCell)	HCoEpiC medium and supplements (ScienCell)
Human cervical epithelium cells (ScienCell)	HCerEpic medium and supplements (ScienCell)
Human neurons (ScienCell)	HN medium and supplements (ScienCell)
Human perineurial cells (ScienCell)	Fibroblast medium and supplements (ScienCell)
Human urothelial cells (ScienCell)	HUC medium and supplements (ScienCell)
HUVEC single donor (PromoCell)	Endothelial cell growth medium and supplements (PromoCell)

3.1.3 Cell lines and media

Table 2: Cell lines and media

Cell type	Supplier	Medium
293Vec-Galv (Packaging cell line)	Biovec Pharma (Québec)	DMEM high glucose complete
DOHH-2 (Follicular lymphoma)	DSMZ (Braunschweig)	RPMI 1640 complete
HEK-293 (Human embryonic kidney)	Quantum Biotechnologies Inc. (Canada)	DMEM high glucose complete
HEK-293T (Human embryonic kidney)	ATCC (USA)	DMEM high glucose complete
HepG2 (Hepatocellular carcinoma)	DSMZ (Braunschweig)	DMEM high glucose complete
JEKO-1 (Mantle cell lymphoma)	DSMZ (Braunschweig)	RPMI 1640 complete
Jurkat (Acute T lymphoblastic leukemia)	DSMZ (Braunschweig)	RPMI 1640 complete
NALM-6 (Acute T lymphoblastic leukemia	Dr. Stephan Mathas (MDC, Berlin)	RPMI 1640 complete
NCI-H929 (Multiple myeloma)	DSMZ (Braunschweig)	RPMI 1640 complete
OCI-Ly7 (Diffuse large B-cell lymphoma)	DSMZ (Braunschweig)	RPMI 1640 complete
Raji (Burkitt's lymphoma)	DSMZ (Braunschweig)	RPMI 1640 complete
REH (Acute B lymphoblastic lymphoma)	Dr. Stephan Mathas (MDC, Berlin)	RPMI 1640 complete
SC-1 (Follicular lymphoma)	DSMZ (Braunschweig)	RPMI 1640 complete
SU-DHL4 (Diffuse large B-cell lymphoma)	DSMZ (Braunschweig)	RPMI 1640 complete
SW620 (Colorectal carcinoma)	CLS Inc. (Eppelheim)	DMEM high glucose complete

Complete: Medium supplemented with 10% FCS, 1x Penicillin/Streptomycin, 1x Non-Essential Amino Acids Solution and 1 mM Sodium Pyruvate

3.1.4 Patient-derived xenografts

Table 3: Patient-derived xenografts

PDX	Supplier
#44685 (Mantle cell lymphoma)	Public Repository of Xenografts (PRoXe) platform of the Dana-Farber Cancer Institute (USA)
#96069 (Mantle cell lymphoma)	Public Repository of Xenografts (PRoXe) platform of the Dana-Farber Cancer Institute (USA)

3.1.5 Antibodies

Table 4: Anti-human antibodies for flow cytometry

Antigen	Fluorescence	Clone	Isotype	Supplier	Dilution
CD1c	FITC	L161	Mouse IgG1	Biolegend	1:100
CD3	BV510	SK7	Mouse IgG1	Biolegend	1:100
CD3	FITC	HIT3a	Mouse IgG2a	Biolegend	1:100
CD3	PB	HIT3a	Mouse IgG2a	Biolegend	1:100
CD4	APC/Cy7	OKT4	Mouse IgG2b	Biolegend	1:100
CD4	BV421	RPA-T4	Mouse IgG1	Biolegend	1:200
CD4	FITC	OKT4	Mouse IgG2b	Biolegend	1:100
CD5	PB	UCHT2	Mouse IgG1	Biolegend	1:165
CD8	APC/Fire750	SK1	Mouse IgG1	Biolegend	1:100
CD8a	APC	HIT8a	Mouse IgG1	Biolegend	1:100
CD8a	APC/Cy7	HIT8a	Mouse IgG1	Biolegend	1:200
CD8a	PE/Cy7	HIT8a	Mouse IgG1	Biolegend	1:100
CD11c	PE/Cy7	Bu15	Mouse IgG1	Biolegend	1:100
CD14	APC	HCD14	Mouse IgG1	Biolegend	1:100
CD19	PB	HIB19	Mouse IgG1	Biolegend	1:200
CD19	BV510	SJ25C1	Mouse IgG1	Biolegend	1:100
CD20	APC	2H7	Mouse IgG2b	Biolegend	1:100
CD25	APC	MOPC-21	Mouse IgG1	Biolegend	1:100
CD45RA	PerCP/Cy5.5	HI100	Mouse IgG2b	Biolegend	1:200
CD45RO	FITC	HCHL1	Mouse IgG2a	Biolegend	1:200
CD56	Pe/Cy7	5.1H11	Mouse IgG1	Biolegend	1:100
CD62L	AF647	DREG-56	Mouse IgG1	Biolegend	1:200
CD197	PE/Cy7	G043H7	Mouse IgG2a	Biolegend	1:200
CD303	APC/Fire750	201A	Mouse IgG2a	Biolegend	1:100
CXCR5	PE	51505	Mouse IgG2b	R&D	1:10

HLA-DR	BV421	L243	Mouse IgG2a	Biolegend	1:100
IgG	Biotin	IS11-12E4.23.20	Mouse IgG1	Miltenyi Biotec	1:10
IgG	FITC	polyclonal	Goat IgG	Southern Biotech	1:400
IgG	PE	polyclonal	Goat IgG	Southern Biotech	1:600
LAG-3	AF647	11C3C65	Mouse IgG1	Biolegend	1:50
PD-1	BV421	EH12.2H7	Mouse IgG1	Biolegend	1:50
PD-1	PE	Eh12.2H7	Mouse IgG1	Biolegend	1:50
TIM-3	BV421	F38-2E2	Mouse IgG1	Biolegend	1:50

Table 5: Anti-mouse antibodies for flow cytometry

Antigen	Fluorescence	Clone	Isotype	Supplier	Dilution
CD3e	APC	145-2C11	Hamster IgG	Biolegend	1:400
CD5	APC	53-7.3	Rat IgG2a	Biolegend	1:400
CD19	FITC	6D5	Rat IgG2a	Biolegend	1:400
CD45.2	PB	104	Mouse IgG2a	Biolegend	1:100
CXCR5	BV421	L138D7	Rat IgG2b	Biolegend	1:50

Table 6: Isotype control antibodies

Antigen	Fluorescence	Clone	Supplier	Dilution
Mouse IgG1	AF647	MOPC-21	Biolegend	1:50
Mouse IgG1	APC	MOPC-21	Biolegend	1:200
Mouse IgG1	Biotin	IS5-21F5	Miltenyi Biotec	1:50
Mouse IgG1	BV421	MOPC-21	Biolegend	1:50
Mouse IgG1	BV510	MOPC-21	Biolegend	1:100
Mouse IgG1	FITC	MOPC-21	Biolegend	1:125
Mouse IgG1	PE	MOPC-21	Biolegend	1:200
Mouse IgG1	PE/Cy7	RMG1-1	Biolegend	1:200
Mouse IgG2a	APC/Fire750	MOPC-173	Biolegend	1:100
Mouse IgG2a	BV421	MOPC-173	Biolegend	1:200
Mouse IgG2b	PE	133303	R&D	1:10
Rat IgG2b	BV421	RTK4530	Biolegend	1:25

3.1.6 Oligonucleotides

Table 7: Oligonucleotides

Primer	Sequence (5'-3')
CXCR5_fwd	GCCTCTCAACATAAGACAGTGAC
CXCR5_rev	AAGGTCTCCGTGGAACTGC
GAPDH_fwd	GGTGAAGGTCGGAGTCAACG
GAPDH_rev	GGACTCCACGACGTACTCAG
CD19_fwd	GGAGTCCCCGCTTAAACCCT
CD19_rev	ATCTCAGGGCGGTCTTTGGC

3.1.7 Kits

BD Biosciences: OptEIA™ Human IFN-γ ELISA Set, PE Quantibrite beads (Phycoerythrin Fluorescence Quantitation Kit)

Miltenyi Biotech: Pan B Cell Isolation Kit II (mouse), Pan T cell isolation Kit II (mouse)

Stemcell Technologies: EasySep Human $CD4^+$ T Cell Isolation Kit, EasySep Human PE Positive Selection Kit

3.1.8 Devices

BD Biosciences: FACSCanto II Cell Analyzer, FACSAria Fusion Cell Sorter

BioTek Instruments: PowerWave X Select microplate UV/VIS reader

Innovatis: CASY Cell Counter TTC

Miltenyi Biotech: MACSQuant Analyzer 10

PerkinElmer: IVIS Spectrum In Vivo Imaging System

ThermoFisher Scientific: Microm HM355S Rotary Microtome

Vilber Lourmat: Quantum Gel Documentation Imaging

Zeiss: AxioCam MRm camera, Axio Imager 2 microscope

3.1.9 Software

Adobe: Illustrator CS6

BD: FACS Diva, Flowjo 10.5.3

GraphPad: Prism 7

ImageJ: ImageJ 2.0.0

Microsoft: Excel 14.7.3, Word 14.7.3

PerkinElmer: Living Image 3.2/4.5

Zeiss: Axio Vision 4.5

3.1.10 Mice

Eμ-Tcl1 mice on a C57BL/6 background were generated by Heinig et al. (Heinig et al., 2014). C57BL/6 and NOD.Cg-Prkdc^{scid} Il2rg^{tm1Wjl}/SzJ (NSG) mice were bred and housed at the MDC

Berlin animal facility. Animal studies were performed in accordance with institutional and Berlin State guidelines (G0373/13; G0050/16; G0104/16).

3.2 Methods

3.2.1 Cell culture

3.2.1.1 Cryoconservation

Cells were resuspended in freshly prepared, cooled FCS (Gibco) with 10% DMSO (Sigma-Aldrich). The cryotubes (Corning) were immediately frozen at -80°C in a cryotube holder (Cell-Camper) and later transferred into liquid nitrogen. Thawing was performed at 37°C in a water bath, the cells were transferred into cold medium, immediately centrifuged (350 g, 5 min) and resuspended in fresh medium.

3.2.1.2 Maintenance of cell lines

Adherent cell lines were cultured in DMEM complete (DMEM high glucose with 10% FCS and 1x Penicillin/Streptomycin, non-essential amino acid solution and sodium pyruvate) and split upon confluency using trypsin/EDTA.

Suspension cell lines were cultured in RPMI complete (RPMI 1640 with 10% FCS and 1x Penicillin/Streptomycin, non-essential amino acid solution and sodium pyruvate) and split every second or third day. Cells were cultured in a Binder CB210 incubator (Thermo Fisher Scientific) at 37°C and 5% CO_2.

3.2.1.3 Cell count determination

In order to determine the quantity of mouse spleen or bone marrow cells, the cell suspension was diluted with CASYton (1:1000) and measured by the CASY Cell Counter TTC. Cell lines and human lymphocytes were counted in a Neubauer hemocytometer with 10% trypan blue in PBS or with the MACSQuant.

3.2.1.4 Culture of primary cells

Primary cells were cultured according to the manufacturer's instructions and detached using Accutase.

3.2.1.5 Isolation of PBMCs from donor blood

Recruiting of voluntary blood donors was approved by the Charité Universitätsmedizin ethics committee. Donor blood was diluted with an equal volume RPMI 1640 and 25 ml were carefully layered over 12.5 ml Biocoll separating solution (Biochrom) in a 50 ml falcon tube. Density gradient centrifugation was performed (650 g, 20 min, RT, without brake), followed by a recovery of the leukocyte containing intermediate phase. The cells were resuspended in 50 ml RPMI 1640 and centrifuged (350 g, 15 min, RT). The cells were again resuspended and centrifuged (300 g, 10 min, RT).

3.2.1.6 Isolation of CXCR5+ CD4+ T cells from PBMCs

$CD4^+$ cells were isolated from PBMCs using the EasySep Human $CD4^+$ T Cell Isolation Kit (Stemcell Technologies) according to the manufacturer's instruction. $CXCR5^+$ cells were isolated from the resulting $CD4^+$ cells with the EasySep Human PE Positive Selection Kit (Stemcell Technologies) according to the manufacturer's instruction after labeling with the CXCR5 PE antibody at 1.3 µg/ml for 15 min at room temperature (R&D).

3.2.1.7 Virus production

Virus for human T cell transduction was produced using virus producing 293Vec-Galv cells lines stably transduced with the MP71 vector. Cells were cultured in DMEM complete (DMEM high glucose with 10% FCS and 1x Penicillin/Streptomycin, non-essential amino acid solution and sodium pyruvate) until 70% confluency was reached. DMEM was removed and 293Vec-Galv cells were cultured in RPMI complete (RPMI 1640 with 10% FCS and 1x Penicillin/Streptomycin, non-essential amino acid solution and sodium pyruvate) at 0.1 ml/cm^2 for 24 h. Viral supernatant was filtered with a 0.45 µm filter and stored at -80°C.

3.2.1.8 Transduction of human T cells

A 24 well non-tissue culture treated plate was prepared by incubation with anti-CD3 (5 µg/ml) and anti-CD28 (1 µg/ml) antibodies in PBS over night at 4°C. The plate was blocked with 2% BSA in PBS at 37°C and washed twice. Human peripheral blood mononuclear cells were seeded at 1-1,3x10^6 cells/well in 1 ml/well RPMI complete (RPMI 1640 with 10% FCS and 1x Penicillin/Streptomycin, non-essential amino acid solution and sodium pyruvate), for *in vivo* experiments and the stress test with 10 ng/ml rhIL7 and rhIL15, for *in vitro* experiments with 10 ng/ml rhIL2 (Miltenyi Biotec). The cells were incubated for 48 h, always at 37°C and 5% CO_2. Another 24 well non-tissue culture treated plate was prepared by incubation with retroNectin (12,5 µg/ml) over night at 4°C. The plate was blocked with 2% BSA in PBS at 37°C and washed twice. Virus solution was added and the plate was centrifuged for 90 min (3000 g, 4°C). The virus solution was removed and the cells were transferred into the virus-precoated wells. Virus solution was added and a final volume of 2 ml/well was obtained by addition of RPMI complete with a final concentration of 10 ng/ml IL7/IL15 or IL2. The plate was centrifuged for 20 min (800 g, 32°C). After 24 h incubation, 1 ml/well was removed and the transduction was repeated. 4 h after centrifugation, the cells were removed from the wells and pooled in cell culture flasks with addition of twice their volume fresh RPMI complete containing 10 ng/ml IL7/IL15 or IL2, cultured in an upright position.

3.2.1.9 T cell culture

T cells were expanded in RPMI complete (RPMI 1640 with 10% FCS and 1x Penicillin/Streptomycin, non-essential amino acid solution and sodium pyruvate) in cell culture flasks in an upright position at 37°C and 5% CO_2. T cells prepared for *in vivo* experiments (10 day culture)

and the stress test (10-14 day culture) were cultured with 10 ng/ml IL7/IL15; for *in vitro* experiments (13 day culture) with 10 ng/ml IL2. IL2 stimulated T cells were cultured in fresh medium with low IL2 (1 ng/ml) for the last three days of culture.

3.2.1.10 Transduction of patient-derived xenograft cells

PDX #96069 cells were thawed and immediately transduced with a lentiviral luciferase-eGFP construct. $3x10^6$ cells/well were seeded in a 24-well plate with 1.5 ml RPMI complete (RPMI 1640 with 10% FCS and 1x Penicillin/Streptomycin, non-essential amino acid solution and sodium pyruvate), 0.5 ml viral supernatant and 16 µl polybrene. After a 2 h centrifugation step (800 g, 37°C), cells were incubated at 37°C and 5% CO_2 for another 2 h. Cells were washed with PBS and immediately injected intravenously in NOD.Cg-Prkdc^{scid} Il2rg^{tm1Wjl}/SzJ (NSG) mice ($3x10^6$ cells/animal). After six weeks, spleens were harvested, eGFP$^+$ cells were sorted by FACS and reinjected in NSG mice. Expansion and sorting was performed twice.

3.2.2 Immunological techniques

3.2.2.1 Flow cytometry

For flow cytometric analysis, $1x10^6$ cells/well were transferred into a 96 well plate. For blocking of unspecific binding sites, cells were centrifuged (350 g, 3 min), the supernatant was discarded and the cells were blocked in 50 µl 5% human serum in FACS buffer (PBS, 2% FCS, 10 mM EDTA) for 10 min at RT. Subsequently, 50 µl FACS buffer containing the antibodies were added. If an IgG antibody (to determine the CAR transduction rate) was used, blocking was omitted and after centrifugation (350 g, 3 min), the supernatant was discarded and 100 µl FACS buffer containing the antibodies were added. The IgG antibody had to be incubated separately, prior to the other antibodies and followed by two wash steps. Ultimately, the cells were stained for 10-15 min at RT in 100 µl FACS buffer. The cells were washed twice with FACS buffer and resuspended in 50-150 µl FACS buffer for the FACS measurement. If 7AAD was used, it was added into the FACS buffer (1:100). The cells were analyzed using a FACSCanto II Cell Analyzer (BD Biosciences). For the quantification of molecules on the cell surface, PE Phycoerythrin Fluorescence Quantibrite beads were used according to the manufacturer's instructions.

3.2.2.2 CAR T cell cocultures

CAR T cells were expanded over the course of 13 days with rhIL2. For the last 3 days, the T cells were resuspended in fresh medium with low IL2 (1 ng/ml) to induce a resting state and subsequently frozen. In order to quantify the effector function of CAR T cells, they were thawed and incubated with various target cells in a 96-well plate. The effector/target cell ratio was 1:1. $5x10^4$ target cells were incubated with $5x10^4$ CAR$^+$ T cells per well. As not all T cells were transduced with the CAR, the total T cell number per well was higher than $5x10^4$. For adherent target cells, flat bottom plates were used and $1x10^4$ cells were seeded after Accutase treatment

one day prior to allow adherence. For suspension target cells, V-bottom plates were used. The cells were incubated in 200 µl RPMI complete (RPMI 1640 with 10% FCS and 1x Penicillin/Streptomycin, non-essential amino acid solution and sodium pyruvate) per well. If the target cells required another medium, 100 µl RPMI complete and 100 µl of the target cell medium were used. For the minimum value, the CAR T cells were incubated without target cells; for the maximum value, they were incubated with 1 µM ionomycin and 5 ng/ml PMA. The plates were incubated for 12-24 h at 37°C and 5% CO_2. The supernatant was frozen at -80°C.

3.2.2.3 CAR T cell blocking coculture

JEKO-1 cells were cocultured with CAR-transduced cells as described under *CAR T cell cocultures*. Peptides synthesized by Biosyntan were added. The peptides were generated by simultaneous multiple peptide synthesis and quality control was performed by mass spectrometry. The epitope peptide is derived from the CXCR5 N-terminus and harbors the epitope recognized by the anti-CXCR5 CAR; the control peptide is derived from a sequence located in the extracellular loop region of CXCR5.

3.2.2.4 Stress test

For the stress test, T cells were expanded for 14 days (for the 1:1 assay) or 10 days (for the 1:10 assay) with rhIL7/15. In order to analyze T cell exhaustion, CAR T cells were cocultured at a 1:1 or 1:10 ratio with JEKO-1 tumor cells in a 24-well plate with 2 ml RPMI complete/well (RPMI 1640 with 10% FCS and 1x Penicillin/Streptomycin, non-essential amino acid solution and sodium pyruvate) supplemented with 1 ng/ml IL7/IL15. For the 1:1 assay, $5x10^5$ T cells were cocultured with $5x10^5$ JEKO-1 cells per well; for the 1:10 assay, $5x10^4$ CAR T cells were cocultured with $5x10^5$ JEKO-1 cells per well. Every third day, the supernatant was collected and frozen at -80°C and the cells were analyzed by flow cytometry.

3.2.2.5 Enzyme-linked immunosorbent assay (ELISA)

The BD OptEIA™ ELISA kit was used to analyze cell culture supernatants according to the manufacturer's instructions. The standard series was performed in duplicates, starting at 8 ng. Data acquisition was performed using a PowerWave X Select microplate UV/VIS reader (Bio-Tek Instruments, USA).

3.2.3 Molecular Biology

3.2.3.1 Polymerase chain reaction

The HMRT103 TissueScan™ Human Normal cDNA Array was analyzed by PCR with the following settings and according to the manufacturer's instruction:

Reaction mix:	5 µl	5x HF buffer
	0.5 µl	10 mM dNTPs
	0.063 µl	100 µM primer mix
	0.25 µl	Phusion polymerase
	ad 25 µl	H_2O

Cycler program:	1. 98°C	0:30 min
	2. 98°C	0:08 min
Annealing	3. 63°C-68°C	0:12 min
	4. 72°C	0:12 min
	Repeat 2.-4. 35x	
	5. 72°C	5:00 min
	6. 4°C	hold

The annealing temperature was 63°C for the CXCR5 PCR, 64°C for the GAPDH PCR and 68°C for the CD19 PCR.

Agarose gel electrophoresis was performed with a 1,5% agarose gel with ethidium bromide at 120 V. O'RangeRuler 100 bp was used to confirm the correct length of the PCR products.

3.2.4 Animal experiments

3.2.4.1 Xenograft mouse model

NOD.Cg-Prkdc^{scid} Il2rg^{tm1Wjl}/SzJ (NSG) mice (8 to 10 weeks old) were used for xenograft experiments. The mice were injected intravenously in the tail vein with 100 µl cell suspension in RPMI 1640 (without additives) with lucifericed tumor cells (JEKO-1 6x10^5). Upon visible tumor growth by IVIS imaging, 3x10^6 CAR T cells were injected in 100 µl RPMI 1640 (without additives) intravenously in the tail vein. The number of total T cells was adjusted using the transduction rate. The tumor challenged mice were analyzed by IVIS imaging twice a week. Their weight and wellbeing was monitored and the experiments were usually terminated before the mice showed visible symptoms of disease.

3.2.4.2 Serum analysis

Peripheral blood was collected by retroorbital puncture and serum was processed by the animal phenotyping facility at the MDC Berlin.

3.2.4.3 Isolation of spleen and bone marrow

Mice were killed with an overdose of the inhalational anesthetic Isoflurane (Abbott Laboratories). Spleen and bone marrow of the femur were isolated at the end point of animal experiments for flow cytometry analysis. Spleens were disrupted in FACS buffer (PBS, 2% FCS, 2 mM EDTA) using the plunger of a 5 ml syringe. Femur was isolated, muscle and skin tissue were removed and the bone was cut open at the epiphysis on both sides. The bone marrow was flushed with PBS using a syringe and a 26-gauge needle (B. Braun). Isolated spleen and bone marrow cells were filtered using a 100 µm cell strainer in FACS buffer. Subsequently, the cells were centrifuged at 350 g for 5 min, supernatant was removed and red blood cell lysis was performed for 5 min (10x lysis buffer: 8,29 g NH_4Cl, 1 g $KHCO_3$, 37,2 mg Na_2-EDTA, ad 1 l H_2O with pH 7,3). The cells were stored in FACS buffer on ice during the experiments.

3.2.4.4 Histology

Lung, colon and liver tissue was fixed in 4 % phosphate-buffered formaldehyde (Carl Roth) for 24 to 48 h and subsequently dehydrated in an ethanol dilution series. The organs were embedded in paraffin for 24 h, with three paraffin changes. 5 µm cuts were made on the Microm HM355S Rotary Microtome (ThermoFisher Scientific), transferred to SuperFrost Plus Menzel slides (ThermoFisher Scientific) and stained with hematoxylin and eosin (H&E) using a Microm HMS 740 robot-stainer (ThermoFisher Scientific). Pictures were recorded with the AxioCam MRm camera an Axio Imager 2 microscope (Zeiss). Processing was performed using Axio Vision 4.5 (Zeiss) and ImageJ 2.0.0 (ImageJ).

3.2.4.5 IVIS in vivo imaging

Mice were anesthetized by isoflurane inhalation in the IVIS induction chamber (PerkinElmer) and injected intraperitoneally with 150 µg luciferin (Biosynth). The mice were incubated for 10 min and transferred into the IVIS Spectrum (PerkinElmer). A photographic image and several bioluminescent images (1-300 sec exposure time) were acquired. The Living Image 3.2 and 4.5 software (PerkinElmer) was used for further analysis.

3.2.4.6 Splenic T cell preparation for RNA single cell sequencing

10-week-old female C57BL/6N mice were injected intravenously with $3x10^6$ *Eµ-Tcl1* tumor cells harvested from the spleens of female transgenic *Eµ-Tcl1* mice. Control animals were injected with $3x10^6$ B cells harvested from the spleens of healthy C57BL/6N mice isolated using the Pan B Cell Isolation Kit II (Miltenyi Biotec). Two weeks after tumor/B cell injection, spleens were harvested and after red blood cell lysis, the tumor load was determined as $CD5^+CD19^+$ cells. 2 mice were pooled per sample. Three samples were processed: Control, high tumor load (45%, 46%) and low tumor load (22%, 31%). $CD3^+$ T cells were isolated using the Pan T cell isolation Kit (Miltenyi). Prior to antibody staining in FACS buffer (PBS, 2% FCS, 2 mM EDTA), cells were blocked with CD16/32. Cells were sorted for 7-AAD and CD19 negativity,

and CD3 and CXCR5 positivity using the FACSAria Fusion sorter (BD Biosciences). Sorting tubes were coated with FCS to prevent sticking of the cells to the tube surface. Cells were sorted into PBS.

3.2.5 RNA single cell sequencing

3.2.5.1 RNA single cell sample processing

Splenic CXCR5^{+} T cells were processed at the Genomics platform at the Berlin Institute for Medical Systems Biology using the Chromium Single Cell 3' Reagent Kit (v3.1 Chemistry, 10x Genomics) according to the manufacturer's instructions. Successful library preparation was confirmed with the Bioanalyzer device (DNA HS kit, Agilent) and KAPA Library Quantification (KK4857, Roche). Library sequencing was performed using Illumina NovaSeq 6000. Barcode processing, mapping, counting of unique molecular identifiers and dimension reduction was conducted using Cell ranger (v3.1.0, 10x Genomics).

3.2.5.2 RNA single cell analysis

Analysis was performed in R (Version 3.6.1) using the package Seurat (Version 3.2.2) (Hafemeister and Satija, 2019; Stuart et al., 2019). Dead cells and doublets were removed by filtering out outliers (cell with less than 2000 or more than 4900 features, percent mitochondrial genes over 8). Contaminating plasma cells and macrophages were excluded. After principal component analysis, cells were visualized upon uniform manifold approximation and projection (UMAP) dimensional reduction (McInnes et al., 2020). Clusters were identified by an algorithm based on shared nearest neighbor (SNN) modularity optimization.

3.2.6 Statistics

Statistical significance was determined using GraphPad Prism (Version 7). Arithmetic mean and standard error of the mean (SEM) are shown and p-values were calculated by applying an unpaired T test (p-values indicated as *P<0.05, **P<0.01, ***P<0.001 unless stated otherwise).

4 Results

The prognosis for patients diagnosed with refractory or relapsed aggressive B-cell lymphomas remains poor. As summarized in the retrospective SCHOLAR-1 study, the two-year survival rate for patients with refractory DLBCL treated with conventional therapy options is 20% (Crump et al., 2017). The advent of CAR T cell therapy finally expanded treatment options for patients with B cell neoplasms. In 2017, thirty years after the first papers about this technology were published, CAR T cell therapy first received approval by the US food and drug administration (FDA) and shortly after by the European Medicines Agency (EMA) (Yu et al., 2018). Up to now, three CAR products, all of them targeting CD19, were approved by the FDA. Axicabtagene ciloleucel, marketed under the name Yescarta, has a CD28 costimulatory domain and is approved for the treatment of relapsed or refractory types of large B-cell lymphoma (diffuse large B cell lymphoma, transformed follicular lymphoma, primary mediastinal B-cell lymphoma) (Jain et al., 2018). Tisagenlecleucel, sold under the name Kymriah, is a 4-1BB CAR product for the treatment of relapsed or refractory DLBCL and B-ALL (Liu et al., 2017; Zavras et al., 2019). This year, a third anti-CD19 CAR entered the clinic with the approval of brexucabtagene autoleucel (Tecartus) for the treatment of refractory and relapsed mantle cell lymphoma (Wang et al., 2020). Of the large B-cell lymphoma patients qualifying for treatment with Yescarta in the ZUMA-1 study, complete responses were noticed in 58% of patients, with a two-year survival rate of around 50% (Locke et al., 2019). For the Kymriah JULIET study, complete response was reported for 40% of patients and 65% showed relapse-free survival 12 months after the initial response (Maziarz et al., 2020; Schuster et al., 2019). Trials of relapsed or refractory chronic lymphocytic leukemia patients treated with CD19 CAR T cells showed that around 20-30% of patients obtained a complete response (Porter et al., 2015; Turtle et al., 2017).

These CD19 CAR products proved extraordinary successful in patients that were previously running out of treatment options. However, many patients are refractory to treatment or relapse after CAR T cell infusion. Numerous mechanisms are involved in treatment failure. They can be caused by loss of CD19 expression, immune evasion, CAR T cell exhaustion and lack of persistence (Abramson et al., 2019).

Oftentimes, CD19 expression is heterogeneous and patients harbor tumor cell populations that lack CD19 or show only dim expression. Lymphoma cells lacking CD19 go unrecognized by CAR T cells and escape CAR-mediated killing, resulting in the outgrowth of loss variants. In B-ALL, CD19 loss variants are frequently observed in relapse. In DLBCL, 10% of relapse cases are CD19 negative (Abramson et al., 2019). Patients with refractory or relapsed B cell lymphomas are still in dire need for treatment options targeting novel antigens. Novel antigens are either tumor-specific antigens exclusive to neoplastic tissue or tumor-associated antigens,

which are strongly expressed in malignant cells, but not restricted to them. A tumor-associated antigen, CXCR5, which functions as the B cell homing receptor to secondary lymphoid organs, was identified as a promising target for CAR T cell therapy.

4.1 The anti-CXCR5 CAR construct was successfully transduced into human T cells

The anti-CXCR5 CAR binds CXCR5 with the single chain variable fragment (scFv) derived from a monoclonal antibody directed towards human CXCR5. The affinity of the antibody was determined, which resulted in a dissociation constant of around 0.7 nM (Emrich, 1995; Förster et al., 1993). The rat hybridoma RF8B2 variable chains were sequenced by ProMab Biotechnologies. The scFv, excluding the complementary determining regions, was humanized according to IgBlast. GeneArt Gene Synthesis synthesized the single chain variable fragments. In detail, the Lk leader was followed by the V_H chain, the Whitlow linker and the V_L chain. The scFv was cloned into an MP71 vector (Bluhm, 2018). The retroviral MP71 vector, which has an optimized 5' untranslated leader region, shows excellent transgene expression in human primary T cells and provides an ideal tool for gene therapy (Engels et al., 2003; Hildinger et al., 1999). The final second generation CAR construct further includes an $IgG_1\Delta$ spacer that connects the variable fragments to the CD28-derived transmembrane domain. The costimulatory domain, also derived from CD28, is intracellular and followed by the CD3ζ activation domain for signal transduction (Figure 3) (Bluhm, 2018).

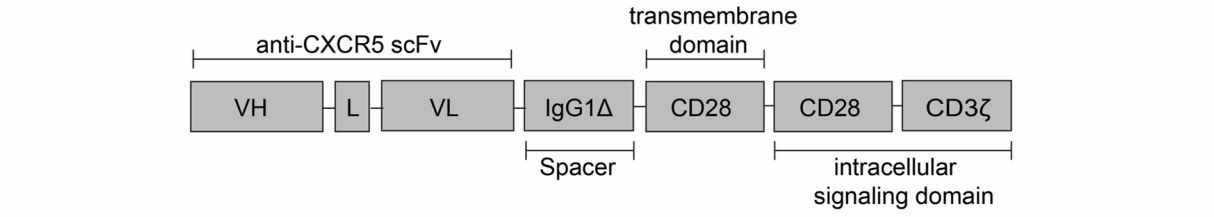

Figure 3: Overview of the anti-CXCR5 CAR construct. The anti-CXCR5 CAR construct is composed of a single chain variable fragment (scFv) of light chain (VL) and heavy chain (VH) connected with a linker (L), an $IgG_1\Delta$ spacer, CD28 transmembrane and costimulatory domains and a CD3ζ activation domain.

The anti-CXCR5, anti-CD19 and anti-SP6 CAR constructs as well as the corresponding virus-producing GalV cells were provided by the group. The construct was successfully transduced into human T cells using γ-retroviral transduction, which stably integrates the transgene in the target genome. GalV cells were used as virus producers. They are a packaging cell line based on HEK-293 with stable production of viral vectors pseudotyped by Gibbon Ape Leukemia Virus-derived envelope proteins. GalV were transduced with the CAR constructs and sorted

for the highest producers, which allowed virus production in large quantities at high titers. Human primary T cells transduced with a chimeric antigen receptor, further called CAR T cells, were identified by flow cytometry after an expansion period of 7 days after transduction or as indicated. Staining was performed with an IgG antibody that binds in the spacer region of the CAR construct (Figure 4A). The transduction rate was determined for every batch of transduced T cells and transduction rates of 50-55% were achieved for the CXCR5, the CD19 and the SP6 construct (Figure 4B). The anti-CD19 CAR T cells were included in most experiments as a reference. The anti-CD19 CAR construct is derived from the murine anti-CD19 mAb FMC63 (Nicholson et al., 1997) and, like the anti-CXCR5 CAR construct, it is a second generation CAR with a CD28 costimulatory domain. The anti-CD19 CAR was ideal for a comparison with the anti-CXCR5 CAR, as the expression profiles of their targeted antigens overlap and many lymphoma entities express both CD19 and CXCR5. Therefore, it was feasible to include the anti-CD19 CAR T cells in both *in vitro* and *in vivo* assays. T cells transduced with the second generation SP6 construct against the not naturally occurring 2,4,6-Trinitrophenyl were included in the assays as a negative control. Additionally, non-transduced T cells (UT) were used as a negative control. CAR T cells were further analyzed for the proportion of $CD4^+$/$CD8^+$ T cell subpopulations. On average, for the CXCR5, the CD19 as well as the SP6 construct, CAR transduced T cells showed a slightly enlarged fraction of $CD8^+$ T cells of around 60%, but the ratio was consistent across constructs and experiments (Figure 4C). As CXCR5 is upregulated on a T cell fraction upon activation (Förster et al., 1994), expansion rates of the CAR were compared in order to determine if the anti-CXCR5 CAR T cells are potentially engaged in fratricide. Viable T cells in the cultures, which were expanded using rhIL7/15 over the course of 10 days after seeding (7 days after transduction), were counted at the end of the expansion period. Each T cell, from the time point of seeding to the end of expansion, multiplied on average 15-27 times, with CXCR5 CAR T cell cultures showing slightly reduced expansion rates (Figure 4D). Nevertheless, it was easily feasible to produce sufficient numbers of CAR T cells for *in vitro* and *in vivo* experiments.

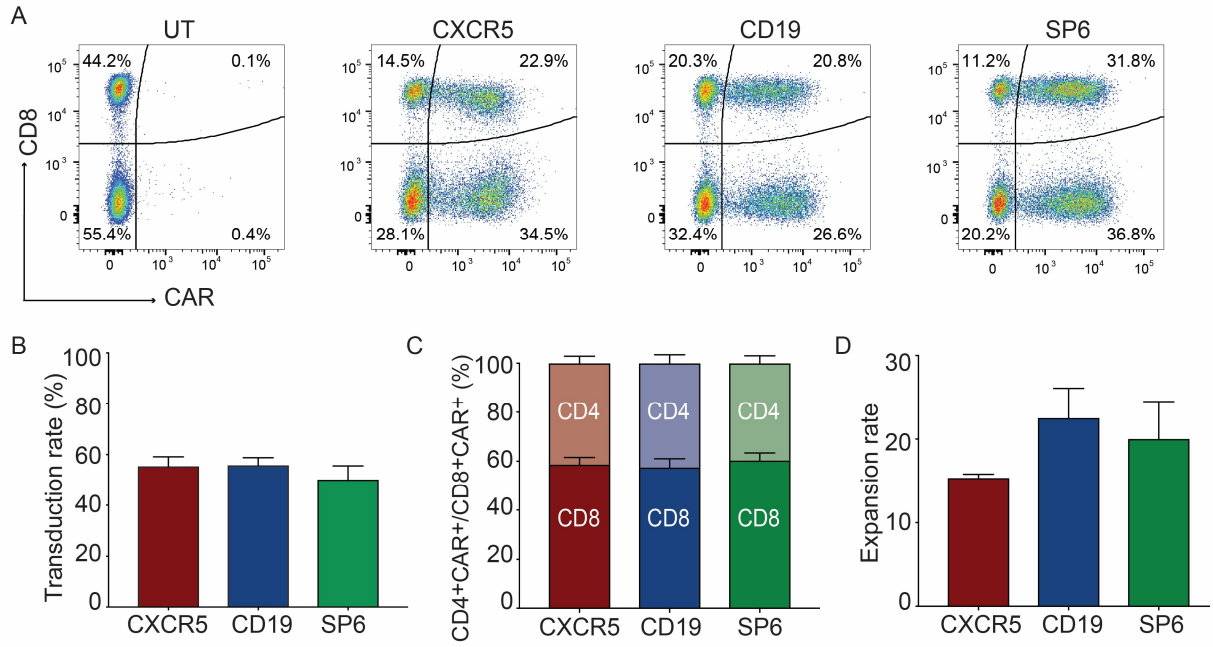

Figure 4: The CXCR5 CAR construct was successfully transduced into human T cells. A Representative flow cytometry plots of non-transduced T cells and CXCR5-, CD19-, and SP6-transduced T cells 7 days after transduction are shown. Cells were gated on singlets. **B** The transduction rates of the CXCR5, CD19 and SP6 CAR constructs transduced into human T cells 7 to 10 days after transduction are shown. Bars represent mean ± SEM of 13 independent experiments (CXCR5 CAR, SP6 CAR) or 8 independent experiments (CD19 CAR). **C** The fractions of $CD4^+$ T cells (defined as $CD8^-$) and $CD8^+$ T cells of positively transduced CAR T cells are shown for human T cells transduced with the CXCR5, CD19 and SP6 CAR constructs 7 to 10 days after transduction. Bars represent mean ± SEM of 13 independent experiments (CXCR5 CAR, SP6 CAR) or 8 independent experiments (CD19 CAR). **D** Expansion rates of CAR T cells expanded using rhIL7/15 for 7 days after transduction are depicted. Bars represent mean ± SEM of 2 independent experiments.

4.2 CXCR5 CAR T cells specifically recognize CXCR5 positive cell lines and PDX cells *in vitro*

4.2.1 CXCR5 is selectively expressed on mature B-NHL cell lines and patient derived xenografts

The expression pattern of CXCR5 on B cell malignancies has been previously described in the literature. CXCR5 was described to be expressed by mature B cell malignancies, such as diffuse large B cell lymphoma, mantle cell lymphoma and follicular lymphoma and to be absent on B cell precursor ALL and multiple myeloma (Dürig et al., 2001; Middle et al., 2015b). In order to verify and expand the expression data, a variety of lymphoma and leukemia cell lines was carefully analyzed for CXCR5 expression on protein level by flow cytometry (Figure 5). This analysis was performed to validate the cell lines as targets for *in vitro* assays, in which the antigen-specific reactivity of the anti-CXCR5 CAR T cells was assessed.

The cell lines were labeled with an anti-CXCR5 monoclonal antibody and, as a control, the corresponding isotype antibody. Cell lines derived from patients that suffered from mature B

non-Hodgkin lymphoma such as diffuse large B cell lymphoma (OCI-Ly7, SU-DHL4), follicular lymphoma (SC-1, DOHH-2), mantle cell lymphoma (JEKO-1) and Burkitt's lymphoma (Raji) were shown to express CXCR5. Cell lines derived from B cell precursor leukemia, such as B acute lymphoblastic leukemia (NALM-6, REH), did not express CXCR5. A cell line that originates from multiple myeloma (NCI-H929), which develops from plasma cells, and Jurkat, a T acute lymphoblastic leukemia cell line were also negative for CXCR5.

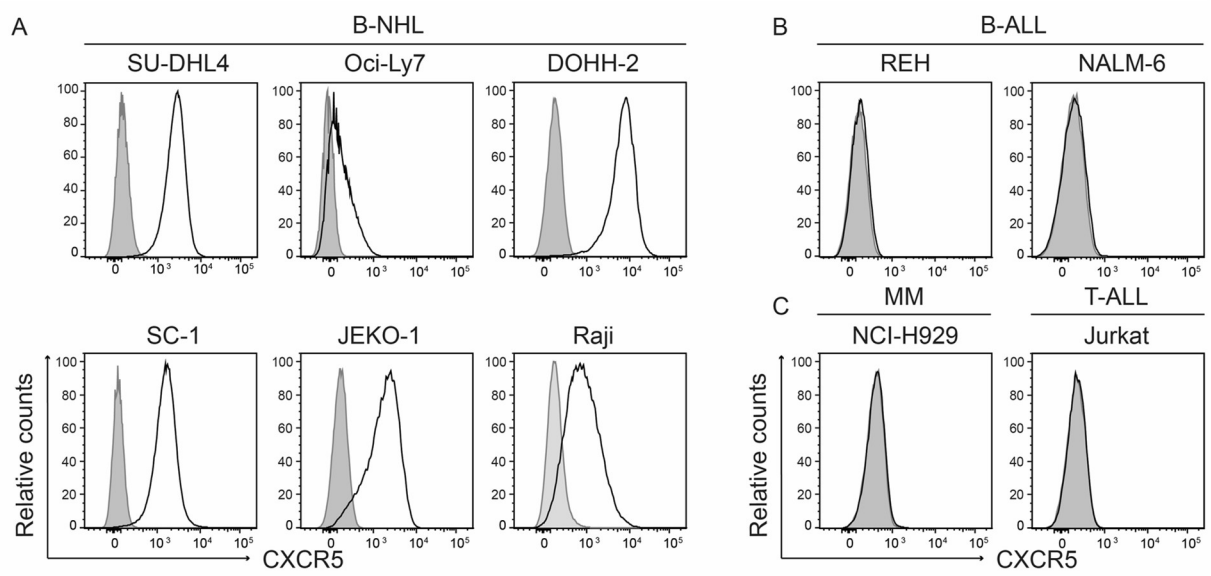

Figure 5: CXCR5 is selectively expressed on mature B lymphoma cell lines. The cell lines were analyzed by flow cytometry after staining with the CXCR5 antibody (black line) or the respective isotype control antibody (grey filled line). Histograms show relative fluorescence intensity of **A** B non-Hodgkin lymphoma (Diffuse large B cell lymphoma (OCI-Ly7, SU-DHL4), follicular lymphoma (SC-1, DOHH-2), mantle cell lymphoma (JEKO-1) and Burkitt's lymphoma (Raji)), **B** B-ALL (REH, NALM-6), **C** MM (NCI-H929) and T-ALL (Jurkat). Representative histograms of at least three independent experiments were selected.

Additionally, Quantibrite beads were applied to analyze the CXCR5 molecule quantity on the cell surface (Figure 6A). In the Quantibrite assay, the cell lines were stained with a PE antibody and measured by flow cytometry, applying the same settings as for the measurement of the Quantibrite PE beads. Subsequently, the number of molecules labeled with the PE antibody could be calculated per cell. The stated values were averaged over at least three independent measurements. DOHH-2 (5146 molecules/cell) had the highest CXCR5 expression. SU-DHL4 (2846 molecules/cell), SC-1 (2602 molecules/cell), JEKO-1 (1667 molecules/cell) and Raji (1287 molecules/cell) showed medium CXCR5 expression. OCI-Ly7 (418 molecules/cell) had the lowest expression level.

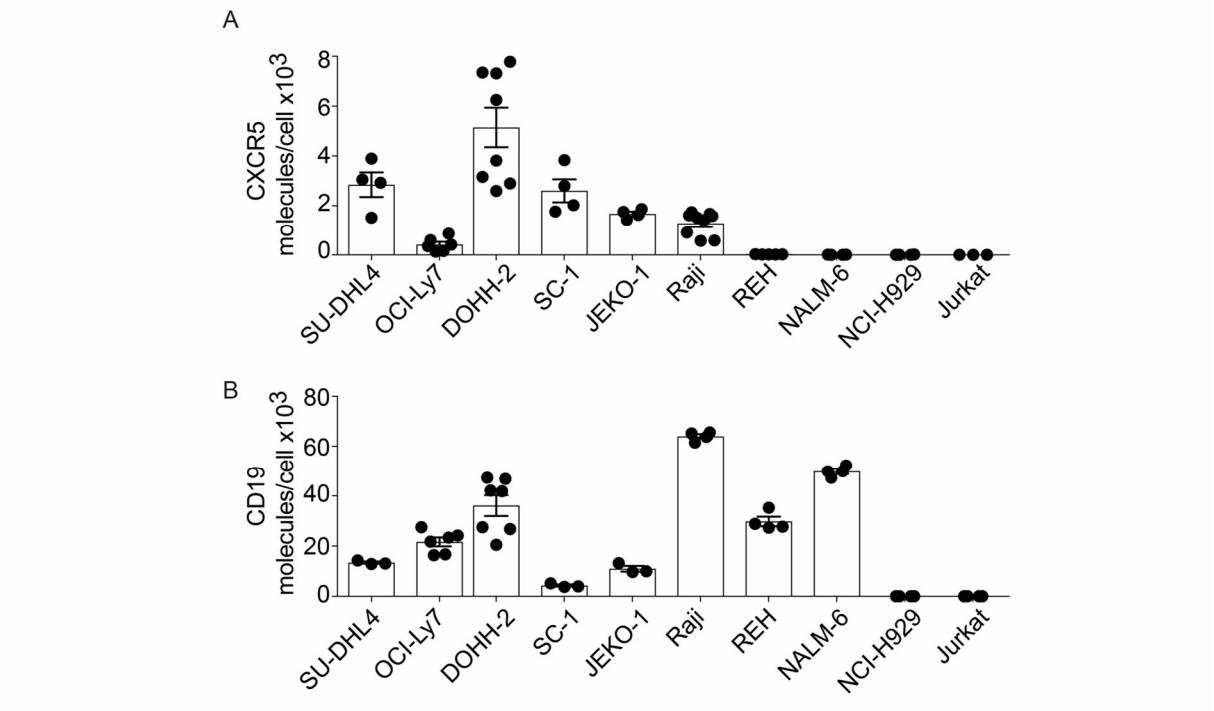

Figure 6: CXCR5 and CD19 were quantified on lymphoma cell lines. Various B-NHL cell lines (SU-HDL4, OCI-Ly7, DOHH-2, SC-1, JEKO-1, Raji), B-ALL (REH, NALM-6), MM (NCI-H929) and T-ALL (Jurkat) were analyzed for surface expression of **A** CXCR5 and **B** CD19 by Quantibrite assay. At least 3 independent measurements were performed; data points represent individual measurements, mean and SEM are shown.

CD19 expression was high on the analyzed lymphoma cell lines (Figure 6B). The highest expression was detected for Raji (64012 molecules/cell) and NALM-6 (49841 molecules/cell), followed by DOHH-2 (36092 molecules/cell), REH (29780 molecules/cell) and OCI-Ly7 (21641 molecules/cell). SU-DHL4 (13392 molecules/cell), JEKO-1 cells (10940 molecules) and SC-1 (4285 molecules/cell) showed the lowest CD19 expression. The multiple myeloma cell line NCI-H929 and the T-ALL cell line Jurkat did not express CD19.

Apart from cell lines, patient derived xenografts (PDX) were analyzed for CXCR5 expression. PDX models are established through xenotransplantation of human primary cancer cells into immunodeficient mice. They provide a tool to study human tumorigenesis *in vivo* (Lai et al., 2017). Two mantle cell lymphoma derived xenografts were analyzed and CXCR5 expression was detected. Quantification using the Quantibrite assay showed that MCL #44685 expressed 726 CXCR5 molecules per cell on average and #96069 had 1109 molecules/cell. CXCR5 quantities on PDX cells were therefore lower than on most analyzed CXCR5$^+$ cell lines, including the mantle cell lymphoma cell line JEKO-1.

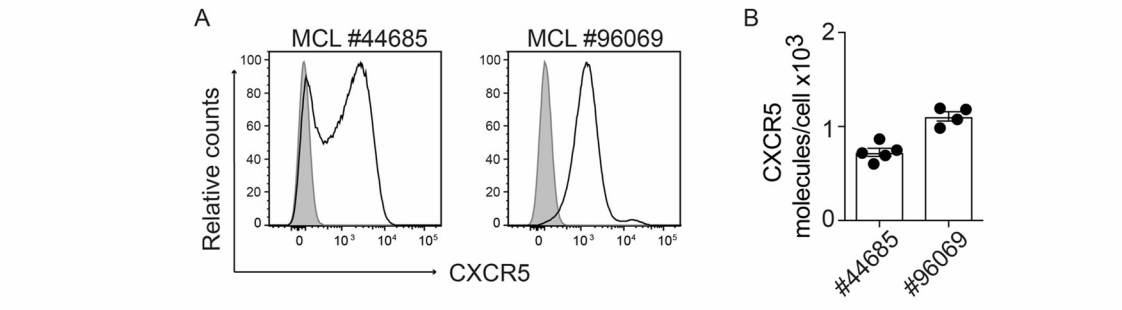

Figure 7: CXCR5 expression was detected on patient-derived MCL xenografts. A MCL PDX #44685 and #96069 were analyzed by flow cytometry after staining with the CXCR5 antibody (black line) or the respective isotype control antibody (grey filled line). Histograms show relative fluorescence intensity. Representative histograms of at least three independent experiments were selected. **B** Surface CXCR5 expression was quantified using the Quantibrite beads. At least 4 independent measurements were performed; data points represent individual measurements, mean and SEM are shown.

Altogether, CXCR5 was present on mature B-NHL cell lines and absent on precursor B/T cell leukemia cell lines and multiple myeloma. Thus, CXCR5 was exclusively detected on cell lines derived from lymphoma that originated from mature B cells. The anti-CXCR5 CAR T cells are expected to react in response to the CXCR5 expressing B-NHL cell lines and patient derived xenografts.

4.2.2 Effector cytokines are released upon incubation of CXCR5 CAR T cells with CXCR5 positive cell lines and patient derived xenografts

Human primary T cells were successfully equipped with the anti-CXCR5 chimeric antigen receptor and expanded over 13 days in the presence of rhIL2, with a three-day low IL2 phase at the end of culture. CAR T cell effector function was analyzed *in vitro* by 24 h coculture with numerous B-NHL cell lines (SU-HDL4, OCI-Ly7, DOHH-2, JEKO-1, Raji), which were confirmed to be $CXCR5^+$ by flow cytometry, and B-ALL (REH, NALM-6), MM (NCI-H929) and T-ALL (Jurkat) cell lines, which lacked CXCR5 expression (Figure 8A). The CAR T cells were incubated at a 1:1 ration with the target cells ($5x10^4$ each per well in a 96-well plate). The readout for effector function was IFNγ release by the CAR T cells, which was quantified in the supernatant by ELISA. The assay was validated with a minimum value (MIN) and a maximum value (MAX). For the minimum value, CAR T cells were incubated without target cells. For the maximum value, the CAR T cells were stimulated with PMA/ionomycin to induce IFNγ release. The effector function of CXCR5 CAR T cells was compared with CD19 CAR T cells; non-transduced cells and SP6 CAR T cells served as negative controls.

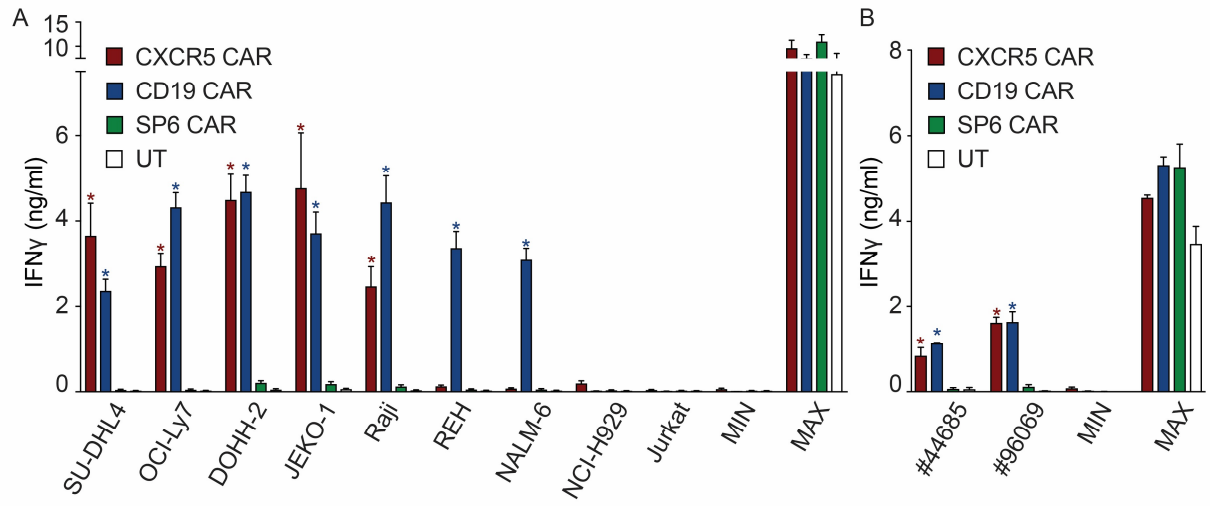

Figure 8: CXCR5 CAR T cells show *in vitro* reactivity against B-NHL cell lines and xenografts. A IFNγ release of CAR T cells or non-transduced cells (UT) upon 24 h incubation with various cell lines of lymphoid origin was quantified by ELISA. Bars represent mean ± SEM of 7 independent donors (CXCR5 CAR, SP6 CAR, UT) or 4 independent donors (CD19 CAR). **B** IFNγ release of CAR T cells or non-transduced cells (UT) upon 24 h incubation with patient-derived mantle cell lymphoma xenografts was quantified by ELISA. Bars represent mean ± SEM of 4 independent donors (CXCR5 CAR, SP6 CAR, UT) or 3 independent donors (CD19 CAR). P-values (*P<0.01) were calculated using an unpaired T test comparing CXCR5-CAR transduced T cells (red) or CD19-CAR transduced T cells (blue) with SP6-CAR transduced T cells. Data was collected in collaboration with Dr. Mario Bunse.

The CXCR5 CAR T cells were shown to be exclusively reactive towards the CXCR5 expressing B-NHL cell lines DOHH-2, OCI-Ly7, SU-DHL4 and JEKO-1 and released IFNγ quantities similar to the CD19 CAR T cells, which was especially remarkable considering the lower antigen density of CXCR5 compared with CD19 on the cell lines. They did not release IFNγ when cocultured with CXCR5 negative cell lines.

IFNγ release for the CD19 positive B cell precursor leukemia cell lines REH and NALM-6 was only detected for the CD19 CAR T cells. NCI-H929 and Jurkat, which are neither CXCR5 nor CD19 positive, were not recognized. For OCI-Ly7, the cell line with the lowest antigen expression, the IFNγ release correlated and showed the lowest amount. Effector function in response to patient-derived mantle cell lymphoma xenografts was evaluated correspondingly (Figure 8B). For both #44685 and #96069, IFNγ release could be detected for the anti-CXCR5 and anti-CD19 CAR T cells. In short, the CXCR5 CAR T cells reacted selectively towards antigen expressing cell lines and patient-derived xenografts, releasing IFNγ levels comparable to the CD19 CAR T cells.

4.3 CXCR5 shows a selective expression profile in the human body

Toxicities in CAR T cell therapy can occur if healthy tissues express the targeted antigen. On-target/off-tumor effects can cause severe organ damage and result in the patient's death. In preclinical CAR development, this issue can be addressed by extensive investigation of antigen expression throughout human tissues (Brudno and Kochenderfer, 2016). Anti-CXCR5 CAR T cells showed effector function in response to incubation with $CXCR5^+$ lymphoma cell lines. If a patient was administered anti-CXCR5 CAR T cells, they would presumably target CXCR5 expressing cells all over the body. Therefore, CXCR5 expression on healthy human tissue had to be carefully investigated.

4.3.1 CXCR5 is selectively expressed in the hematopoietic compartment

CXCR5 expression on lymphoid cells was first described in 1994 by Förster et al. Mature B cells and small fractions of $CD4^+$ and $CD8^+$ T cells were shown to express CXCR5 (Förster et al., 1994). Blood cells are the first cells to be encountered by CAR T cells upon infusion; thus, knowledge about CXCR5 expression in hematopoietic cells allows risk assessment.

In this thesis, in-depth analysis of CXCR5 expression in the hematopoietic compartment of the peripheral blood, both on cells of lymphoid and myeloid origin, was performed.

Peripheral blood from healthy donors was freshly prepared to analyze the expression of CXCR5 on untouched cells of the hematopoietic compartment. In the lymphoid lineage, $CD4^+$ T cells, in particular $CD4^{high}CXCR5^+PD\text{-}1^+CD25^-$ T_{FH} cells, $CD8^+$ T cells and $CD56^+$ NK cells were analyzed by means of flow cytometry (Figure 9). The cells were gated on single cells, lymphocytes and live cells. After gating on $CD8^+$, $CD4^{high}$ (Figure 9A), $CD56^+$ or $CD19^+$ (Figure 9B), the subset of $CXCR5^+$ cells was quantified. On average among the three donors, 12% of $CD4^{high}$ T cells, 3.2% of $CD8^+$ T cells and 97% of $CD19^+$ B cells were CXCR5 positive. $CD56^+$ NK cells were CXCR5 negative (Figure 9B). The mean CXCR5 expression on lymphoid cells was quantified by Quantibrite assay as previously described. B cells showed the highest CXCR5 expression with a mean of 8544 molecules/cell. The $CD8^+$ T cells had the lowest CXCR5 expression with 992 molecules/cell. $CD4^{high}$ T cells had on average 1860 CXCR5 molecules on their surface and T_{FH} cells, defined as $CD4^{high}CXCR5^+PD\text{-}1^+CD25^-$, expressed 1890 molecules/cell (Figure 9C).

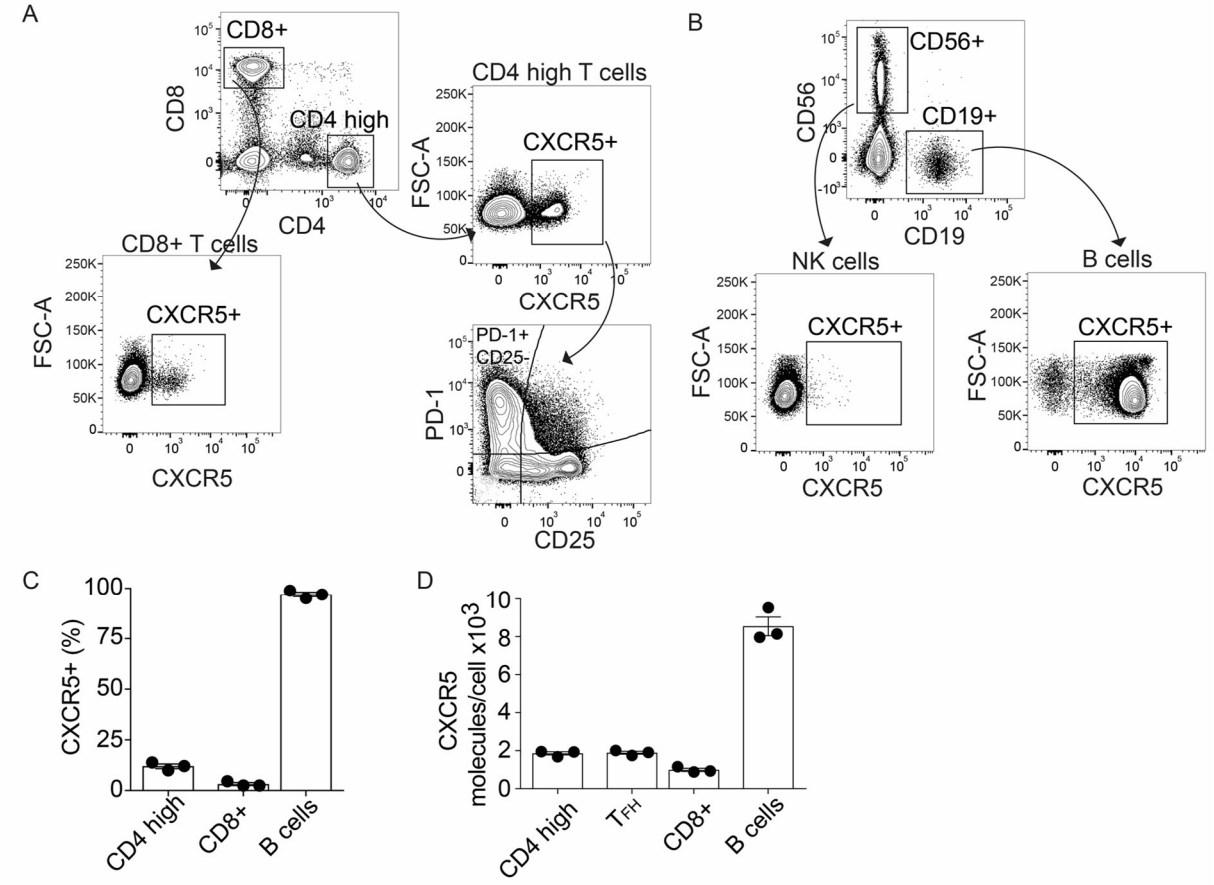

Figure 9: CXCR5 is expressed on subsets of peripheral blood lymphoid cells. The cells were gated on singlets, lymphocytes and live cells by 7AAD$^+$ exclusion. The cells were further gated on **A** CD8$^+$ or CD4^{high}. CD4^{high} cells were additionally analyzed for their PD-1 and CD25 expression. **B** CD56$^+$ or CD19$^+$. CXCR5 expression was analyzed on these subsets. **C** The fraction of CXCR5$^+$ cells is shown for CD4^{high}, CD8$^+$ and CD19$^+$ B cells. **D** CXCR5 molecules per cell were quantified using the Quantibrite assay. Molecules/cell were quantified for CXCR5$^+$CD4^{high} cells, T_{FH} cells (CD4^{high}CXCR5$^+$PD-1$^+$CD25$^-$), CD8$^+$ cells and CD19$^+$ B cells. Data points represent individual measurements, mean and SEM are shown (n=3).

Apart from cells of the lymphoid lineage, myeloid cells were analyzed. Monocytes (CD14$^+$CD11c$^+$HLA-DR$^+$) and dendritic cells (CD11c$^+$HLA-DR$^+$), in more detail CD303$^+$ plasmacytoid dendritic cells (pDC) and CD1c$^+$ myeloid dendritic cells (mDC1) were analyzed for their CXCR5 expression by flow cytometry (Figure 10A). After gating on single cells, lymphocytes and live cells, the subset of CXCR5$^+$ cells of monocytes and dendritic cells was quantified (Figure 10B). CXCR5 was virtually absent on these myeloid cells, with a mean frequency of less than 0.7%.

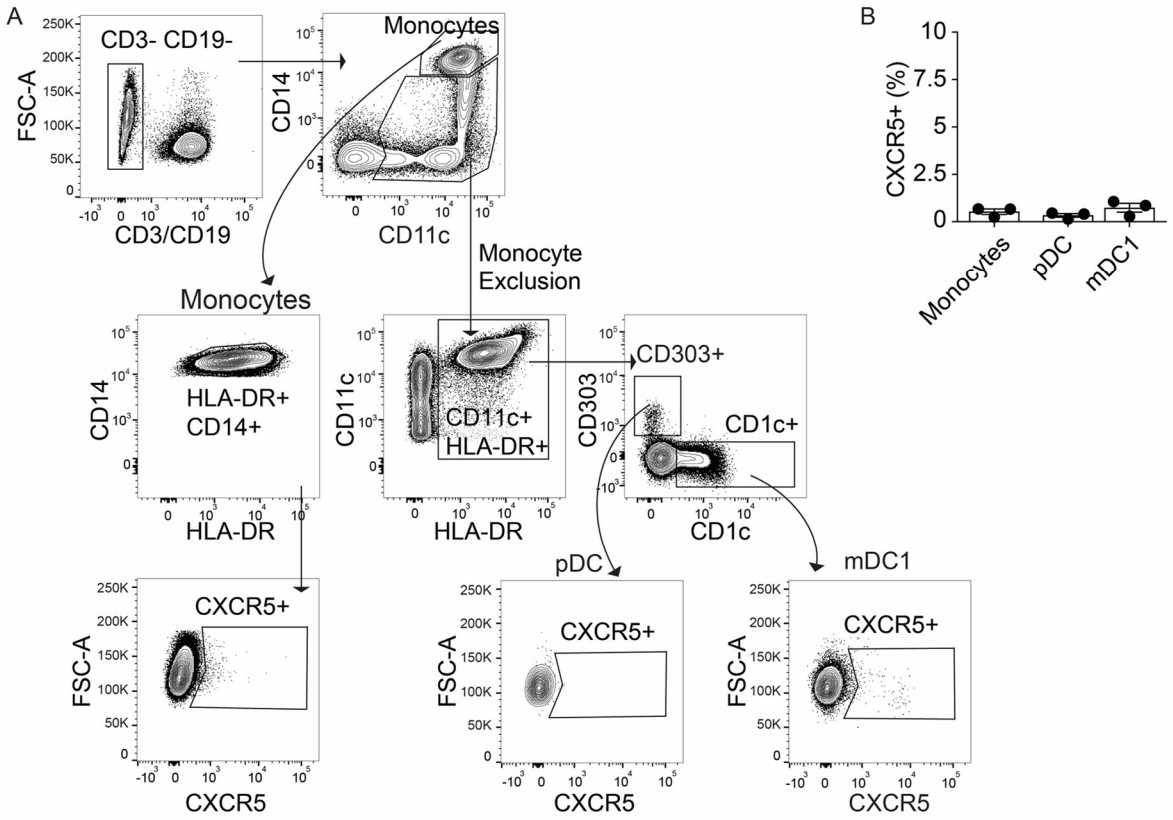

Figure 10: CXCR5 is virtually absent on peripheral blood myeloid cells. A The cells were previously gated on singlets, lymphocytes and live cells by 7AAD$^+$ exclusion. The cells were further gated on CD14$^+$CD11c$^+$HLA-DR$^+$ monocytes and CD11c$^+$HLA-DR$^+$ dendritic cells, additionally defined by CD303$^+$ plasmacytoid DCs (pDC) and CD1c$^+$ myeloid DCs (mDC1). **B** The fraction of CXCR5$^+$ cells is shown for monocytes, plasmacytoid dendritic cells (pDC) and myeloid dendritic cells (mDC) gated applying the scheme from A. Data points represent individual measurements, mean and SEM are shown (n=3).

4.3.2 CXCR5 CAR T cells react towards benign B cells *in vitro*

Commonly, malignant lymphocytes express or overexpress the chemokine receptors expressed by their benign counterparts (López-Giral et al., 2004). As shown by flow cytometry, CXCR5 is highly expressed on mature B cells in the peripheral blood of healthy donors. Recognition of mature B cells by anti-CXCR5 CAR T cells would induce removal of B cells in patients. This condition, which is called B cell aplasia, is a frequent side effect observed in the treatment with anti-CD19 CAR T cells, but can be clinically managed (Bhoj et al., 2016). Therefore, in order to assess whether anti-CXCR5 CAR T cells react towards benign B cells, coculture experiments were performed.

B cells from peripheral blood of a healthy donor were incubated with CAR T cells in a 24 h coculture assay at a 1:1 ratio (Figure 11A). The anti-CXCR5 CAR T cells released IFNγ in response to these benign B cells. Additionally, anti-CXCR5 CAR T cells were able to kill mature B cells of a healthy donor in a 72 h coculture (Figure 11B). The removal of B cells in this coincubation experiment was confirmed in flow cytometry and, for clearer visualization, normalized to the percentage of B cells in the samples incubated with non-transduced T cells.

These results illustrate that anti-CXCR5 CAR T cells show *in vitro* reactivity towards benign CXCR5$^+$ mature B cells.

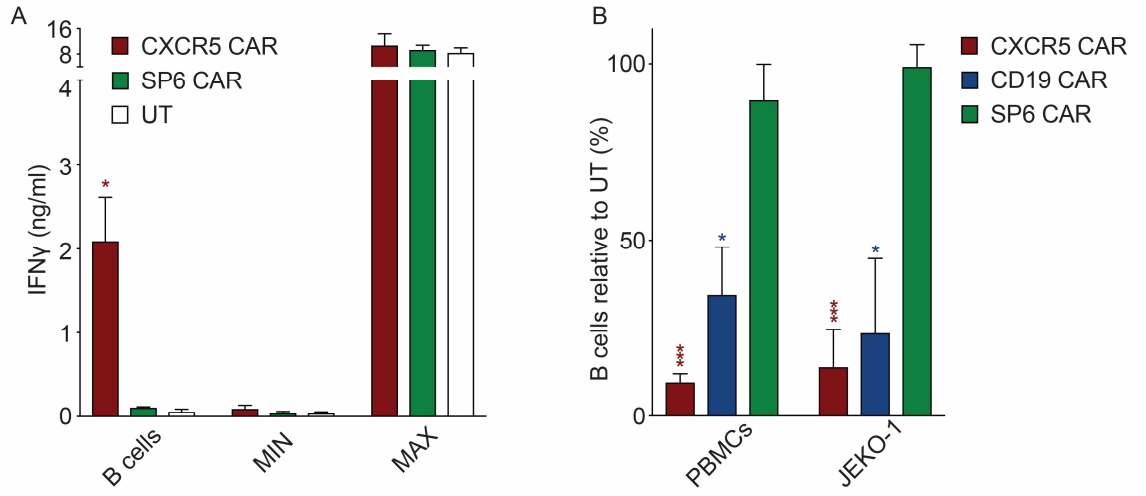

Figure 11: CXCR5 CAR T cells show *in vitro* reactivity towards benign mature B cells. A IFNγ release of CAR T cells or non-transduced cells (UT) upon 24 h incubation with B cells isolated from the blood of a healthy donor was quantified by ELISA. Bars represent mean ± SEM of 3 independent donors. **B** Cocultures of PBMCs isolated from the blood of a healthy donor at 1:1 ratio with CXCR5, CD19 and SP6 CAR T cells and non-transduced cells were analyzed by flow cytometry. Cells were gated on single cells and 7-AAD$^-$. Percentages shown are B cell fractions (CD3$^-$CXCR5$^+$) relative to non-transduced (UT) cells. Bars represent mean ± SEM of 4 independent donors (CXCR5 CAR, SP6 CAR, UT) or 3 independent donors (CD19 CAR). P-values (*P<0.05, **P<0.01, ***P<0.001) were calculated using an unpaired T test comparing CXCR5-CAR transduced T cells (red) or CD19-CAR transduced T cells (blue) with SP6-CAR transduced T cells.

4.3.3 CXCR5 is selectively expressed in human tissue

CXCR5 is expressed on cells of the hematopoietic compartment; however, its expression in unrelated human tissue had to be carefully examined in order to exclude on-target/off-tumor toxicity of CXCR5 CAR T cell treatment. The HMRT103 TissueScan Human Normal cDNA Array was applied to screen for *Cxcr5* RNA expression in numerous human tissues (Figure 12). Apart from the *Gapdh* PCR that served as a cDNA quantity control, the *Cd19* PCR was performed to detect *Cd19* expressing B cells in the tissue samples.

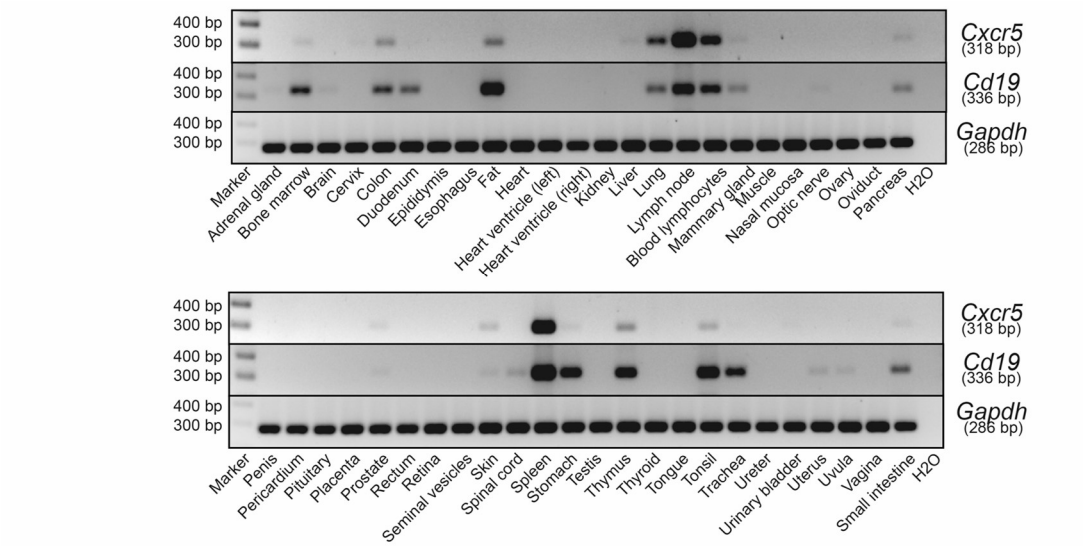

Figure 12: *Cxcr5* tissue expression was analyzed by a cDNA library PCR. *Cxcr5* PCR was performed on the HMRT103 TissueScan Human Normal cDNA Array to screen for *Cxcr5* tissue expression. Additionally, a *Cd19* PCR and a *Gapdh* PCR were performed as controls. A marker was applied to confirm the correctness of the fragments at 318, 336 and 286 base pairs.

The majority of tissues were *Cxcr5* negative. *Cxcr5* was coexpressed with *Cd19* in lymphoid tissue (bone marrow, lymph node, blood lymphocytes, spleen, thymus, tonsil), indicating the presence of mature B cells. Some non-lymphoid tissue (colon, fat, lung, mammary gland, pancreas, prostate, skin, stomach, small intestine) showed *Cxcr5*, but also *Cd19* expression. Most likely, these tissues harbored lymphocytic infiltrates, which contained $CD19^{+}CXCR5^{+}$ mature B cells. *Cd19* expression independent from *Cxcr5* expression was detected in some tissues (e.g. duodenum, stomach and trachea), indicating the presence of $Cd19^{+}Cxcr5^{-}$ plasmablasts (Llinàs et al., 2011). *Cxcr5* expression was selectively detected in tissues with *Cd19* expression in lymphoid and non-lymphoid organs, but not on other, unrelated tissues. Minor bands for CXCR5 expression were detected for liver, cervix and urinary bladder; primary cells of these tissues were therefore subsequently analyzed for protein expression. Summing up the tissue distribution of *Cxcr5*, *Cxcr5* mRNA expression was highly selective in non-lymphoid tissue and almost always coincided with *Cd19* expression. Making the presumable assumption that anti-

CXCR5 CAR T cells spare these *Cxcr5* negative tissues, the *Cxcr5* mRNA expression data largely excluded potential safety risks for a large number of tissues.

4.3.4 CXCR5 is absent on non-hematopoietic primary cells and cell lines

The CXCR5 expression on numerous primary cells (Figure 13A) and cell lines (Figure 13B) of non-hematopoietic origin was analyzed by flow cytometry. HUVEC (Human Umbilical Vein Endothelial Cell) and HUAEC (Human Umbilical Artery Endothelial Cell) are vascular primary cells in immediate proximity of CAR T cells upon infusion. Thus, CXCR5 negativity had to be ensured in order to being able to safely administer anti-CXCR5 CAR T cells to patients. Human Cervical Epithelial Cells (HCerEpiC), Human Urothelial Cells (HUC) and the hepatocellular carcinoma cell line HepG2 were further investigated as low *Cxcr5* mRNA levels were detected for liver, cervix and urinary bladder in the HMRT103 TissueScan Human Normal cDNA Array. Human Perineurial Cells (HPNC), Human Astrocytes (HA) and Human Neurons (HN) were analyzed in order to exclude potential neurotoxic events due to CXCR5 expression on tissues of the nervous system. Additionally, the CXCR5 expression on the gastro-intestinal primary cells HCoEpiC (Human Colonic Epithelial Cells) and cell line SW620 (colorectal carcinoma), and HEK-293 (Human Embryonic Kidney) was measured. The adherent cells were gently dissociated using Accutase and subsequently labeled with the CXCR5 antibody or the isotype control antibody, dead cells were excluded by 7AAD positivity. All primary cells and cancer cell lines were shown to be CXCR5 negative.

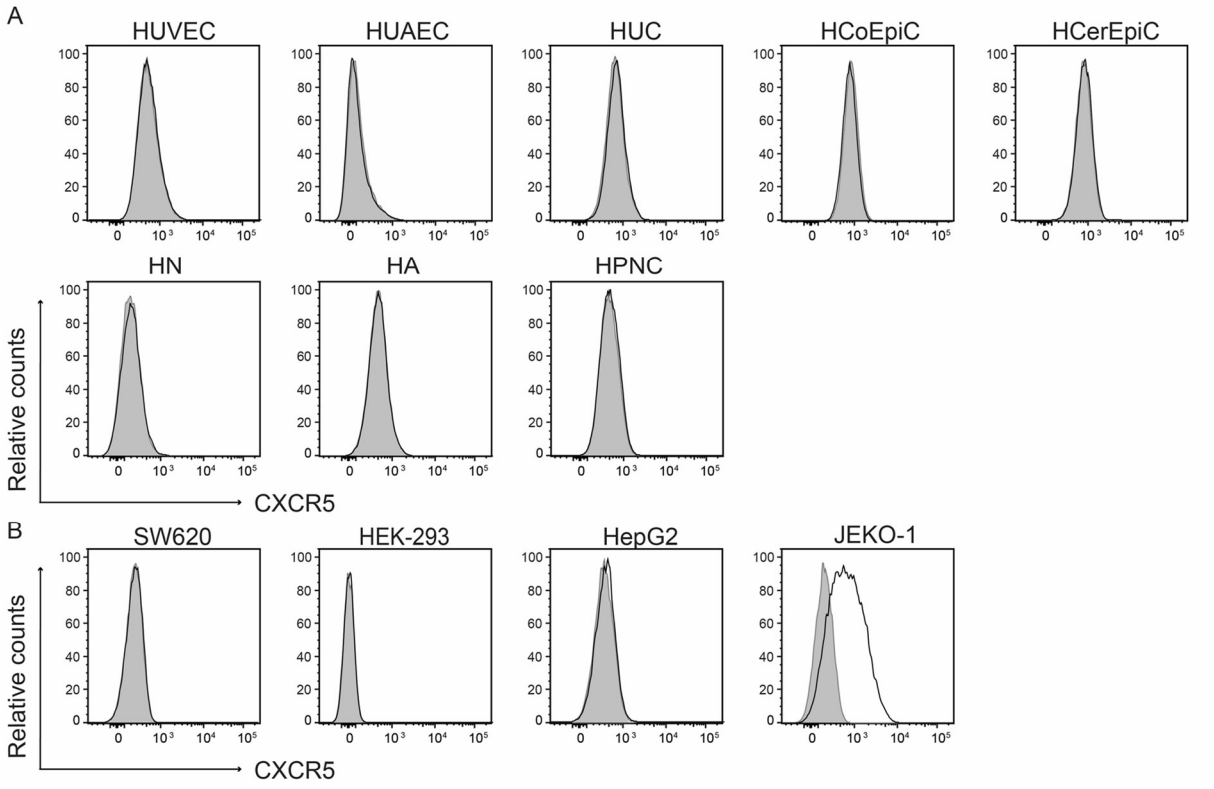

Figure 13: CXCR5 is absent on unrelated primary cells and cell lines. Primary cells and cell lines were analyzed by flow cytometry after labeling with the CXCR5 antibody (black line) or the isotype control antibody (grey filled line). Representative histograms of at least three independent experiments were selected. **A** CXCR5 expression was plotted for the human primary cells HUVEC (Human Umbilical Vein Endothelial Cell), HUAEC (Human Umbilical Artery Endothelial Cell), Human Urothelial Cells (HUC), Human Colonic Epithelial Cells (HCoEpiC), Human Cervical Epithelial Cells (HCerEpiC), HN (Human Neurons), HA (Human Astrocytes) and HPNC (Human Perineurial Cells). **B** CXCR5 expression was plotted for the human gastro-intestinal cancer cell lines HepG2 (hepatocellular carcinoma), SW620 (colorectal carcinoma) and HEK-293 (Human Embryonic Kidney). JEKO-1 lymphoma cells are shown as positive control. Data was collected in collaboration with Dr. Mario Bunse.

4.3.5 CXCR5 is absent on non-hematopoietic primary cells under inflammatory conditions

Jiang et al. published that murine astrocytes expressed CXCR5 in a neuropathic pain model. The authors utilized a spinal nerve ligation model, in which they found upregulation of CXCL13 in inflamed neurons and induction of CXCR5 on activated murine astrocytes (Jiang et al., 2016) Therefore, it was necessary to further exclude possible anti-CXCR5 CAR-mediated on-target/off-tumor effects under inflammatory conditions. Primary vascular cells (HUVEC and HUAEC), primary perineurial cells (HPNC) and astrocytes (HA) were incubated with 25 ng/ml IFNγ for 24 h to induce an inflammatory status. Subsequently, they were gently dissociated using Accutase and labeled. 7AAD was used to exclude dead cells. The inflammatory status was confirmed by MHC I upregulation (Figure 14A). FACS analysis confirmed that CXCR5 was not upregulated upon IFNγ stimulation in the primary cells (Figure 14B).

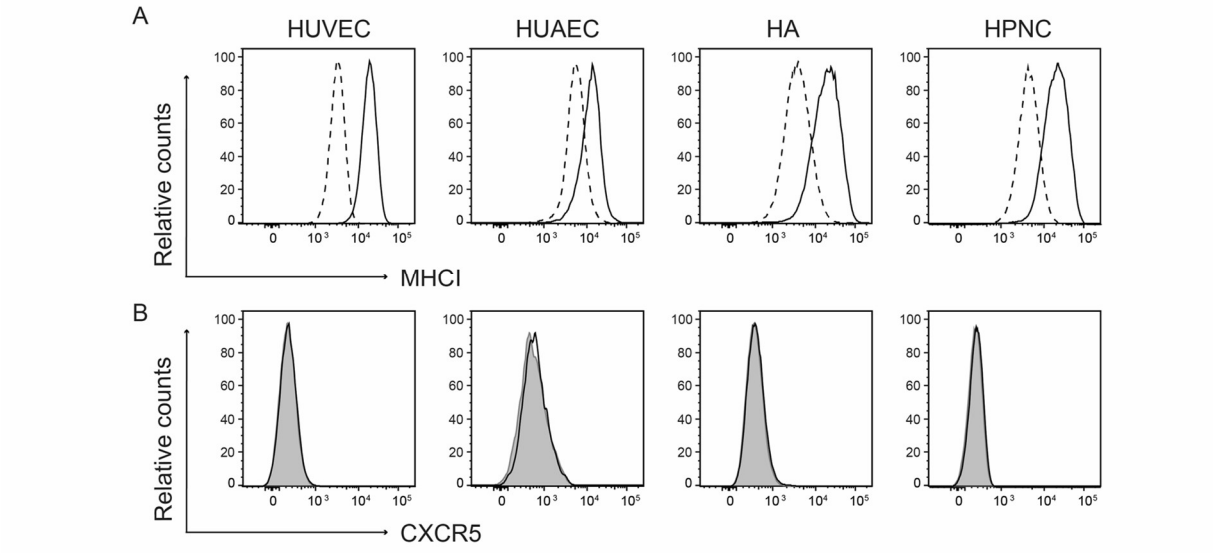

Figure 14: Primary cells do not express CXCR5 under inflammatory conditions. HUVEC (Human Umbilical Vein Endothelial Cell), HUAEC (Human Umbilical Artery Endothelial Cell), HPNC (Human Perineurial Cells) and HA (Human Astrocytes) were incubated with 25 ng/ml IFNγ for 24 h and further analyzed by flow cytometry (n=2). **A** The staining of the MHC I antibody is shown. The continuous line represents cells incubated with 25 ng/ml IFNγ for 24 h, the dotted line represents untreated cells. **B** The black line represents staining with the CXCR5 antibody, the grey filled line shows the staining with the isotype control antibody. Data was collected in collaboration with Dr. Mario Bunse.

4.4 CXCR5 CAR T cells do not recognize CXCR5 negative cells *in vitro* and *in vivo*

The expression profile of CXCR5 on mRNA level was investigated for a plethora of tissues. Additionally, extensive expression analysis by flow cytometry was performed for human primary cells and cell lines in order to exclude CXCR5 expression on non-hematopoietic tissues on protein level. However, most importantly, it had to be confirmed that anti-CXCR5 CAR T cells do not react towards these unrelated cells upon direct contact. Experiments were performed to cover on-target/off-tumor as well as off-tumor/off-target effects. On-target/off-tumor effects occur upon CXCR5 expression by unrelated tissues, off-tumor/off-target effects describe unspecific reactions of CAR T cells against CXCR5 negative benign tissues.

4.4.1 Effector cytokines are not released upon incubation of CXCR5 CAR T cells with CXCR5 negative primary cells and cell lines

Cocultures were performed with anti-CXCR5 CAR T cells as effector cells and various human primary cells (HUVEC, HUAEC, HPNC, HA, HUC, HCerEpiC and HCoEpiC) and gastro-intestinal cancer cell lines (HepG2, SW620 and HEK-293) as targets (Figure 15). Effector and target cells were cocultured at a 1:1 ratio ($5x10^4$ cells per well each, in a 96-well plate). The target cells were seeded one day prior, upon gentle Accutase dissociation, to allow adherence. After a 24 h incubation period, IFNγ in the supernatant was quantified by ELISA. The CXCR5 CAR T cells did not release IFNγ in response to incubation with CXCR5 negative primary cells and cell lines, showing that they did not recognize their epitope. Thus, the absence of CXCR5 on these cells, as shown by flow cytometry, could be confirmed. Also, this indicates that the CXCR5 CAR T cells do not react to other, undefined structures on the target cells. To validate the assay, CXCR5 CAR T cell functionality was confirmed using JEKO-1 cells as a positive control.

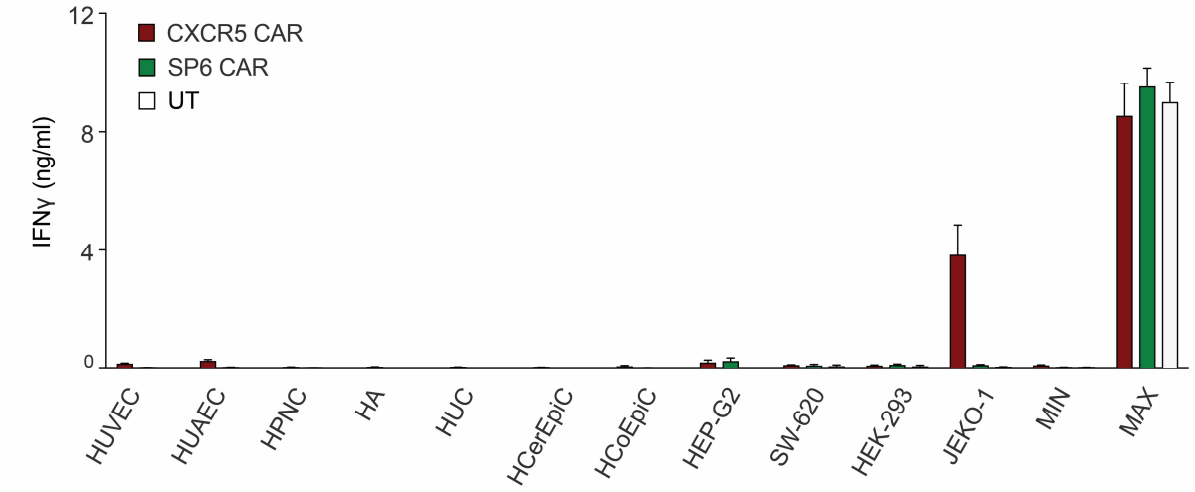

Figure 15: CXCR5 CAR T cells do not show *in vitro* reactivity against CXCR5 negative primary cells and cell lines. IFNγ release of CAR T cells or non-transduced cells (UT) upon 24 h incubation with the human primary cells HUVEC (Human Umbilical Vein Endothelial Cell), HUAEC (Human Umbilical Artery Endothelial Cell), Human Urothelial Cells (HUC), Human Colonic Epithelial Cells (HCoEpiC), Human Cervical Epithelial Cells (HCerEpiC), HN (Human Neurons), HA (Human Astrocytes), HPNC (Human Perineurial Cells) and the human gastro-intestinal cancer cell lines HepG2 (hepatocellular carcinoma), SW620 (colorectal carcinoma) and HEK-293 (Human Embryonic Kidney) was quantified by ELISA. JEKO-1 CXCR5$^+$ lymphoma cells served as a positive control. Bars represent mean ± SEM of 7 independent donors. Data was collected in collaboration with Dr. Mario Bunse.

4.4.2 Effector cytokines are not released upon incubation of CXCR5 CAR T cells with CXCR5 negative primary cells under inflammatory conditions

As demonstrated by flow cytometry, primary vascular (HUVEC) and perineurial (HPNC) cells, as well as primary astrocytes (HA) did not upregulate CXCR5 expression upon induction of an inflammatory status by IFNγ incubation. Additionally, it was investigated whether CXCR5 CAR T cells showed *in vitro* reactivity against these inflamed cells. HUVEC, HPNC and HA were first stimulated for 24 h with 25 ng/ml IFNγ to induce inflammation. After washing, they were coincubated with CAR T cells for 24 h at a 1:1 ratio. CXCR5$^+$ JEKO-1 cells were included in the coculture as a positive control for CXCR5 CAR T cell activity; CXCR5$^-$ Jurkat cells served as a negative control. IFNγ in the supernatant was quantified by ELISA (Figure 16). The CXCR5 CAR T cells did not release IFNγ in response to untreated or IFNγ-treated (+) target cells, indicating that CXCR5 expression was not induced upon inflammation in the analyzed primary cells.

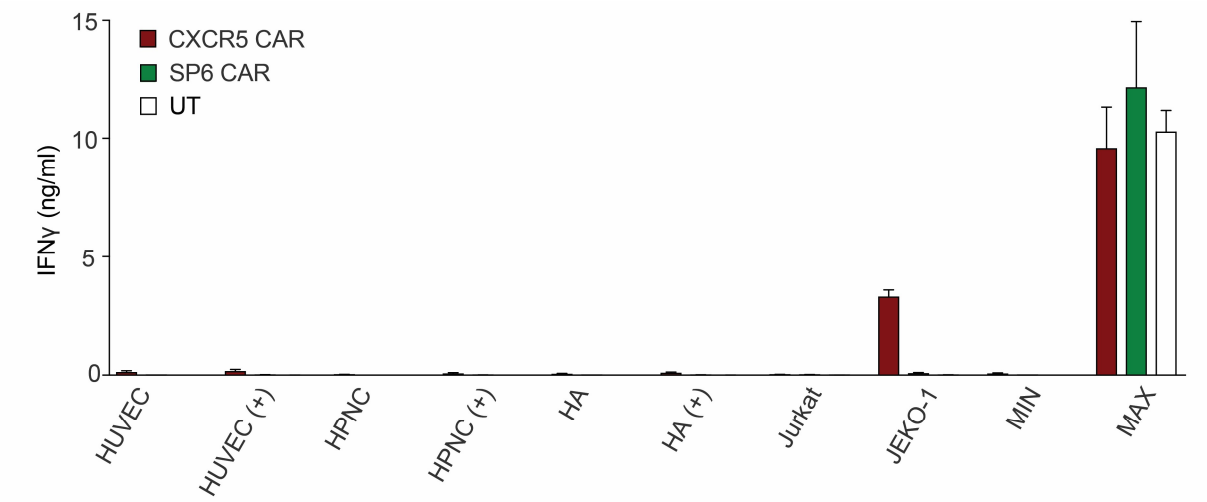

Figure 16: CXCR5 CAR T cells do not show *in vitro* reactivity against CXCR5 negative primary cells under inflammatory conditions. HUVEC (Human Umbilical Vein Endothelial Cell), HPNC (Human Perineurial Cells) and HA (Human Astrocytes) were incubated with 25 ng/ml IFNγ for 24 h to induce an inflammatory status. Subsequently CAR T cells or non-transduced cells (UT) were coincubated with the non-stimulated or stimulated (+) primary cells and IFNγ in the supernatant was quantified by ELISA. Jurkat CXCR5$^-$ cells served as a negative control. JEKO-1 CXCR5$^+$ lymphoma cells served as a positive control. Bars represent mean ± SEM of 7 independent experiments. Data was collected in collaboration with Dr. Mario Bunse.

4.4.3 CXCR5 CAR T cells do not show off-target reactivity *in vivo*

In cocultures with CXCR5$^-$ non-hematopoietic primary cells and cell lines, it was demonstrated that anti-CXCR5 CAR T cells do not react towards unrelated structures on the target cells in a nonspecific manner *in vitro*. Subsequently, it was investigated whether anti-CXCR5 CAR T cells recognize unrelated epitopes *in vivo*. For this purpose, immunodeficient NOD.Cg-Prkdc^{scid} Il2rg^{tm1Wjl}/SzJ (NSG) mice were injected with CXCR5 CAR T cells ($1x10^6$ or $1x10^7$ T cells per mouse). Immunodeficient mice were used to avoid reactions of the murine immune system against the human T cells. After one and three days, serum parameters were analyzed in peripheral blood collected by retroorbital puncture. It was shown that the liver markers alanine transaminase (ALT) and aspartate transaminase (AST) were not elevated compared with naive mice, indicating that liver tissue was not harmed by the CXCR5 CAR T cells. AST upregulation is additionally associated with damage of cardiac and skeletal muscle, which could also be excluded. Creatinine, a marker of renal function, was comparable between the groups. General tissue damage could be excluded as lactate dehydrogenase (LDH) values were not increased in the treated mice. Altogether, the CAR T cells did not cause an increase in serum markers associated with tissue damage (Figure 17A). Paraffin embedded tissue sections of lung, liver and colon, which were stained with hematoxylin and eosin, were screened for lymphoid infiltrates caused by CAR T cells attacking the tissues, but such infiltrates were absent and there were no differences visible between the treated and naive mice (Figure 17B). Thus, CXCR5 CAR T cells did not show off-target reactivity *in vivo* by reacting towards unrelated epitopes in the NSG mouse model.

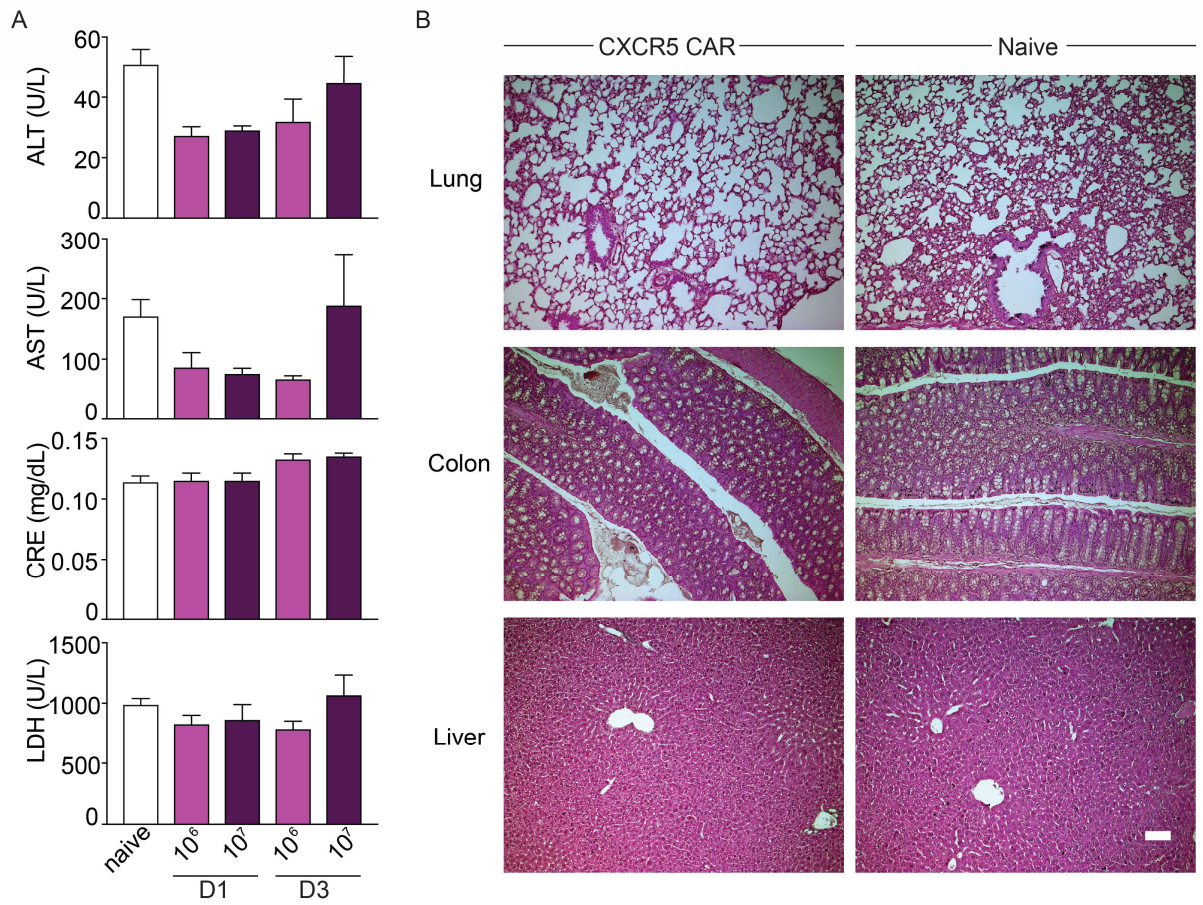

Figure 17: CXCR5 CAR T cells do not show off-target reactivity *in vivo*. A Representative hematoxylin and eosin stainings show lung, colon and liver sections of CXCR5 CAR T cell injected mice and naive mice three days after injection. **B** Markers for liver damage (ALT, AST), kidney damage (CRE) and general organ damage (LDH) were analyzed in the serum of naive mice and mice injected with CXCR5 CAR T cells (1x10^6 or 1x10^7 T cells) one or three days after injection (n=3-8).

4.5 CXCR5 CAR T cells recognize CXCR5 positive primary B-NHL patient samples *in vitro*

4.5.1 CXCR5 is highly expressed on B-NHL patient samples

Clinical trial eligibility criteria include, among others, prior treatments and physical condition of the patient, but most importantly disease characteristics (Gerber et al., 2015). For a prospective CXCR5 CAR trial and potential therapeutic use in patients, it had to be confirmed that CXCR5 is an epitope frequently expressed on primary malignant cells of B-NHL patients. In the literature, CXCR5 expression on mature B cell malignancies, such as chronic lymphocytic leukemia (CLL), mantle cell lymphoma (MCL), follicular lymphoma (FL) and marginal zone lymphoma (MZL) has been described (Dürig et al., 2001; Middle et al., 2015b).

First, antigen expression on patient biopsies was evaluated by flow cytometry. Bone marrow (FL #85, #1054, #1100, #1129; MCL #545, #777; CLL #890, #821) or peripheral blood mononuclear cell patient samples (FL #252, #457, #563; MCL #114, #578, #624, #988; MZL #421,

#441, #728, #769; CLL #12, #31, #33, #47, #75, #819) were kindly provided by Prof. Jörg Westermann (Department of Hematology, Oncology and Tumorimmunology; Charité-University Medicine).

The samples were labeled with the CXCR5 antibody or the corresponding isotype control antibody. Gating included doublet, dead cell, and $CD3^+$ exclusion. Histograms showing profound CXCR5 expression on the B tumor population demonstrated that CXCR5 was expressed on the majority of samples, supporting the findings in the literature (Figure 18). Additionally, apart from confirming CXCR5 expression on the primary patient samples, the antigen quantity per cell was determined using Quantibrite beads, which added novel information to the expression data. The highest mean expression was measured for the CLL samples (4452 molecules/cell), followed by MCL (2035 molecules/cell). 1813 molecules/cell were detected on average on the FL samples. MZL showed mean CXCR5 expression of 672 molecules/cell, with one sample showing high expression and three samples having low expression (Figure 18E). Altogether, CXCR5 was strongly expressed in almost all analyzed patient samples, with quantities comparable to the analyzed mature B-NHL cell lines.

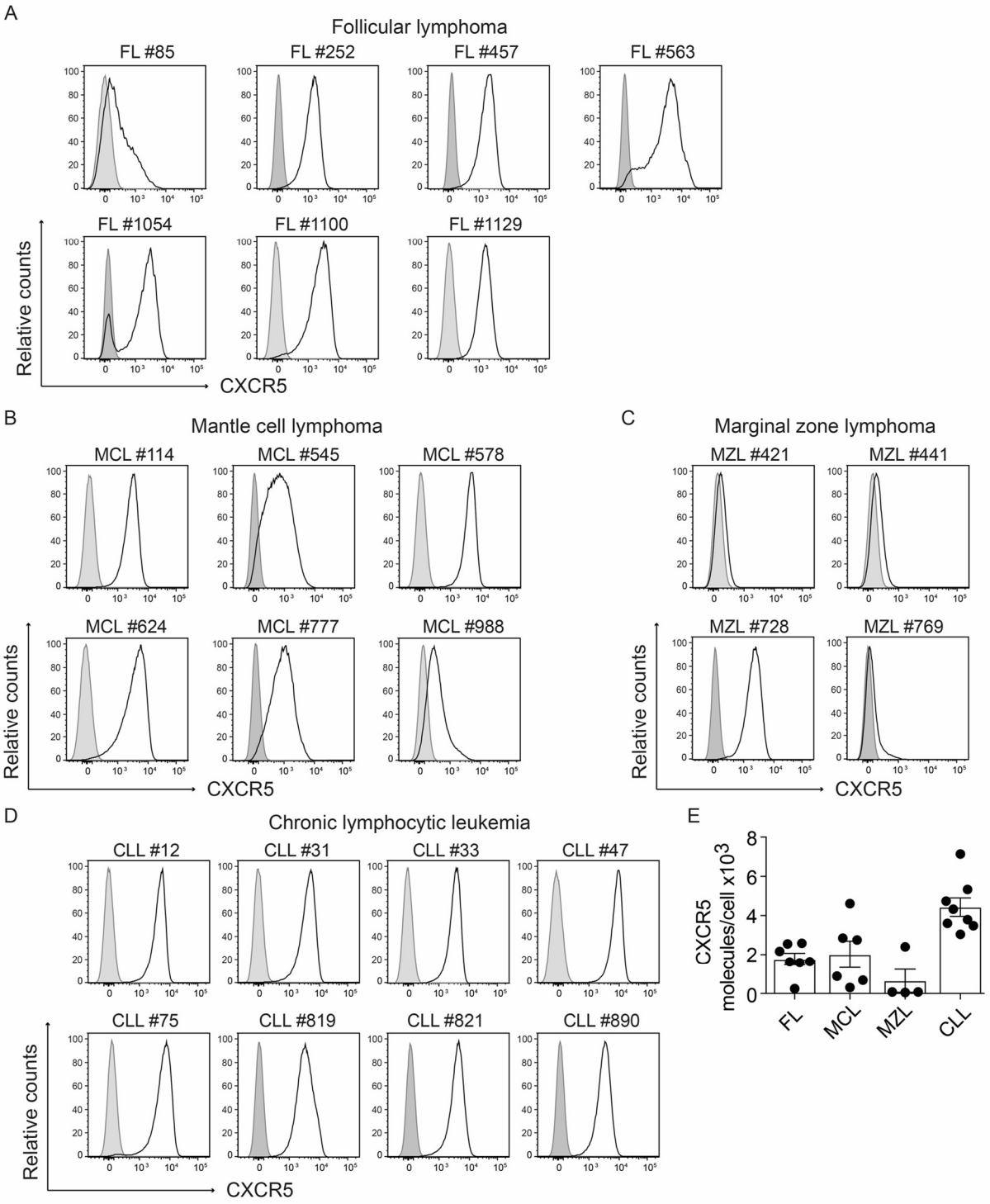

Figure 18: B-NHL biopsies frequently express high levels of CXCR5. CXCR5 expression on B-NHL patient samples was assessed by flow cytometry. Doublets, dead cells, and $CD3^+$ cells were excluded. Each sample was measured once due to limited material. CXCR5 expression on **A** follicular lymphoma, **B** mantle cell lymphoma, **C** marginal zone lymphoma and **D** chronic lymphocytic leukemia patient samples was depicted in histograms. Black lines show staining with the CXCR5 antibody; grey filled lines depict staining with the isotype control antibody. Histograms show relative fluorescence intensity. **E** CXCR5 molecules on the cell surface of B-NHL patient samples were quantified with the Quantibrite assay. Data points represent individual measurements, mean and SEM are shown. Data was collected in collaboration with Dr. Mario Bunse.

For each patient biopsy, CXCR5 and CD19 expression was depicted in plots (Figure 19). A healthy donor peripheral blood sample illustrated the difference to the tumor samples. In healthy blood, only 17% of $CD3^-$ cells were mature B cells and expressed CD19 and CXCR5 (Figure 19A). In the lymphoma/leukemia primary samples, the fraction of cells expressing CD19/CXCR5 was strongly increased, indicating that the majority of cells in these samples were tumor cells. FL biopsies expressed CXCR5 and CD19 to various degrees. CD19 expression was the least homogeneous in FL. In some FL samples, a fraction of tumor cells was $CD19^-CXCR5^+$ (#252, #457, #563, #1054). All FL patient samples, except #85, showed robust CXCR5 expression. FL #85, which is a bone marrow biopsy, also harbored a $CXCR5^-$ subset, possibly due to immature $CD19^+CXCR5^-$ B cells (Figure 19B). In MCL, half the samples highly expressed CXCR5 (#114, #578, #624) and half of them showed lower expression levels (#545, #777, #988). The MCL samples were positive for CD19 (Figure 19C). Of the four MZL samples, only one strongly expressed CXCR5 (#728); the other three samples showed only minor expression levels on a small subset of tumor cells. CD19 was abundant on MZL biopsies (Figure 19D). CLL samples strongly and homogeneously expressed CD19 and CXCR5. CLL #819 harbored a fraction of $CD19^-CXCR5^+$ cells (Figure 19E). The fraction of $CXCR5^+CD19^+$ cells is drastically enriched in the primary patient samples compared with the healthy donor sample. It can be assumed that benign mature B cells were virtually absent and replaced by malignant cells in these samples. As the fraction of tumor cells in these samples was very high, complete patient samples, which were not specifically enriched for tumor cells, were used in subsequent *in vitro* assays.

For patient samples that lack CD19 expression on a subset of tumor cells, anti-CD19 CAR T cells would not be able to target the tumor cells homogeneously. However, if CXCR5 is expressed on all tumor cells, anti-CXCR5 CAR T cells would be able to completely eradicate all tumor cells. The activity of anti-CXCR5 and anti-CD19 CAR T cells was further studied in co-cultures, which shed light on the cytokine secretion and killing capacity upon incubation with the various B-NHL biopsies.

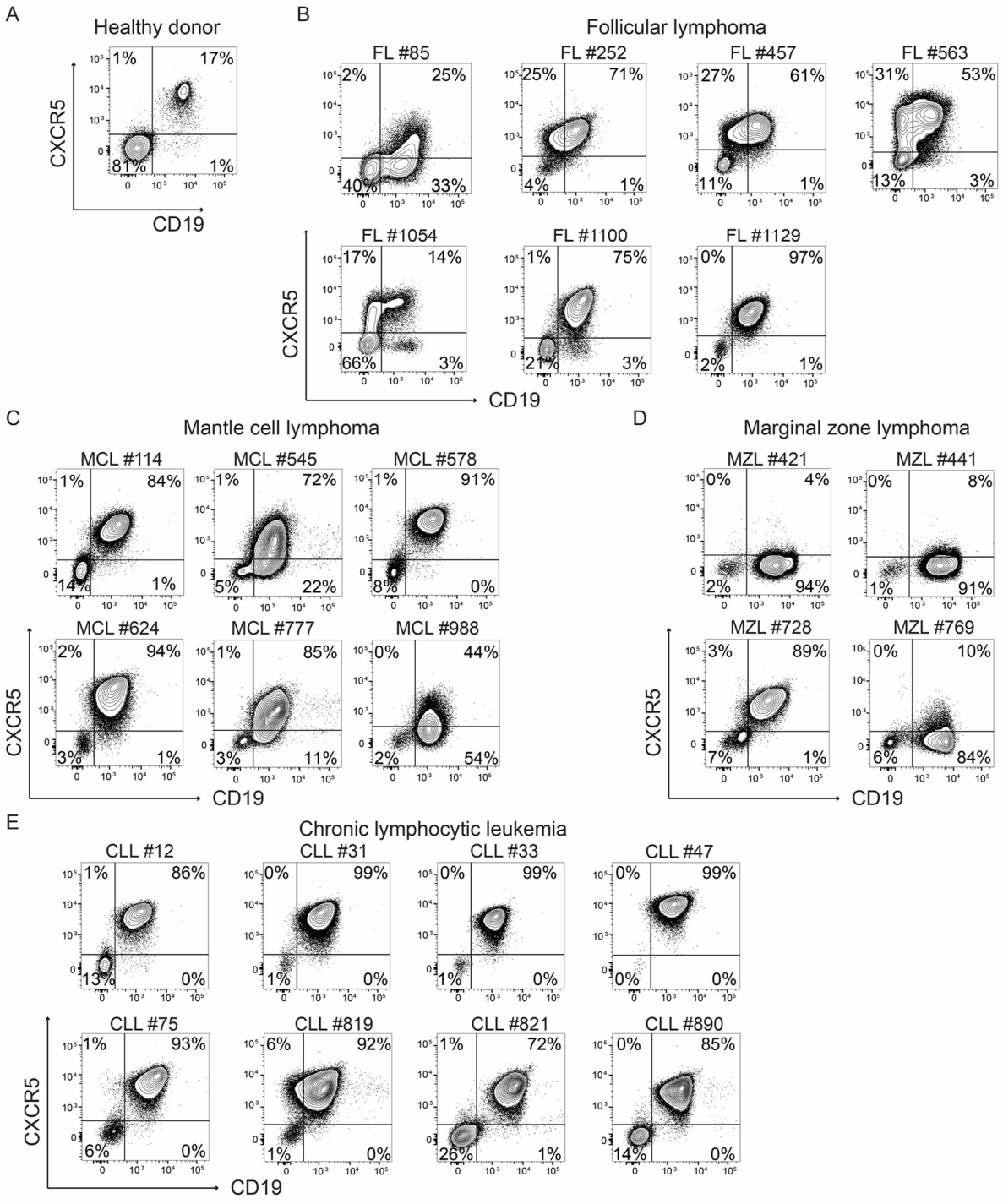

Figure 19: CD19 and CXCR5 expression was assessed on B-NHL patient material. Expression of CXCR5 and CD19 was assessed on $CD3^-$ cells in primary material from **A** a healthy donor, **B** follicular lymphoma, **C** mantle cell lymphoma, **D** marginal zone lymphoma and **E** chronic lymphocytic leukemia. Cells were pregated on singlets and live cells. Quadrant gate was adjusted according to isotype controls. Each sample was measured once due to limited material. Data was collected in collaboration with Dr. Mario Bunse.

4.5.2 CXCR5 CAR T cells release IFNγ upon incubation with CXCR5 positive B-NHL patient samples

Strong CXCR5 expression was demonstrated for the majority of patient material. For the treatment of patients, it is crucial that the CXCR5 CAR T cells recognize and react towards CXCR5 positive primary patient material. CAR T cells were incubated with the lymphoma patient samples for 12-24 h at a 1:1 ratio of target and effector cells ($5x10^4$ cells each). IFNγ release in the supernatant was quantified by ELISA (Figure 20). As a positive control for CAR T cell activity, the $CXCR5^+CD19^+$ cell line JEKO-1 was used. Generally, the anti-CXCR5 CAR T cells released more IFNγ than the anti-CD19 CAR T cells in response to FL, MCL and CLL samples. In FL, anti-CXCR5 CAR T cells reacted stronger towards #252, #457, #563, #1054 (which harbored CD19 negative tumor cell fractions) and #1100. For #457 and #1054, anti-CD19 CAR T cells even lacked IFNγ release. #85, which only weakly expressed CXCR5, elicited a stronger response in the anti-CD19 CAR T cells. For unknown reasons, #1129, which expressed both CXCR5 and CD19, did not trigger a response by any of the CAR T cells (Figure 20A). Anti-CXCR5 CAR T cells released more IFNγ than the anti-CD19 CAR T cells in response to the MCL samples #114, #545, #578, #624 and #777. MCL #988 barely triggered any release by any of the CAR T cells, but the reason for this is unclear, as the tumor cells expressed CD19 and CXCR5 (Figure 20B). Despite very weak CXCR5 expression on three MZL samples (#421, #441, #769), the anti-CXCR5 CAR T cells released some IFNγ. The reaction of the anti-CD19 CAR T cells was stronger towards these samples, as they expressed higher levels of CD19. MZL #728, which expressed both CXCR5 and CD19, triggered robust IFNγ release of both CAR T cell types, with stronger release by the anti-CD19 CAR T cells (Figure 20C). CLL patient samples, which showed very homogeneous CXCR5 and CD19 expression in flow cytometry, generally triggered a stronger reaction of the anti-CXCR5 CAR T cells (Figure 20D). It can be concluded that the anti-CXCR5 CAR T cells react towards the CXCR5 positive patient samples. Frequently, they show greater activity than the anti-CD19 CAR T cells.

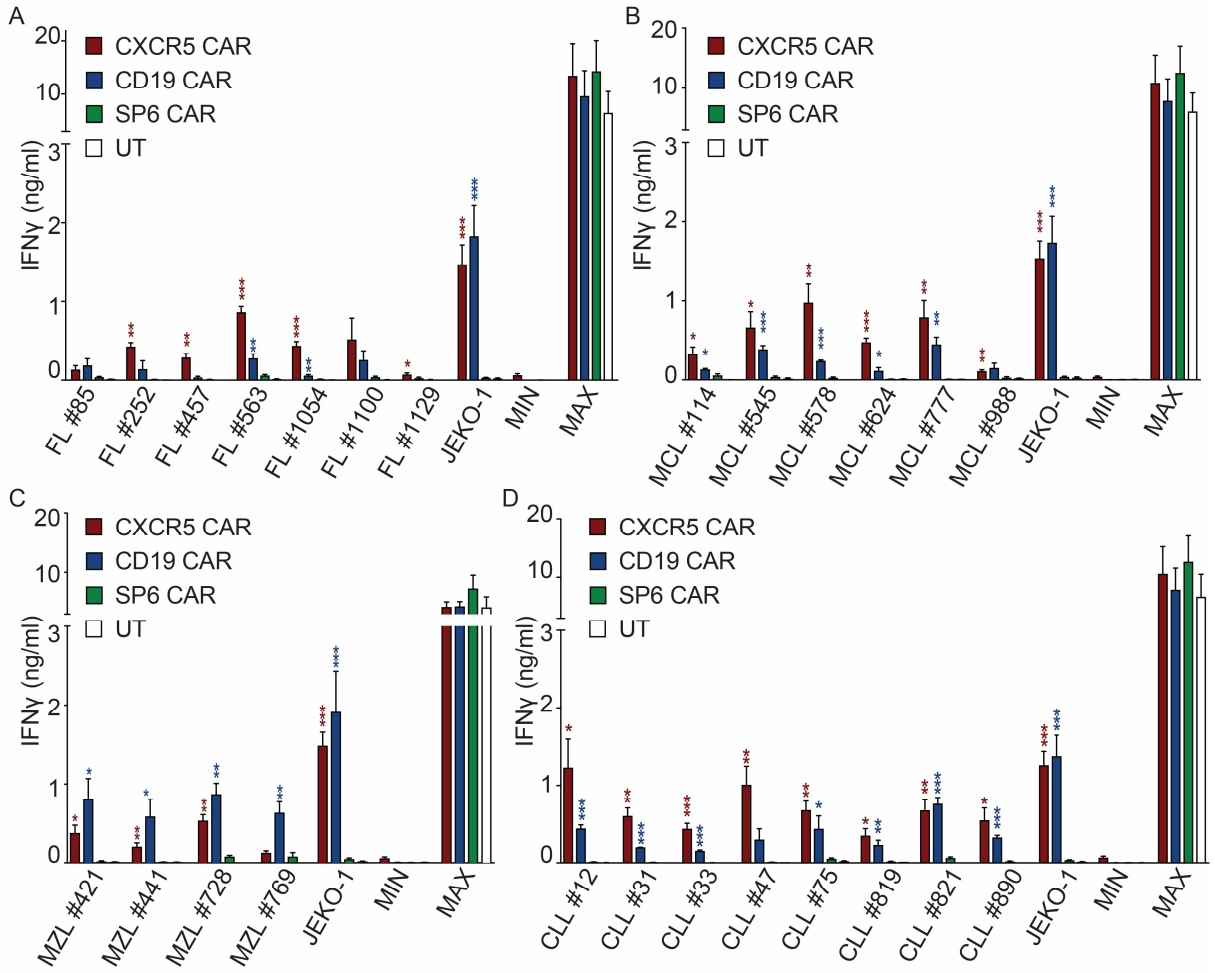

Figure 20: CXCR5 CAR T cells show *in vitro* reactivity against B-NHL biopsies. Patient B-NHL cells were incubated with CAR transduced cells or non-transduced T cells for 12-24 h. IFNγ in the supernatant was quantified by ELISA. CXCR5$^+$ JEKO-1 cells served as a positive control. Bars represent mean ± SEM of 4 independent donors (CXCR5 CAR, SP6 CAR, UT) or 3 independent donors (CD19 CAR). P-values (*P<0.05, **P<0.01, ***P<0.001) were calculated using an unpaired T test comparing CXCR5-CAR transduced T cells (red) or CD19-CAR transduced T cells (blue) with SP6-CAR transduced T cells. **A** Follicular lymphoma (FL), **B** mantle cell lymphoma (MCL), **C** marginal zone lymphoma (MZL) and **D** chronic lymphocytic leukemia (CLL) patient samples were analyzed. Data was collected in collaboration with Dr. Mario Bunse.

4.5.3 CXCR5 CAR T cells kill tumor cells in B-NHL patient samples

It was demonstrated that CXCR5 CAR T cells released IFNγ in response to lymphoma patient samples. Another crucial functional feature of CAR T cells for clinical application is efficient killing of malignant cells. Lymphoma cell killing in patient samples *in vitro* was further analyzed in a coculture. Previously, numerous experiments were performed to establish a solid protocol for *in vitro* primary lymphoma killing. Ultimately, a time frame of 48 h yielded the best results, considering patient cell viability and CAR T cell activity. Patient cells and CAR-transduced cells were incubated at a 1:1 ratio ($5x10^4$ cells each). To facilitate further analysis, the amount of T cells per donor was kept constant by adding non-transduced T cells. After two days, the cells

were analyzed by flow cytometry and gated for the CXCR5$^+$, CD20$^+$ or CD5$^+$ tumor fraction. Patient material of follicular lymphoma (Figure 21A), mantle cell lymphoma (Figure 21B), marginal zone lymphoma (Figure 21C) and chronic lymphocytic leukemia (Figure 21D) was included in the assay. The amount of viable tumor cells at the end of the culture was highly variable between patient samples; therefore, the tumor cell fraction was depicted in relation to the viable tumor cells in the control sample incubated with non-transduced T cells. Interestingly, anti-CD19 CAR T cell-mediated killing was weak and not statistically significant, despite proving its activity against the MCL cell line JEKO-1, which was included as a positive control. The anti-CXCR5 CAR T cells showed strong tumor eradication towards most FL and MCL samples. Against MZL samples with minor CXCR5 expression, the anti-CXCR5 CAR T cell killing was weak. CLL samples were eliminated by the anti-CXCR5 CAR T cells to strongly varying degrees. In this *in vitro* killing assay, the anti-CXCR5 CAR T cells showed stronger functionality in comparison with the anti-CD19 CAR T cells.

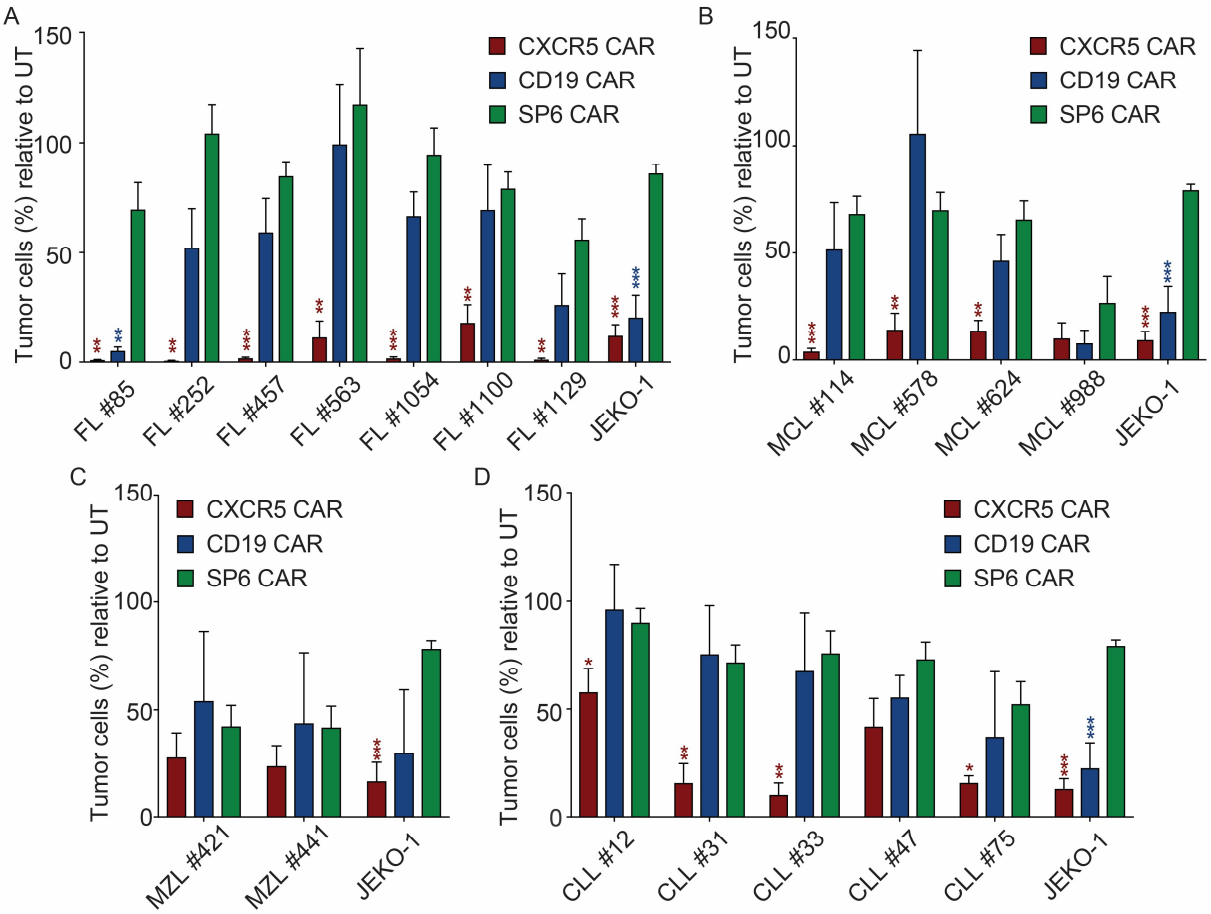

Figure 21: CXCR5 CAR T cells kill primary B-NHL lymphoma cells *in vitro*. Cocultures of lymphoma patient cells at a 1:1 ratio with CXCR5, CD19 and SP6 CAR T cells and non-transduced cells were analyzed by flow cytometry. Cells were gated on single cells and 7-AAD$^-$. Percentages shown are tumor cell fractions (CXCR5$^+$, CD20$^+$ or CD5$^+$) relative to tumor cell fractions in the samples with non-transduced T cells. Bars represent mean ± SEM of 4 independent donors (CXCR5 CAR, SP6 CAR, UT) or 3 independent donors (CD19 CAR). P-values (*P<0.05, **P<0.01, ***P<0.001) were calculated using an unpaired T test comparing CXCR5-CAR transduced T cells (red) or CD19-CAR transduced T cells

(blue) with SP6-CAR transduced T cells. **A** Follicular lymphoma (FL), **B** mantle cell lymphoma (MCL), **C** marginal zone lymphoma (MZL) and **D** chronic lymphocytic leukemia (CLL) patient samples were analyzed. Data was collected in collaboration with Dr. Mario Bunse.

4.6 CXCR5 CAR T cells recognize CXCR5 expressing T cells *in vitro*

CXCR5 is not only expressed on mature B cells, but also on subsets of $CD4^+$ T cells. Follicular helper T (T_{FH}) cells are classified as $CD4^+$ helper T cells in the B cell follicle and germinal centers. They are able to enter these B cell areas upon CXCR5 expression and provide B cell help (Breitfeld et al., 2000; Schaerli et al., 2000b). They are commonly described to coexpress PD-1 and/or ICOS. Further, they were described to actively contribute to pathogenesis in follicular lymphoma and chronic lymphocytic leukemia. Their counterparts in the peripheral blood were termed circulating follicular helper T (cT_{FH}) cells and preferentially studied in disease due to their easy accessibility in patients (Crotty, 2014).

4.6.1 CXCR5 CAR T cells release IFNγ upon incubation with CXCR5 expressing T cells

Human $CXCR5^+$ T cells were isolated from peripheral blood. Immunomagnetic sorting was chosen over fluorescence-activated cell sorting (FACS), as it was not feasible to obtain sufficient numbers of viable cells by FACS. Therefore, it was not possible to isolate $PD\text{-}1^+CD25^-$ cT_{FH} cells, but in a rather general approach, $CXCR5^+CD4^+$ cells were harvested, which included cT_{FH} cells. First, an immunomagnetic negative sort for $CD4^+$ cells was performed, followed by a positive sort for $CXCR5^+$ cells. Flow cytometry analysis confirmed that $CD4^+CXCR5^+$ cells were strongly enriched in the positive sort fraction and absent from the negative sort fraction (Figure 22A). The CXCR5 negative and positive sort fractions were co-cultured in an overnight assay with the anti-CXCR5, anti-CD19 and SP6-transduced T cells and non-transduced T cells at a 1:1 ratio ($5x10^4$ cells each per well) (Figure 22B). JEKO-1 tumor cells were included as a positive control. The anti-CD19 CAR T cells did not release IFNγ in response to the $CD4^+$ T cell fractions. The anti-CXCR5 CAR T cells however secreted IFNγ exclusively in response to the $CD4^+CXCR5^+$ fraction. The $CD4^+CXCR5^-$ fraction was not recognized by the CAR T cells. This demonstrated that the anti-CXCR5 CAR T cells react specifically towards CXCR5 expressing helper T cells in the peripheral blood, which include the cT_{FH} cells.

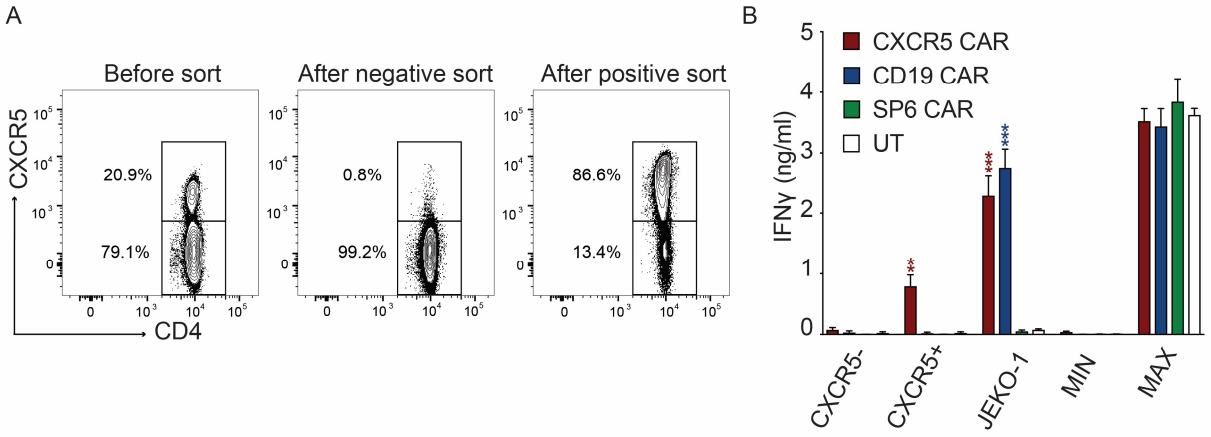

Figure 22: CXCR5 CAR T cells show *in vitro* reactivity against CXCR5⁺ T cells. A Cells from peripheral blood were analyzed for CD4⁺CXCR5⁺ cells before magnetic sorting and afterwards. Doublets and dead cells were excluded. Plots are shown before the sort and of the negative and positive CXCR5 sort fractions. **B** CD4⁺ T cells from peripheral blood magnetically sorted into the CXCR5⁻ and CXCR5⁺ fractions were incubated with CAR transduced cells or non-transduced T cells for 16 h. IFNγ in the supernatant was quantified by ELISA. CXCR5⁺ JEKO-1 cells served as a positive control. Bars represent mean ± SEM of 4 independent donors (CXCR5 CAR, SP6 CAR, UT) or 3 independent donors (CD19 CAR). P-values (*P<0.05, **P<0.01, ***P<0.001) were calculated using an unpaired T test comparing CXCR5-CAR transduced T cells (red) or CD19-CAR transduced T cells (blue) with SP6-CAR transduced T cells. Data was collected in collaboration with Dr. Mario Bunse.

4.6.2 CXCR5 CAR T cells kill follicular helper T cells in follicular lymphoma and chronic lymphocytic leukemia patient samples

Follicular helper T cells were described to support malignant cells in follicular lymphoma and chronic lymphocytic leukemia. They stimulate the tumor cells with mechanisms intended for the support of B cell proliferation, such as IL4/21 production and CD40/CD40L signaling. For CLL, expansion of cT_{FH} cells in the blood was described (Ahearne et al., 2013; Amé-Thomas et al., 2012). First, peripheral blood samples from FL patients, CLL patients and healthy donors were analyzed by flow cytometry for cT_{FH} cells. After exclusion of dead cells and doublets, CD4⁺CD25⁻ cells were selected and expression of CXCR5 and PD-1 was analyzed. Double positive cells represented the cT_{FH} cell fraction (Figure 23A). Healthy donors harbored cT_{FH} cell fractions of around 5%. For the two analyzed FL samples, cT_{FH} cell fractions were in a similar range, indicating that cT_{FH} cells were not enriched in these patients. Five CLL samples were measured, of which three showed strongly enlarged cT_{FH} cell fractions from 9% to 26%. Due to the low sample number, these percentages are not intended to describe the cT_{FH} cell fractions in FL or CLL patients, but rather to demonstrate that cT_{FH} cells were present at the onset of the killing assay. In addition to showing *in vitro* killing of the tumor cells, flow cytometry of cT_{FH} cells after coculture was performed to assess whether the CAR T cells are capable of killing them. The FL and CLL samples were incubated with the CAR T cells for 48 h. After gating on CD4⁺CD25⁻, the cT_{FH} fractions are shown as PD-1⁺CXCR5⁺ (Figure 23B). The T_{FH} fractions of the peripheral blood samples are depicted after incubation with the CXCR5, CD19

and SP6 CAR T cells (Figure 23C). PBMCs from healthy donors were included as controls. Incubation with the anti-CXCR5 CAR T cells, and not with anti-CD19 CAR T cells, could exclusively deplete the cT_{FH} population in the FL and CLL samples.

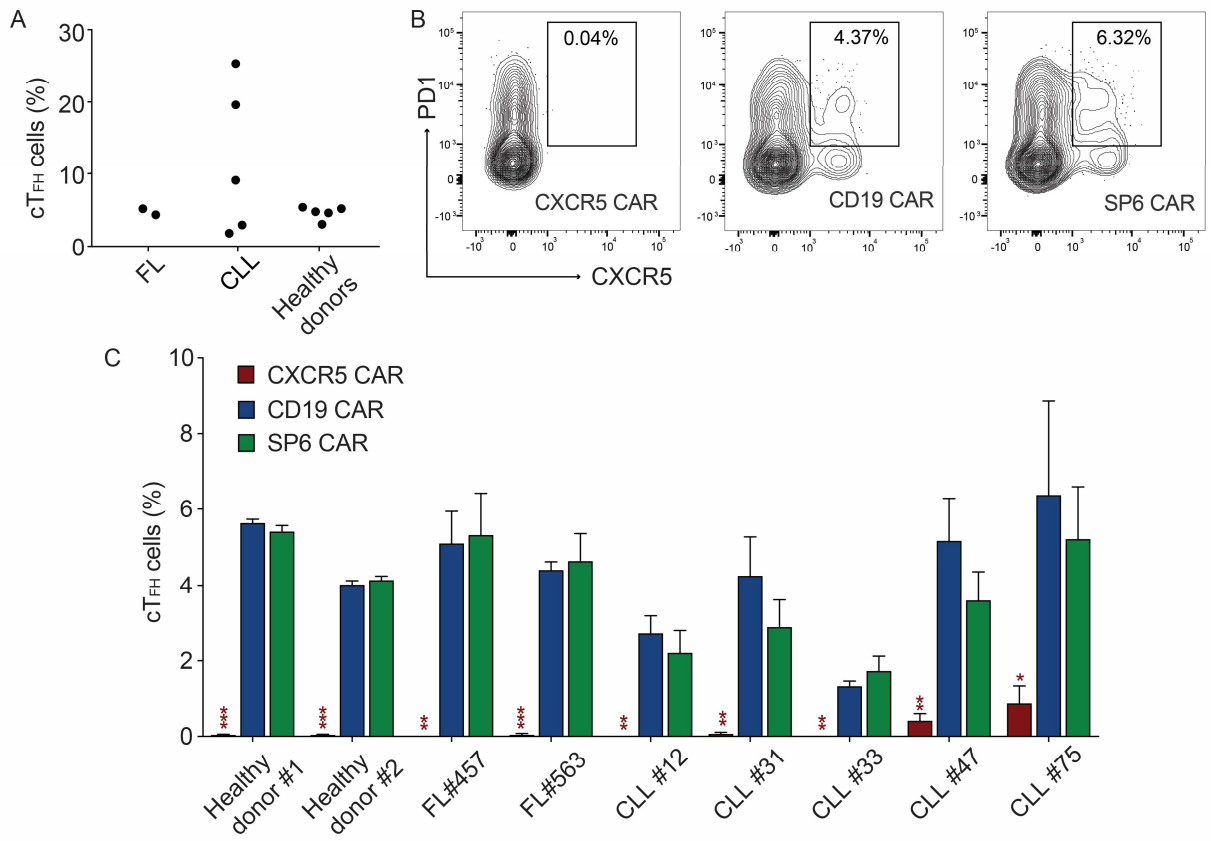

Figure 23: CXCR5 CAR T cells kill primary follicular helper T cells derived from FL and CLL biopsies. T_{FH} cell fractions are defined as PD-1$^+$CXCR5$^+$ of CD4$^+$CD25$^-$ cells. **A** Distribution of T_{FH} cell fractions of peripheral blood patient biopsis of FL, CLL and healthy donors are depicted. **B** Cocultures of follicular lymphoma patient cells with CXCR5, CD19 and SP6 CAR T cells were analyzed by flow cytometry. Cells were gated on single cells, 7-AAD$^-$ and CD4$^+$CD25$^-$. Percentages shown are follicular helper T cell fractions. Representative contour plots of 3-4 independent experiments are shown. **C** The T_{FH} cell fraction determined as described in B is depicted. Bars represent mean ± SEM of 4 independent donors (CXCR5 CAR, SP6 CAR, UT) or 3 independent donors (CD19 CAR). P-values (*P<0.05, **P<0.01, ***P<0.001) were calculated using an unpaired T test comparing CXCR5-CAR transduced T cells (red) or CD19-CAR transduced T cells (blue) with SP6-CAR transduced T cells. Data was collected in collaboration with Dr. Mario Bunse.

4.7 CXCR5 CAR T cells show a strong anti-tumor effect *in vivo* against B-NHL

NOD.Cg-Prkdc^{scid} Il2rg^{tm1Wjl}/SzJ (NSG) mice, which lack B and T cells and are defective in functions of the innate immune system, were used in a xenograft mouse model (Shultz et al., 2005). Due to these deficiencies, human cells, including lymphoma cell lines or patient-derived xenografts, engraft in the mice. The mice can also be subsequently administered with human CAR T cells to investigate an antigen-specific anti-tumor effect.

It is of particular interest to not only analyze mice at the end point of an experiment, but also at earlier time points to gain a better understanding of tumor kinetics and the anti-tumor function of CAR T cells. *In vivo* bioluminescence imaging using the IVIS spectrum device allowed visualization of luciferized tumor cells within the mice, without the need to sacrifice animals at different time points during the experiment. IVIS is equipped with a sensitive camera to detect the emission of bioluminescence in cells within the living animal. These cells must express luciferase, an enzyme derived from firefly or sea pansy. At the time of measurement, the mice are injected with the corresponding substrate called luciferin. The substrate is transformed by the luciferase and light is emitted.

4.7.1 PDX cells could not be sufficiently luciferized to be used in a xenograft NSG mouse model

A couple of CXCR5 expressing cell lines were tested in order to find a candidate that engrafts upon intravenous injection in a lymphoma-typical pattern. Ultimately, two mantle cell lymphoma entities, the cell line JEKO-1 and the patient-derived xenograft (PDX) #96069, were shown to be suitable for the xenograft experiments. Luciferized JEKO-1 cells were provided at the start of the project; the PDX cells were transduced as part of this thesis.

A PDX is established by injecting human tumor cells, originating from a patient, into immunodeficient mice, as they lack the immune system to reject the graft. They are gradually adapted to the murine environment by passaging. PDX cells have to be expanded *in vivo*, because they do not proliferate in cell culture, which required the application of a special transduction protocol to equip them with a luciferase-eGFP construct. After transduction, the cells were immediately injected in mice and after several weeks, the spleen was harvested, sorted for positively transduced cells and reinjected into a mouse to expand these cells. Sorting was performed twice in order to create a highly enriched population of transduced PDX cells. (Figure 24A-C).

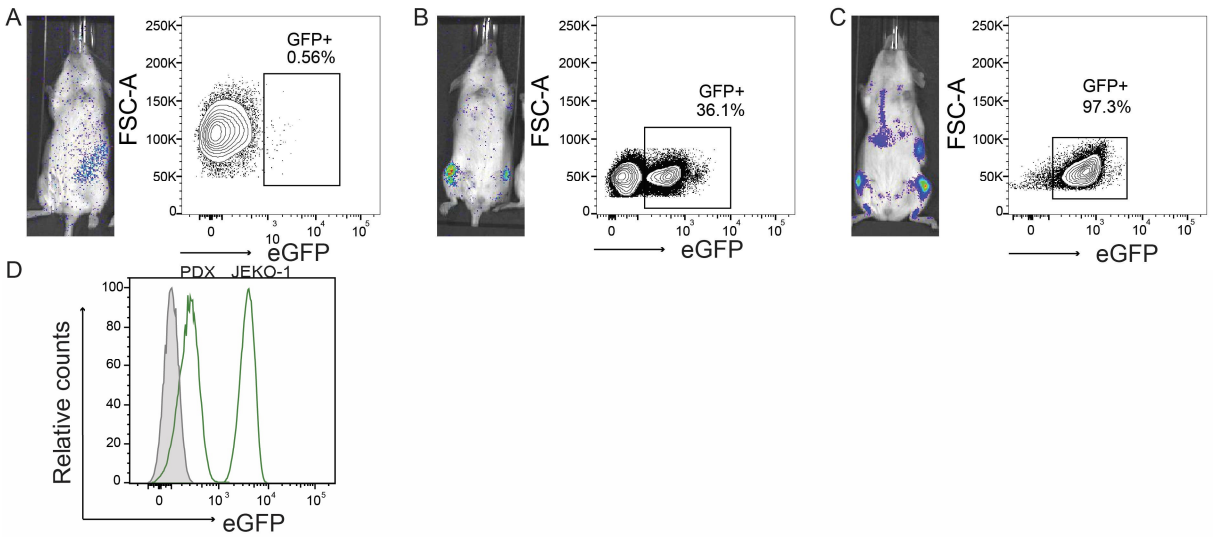

Figure 24: Mantle cell lymphoma PDX #96069 cells were luciferized by viral transduction. PDX #96069 cells were transduced, expanded in NSG mice and sorted twice. IVIS images of the injected mice and analysis of cells harvested from the spleen by flow cytometry after single cell gating are shown. **A** IVIS image with 240 s exposure time six weeks after the first injection, flow cytometry showed that only a minor cell fraction is positively transduced and expresses eGFP. These cells were sorted and reinjected into an NSG mouse. **B** IVIS image with 240 s exposure time six weeks after injection of once sorted PDX cells, flow cytometry revealed that the eGFP$^+$ fraction is strongly enriched. The eGFP$^+$ cells were sorted and expanded in NSG mice. **C** The IVIS image with 60 s exposure time and flow cytometry analysis show that the majority of PDX cells are GFP$^+$ after sorting them twice. **D** JEKO-1 eGFP transduced tumor cells, eGFP transduced PDX cells and non-transduced JEKO-1 cells were analyzed for eGFP expression by flow cytometry, gated on singlets and live cells by 7-AAD negativity. eGFP histograms are shown.

The MCL PDX cells were subsequently used in an NSG mouse experiment to analyze the anti-tumor effect of CXCR5-CAR T cells. However, the PDX cells did not show sufficient expression of bioluminescence during the course of the experiment. Compared to luciferase-eGFP transduced JEKO-1 cells, fluorescence intensity of eGFP was around 10-fold lower in the PDX cells (Figure 24D). It was not possible to generate PDX cells with high expression levels and they were not suitable to monitor the course of the experiment by bioluminescence imaging. JEKO-1 cells with a higher luciferase-eGFP expression were preferred for the following experiments to assess the anti-tumor activity of the anti-CXCR5 CAR T cells against mantle cell lymphoma *in vivo*.

4.7.2 CXCR5 CAR T cells show a strong anti-tumor effect *in vivo* against a mantle cell lymphoma cell line

JEKO-1 was used as a target cell line in the xenotransplantation model due to its high luciferase expression and ideal engraftment upon intravenous injection. For *in vivo* experiments, JEKO-1 cells were expanded before injection and culture medium was added a day prior to ensure high viability. 6x10^5 JEKO-1 cells per mouse were injected intravenously. CAR T cells were expanded supplemented with rhIL7/15 over the course of 10 days. The T cells were frozen after expansion, stored in liquid nitrogen and thawed before injection. For CAR T cell

administration, transduction rates were considered and a fixed number of CAR T cells was injected ($3x10^6$), the total T cell number was higher.

The JEKO-1 xenotransplantation experiment was performed twice with a comparison between the anti-CXCR5 and anti-CD19 CAR T cells. In the first experiment, onset of tumor growth was confirmed by bioluminescence imaging on day 7 at 300s (Figure 25A). In the second experiment, onset of growth was already visible on day 5 at 120 s exposure time (Figure 26A). The tumor cells predominantly locate to the bone marrow. Upon visible tumor growth, anti-CXCR5, CD19 and SP6 CAR T cells were injected the following day and progression was monitored by IVIS. An exposure time of 15 s was selected, which allowed showing the images of all groups without oversaturating the images of the SP6 CAR group that had stronger bioluminescence signals (Figure 25+Figure 26B). The antigen-specific CXCR5 and CD19 CAR T cells were able to reduce tumor growth over the course of the experiment. No reduction of tumor growth was observed in the SP6 group, except of a single animal in the first experiment. As tumor load increased, bioluminescence signals were detected mostly in the bone marrow of the femur and chest area; in one animal they were localized in the spleen (Figure 25B) In the second experiment, tumor removal by the anti-CXCR5 and anti-CD19 CAR T cells was less efficient and residual tumor mass, especially in the head region was increasingly detected during the course of the experiment (Figure 26B). Quantification of bioluminescence signals of the luciferized tumor cells illustrated that tumor load was decreased in the CXCR5 CAR and CD19 CAR groups compared with the SP6 group (Figure 25+Figure 26C). At the end point of the experiments, mice were sacrificed, spleen and bone marrow of the femur were harvested. Flow cytometry analysis confirmed that the tumor cells strongly located to the bone marrow of SP6 mice. In the CXCR5 CAR and CD19 CAR groups of the first experiment, JEKO-1 cells were virtually absent from bone marrow; only one mouse in the CXCR5 CAR group harbored tumor cells in the spleen (Figure 25D). The tumor load was generally higher in the second experiment than in the first experiment. Tumor load in the SP6 group was on average 7% in the bone marrow and 0.1% in the spleen in the first experiment; for the second experiment, the tumor load was 69% and 31%, respectively (Figure 25+Figure 26D). IVIS imaging and flow cytometry analysis illustrated the strong anti-tumor effect of the anti-CXCR5 and anti-CD19 CAR T cells, especially at the primary site of lymphomagenesis, the bone marrow. The anti-CD19 CAR T cells showed slightly stronger anti-tumor efficacy in the first experiment, while the anti-CXCR5 CAR T cells performed better in the second experiment. The JEKO-1 tumor cells were analyzed concerning their CXCR5 expression. In both experiments, expression was consistent among the groups, which excluded the outgrowth of antigen-loss variants (Figure 25+Figure 26E). Further, expression of the exhaustion marker PD-1 was assessed to get an impression of the T cell exhaustion status. PD-1 levels of the antigen-specific CAR T cells were not

increased compared with the anti-SP6 CAR T cells, indicating that the CAR T cells did not suffer from exhaustion (Figure 25+Figure 26F).

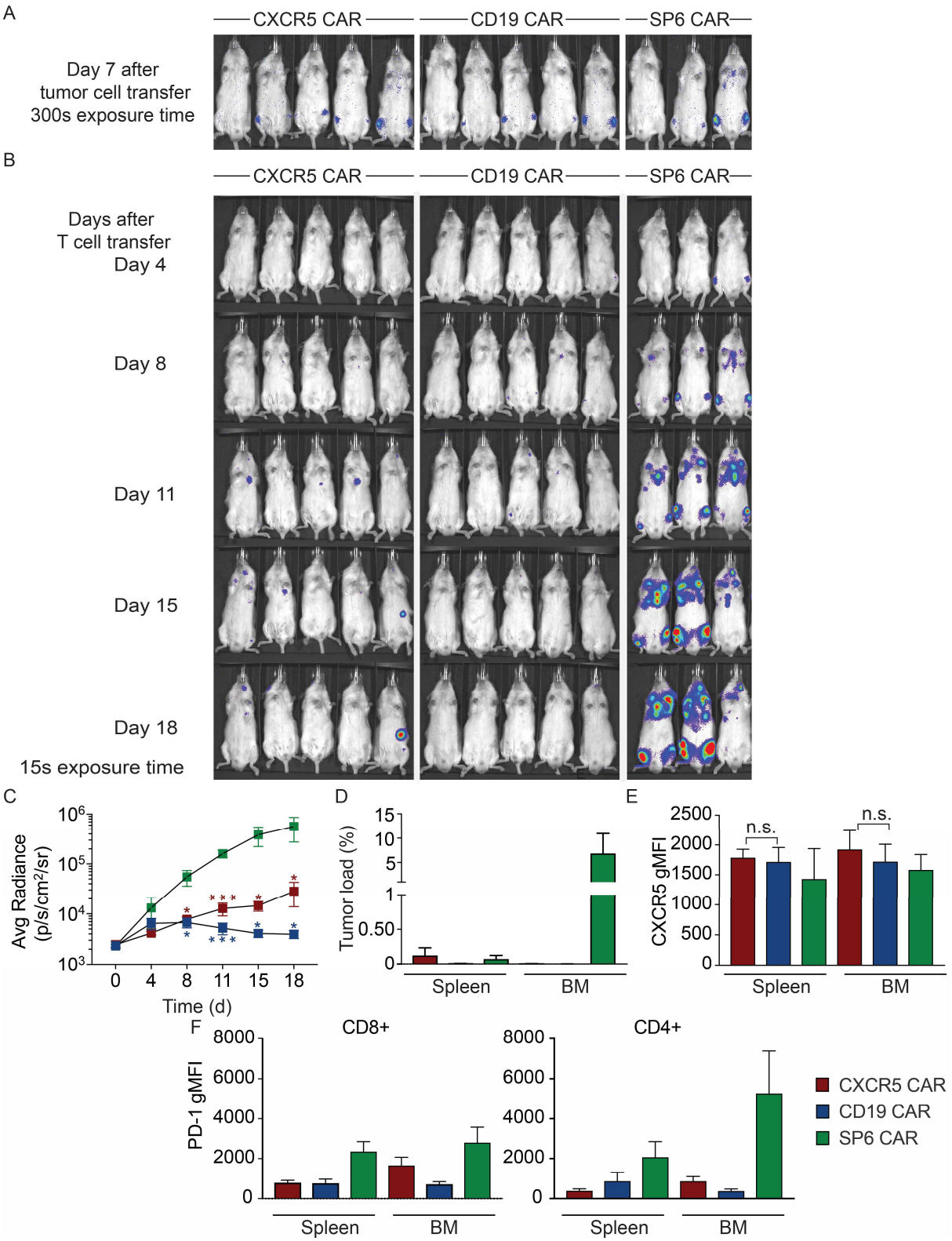

Figure 25: CXCR5 CAR T cells show a strong anti-tumor activity in vivo. NSG mice were injected with 6x10^5 JEKO-1 tumor cells and subsequently with CXCR5, CD19 or SP6 CAR T cells (3x10^6 CAR T cells per mouse). **A** Tumor growth was verified on day 7 after tumor cell injection by IVIS (exposure time 300s). **B** Progression of tumor growth was monitored by IVIS (exposure time 15s) over the course

of 18 days after T cell injection. **C** Average Radiance is depicted for the different groups (n=3-6 mice per group). P-values (*P<0.05, **P<0.01, ***P<0.001) were calculated using an unpaired T test comparing animals of the CXCR5 group (red) or animals of the CD19 group (blue) with SP6 animals. Cells were analyzed by flow cytometry on day 19 and 20. **D** Tumor load as fraction of viable JEKO-1 cells is shown for the spleen and the bone marrow. **E** CXCR5 gMFI on JEKO-1 tumor cells is depicted. An unpaired T test comparing animals of the CXCR5 and the CD19 group was conducted. **F** Expression of PD-1 (gMFI) is shown for $CD4^+$ and $CD8^+$ T cells in the spleen and bone marrow.

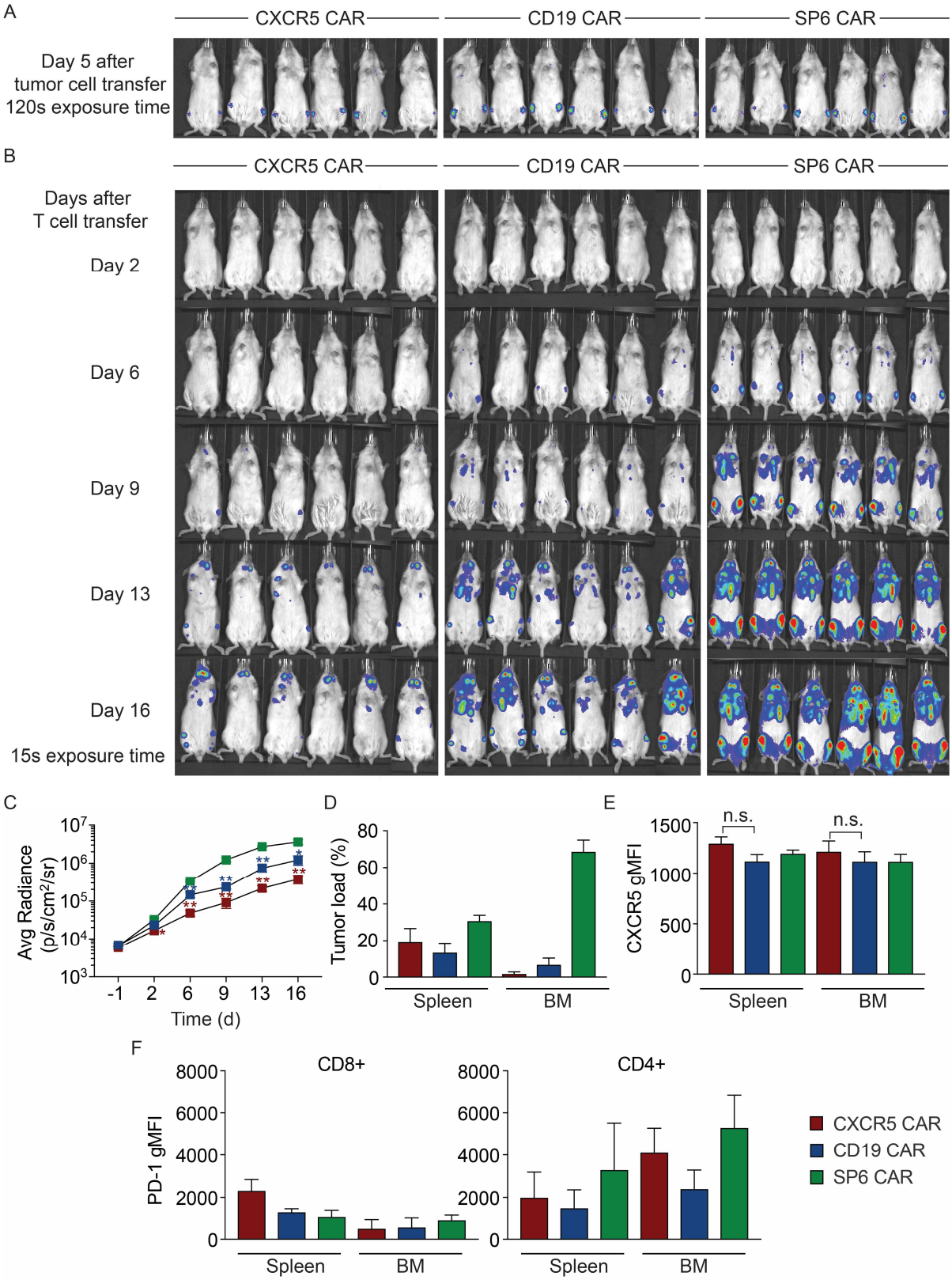

Figure 26: CXCR5 CAR T cells mediate potent anti-tumor activity *in vivo*. NSG mice were injected with 6x10^5 JEKO-1 tumor cells and subsequently with CXCR5, CD19 or SP6 CAR T cells (3x10^6 CAR T cells per mouse) **A** Tumor growth was verified on day 5 after tumor cell injection by IVIS (exposure time 120s). **B** Progression of tumor growth was monitored by IVIS (exposure time 15s) over the course of 16 days after T cell injection. **C** Average Radiance is depicted for the different groups. Values are depicted as mean ± SEM of n=6 mice per group. P-values (*P<0.01, **P<0.001) were calculated using

an unpaired T test comparing animals of the CXCR5 group (red) or animals of the CD19 group (blue) with SP6 animals. Cells were analyzed by flow cytometry on day 19 and 20. **D** Tumor load as fraction of viable JEKO-1 cells is shown for the spleen and the bone marrow. **E** CXCR5 gMFI on JEKO-1 tumor cells is depicted. An unpaired T test comparing animals of the CXCR5 and the CD19 group was conducted. **F** Expression of PD-1 (gMFI) is shown for CD4 and CD8 CAR T cells in the spleen and bone marrow.

A strong anti-tumor effect of the anti-CXCR5 CAR T cells could be demonstrated in both *in vivo* JEKO-1 xenograft experiments, with an efficacy slightly stronger than the anti-CD19 CAR T cells in one experiment and slightly weaker in the other. Nevertheless, the antigen-specific CAR T cells did not completely eradicate the lymphoma cells. Progressive tumor growth in the anti-CXCR5 CAR group, but also the anti-CD19 CAR group, especially in the spleen was still observed. A reason for this could be decreased T cell functionality due to exhaustion. Exhausted T cells are dysfunctional, cannot proliferate and lack effector functions. Programmed cell death protein 1 (PD-1) is one of the markers upregulated on exhausted T cells, as originally investigated in chronic infection models. These findings in infection were also applicable in cancer research (Sakuishi et al., 2010). PD-1 signaling was also shown to induce T cell exhaustion in hematologic malignancies (Mumprecht et al., 2009; Yamamoto et al., 2008). However, in both JEKO-1 xenotransplantation experiments, PD-1 upregulaton was not observed. Thus, T cell exhaustion appeared to be not causal for tumor progression. Progressive tumor growth can therefore most likely be attributed to the limitation of the NSG mouse model, in which human T cells lack support. NSG mice lack the cytokines IL2, IL4, IL7, IL9, IL15 and IL21 due to their *Il2rg* null mutation (Shultz et al., 2012). Another major impairment for human T cell function in the NSG model is the insufficient cross-reactivity of murine cytokines on human receptors (Willinger et al., 2011). In summary, these results showed that, despite limitations of the NSG mouse model, the anti-CXCR5 CAR T cells achieved a significant anti-tumor effect *in vivo*, in a range comparable to the anti-CD19 CAR T cells.

4.8 The CXCR5 CAR is not hampered by the soluble CXCR5 N-terminus

In the previous xenotransplantation experiments, the CAR T cells did not completely eradicate the tumor cells. CAR T cell function is dependent on the interaction between the antigen-binding domain of the CAR T cell and the antigen expressed by the target cell. This interaction can possibly be disturbed by soluble antigen binding to the CAR. For B-cell maturation antigen (BCMA), shedding of the extracellular domain is described (Laurent et al., 2015). For CXCR5, similar mechanisms have not been reported and tumor cells with reduced antigen expression have not been found in the JEKO-1 xenotransplantation experiments. However, to exclude the possibility that antigen shedding inhibits CAR function, it was assessed whether anti-CXCR5 CAR T cell function is compromised by the soluble CXCR5 N-terminus (Figure 27). CAR T cells were, analogous to previous coculture experiments, coincubated with $CXCR5^{+}CD19^{+}$

JEKO-1 tumor cells at a 1:1 ratio ($5x10^4$ cells/well each). Anti-CXCR5, anti-CD19 and anti-SP6 CAR T cells were included in the assay. 60 nM of a synthesized peptide were added, which included the region of the anti-CXCR5 CAR-targeted N-terminal epitope. This concentration was chosen as it was similar to the median soluble BCMA concentration measured in the blood of multiple myeloma patients. At this concentration, soluble BCMA interfered with BCMA antibody binding to tumor cells (Sanchez et al., 2012). Moreover, the effect of 500 nM of the epitope peptide was evaluated to compare if non-physiological concentrations might interfere with CAR binding. As a control, a synthesized peptide of the CXCR5-loop region, which is not recognized by the anti-CXCR5 CAR T cells, was added at the same concentrations as the CAR-targeted epitope peptide. As always, a minimum value with solely CAR T cells and a maximum value induced by PMA/ionomycin stimulation were included. IFNγ release by CAR T cells was measured after a 24 h incubation period. IFNγ secretion of the anti-CXCR5 CAR T cells was not decreased by addition of the CXCR5-CAR targeted-epitope, even at 500 nM, compared with addition of the control peptide or without the addition of any peptides. This finding showed that the presence of the CAR-targeted CXCR5 N-terminal epitope even at non-physiological concentrations did not inhibit CAR-mediated T cell activity and potential CXCR5 shedding is not expected to interfere with anti-tumor efficacy in the NSG xenotransplantation model or in the prospective anti-CXCR5 CAR T cell administration to patients.

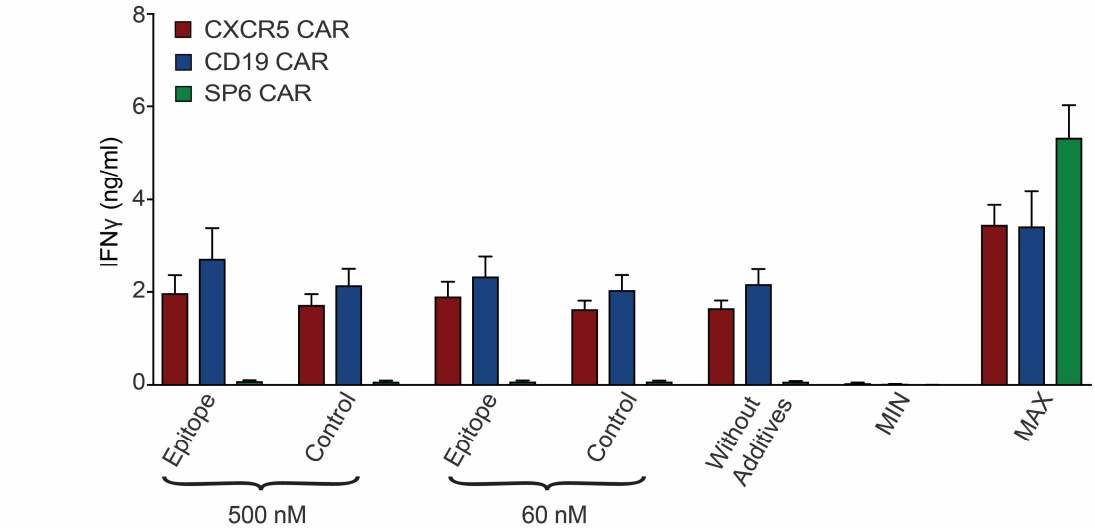

Figure 27: CXCR5 CAR T cells do not show decreased *in vitro* activity upon incubation with the soluble CXCR5 N-terminus. IFNγ release of CAR T cells upon 24 h incubation with JEKO-1 tumor cells was quantified by ELISA. The CXCR5 CAR epitope peptide or a control peptide were added to the culture at 500 nM and 60 nM. Bars represent mean ± SEM of 6 independent donors.

4.9 CXCR5 CAR T cells are not exhausted at the time of tumor cell outgrowth

Tumor relapse or insufficient tumor elimination by the CAR T cells in the previous experiments did not seem to be caused by the outgrowth of antigen-loss variants or by CAR-blocking by the soluble CXCR5 N-terminus. However, it was not yet fully addressed whether the CAR T cells experience exhaustion, which diminishes their anti-tumor efficacy. The *in vivo* persistence of anti-CXCR5 CAR T cells was studied at the time of tumor cell outgrowth to gain a better understanding about why NSG mice suffer from tumor relapse. To this end, CXCR5 CAR T cells were studied in a short-term animal experiment analogous to the previous JEKO-1 experiments. NSG mice were injected with $6x10^5$ JEKO-1 mantle cell lymphoma cells and tumor growth was confirmed by IVIS on day 5 (Figure 28A). Subsequently, $3x10^6$ anti-CXCR5 or anti-SP6 CAR T cells were administered and tumor growth was monitored by IVIS (Figure 28B). On day 8 and 13, four to five mice were sacrificed and femoral bone marrow and spleen tissues were analyzed by flow cytometry. On day 8, the tumor load was still low, but rapidly increased in the SP6 CAR group in the following days. On day 13, the average tumor load in the SP6 group was 12% in the bone marrow and 0.3% in the spleen. The tumor load was strongly reduced in the CXCR5 CAR group. The final average tumor load in the CXCR5 CAR group was 0.25% in the bone marrow and 0.13% in the spleen (Figure 28C). For the JEKO-1 tumor cells, CXCR5 expression was assessed for the different organs and groups on day 8 and 13. CXCR5 was not significantly downregulated on the tumor cells in the mice treated with the anti-CXCR5 CAR T cells, supporting that tumor recurrence was not caused by antigen-loss variants (Figure 28D). Further analysis was focused on CAR T cell proliferation and exhaustion characteristics of anti-CXCR5 and anti-SP6 CAR T cells recovered from sites of lymphomagenesis. CAR T cells were quantified and total cell numbers in the spleen and femoral bone marrow were determined (Figure 28E). $CD8^+$ T cell numbers were low and mostly $CD4^+$ T cells were present in the tissues, with expansion of antigen-specific $CD4^+$ anti-CXCR5 CAR T cells on day 8 in the bone marrow and on day 13 in the spleen. This expansion pattern for the anti-CXCR5 CAR T cells is in accordance with earlier and stronger tumor progression in the bone marrow, opposed to the spleen, as seen in the SP6 CAR group. Anti-CXCR5 CAR T cells could still be detected at the sites of lymphoma homing at the endpoint of the experiment at day 13.

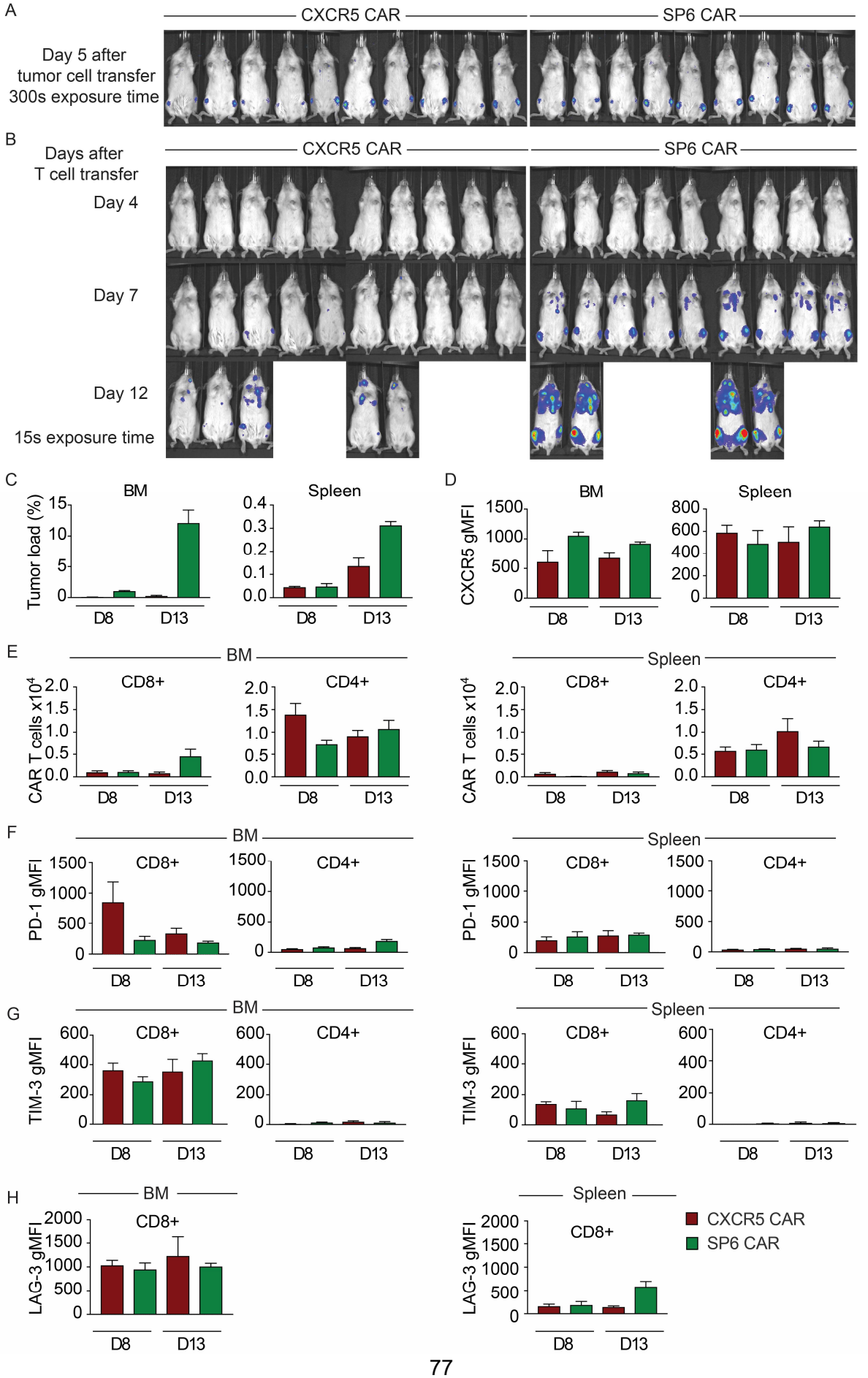
A
CXCR5 CAR
SP6 CAR
Day 5 after
tumor cell transfer
300s exposure time
B
Days after
T cell transfer
Day 4
Day 7
Day 12
15s exposure time
C
BM
Spleen
Tumor load (%)
D8
D13
D
CXCR5 gMFI
E
CD8+
CD4+
CAR T cells x10^4
F
PD-1 gMFI
G
TIM-3 gMFI
H
LAG-3 gMFI

Figure 28: CXCR5 CAR T cells are not exhausted at the time of tumor cell outgrowth. NSG mice were injected with JEKO-1 tumor cells and subsequently with CXCR5 or SP6 CAR T cells ($3x10^6$ CAR T cells per mouse). **A** Tumor growth was verified on day 5 after tumor cell injection by IVIS (exposure time 300s). **B** Progression of tumor growth was monitored by IVIS (exposure time 15s) over the course of 12 days after T cell injection. Cells were analyzed by flow cytometry on day 8 and 13. **C** Tumor load as fraction of viable JEKO-1 cells is shown for the spleen and the bone marrow. **D** CXCR5 gMFI on JEKO-1 tumor cells is depicted. **E** Absolute CAR T cell numbers are shown for CD8 and CD4 T cells in the spleen and bone marrow. **F, G, H** Expression of PD-1, TIM-3 and LAG-3 (gMFI) is shown for CD8 and CD4 T cells in the spleen and bone marrow. Bars represent mean ± SEM of 4-5 mice.

Expression of the exhaustion markers PD-1, T-cell immunoglobulin and mucin-domain containing-3 (TIM-3) and Lymphocyte-activation gene 3 (LAG-3) was analyzed on the CAR T cells (Figure 28F-H). On $CD4^+$ T cells, the markers were virtually absent. $CD8^+$ T cells expressed the markers; however, they were not differently regulated in the CXCR5 CAR group compared with the SP6 CAR group. $CD8^+$ T cells did upregulate PD-1 on day 8 in the bone marrow; nevertheless, exhaustion would be expected to induce upregulation of more than one of the exhaustion markers.

In summary, anti-CXCR5 CAR T cells showed a robust anti-tumor response at day 8 and day 13 in the bone marrow and spleen. The CAR T cells did not exhibit an exhausted phenotype and the tumor cells did not downregulate CXCR5. Hence, CAR T cell exhaustion or antigen loss appears to be an unlikely cause of insufficient tumor control.

4.10 CXCR5 CAR T cells do not show signs of exhaustion upon repetitive antigenic stimulation

In vivo, the CAR T cells did not show signs of exhaustion. Subsequently, this question was further addressed in an *in vitro* stress test, in which potential T cell dysfunction and exhaustion upon repetitive antigenic stimulation was studied. In this assay, the anti-CXCR5 and anti-CD19 CAR T cells were incubated with JEKO-1 tumor cells. Every third day, the CAR T cells were transferred into culture dishes with fresh tumor cells in order to reconstitute a constant CAR T cell to tumor cell ratio. In initial experiments, T cells and tumor cells were incubated at a 1:1 ratio (Figure 29A). Five stimulation rounds were performed and after every round, the T cells and the supernatant were analyzed. Before the assay, the cells were expanded with rhIL7/15 for 14 days; thus, the cells were in culture for 29 days altogether. The specific CXCR5 and CD19 CAR T cells were able to kill virtually all the tumor cells repetitively over the course of the experiment. The non-transduced T cells did not reduce the tumor load (Figure 29B). Moreover, the specific CAR T cells produced IFNγ and proliferated to twice their original number in every round over 15 days (Figure 29C+D). The transduction rate was already at least 75% at the beginning and still increased slightly over the course of the experiment to almost 100% (Figure 29E).

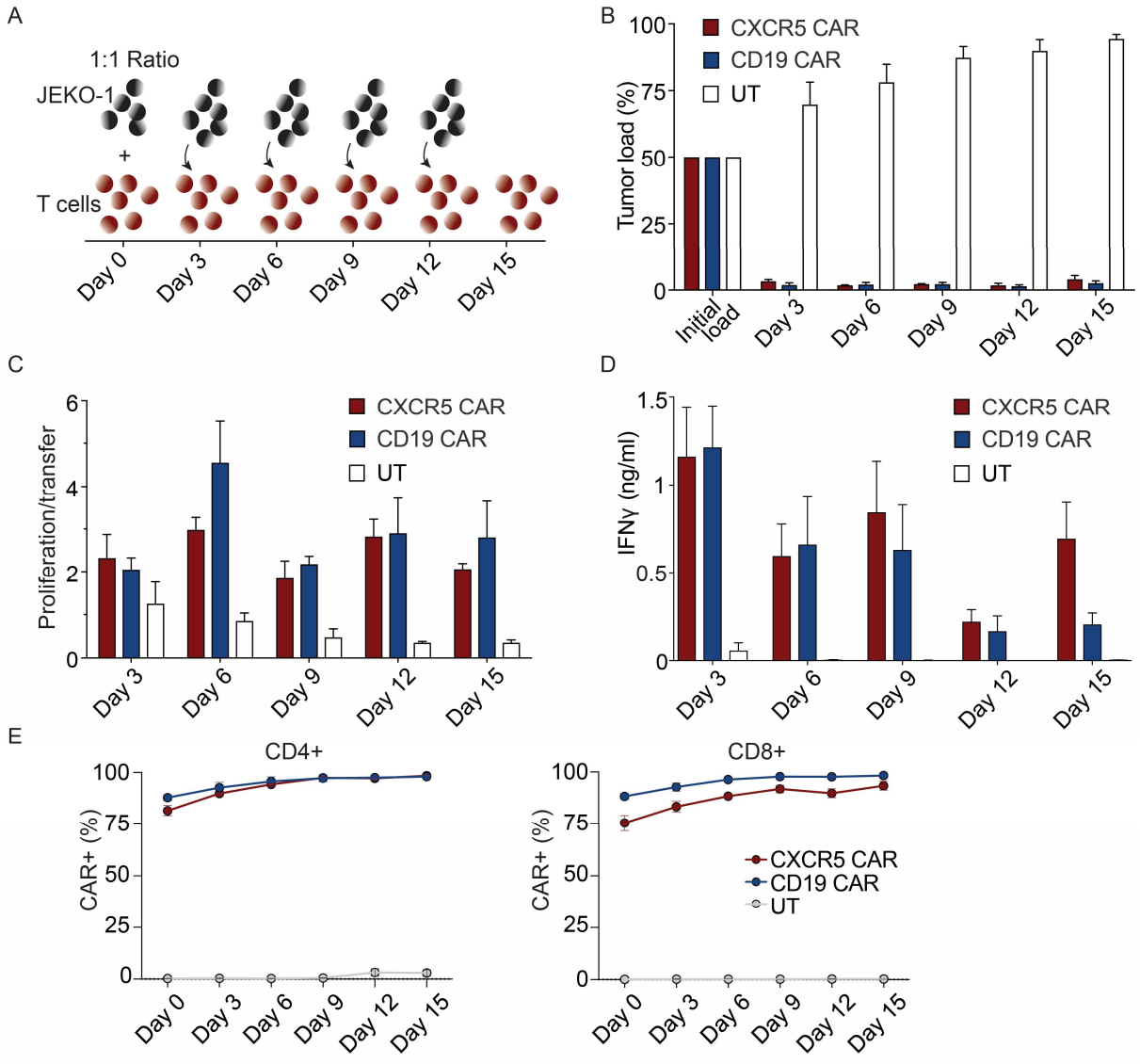

Figure 29: CXCR5 CAR T cells do not show signs of functional exhaustion upon repetitive antigenic stimulation. A T cells and JEKO-1 tumor cells were coincubated at a 1:1 ratio. Analyses were conducted every third day and the T cell to tumor cell ratio was reconstituted**. B** Tumor load is shown as percentage of viable JEKO-1 tumor cells in the culture. **C** Proliferation rate per transfer was calculated by counting the number of T cells and calculating the ratio in relation to the input T cell number. **D** IFNγ release in the supernatant was quantified by ELISA. **E** The fraction of CAR$^+$ cells was quantified for CD4$^+$ and CD8$^+$ T cells. Bars and dots represent mean ± SEM of 4 independent donors (UT, CD19) or 5 independent donors (CXCR5). Data was collected in collaboration with Dr. Mario Bunse.

The exhaustion markers PD-1, LAG-3 and TIM-3 were also measured every 72 h (Figure 30). $CD8^+$ T cells did not upregulate these markers during the experiment. $CD4^+$ T cells expressed higher levels of PD-1, which increased during the course of the experiment in anti-CXCR5 and anti-CD19 CAR T cells (Figure 30A). On $CD4^+$ T cells, the expression levels of TIM-3 and LAG-3 were lower than on $CD8^+$ T cells (Figure 30B+C). Only for LAG-3, anti-CXCR5 CAR T cells expressed higher levels compared with anti-CD19 CAR T cells (Figure 30C). Nevertheless, general upregulation of the exhaustion markers PD-1, LAG-3 and TIM-3 was not detected, indicating that the CAR T cells did not suffer from exhaustion.

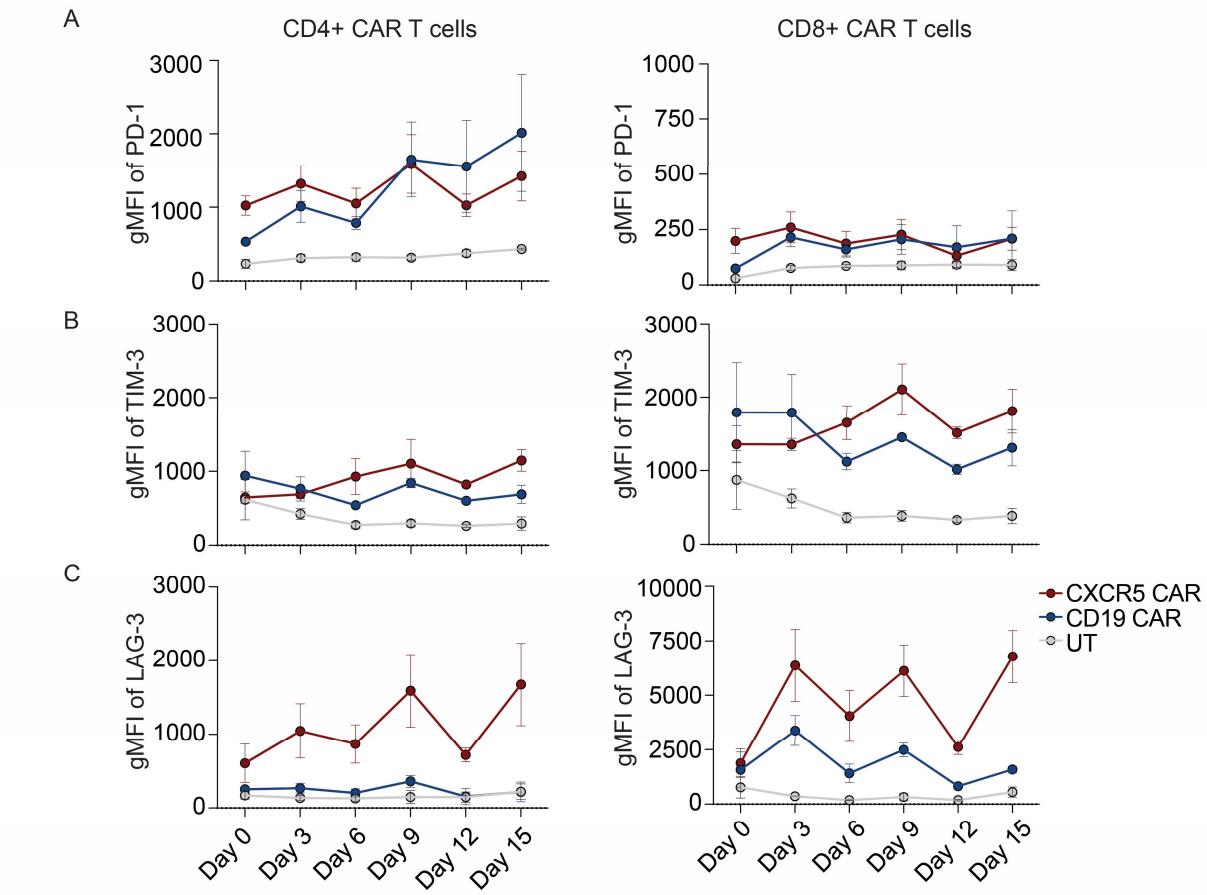

Figure 30: CXCR5 CAR T cells do not upregulate exhaustion markers upon repetitive antigen stimulation. The gMFI for the exhaustion markers A PD-1, B TIM-3 and C LAG-3 is shown for CD4+ and CD8+ CAR T cells. Cells were analyzed by flow cytometry every third day over the course of 15 days and gated for singlets and 7-AAD negative cells. Dots represent mean ± SEM of 4 independent donors (UT, CD19) or 5 independent donors (CXCR5). Data was collected in collaboration with Dr. Mario Bunse.

Additionally, the differentiation of CAR T cells into memory T cell subtypes was assessed during the course of the experiment. In the literature, around 19% of peripheral blood $CD4^+$ memory T cells ($CD45RA^-$) were described to express CXCR5 (Morita et al., 2011). Preferred T cell subtypes for adoptive T cell therapy are undifferentiated naïve T cells or central memory

T cells that are arrested at an early stage of differentiation and retained some plasticity (McLellan and Ali Hosseini Rad, 2019). CAR T cells for the *in vitro* stress test were expanded for 14 days under rhIL7/15 supplementation to support the formation of memory cells, and then assessed by flow cytometry for the distribution of the naive/memory markers CD45RA and CD45RO. As expected, the fraction of memory T cells ($CD45RA^-CD45RO^+$) was over 90% for the anti-CXCR5 CAR $CD4^+$ T cells and slightly lower for the $CD8^+$ T cells. The anti-CD19 CAR T cells harbored memory T cells in a comparable range. The large fraction of memory T cells within the anti-CXCR5 CAR T cells showed that depletion of $CXCR5^+$ T cells due to fratricide during expansion with homeostatic cytokines did not hamper memory formation. Next, the development of memory subsets in the *in vitro* stress test under inflammatory conditions was investigated.

Two main subsets of memory T cells are defined: central memory T (T_{CM}) cells ($CD62L^+CCR7^+$), which home to SLOs, and effector memory T (T_{EM}) cells ($CD62L^-CCR7^-$), which home to tissues and are equipped with cytotoxic effector functions (Sallusto et al., 1999). The majority of $CXCR5^+CD4^+$ T cells in the blood coexpresses CD62L and CCR7, which classifies them as T_{CM} cells (Schaerli et al., 2000b).

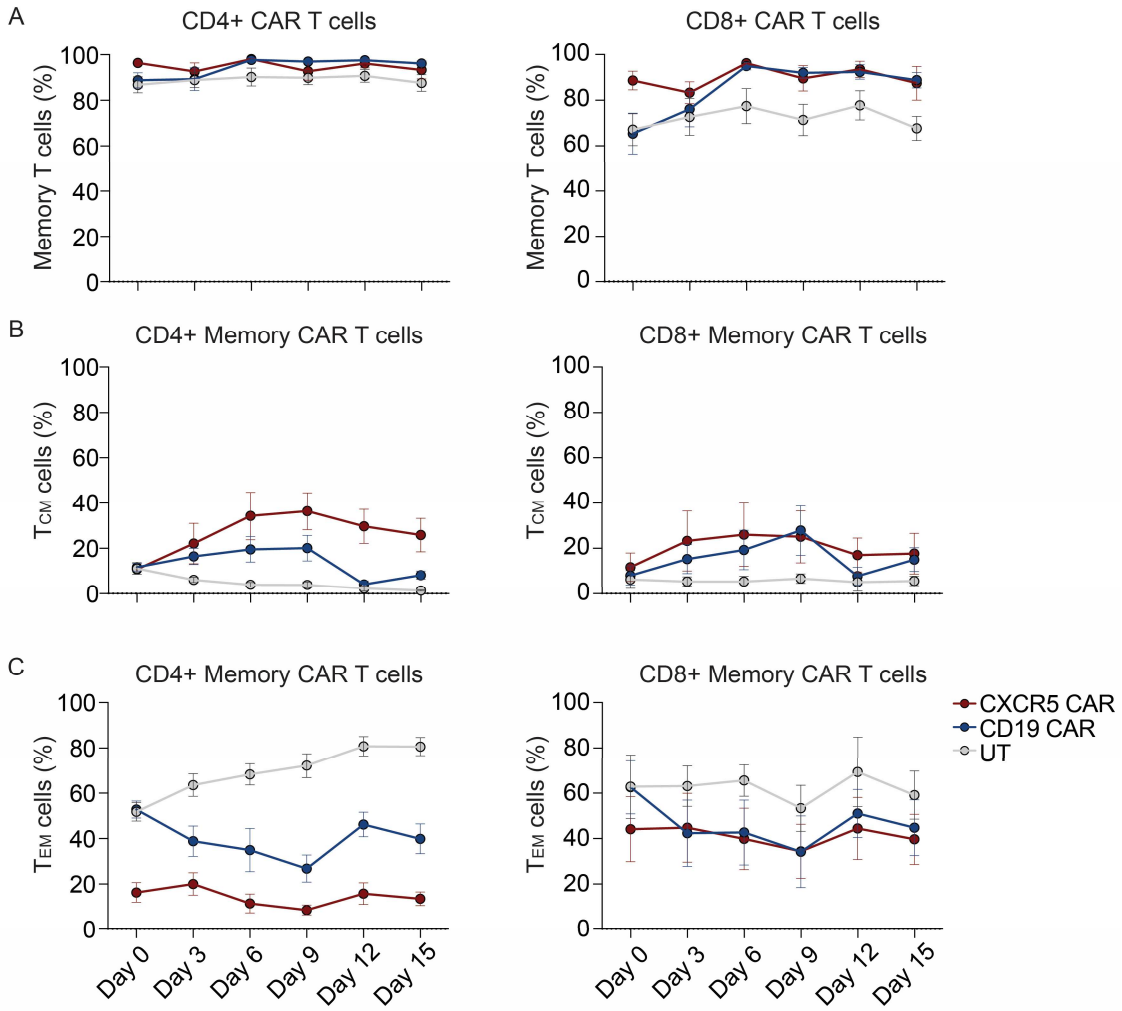

Figure 31: Anti-CXCR5 CAR T cells show a memory phenotype *in vitro*. CAR T cells were analyzed by flow cytometry every third day over the course of 15 days and gated for singlets and 7-AAD negative cells. Dots represent mean ± SEM of 4 independent donors (UT, CD19) or 5 independent donors (CXCR5). **A** Memory subsets defined as $CD45RA^{-}CD45RO^{+}$ are depicted. **B** Central memory T cells ($CD62L^{+}CCR7^{+}$) as fractions of memory cells are shown. **C** Effector memory T cells ($CD62L^{-}CCR7^{-}$) as fractions of memory cells are shown.

Despite showing low cytotoxic potential, T_{CM} cells perform better in adoptive T cell transfer than T_{EM} cells (McLellan and Ali Hosseini Rad, 2019). The CAR T cells in the *in vitro* stress test were evaluated concerning their memory subtype at the beginning of the assay and every third day. In the $CD8^{+}$ compartment, anti-CXCR5 and anti-CD19 CAR T cells had very similar fractions of T_{CM} and T_{EM} cells, with a low fraction of central memory cells and a higher fraction of effector memory cells. The $CD4^{+}$ anti-CXCR5 CAR T cells were however enriched in their central memory fraction and harbored a very small effector memory fraction compared with the anti-CD19 CAR T cells. In summary, the anti-CXCR5 CAR T cells were shown to harbor comparable memory subsets as the anti-CD19 CAR T cells, when expanded under rhIL7/15, with potentially beneficial deviations in the $CD4^{+}$ memory T cell compartment.

In the first *in vitro* stress tests, the T cells were cocultured at a 1:1 ratio with JEKO-1 tumor cells following a 14-day expansion. In this set-up, signs of T cell dysfunction or exhaustion could not be detected and the anti-CXCR5 CAR product showed a robust anti-tumor response *in vitro*. Nevertheless, in order to validate the protocol for the *in vitro* stress test, a more challenging set-up had to be applied to ultimately induce dysfunction. Therefore, CAR T cells were cocultured at a 1:10 ratio with JEKO-1 cells. Additionally, a first generation anti-CXCR5 CAR without CD28 costimulatory domain was included in the assay. First generation CARs with a CD3ζ intracellular domain generally lacked sufficient cytotoxicity and proliferation, resulting in their replacement by second generation CARs with a costimulatory domain that showed enhanced function and survival (Tokarew et al., 2019). As expansion of first generation anti-CXCR5 CAR T cells proved difficult, the expansion period for all CAR T cells was shortened to 10 days in order to improve viability at the onset of the assay. In the *in vitro* stress test, the first generation anti-CXCR5 CAR T cells showed efficient tumor cell killing in the first two rounds (Figure 32A); however, they did not proliferate and could not be assessed beyond day 6 (Figure 32B). The anti-CXCR5 and anti-CD19 CAR T cells showed a strong anti-tumor response in the first two rounds, despite the excessive amount of tumor cells. In the following days, their anti-tumor capacity decreased, resulting in the complete lack of tumor removal for both CAR products on day 15 (Figure 32A). The anti-CD19 CAR T cells strongly proliferated over 4 rounds, whereas the anti-CXCR5 CAR T cells proliferated less after the first two rounds; in the fifth round, the anti-CXCR5 and anti-CD19 CAR T cells did not proliferate (Figure 32B). IFNγ release by all antigen-specific CAR T cells was robust for the first two rounds. After day 6, the anti-CXCR5 and anti-CD19 CAR T cells produced only minor amounts of IFNγ (Figure 32C). Further, expression of the exhaustion marker PD-1 was measured on the CAR T cells. $CD4^+$ CAR T cells generally expressed higher levels and PD-1 expression increased over the course of the experiment. $CD8^+$ CAR T cells showed lower expression and only anti-CXCR5 CAR T cells upregulated PD-1 at the end of the assay (Figure 32D). Summing up, the lack of effective tumor killing, proliferation and IFNγ secretion upon repetitive stimulation with excessive amounts of tumor cells indicated that the CAR T cells suffered from functional exhaustion. The CAR T cells, including the anti-CXCR5 CAR T cells, could not maintain their function in the 1:10 assay, as opposed to in the previous 1:1 *in vitro* stress test. Long-term cocultures of tumor cells with CAR T cells were able to induce T cell dysfunction, which validated the set-up chosen for the assays. Most importantly, it can be emphasized that the anti-CXCR5 CAR T cells remained highly functional during the 1:1 *in vitro* stress test and were able to maintain their function over the first rounds of the 1:10 incubation with excessive amounts of tumor cells.

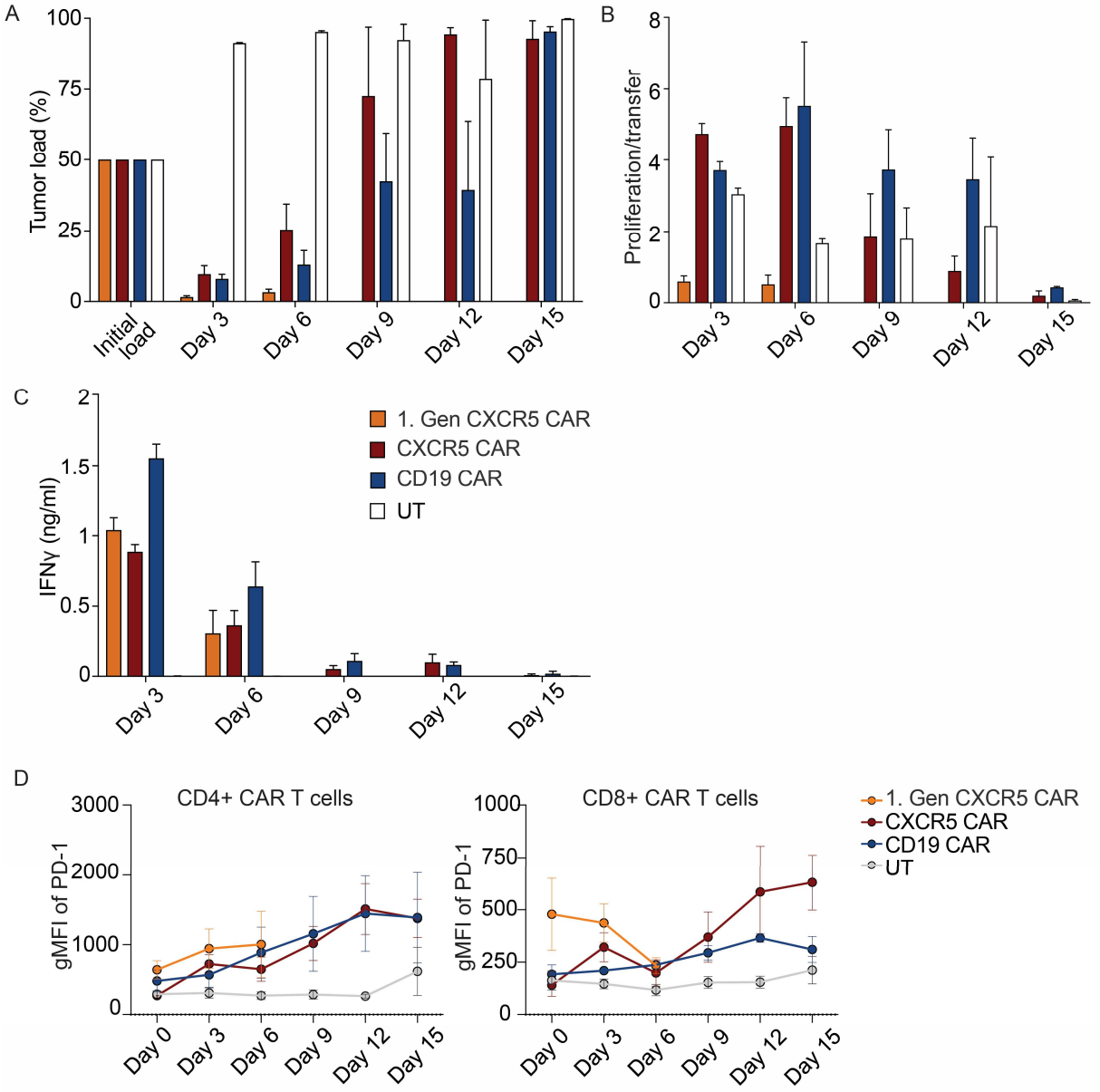

Figure 32: CAR T cells show signs of functional exhaustion upon repetitive antigen stimulation with excessive amounts of tumor cells. CAR T cells or non-transduced T cells and JEKO-1 tumor cells were coincubated at a 1:10 ratio. **A** Tumor load is shown as percentage of viable JEKO-1 tumor cells in the culture. **B** Proliferation rate per transfer was calculated by counting the number of T cells and calculating the ratio in relation to the input T cell number. **C** IFNγ release in the supernatant was quantified by ELISA. Bars represent mean ± SEM of 3 independent donors (1. Generation CXCR5 CAR until day 6).

Collectively, the data show that CXCR5 has a favorable expression pattern throughout the body in order to be targeted by CAR T cell therapy. It provides a valuable target as it is frequently strongly expressed by primary lymphoma/leukemia and especially because it allows dual targeting of tumor cells and tumor-supportive follicular helper T cells. The anti-CXCR5 CAR T cells showed promising characteristics concerning their *in vitro* and *in vivo* reactivity for a prospective use in clinical application.

4.11 The murine splenic CXCR5$^+$ T cell compartment undergoes changes upon lymphoma challenge

As previously mentioned, physiological CXCR5 expression is not restricted to mature B cells. Subsets of CD4$^+$ and CD8$^+$ T cells express CXCR5 as well. CD4$^+$CXCR5$^+$ T cells, which coexpress PD-1 and/or ICOS are commonly termed follicular helper T cells. As these T cells express CXCR5, they are most definitely targeted by the anti-CXCR5 CAR T cells. In the NSG xenotransplantation model, it was possible to assess the anti-tumor effect of CXCR5 CAR T cells by administration of human tumor cells and human CAR T cells. However, this immunodeficient mouse model, which lacks endogenous T cells, is not suitable to study the effect of anti-CXCR5 CAR T cells on the CXCR5$^+$ T cell compartment. A syngeneic mouse model is needed, in which the effect of murine CAR T cells targeting murine CXCR5 on murine lymphoma and the endogenous CXCR5$^+$ T cells can be studied. The generation of a murine anti-CXCR5 CAR was beyond the scope of this thesis; however, it was possible to investigate the influence of lymphoma challenge on the splenic CXCR5$^+$ T cell compartment in a syngeneic mouse model, which provides valuable information about how the transcriptome of CXCR5$^+$ T cells changes upon tumor progression. Single cell RNA sequencing of the murine splenic T cell compartment was the method of choice to study the CXCR5$^+$ T cell types in great detail, with a special focus on follicular helper T cells. In an effort to get an overview of the changes in the CXCR5$^+$CD3$^+$ compartment upon lymphoma challenge, C57BL/6N mice were either injected with benign B cells or *Eμ-Tcl1* tumor cells ($3x10^6$ cells per mouse) harvested from the spleen of transgenic *Eμ-Tcl1* mice. The murine *Eμ-Tcl1* lymphoma model recapitulates the progression of human chronic lymphocytic leukemia. In this mouse model, it is especially interesting to analyze the impact of tumor progression on follicular helper T cells, as expansion of cT_{FH} cells is described in CLL patients (Ahearne et al., 2013). After two weeks, murine spleens of control mice, which were injected with benign murine B cells, and diseased mice, which were injected with *Eμ-Tcl1* cells, were harvested. The diseased mice were grouped in high tumor load (45%, 46%) and low tumor load (22%, 31%) in the spleen. Two animals were pooled per sample. The spleens were homogenized and lysis was performed to remove erythrocytes. CD3$^+$ T cells were obtained after magnetic sorting. By fluorescence-activated cell sorting, doublets and dead cells were excluded, CD3$^+$CD19$^-$ cells were selected and ultimately, CXCR5 expressing cells were sorted according to the gating scheme presented in Figure 33.

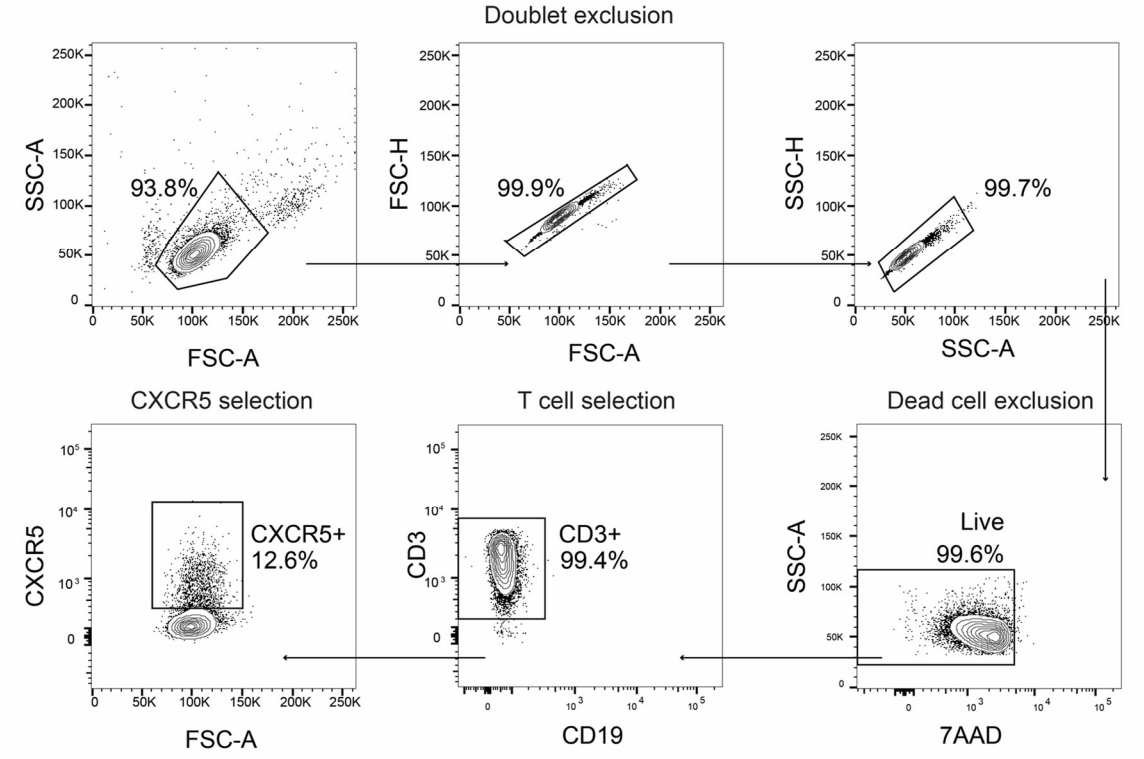

Figure 33: CXCR5 positive T cells for single cell analysis were sorted by flow cytometry. Before single cell analysis, CD3⁺ T cells were isolated by magnetic sort and further sorted by flow cytometry. Doublets and dead cells were excluded. CD3⁺ T cells and CXCR5⁺ cells were gated using an isotype control. CD3⁺CXCR5⁺ cells were further analyzed by single cell RNA sequencing.

The sorted cells were handed over to the Genomics platform at the Berlin Institute for Medical Systems Biology for single cell RNA sequencing, bioinformatical preprocessing was performed by Tadhg Crowley. Using the 10x Genomics system, the cells were first encapsulated in a barcoded gel bead, one cell per bead. Inside the bead, reverse transcription took place. cDNA derived from each cell was labeled with a unique barcode. The resulting barcoded library was then sequenced, which made it possible to obtain the gene expression profile at single cell level. The data was analyzed using the single cell genomics toolkit Seurat.

4.11.1 Murine splenic CD4⁺ and CD8⁺ T cells both express CXCR5

As magnetic sorting for CD3⁺ T cells was performed, cells in the analysis were shown to express either the *Cd8a* or *Cd4* gene (Figure 34A). The T cells were correspondingly grouped into two clusters upon visualization by Uniform Manifold Approximation and Projection for Dimension Reduction (UMAP) projection, which separated the *Cd8a*⁺ cytotoxic T cells (Cluster 1) and the *Cd4*⁺ helper T cells (Cluster 2) (Figure 34B). 66% of the cells were assigned to cluster 1 and 34% were assigned to cluster 2. These percentages might not be representative for the CXCR5⁺ CD4/CD8 T cell ratio in the murine spleen, as sample preparation and sorting

might have unevenly diminished the number of more fragile T cell subsets, but rather gives an overview of the T cells included in the following analysis.

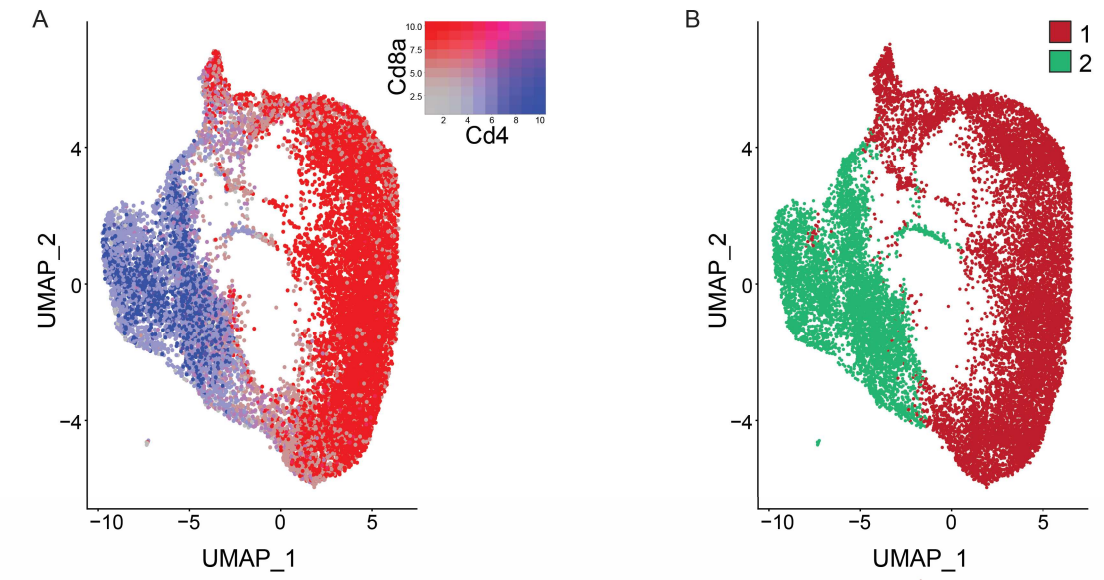

Figure 34: CXCR5⁺ *Cd8a*⁺ and *Cd4*⁺ T cells are present in the spleen. A mRNA expression of *CD4* (blue) and *Cd8a* (red) was depicted for murine splenic CXCR5⁺ T cells. **B** UMAP projection of CXCR5⁺ T cells grouped into two distinct clusters. Two mice were pooled for each of the three conditions.

4.11.2 The fraction of effector cells is increased in the murine splenic CXCR5⁺CD8⁺ T cell compartment upon tumor challenge

As expansion of circulating follicular helper T cells was described in the literature for chronic lymphocytic leukemia, follicular helper T cells were the main focus of analysis (Ahearne et al., 2013). However, it became evident that tumor challenge also impacted the CD8 compartment. Therefore, *Cd8a*⁺ T cells were analyzed in more detail. Cells of cluster 1, which was dominated by *Cd8a* expression, could be grouped into two distinct clusters. The smaller subset was enriched in mice challenged with low and high tumor load in the spleen (14%) compared with the control mice (7%), indicating that the enrichment was initiated early in tumor progression (Figure 35A). This smaller cluster differed from the bulk population by upregulation of effector genes (Figure 35B). In this effector subset, expression of the genes for perforin and granzyme B was increased, hinting that cytotoxicity is enhanced upon tumor challenge.

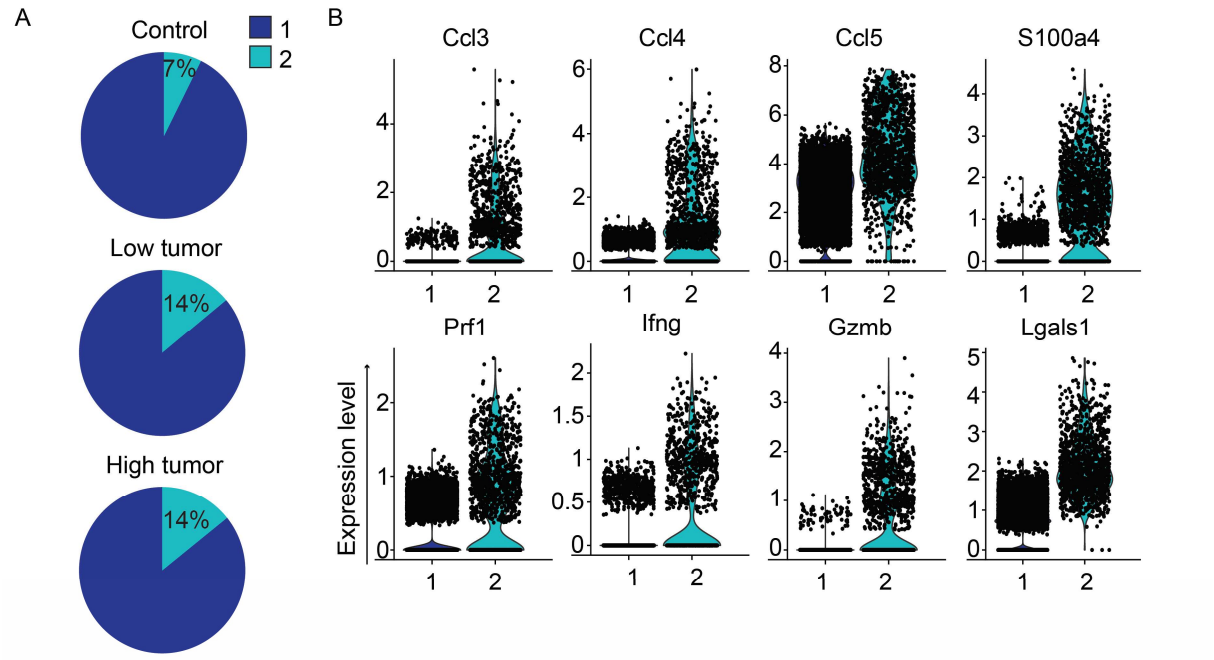

Figure 35: The fraction of effector *Cd8a*⁺ T cells is expanded upon tumor challenge. A *Cd8a*⁺ T cell fractions are depicted in pie charts. **B** Expression of cluster 2 effector CD8 T cell-specific genes is depicted for *Ccl3*, *Ccl4*, *Ccl5*, *S100a4*, *Prf1*, *Ifng*, *Gzmb* and *Lgals1* in violin plots. Two mice were pooled for each of the three conditions.

4.11.3 A T_{FH} cell-harboring cluster is expanded upon lymphoma challenge

CXCR5 expressing *Cd4*⁺ T cells were grouped into three distinct clusters after visualization by UMAP projection (Figure 36A). Expression of certain T_{FH}-specific genes, such as *Pdcd1* (which encodes PD-1), *Icos* (Wing et al., 2017), *Sostdc1* (Wu et al., 2020), *Izumo1r* (Künzli et al., 2020), *Cd200* (Chtanova et al., 2004) and *Tox* (Xu et al., 2019) was investigated within these clusters (Figure 36B). In particular, cluster 2 displayed high expression of T_{FH}-specific genes, indicating that this subpopulation harbored T_{FH} cells. Cluster 2 was further shown to be enriched upon tumor development. The T_{FH}-harboring cluster 2 was increased within *Cd4*⁺ T cells in low (39%) and high (36%) tumor load, compared to mice without tumor challenge (29%).

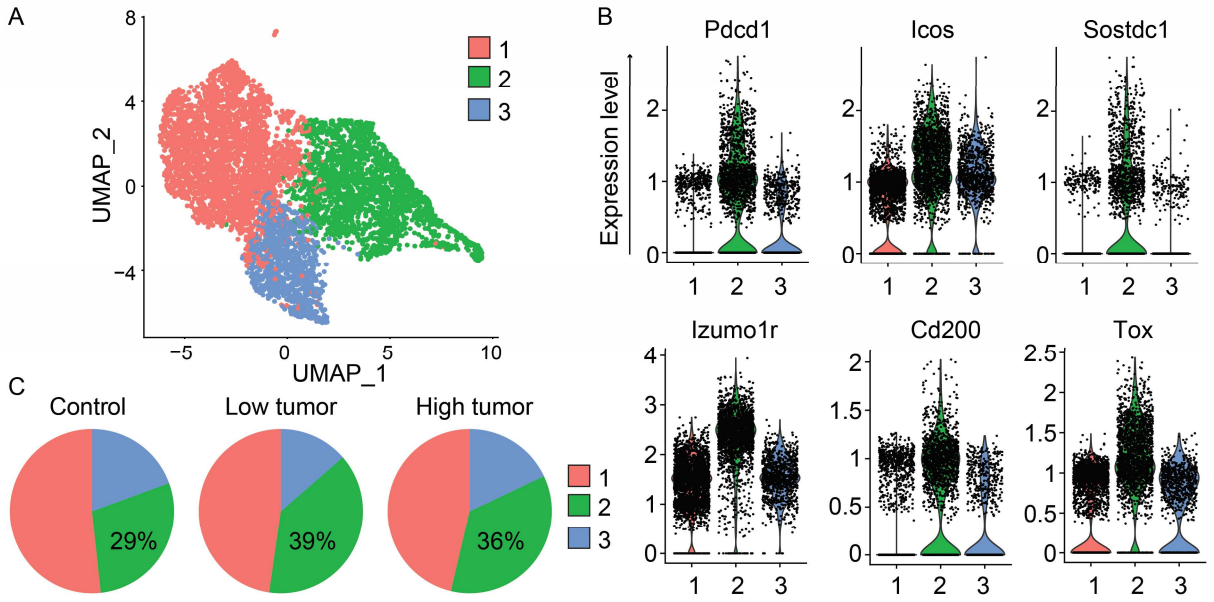

Figure 36: A follicular helper T cell-harboring cluster is expanded upon tumor challenge. A *Cd4*⁺ T cells grouped in three distinct clusters as visualized by UMAP. **B** Expression of T_{FH}-specific genes (*Pdcd1*, *Icos*, *Sostdc1*, *Izumo1r*, *Cd200* and *Tox*) is depicted in violin plots for the three *Cd4*⁺ T cell clusters. **C** The *Cd4*⁺ T cell fractions are depicted in pie charts. Two mice were pooled for each of the three conditions.

4.11.4 Follicular helper T cells and follicular regulatory T cells were successfully separated in a biased clustering

Cells of the T_{FH} cell-harboring cluster 2 were however shown to express *Foxp3*, which is a master regulator in the development of regulatory T cells. *Foxp3* expression indicated that Cluster 2 did not only include follicular helper T cells, but also follicular regulatory T (T_{FR}) cells, which fulfill regulatory functions in the B cell follicle (Linterman et al., 2011). It was not possible to separate T_{FH} and T_{FR} cells in an unbiased clustering, as both cell types express typical T_{FH} genes and regulatory gene expression was not strong enough to dominate the clustering. Therefore, biased clustering was performed, using high and low expressing populations of the T_{FR}-specific genes *Foxp3*, *Ikzf2, Tnfrsf18* and *Prdm1* as a basis to calculate the parameters for the clustering. Using this approach, it was possible to separate the T_{FR} cell population from the T_{FH} cells (Figure 37A). Both cell populations expressed the T_{FH}-specific genes *Pdcd1* and *Icos* at high levels, with higher *Icos* expression for T_{FR} cells. *Bcl6*, the T_{FH} master regulator commonly expressed by T_{FH} as well as T_{FR} cells, was not expressed strongly in either cluster, but rather in T_{FH} cells than in T_{FR} cells (Figure 37B). T_{FR}-specific genes, such as *Foxp3*, *Ikzf2* (which encodes Helios), *Tnfrsf18*, *Ctla4* and *Prdm1* (which encodes BLIMP-1) were strongly enriched in the T_{FR} cell cluster (Figure 37C). The gene expression of *Il21*, which is usually absent in T_{FR} cells, was indeed restricted to the T_{FH} cell cluster (Figure 37D). All in all, the

expression pattern of T_{FR} and T_{FH} cell-specific genes validated the biased clustering approach. Upon tumor challenge, the fraction of T_{FR} cells was increased in mice with a high tumor load (16%), compared with low tumor-mice (9%) and control mice (8%) (Figure 37E).

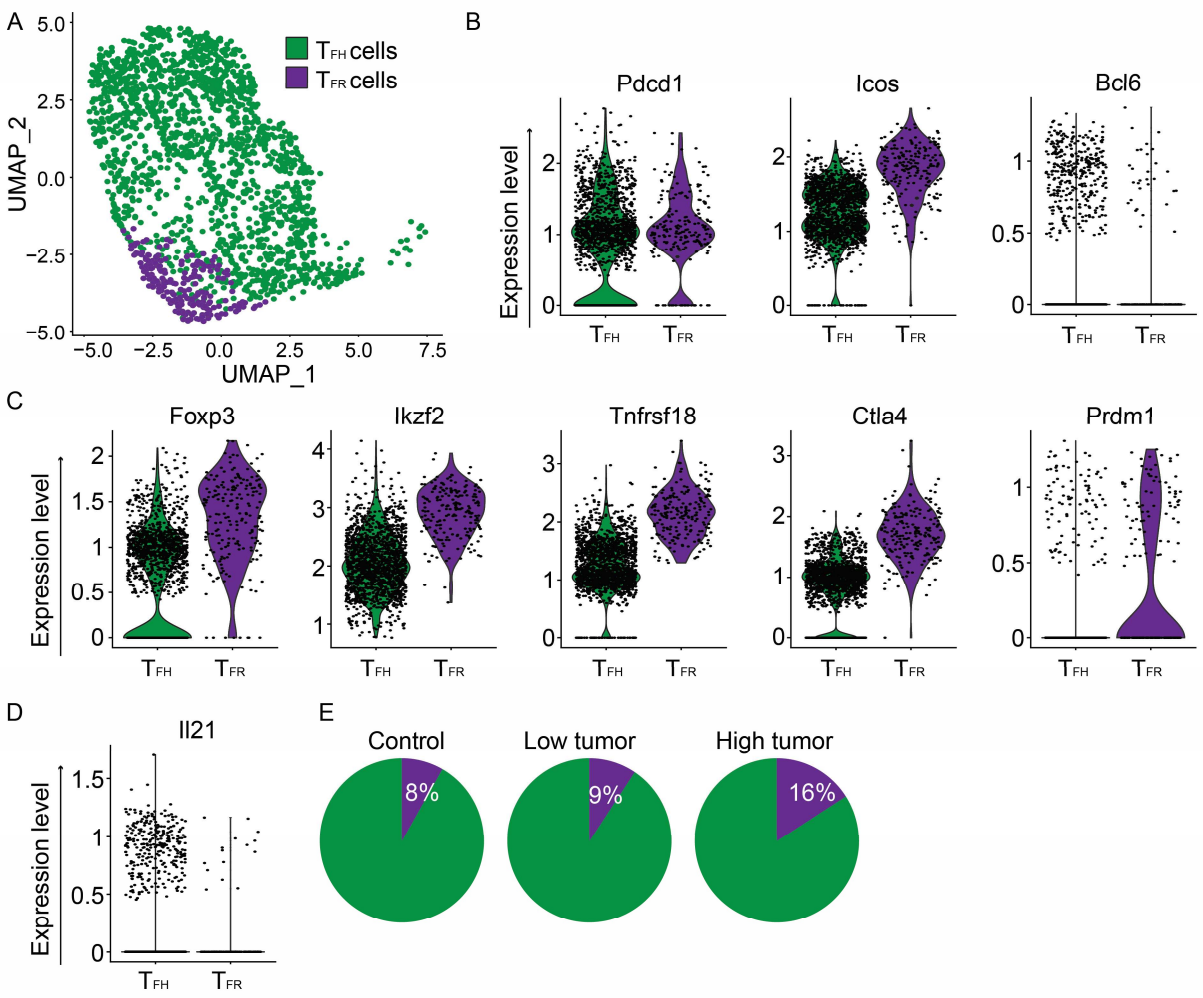

Figure 37: Follicular regulatory T cells were separated from T_{FH} cells in a biased clustering. A $CD4^+$ T cells were grouped in two distinct clusters upon biased clustering. **B** Expression of *Pdcd1*, *Icos* and *Bcl6*, which are genes equally specific for T_{FH} and T_{FR} cells, is depicted in violin plots for the T_{FH} and T_{FR} cell clusters. **C** Expression of genes specific for T_{FR} cells (*Foxp3*, *Ikzf2*, *Tnfrsf18*, *Ctla4*, *Prdm1*) is depicted in violin plots for the T_{FH} and T_{FR} cell clusters **D** *Il21* expression specific for T_{FH} cells is depicted in a violin plot for the T_{FH} and T_{FR} cell clusters. **D** The *Cd4*$^+$ T cell fractions are depicted in pie charts. Two mice were pooled for each of the three conditions.

4.11.5 Lymphoma challenge showed profound influence on T_{FH} cells and T_{FR} cells

T_{FH} cells and T_{FR} cells were analyzed regarding their expression pattern of certain chemokines, cytokines, transcription factors, costimulatory molecules and tissue residence genes corresponding to the expression analysis by Magen et al. (Magen et al., 2019). Oftentimes, gene expression gradually changed with increasing tumor load. It was however particularly remarkable that low tumor load induced differential gene expression, which in many cases differed

from control samples and the samples with high tumor load. Chemokine/chemokine receptor expression was not changed in tumor-challenged T_{FH} cells, apart from a decrease in *Cxcr4* and *Cxcr5* expression in spleens with a high tumor load (Figure 38A).

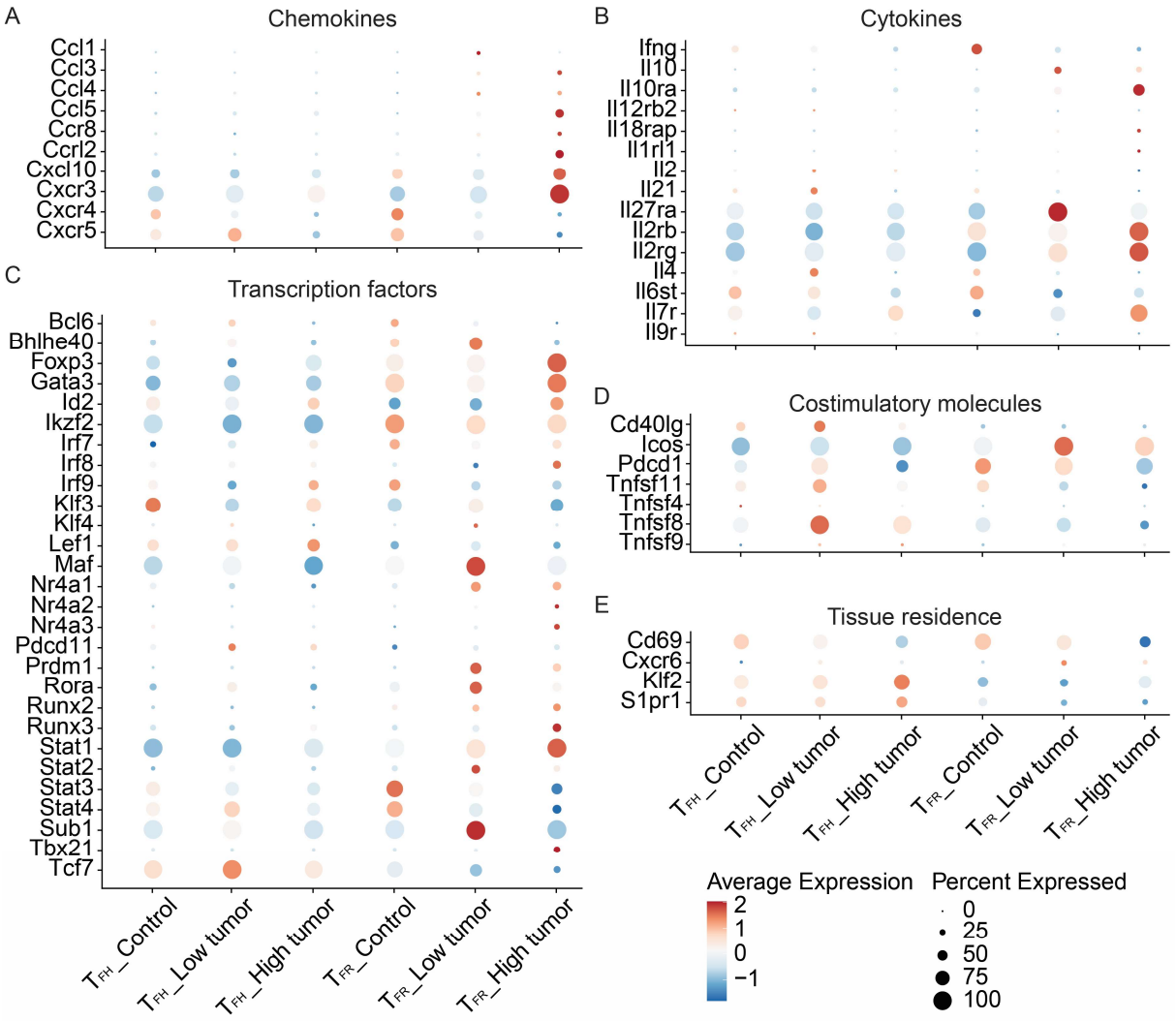

Figure 38: Gene expression is altered upon lymphoma challenge in T_{FH} and T_{FR} cells. Expression of **A** chemokine genes, **B** cytokine genes, **C** transcriptions factors, **D** genes encoding costimulatory molecules and **D** genes encoding tissue residence markers was analyzed for T_{FH} and T_{FR} cells in mice without lymphoma challenge (Control) and mice with low and high splenic tumor load. The color scale shows average gene expression; dot size depicts percentage of cells expressing the gene within the cluster. Two mice were pooled for each of the three conditions.

T_{FR} cells increasingly expressed chemokine genes, but *Cxcr4* and *Cxcr5* expression was likewise downregulated upon high tumor challenge. Especially *Cxcr3* was strongly expressed by T_{FR} cells in spleens with a high tumor load. T_{FH} cells upregulated cytokine expression of *Il4* and *Il21* uniquely upon low tumor challenge (Figure 38B). T_{FR} cells lost *Ifng* expression upon tumor challenge, but upregulated *Il10* and *Il27ra* when challenged with low tumor load, and *Il10ra*, *Il2rb/g* and *Il7r* when challenged with high tumor load. Lymphoma challenge had profound

influence on the gene expression of transcription factors, especially in T_{FR} cells (Figure 38C). In T_{FH} cells, *Klf3* was decreased upon tumor challenge. *Pdcd11* and *Tcf7* were increased in mice challenged with a low tumor load; *Irf9* and *Lef1* were induced in high tumor load. In T_{FR} cells, *Maf* and *Sub1* was strongly increased in low tumor load; *Foxp3*, *Gata3*, *Stat1* are upregulated upon high tumor challenge. T_{FH} cells upregulated expression of the costimulatory molecules *CD40lg*, *Tnfsf8* and *Tnfsf11*, whereas T_{FR} cells showed enhanced *Icos* expression in low tumor load (Figure 38D). Additionally, expression of genes involved in tissue residence differed upon tumor challenge (Figure 38E). In T_{FH} cells and T_{FR} cells, *Cd69* was downregulated; *Klf2* and *S1pr1* were upregulated with increasing tumor load in T_{FH} cells.

4.11.6 Lymphoma challenge profoundly influenced T_{FH} cells and T_{FR} cells

For better visualization of the differences in T_{FH} gene expression induced by tumor challenge, differentially expressed genes were depicted in volcano plots (Figure 39). Splenic T_{FH} cells harvested from control mice were compared with cells from mice challenged with low tumor load or high tumor load. Genes with a p-value smaller than 0.05 and a $\log_2$ fold change smaller than -0.5 or bigger than +0.5 are shown in red. For T_{FH} cells challenged with a low tumor load, *Ly6a*, *Ifi27l2a*, *Sostdc1* and *S100a11* were upregulated and fulfilled the mentioned criteria (Figure 39A). Upon high tumor challenge, *Ly6a* and *Ifi27l2a* were continuously upregulated and expression of *Tnfrsf4* was increased (Figure 39B). *Malat1* was downregulated in both low and high tumor load.

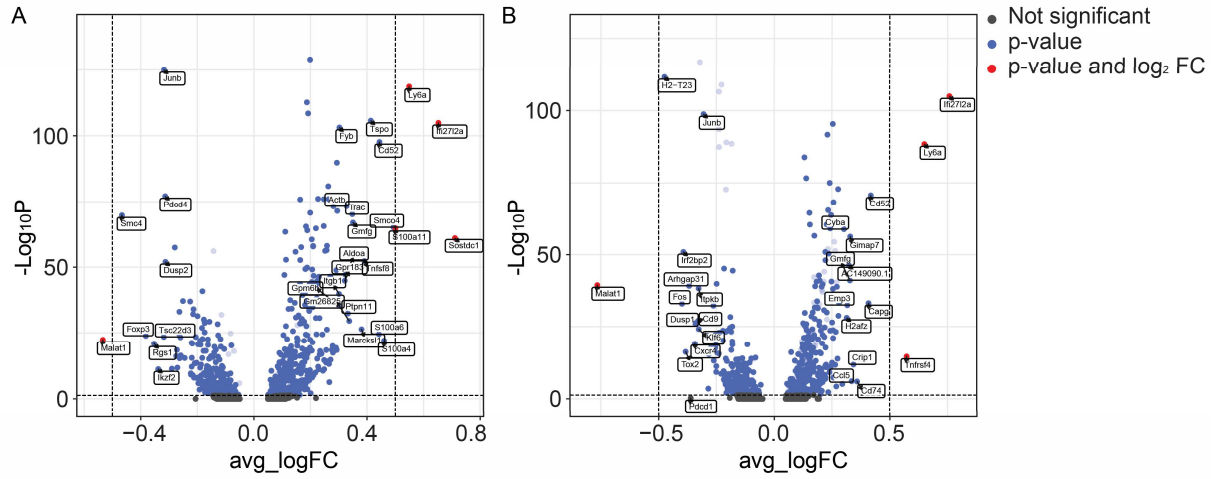

Figure 39: Lymphoma challenge induces upregulation of specific genes in T_{FH} cells. Non-significantly differentially regulated genes are depicted in grey. Genes with a p-value <0.05 are depicted in blue; genes with a p-value <0.05 and $\log_2$FC< -0.5/ $\log_2$FC> +0.5 are depicted in red. Labels are shown for genes with a p-value <0.05 and $\log_2$FC< -0.3/ $\log_2$FC> +0.3. These values are additionally indicated by dashed lines. Mice without tumor were compared with mice challenged with a **A** low tumor load or a **B** high tumor load. On the y-axis, the negative log with base 10 of the p-value is plotted; on the x-axis, the log of the fold change is plotted.

In summary, *Eμ-Tcl1* lymphoma growth induced profound changes in the murine splenic CXCR5$^+$ T cell compartment, both in CD8$^+$ and CD4$^+$ T cells. Tumor challenge influenced the T cell ratios within the subpopulations. In the CD8$^+$ subset, the fraction of cells expressing cytotoxic effector genes was increased. In the CD4$^+$ subset, the fractions of T_{FH} and T_{FR} cells were enlarged, with the T_{FH} cells being increased early on upon low tumor challenge and the T_{FR} cells later at a high tumor load. Single cell RNA sequencing analysis allowed to obtain gene expression data at single cell level. It was shown that lymphoma growth changed expression levels in both T_{FH} and T_{FR} cells for chemokines, cytokines, transcription factors, costimulatory molecules and tissue residence genes and induced upregulation of certain genes. Remarkably, low tumor induced a unique gene expression pattern, which was different from the control and the high tumor sample. The collected data give a comprehensive insight in the CXCR5$^+$ T cell subsets upon tumor challenge and provide information about the environment anti-CXCR5 CAR T cells would encounter in the spleen.

5 Discussion

5.1 CXCR5 is a promising novel target for CAR T cell therapy

Since the introduction of CAR T cell therapy, the prognosis for relapsed and refractory patients of aggressive B-cell lymphomas has strongly improved. The median survival has increased from 6 months with conventional therapy to more than two years with anti-CD19 CAR T cell therapy, as shown in the ZUMA-1 study (Crump et al., 2017; Locke et al., 2019). CAR T cell therapy has given hope to patients previously running out of treatment options. Nevertheless, a large fraction of patients is refractory to anti-CD19 CAR treatment or relapses. Reasons for treatment failure are complex and involve CAR T cell dysfunction and insufficient persistence in the patient, immune evasion, but also loss of CD19 expression. CD19 expression on the tumor population is often not homogeneous and subsets lack or express low levels of CD19 (Abramson et al., 2019). Mechanisms of CD19 loss include genetic alteration, such as frameshift mutations, and loss of heterozygosity, resulting in a lack of surface antigen (Orlando et al., 2018). Other mutational events cause alternative splicing, which leads to CD19 variants that lack the epitope targeted by the CAR (Sotillo et al., 2015). CD19 loss can also result from alterations in the associated molecules CD21 and CD81 that form the coreceptor complex, which disrupts CD19 membrane transport (Braig et al., 2017; Velasquez and Gottschalk, 2017). These lymphoma cells are not recognized and killed by the CD19 CAR T cells, which causes the outgrowth of loss variants. Other treatment options for patients suffering from refractory or relapsed aggressive B cell neoplasms, which target novel tumor-specific or tumor-associated antigens, are still urgently needed. The tumor-associated chemokine receptor CXCR5 was identified as a promising target for CAR T cell therapy.

5.1.1 CXCR5 is highly expressed in B-NHL

The chemokine receptor CXCR5 is crucial in directing B cells to the B cell zones of secondary lymphoid organs (Förster et al., 1996). Chemokine receptor expression on neoplastic B cells commonly mirrors the expression pattern of their healthy counterparts. CXCR5 was accordingly found on B non-Hodgkin lymphomas derived from mature B cells, especially in lymphomas with nodular dissemination (López-Giral et al., 2004). Large-scale mRNA data accessible on genevestigator.com visualized *Cxcr5* expression for a broad range of malignancies. A query of the HS_AFFY_U133PLUS_2-0 microarray database, which includes 710 cancer categories, showed very high *Cxcr5* expression for chronic lymphocytic leukemia (n=1039), mantle cell lymphoma (n=37), follicular lymphoma (n=196), diffuse large B cell lymphoma (n=854), marginal zone lymphoma (n=52) and Burkitt's lymphoma (n=16), with especially high expression in CLL, MCL and FL. Additionally, this dataset contained information about the *Cxcr5* expression level for each patient. Of 1039 CLL samples, 998 showed high expression and 41 showed

medium expression. In all 37 MCL samples, high *Cxcr5* mRNA expression was detected. 191 FL patients had high *Cxcr5* expression and 5 FL patients had medium expression levels. In 854 diffuse large B cell lymphoma samples, 721 biopsies highly expressed *Cxcr5*, 131 samples showed medium expression levels and 2 patients had low *Cxcr5* expression. Of 52 marginal zone lymphoma samples, *Cxcr5* was highly expressed by 39, 13 had medium expression. 12 Burkitt's lymphoma samples highly expressed *Cxcr5* and 4 showed medium expression levels. In the literature, the CXCR5 expression pattern in these B-NHL entities was confirmed on protein level by flow cytometric analysis. Precursor B acute lymphoblastic leukemia, which is a neoplasm of immature B cells, and multiple myeloma, which originates from plasma cells, lacked CXCR5 expression (Dürig et al., 2001; Middle et al., 2015b). Dürig et al. published individual patient data and showed CXCR5 expression by flow cytometry on all 23 CLL, 4 MCL and 3 FL samples (Dürig et al., 2001).

In the presented thesis, extensive CXCR5 expression analysis of B cell lines and primary B-NHL patient material supported and expanded the expression pattern described in the literature. An important aspect in clinical application of immunotherapy is also the antigen frequency within the tumor cell population; antigen absence on a subset can lead to the outgrowth of antigen-loss variants. In the analyzed patient samples, robust and ubiquitous CXCR5 expression was detected for FL and CLL. In MCL, expression ranged from low to high; half the samples lacked CXCR5 on a fraction of cells. In MZL, one of four samples showed robust CXCR5 expression on the main population. CXCR5 negativity was further confirmed for B cell precursor neoplasms and MM.

Abundant expression on mature B cell neoplasms makes CXCR5 a valuable target in CAR T cell therapy, as large amounts of patients harbor CXCR5 expressing tumors and could benefit from treatment with anti-CXCR5 CAR T cell therapy.

5.1.2 CXCR5 is expressed on B cell-supportive follicular helper T cells

Germinal center (GC) reactions ensure the production of high affinity antibodies in secondary lymphoid organs in response to an infection. In GCs, B cells undergo selective proliferation and differentiation. Most importantly, their antibody genes are mutated in a process called somatic hypermutation, which results in antibodies of higher affinity. Follicular helper T cells play a central role in the processes in the germinal centers. They are $CD4^+$ cells characterized by the expression of CXCR5, which allows them to access B cell follicles and GCs. Further, they are described as PD-1^+ and $ICOS^+$ (Victora and Nussenzweig, 2012). B cells in the germinal center circulate between the light and the dark zone. In the light zone, B cells have access to antigen. The B cells bind the antigen and present it in an MHC complex to T_{FH} cells, which subsequently provide them with proliferation and survival stimuli. Stimulated B cells make their

way to the dark zone, in which they further proliferate and undergo somatic hypermutation. When they return to the light zone, the B cells with the highest antigen affinity are again selected by the follicular helper T cells (Crotty, 2014). T_{FH} cells influence many steps in germinal center processes, either by cytokine secretion (IL4 and IL21) or interaction of costimulatory molecules (PD-1, ICOS, CD40L). Cytokines produced by T_{FH} cells, especially IL4 and IL21, are major inducers of GC B cell survival, proliferation and class switch (Crotty, 2011). Further, T_{FH}-derived IL21 was shown to regulate germinal center size and to promote plasmablast development from germinal centers. IL21 is strongly expressed by T_{FH} cells and GC B cells upregulate expression of the IL21 receptor, favoring plasma cell differentiation (Zhang et al., 2018). The PD-1/PD-L1/2 interaction between follicular helper T cells and B cells was described to regulate long-lived plasma cell differentiation. In the absence of PD-1, cell death in the GC was increased and T_{FH} cytokine production was reduced (Good-Jacobson et al., 2010). T_{FH} cells additionally express ICOS and CD40L at high levels, which activate B cells (Breitfeld et al., 2000).

The counterparts of classical T_{FH} cells in secondary lymphoid organs are circulating T_{FH}-like (cT_{FH}) cells in the blood, which are $CD4^+$ cells characterized by CXCR5 expression. They have similar functional characteristics as T_{FH} cells in the germinal centers and support humoral immune responses (Morita et al., 2011; Ueno, 2016). Peripheral blood cT_{FH} cells are easily accessible in humans and were therefore preferentially the subject of studies.

As described in the literature, peripheral blood cT_{FH} cells are significantly enriched in B-NHL patients and the plasma concentration of the T_{FH} key cytokine IL21 is increased, which was both correlated with negative prognosis (Zhou et al., 2017). In particular for chronic lymphocytic leukemia and follicular lymphoma, a tumor-supportive function of T_{FH} cells was discussed. In CLL patients, the cT_{FH} population is increased, especially in advanced disease stages (Ahearne et al., 2013; Cha et al., 2013). T_{FH} cells are also strongly expanded in the lymph nodes of CLL patients (de Weerdt et al., 2019). IL4 and IL21 are the main cytokines produced by T_{FH} cells. Cytokine-mediated effects on patient-derived CLL cells *in vitro* have been described. IL4 increased CLL cell survival and apoptosis resistance (Dancescu et al., 1992). IL21 stimulation induced apoptosis in leukemic cells (de Totero et al., 2008). Combined IL4/21 signaling however induced proliferation in leukemic cells, without differentiation or apoptosis. IL21 additionally promoted proliferation of side population cells, which are related to enhanced chemotherapy resistance (Ahearne et al., 2013). CD40 stimulation additionally induced upregulation of IL21 receptor expression on leukemic cells and enhanced the effect of IL21 stimulation (de Totero et al., 2006). IL21 in combination with CD40/CD40L signaling also induced CLL proliferation (Pascutti et al., 2013). *In vivo*, IL4 supplementation in a clinical trial with CLL patients was shown to increase the number of CLL cells (Lundin et al., 2001). Not only the

influence of T_{FH}-associated factors on CLL cells, but also the reciprocal effect of CLL progression on the T cell compartment has been investigated. In a study with CLL patients, cT_{FH} cells were shown to be shifted towards a T_H2 and T_H17-like cT_{FH} cells, which as opposed to T_H1-like cT_{FH} cells, secrete IL21 (Cha et al., 2013). Mouse models, such as the *Eμ-Tcl1* mouse model, which is the most widely used and validated murine model for human CLL, were utilized to study how leukemia growth affects T cells. The validity of the *Eμ-Tcl1* mouse model was further confirmed by Gorgun et al., who showed that changes in the function and $CD4^+$/$CD8^+$ gene expression profiles of T cells induced by *Eμ-Tcl1* in the mouse model were similar to changes between CLL patients and healthy donors (Gorgun et al., 2009). Hofbauer et al. observed that absolute T cell numbers increased and that the T cell subsets were skewed towards an antigen-experienced memory phenotype in *Eμ-Tcl1* tumor-challenged mice (Herek and Cutucache, 2017; Hofbauer et al., 2011).

However, to our knowledge, an in-depth study of the tumor cell-induced changes in the T cell subsets with a focus on follicular helper T cells, especially on single-cell gene expression level, has not been conducted. In this thesis, single cell RNA sequencing of the tumor-challenged murine splenic $CXCR5^+$ T cell compartment was performed and a profound impact of CLL pathogenesis on follicular helper T cells was described. In mice challenged with *Eμ-Tcl1* lymphoma cells, the fraction of splenic T_{FH} cells was enlarged. Early in tumor progression, the T_{FH} cells were shown to upregulate *Il4*, *Il21* and *Cd40lg*. These findings were in line with the previous findings in the literature and support the importance of T_{FH}-mediated IL4, IL21 and CD40L signaling especially in the early stages of CLL. Upon *Eμ-Tcl1* lymphoma challenge, murine splenic T_{FH} cells upregulated *Ifi27l2a*, which is an interferon-stimulated gene (ISG). ISGs are generally involved in the inhibition of viral infections (Schoggins, 2019). Also, *Ly6a* was upregulated, which is known as an activation marker linked to proliferation, indicating an enhanced activation status in tumor-challenged T_{FH} cells (Hsu et al., 2014; Malek et al., 1986). The T_{FH}-specific gene *Sostdc1* was upregulated early in tumor progression and *Sostdc1* expressing T_{FH} cells are described to promote follicular regulatory T cell differentiation, which is in line with an enriched T_{FR} fraction in the advanced tumor stage (Wu et al., 2020). *Tnfrsf4*, which encodes CD134/OX4, is upregulated in T_{FH} cells upon high splenic tumor load. OX40 is a costimulatory receptor, which promotes survival, proliferation and cytokine production in T cells upon OX40 ligand binding. It also serves as a T cell activation marker (Croft et al., 2009). Also, OX40 signaling induces CXCR5 and IL4 expression in $CD4^+$ T cells (Flynn et al., 1998; Walker et al., 1999). *Malat1*, which encodes a long noncoding RNA, was downregulated in T_{FH} cells upon lymphoma challenge. As suppression of Malat1 is a hallmark of $CD4^+$ T cell activation, this is in accordance with the collective findings presented in this thesis that murine splenic

T_{FH} cells showed an activated phenotype when challenged with chronic lymphocytic leukemia-like tumor cells (Hewitson et al., 2020).

As mentioned earlier, the second B-NHL tumor entity, for which tumor support by follicular helper T cells is discussed, is follicular lymphoma. Pangault et al. analyzed the gene expression profile of the non-B cell compartment in lymph nodes of follicular lymphoma patients. They found a T_{FH} gene signature and upregulation of genes relevant for T cell proliferation and activation, including *Il4* and *Tnfrsf4*, which were also upregulated in *Eμ-Tcl1* CLL lymphoma challenged murine splenic T_{FH} cells as presented in this thesis. The authors were able to confirm T_{FH} cells as the IL4 source and also described T_{FH} cell enrichment in the FL lymph node microenvironment (Pangault et al., 2010). *In vitro*, FL cells profited from T_{FH} cell coculture and were rescued from spontaneous apoptosis. The authors also analyzed FL-derived T_{FH} cells in detail and detected upregulation of *Il4* and *Cd40lg*, which were also shown to be upregulated in the *Eμ-Tcl1*-challenged T_{FH} cells in this thesis. FL cell culture with anti-CD40L and anti-IL-4Rα neutralizing mAbs confirmed that IL4 and CD40 ligand contribute to lymphoma cells survival (Amé-Thomas et al., 2012). It was further demonstrated that IL4 additionally contributes to FL tumorigenesis in an indirect manner by inducing CXCL12 in stromal cells. Induction of the CXCL12/CXCR4 loop promotes lymphoma cell activation and migration (Pandey et al., 2017). In this work, $CD4^+CXCR5^+$ cells were isolated from human peripheral blood by magnetic separation; the positive ($CD4^+CXCR5^+$) and negative ($CD4^+CXCR5^-$) sort fractions were subsequently cocultured with CAR T cells. It was possible to show that anti-CXCR5 CAR T cells specifically secreted IFNγ in response to the positive sort fraction that included the cT_{FH} cells. Anti-CD19 CAR T cells did not show this reaction as CD19 was absent from T cells. This work could further demonstrate that cT_{FH} cells in patient samples of FL and CLL were killed *in vitro* upon incubation with anti-CXCR5 CAR T cells. cT_{FH} killing was exclusively performed by anti-CXCR5 CAR T cells; anti-CD19 CAR T cell-mediated killing was restricted to CD19 expressing B cells. Malignant B cells are provided with strong proliferation and survival stimuli by T_{FH} cells. Thus, removal of T_{FH} cells by CAR T cell therapy could be beneficial for FL and CLL patients.

T_{FH} cells are also involved in the pathogenesis of autoimmune disorders. A characteristic feature of autoimmune disease is the presence of autoantibodies, which target the body's own tissues (Ma et al., 2017). Interestingly, for numerous autoimmune diseases, an increase of cT_{FH} cells in the blood is described (Crotty, 2014). Patients with severe systemic lupus erythematosus (SLE) present with increased fractions of cT_{FH} cells in the blood, which express the associated molecules ICOS and PD-1 at high levels (Simpson et al., 2010). In an SLE mouse model, cT_{FH} cells were shown to expand in proportion to GC T_{FH} cells. Autoimmunity was described to be dependent on germinal center formation and aberrant enhanced positive selection by T_{FH} cells. Additionally, the authors showed that autoimmune symptoms in the mice

improved upon loss of an allele for *Bcl6*, the T_{FH} master regulator, or *Sap*, which encodes a T_{FH} adaptor protein (Linterman et al., 2009). Enhanced IL21 production and CD40/CD40L interactions were described to promote survival and plasma cell differentiation of autoreactive B cells in these mice (Han et al., 2015). Elevated cT_{FH} cell percentages were found in Sjögren's syndrome and correlated with increased autoantibody levels (Szabo et al., 2013). T_{FH} cell-mediated B cell hyperactivity could be reduced by treating patients with a T cell inhibitory antibody, resulting in reduced T_{FH} cell numbers, ICOS expression and IL21 levels, and ultimately lower disease scores in Sjögren's patients (Verstappen et al., 2017). Another autoimmune disease, in which cT_{FH} cells are expanded, is rheumatoid arthritis. In these patients, T_{FH} cell expansion correlated with autoantibody levels and plasma IL21 was increased (Ma et al., 2012). IL21 in rheumatoid arthritis patients was further shown to induce B cell differentiation to plasmablasts and promote antibody production (Liu et al., 2012). In a murine arthritis model, pathogenesis was strikingly dependent on CXCR5 and mice lacking CXCR5 on T cells did not develop disease, indicating that colocalization of B cells and T_{FH} cells is crucial for disease onset (Moschovakis et al., 2017). Traditional therapy of autoimmune disorders mostly depends on immunosuppressive agents, but long-term treatment can be tricky and can result in opportunistic infections (Rosenblum et al., 2012). CAR T cell therapy provides a new tool of targeted therapy. In a murine lupus model, it was demonstrated that anti-CD19 CAR T cells stopped autoantibody-production. Treated mice had increased survival and disease progression was reversed in organs typically targeted by autoantibodies in lupus (Kansal et al., 2019). Some clinical trials for patients with autoimmune disorders are currently in progress: Patients suffering from myasthenia gravis are treated with a CAR product targeting the B cell maturation antigen (BCMA) (NCT04146051). Systemic lupus erythematosus patients receive anti-CD19 CAR T cells (NCT03030976) and pemphigus vulgaris patients are administered T cells targeting specific autoantibody producing B cells (NCT04422912) (clinicaltrials.gov, 2020). Reighard et al. proposed treatment of autoimmune patients by eliminating T_{FH} cells with CAR natural killer (NK) cells. The authors developed a CAR with a PD-1 ligand domain, which binds selectively to T_{FH} cells, which show high PD-1 expression. The CAR NK cells were able to kill T_{FH} cells and reduce T cell-induced B cell activity. In a humanized lupus-like mouse model, it was possible to reduce symptoms upon treatment with anti-PD-1 CAR NK cells (Reighard et al., 2020). As anti-CXCR5 CAR T cells also target T_{FH} cells, autoimmune patients could possibly benefit from treatment with these CAR T cells in a similar way and disease progression could be slowed down.

5.1.3 CXCR5 as a target on malignancies beyond B cell neoplasms

CXCR5 is not only a target in the treatment of B cell neoplasms, but is also involved in the pathogenesis of other malignancies. Angioimmunoblastic T cell lymphoma (AITL) is a rare, aggressive neoplasm of follicular helper T cells. It is a mature peripheral T cell lymphoma, which accounts for 1-2% of non-Hodgkin lymphomas. The malignant cells commonly express the T cell markers CD3, CD4 and the typical T_{FH} co-stimulatory molecules PD-1, ICOS, the chemokine receptor CXCR5 and the transcription factor BCL6 (Gaulard and de Leval, 2011; Lunning and Vose, 2017). Additionally, the cells uniformly express the ligand for CXCR5, the chemokine CXCL13 (Dupuis et al., 2006; Grogg et al., 2005). In AITL patients, the lymph node structure is destroyed and follicles are absent. Follicular dendritic cells are expanded and HEVs proliferate. Moreover, patients present with symptoms of B cell expansion (Ansel et al., 2000; Dupuis et al., 2006). The prognosis is poor, with a 5-year median survival of 32%. Oftentimes, induction therapy induces a strong response, but the patients relapse quickly. As of now, there is no gold standard in therapy; first-line treatment is usually CHOP (cyclophosphamide, doxorubicin, vincristine, prednisone) combined chemotherapy. Chemotherapy can be combined with targeted drugs such as lenalidomide, an immunomodulatory substance used in the treatment of B cell malignancies, the anti-CD52 antibody alemtuzumab, which targets both B and T cells, or the histone deacetylase (HDAC) inhibitor romidepsin (Lunning and Vose, 2017). As the prognosis is poor and treatment options are limited, patients are still in dire need of novel therapies against this aggressive T cell lymphoma subtype. As CXCR5 is expressed on follicular helper T cells, the anti-CXCR5 CAR T cells are expected to recognize and deplete the tumor cells in the patient.

Follicular dendritic cell sarcoma is another tumor entity, whose patients might benefit from treatment with anti-CXCR5 CAR T cells. It is an aggressive neoplasm of follicular dendritic cells (FDCs), which guide $CXCR5^+$ mature B cells into the follicle by secreting CXCL13 and engage them in a CXCL13/lymphotoxin positive feedback loop. Most patients present with lymphadenopathy and receive chemotherapy, radiation and surgery, but 81% of them relapse (Soriano et al., 2007). In follicular dendritic cell sarcoma, neoplastic FDCs were also shown to secrete CXCL13 (Vermi et al., 2008). CXCL13 secreted by FDCs induces upregulation of membrane lymphotoxin in B cells (Ansel et al., 2000). Lymphotoxin then in turn activates FDCs (Myers et al., 2013). As the maintenance of FDC networks requires continues interaction with B cells expressing lymphotoxin, signaling inhibition quickly results in FDC disturbance (Mackay and Browning, 1998). Most likely, follicular dendritic cell sarcoma cells also express the lymphotoxin receptor and disturbance of the lymphotoxin axis might reduce activation signals. This could be achieved by inducing B cell aplasia by treatment with anti-CXCR5 CAR T cells.

The CXCR5/CXCL13 axis was further suggested to play a role in some solid tumors (Kazanietz et al., 2019). Numerous benign solid tissues were shown to be CXCR5 negative on mRNA and protein level in the scope of this work. However, certain malignant cells, such as breast cancer cells, were described in the literature to upregulate CXCR5 expression. Panse et al. detected weak protein expression of CXCR5 by western blot in breast cancer lysates, but not in healthy tissue. Nevertheless, it has to be considered that the samples might not be free from CXCR5 expressing immune cells. Interestingly, breast cancer cell lines, which were CXCR5 positive in real-time PCR and western blot, only showed intracellular CXCR5 expression in flow cytometry; surface expression was not detected (Panse et al., 2008). It has to be carefully analyzed if CXCR5 is indeed expressed on the surface of malignant cells derived from solid tumors. Ideally, reactivity of anti-CXCR5 CAR T cells against potential CXCR5 expressing target cells should be investigated in *in vitro* cocultures.

For many tumor entities, survival benefits from tertiary lymphoid structures within or near the tumor mass, which depend on the CXCR5/CXCL13 axis, were described. Tertiary lymphoid structures, which are also present in inflamed and infected tissues, resemble lymph nodes, are correspondingly divided in T- and B-cell zones and harbor germinal centers. They give rise to cells that initiate and sustain the anti-tumor immune response. The presence of these tertiary structures is a positive prognosis marker, especially in patients treated with immunotherapies (Dieu-Nosjean et al., 2014). In triple-negative breast cancer, lymphocytic infiltrates are associated with improved overall survival (Luen et al., 2019). In this type of breast cancer, patients with high CXCL13 levels showed longer disease-free survival (Schmidt et al., 2018). Analysis of the CD4 populations in breast tumors revealed that the presence of CXCL13-producing T_{FH} cells is characteristic of extensive lymphocytic infiltration organized in tumor adjacent tertiary lymphoid structures and beneficial for patient survival and response to chemotherapy (Gu-Trantien et al., 2013). The presence of lymphocyte infiltrates might however not necessarily be causal for improved survival by eliciting an adaptive immune response against the cancerous tissue (Gu-Trantien et al., 2013). They might rather be an indicator of a less immunosuppressive tumor microenvironment, which permits the proliferation of lymphocytes. Thus, if the CAR T cells efficiently eradicate the tumor cells, the benefits of tumor removal might outweigh the destruction of possibly beneficial tertiary lymphoid structures.

5.2 The CXCR5 CAR shows a satisfactory safety profile

Toxicities in CAR T cell therapy can be caused by cytokine release syndrome (CRS), neurotoxicity, on-target/off-tumor autoimmune effects from attacking healthy antigen expressing tissues and off-target toxicities by CAR T cells recognizing unintended antigens (Bonifant et al.,

2016). The cytokine release syndrome is a frequent and well-known side effect. CRS can be triggered by cytokine release after direct cell lysis or T cell activation, inducing a cytokine release cascade in the surrounding cells. Patients present with a broad spectrum of symptoms, ranging from fever to organ failure and are treated with antihistamines, antipyretics or antibodies against the IL6 receptor (Shimabukuro-Vornhagen et al., 2018). Neurological toxicity, with symptoms like confusion and seizures, is often reversible. Pathophysiology is not well understood, but possibly related to increased cytokine levels (Bonifant et al., 2016).

The other two types of toxicities, on-target/off-tumor toxicity and general off-target toxicity have to be considered in the development of novel CAR T cell therapies and can be addressed in *in vitro* and *in vivo* experiments.

5.2.1 CXCR5 is a safe target for CAR T cell therapy

For the safety of a CAR T cell therapy, it is crucial to be well aware of the expression pattern of the target. Ideally, the targeted antigen is a tumor-specific neoantigen and restricted to the malignant cells. Unfortunately, this is very rarely the case. More frequently, the antigen is tumor-associated and can be also found on healthy tissues. Therefore, in order to avoid on-target/off-tumor toxicity, it has to be scrutinized whether the antigen-expressing tissues are vital and if not, if the tissue destruction by the CAR T cells can be clinically managed. An example of a tumor-associated antigen is carcinoembyronic antigen (CEA), which is not only expressed on many solid tumors, but also in the gastrointestinal tract. Targeting CEA with adoptive T cell therapy induced severe colitis (Parkhurst et al., 2011). A fatal case was described for a patient treated with anti-ERBB2 CAR T cells targeting metastatic colon cancer, which recognized low level of ERBB2 on lung epithelium (Morgan et al., 2010).

The first CAR products approved for therapy by the U.S. Food and Drug Administration targeted the CD19 antigen (Boyiadzis et al., 2018). CD19 is expressed on malignant B cells, but also on benign B cells. Therefore, successful therapy initially eradicates the benign B cell compartment. The patients benefit from the treatment; reduction of the tumor mass outweighs the negative effects of having a compromised humoral immune answer. B cell aplasia is a positive indicator of CAR T cell functionality in these patients, as functional CAR T cells efficiently remove $CD19^+$ benign as well as malignant B cells (Maude et al., 2014). Long-term B cell aplasia can also be addressed by immunoglobulin supplementation (Doan and Pulsipher, 2018). Altogether, the effects of CD19 CAR therapy on the B cell compartment have been extensively studied and have been found to be nonhazardous.

Immunotherapy in cancer targeting chemokine receptors has entered clinical practice. So far, a monoclonal antibody has been approved for the treatment of T cell malignancies and a small molecule competitive antagonist of CXCR4, which mobilizes hematopoietic stem cells to the

peripheral blood, was approved for autologous transplantation in non-Hodgkin Lymphoma and multiple myeloma (De Clercq, 2019; Subramaniam et al., 2012). Several inhibitors of chemokine receptors are in pre-clinical testing or clinical trials (Mollica Poeta et al., 2019).

Targeting chemokine receptors in CAR T cell therapy is a very novel field and, to our knowledge, only an anti-CCR4 CAR has been generated to date. Perera et at. suggested targeting CCR4, which is not only expressed on regulatory T cells, T_H2 and T_H17 T cells and platelets, but also frequently detected on T cell lymphomas (Perera et al., 2017)

Immunotherapeutic targeting of CXCR5 was proposed by Panjideh et at. The authors demonstrated that a bispecific CXCR5::CD3 antibody recruits T cells to malignant B cells and efficiently induces T cell activation *in vitro*. In a xenograft mouse model of Burkitt's lymphoma, anti-tumor effects of the CXCR5::CD3 bispecific antibody and of the parental CXCR5 antibody were shown (Panjideh et al., 2014). One clinical trial targeting CXCR5 has been conducted to our knowledge (NCT02321709 by Sanofi). In a dose study conducted from 2014 to 2016 with systemic lupus erythematosus patients, anti-CXCR5 antibodies were injected subcutaneously. Severe side effects were not observed (clinicaltrials.gov, 2020; Ming, Jeffrey et al., 2018).

However, to date, no other clinical trials targeting CXCR5 have been registered and anti-CXCR5 therapy has never been administered systemically to patients (clinicaltrials.gov, 2020). In order to safely treat patients with the anti-CXCR5 CAR product, CXCR5 tissue expression had to be analyzed carefully.

In this work, it was shown that CXCR5 is restrictively expressed in the hematopoietic compartment. By flow cytometry, it was confirmed that CXCR5 expression is restricted to B cells and small subsets of $CD4^+$ and $CD8^+$ T cells in peripheral blood of healthy donors. This corresponds to the expression pattern described in the literature (Förster et al., 1994). Additionally, experiments presented in this thesis showed that the anti-CXCR5 CAR T cells reacted against CXCR5 expressing benign B cells *in vitro*. Thus, treating patients with anti-CXCR5 CAR T cells will presumably remove their benign mature B cells. However, as mentioned earlier, B cell aplasia is well described in patients treated with anti-CD19 CAR T cell therapy and was shown to be tolerable. B cell depletion has been widely used in therapy for about twenty years. Long-term B cell depletion has been especially studied upon treatment with the anti-CD20 monoclonal antibody Rituximab in autoimmune patients. It became evident that B cell depletion did not increase the risk for malignancy or infection, except for hepatitis B reactivation, and was overall well tolerated, even for a long period of time. However, it has to be considered that the vaccine response and immune responses to novel antigens are impaired in these patients (Chen and Cohen, 2012). In contrast to CD19 or CD20, CXCR5 is restrictively expressed on mature B cells. Anti-CXCR5 CAR T cells did not show reactivity towards B cell precursor leukemia,

suggesting that they also spare benign B cell precursors and the B cell aplasia is less pronounced than for the anti-CD19 CAR T cells.

Apart from B cells, CAR T cell reactivity against CXCR5 expressing $CD4^+$ cells was shown in this work. Upon CAR T cell infusion, $CXCR5^+CD4^+$ and $CXCR5^+CD8^+$ T cells will likely be depleted in the patient. T cell aplasia is much more severe than B cell aplasia and puts the patients at risk for potentially fatal infections (Scherer et al., 2019). However, only small T cell fractions are targeted by the anti-CXCR5 CAR T cells. The group could show in a syngeneic mouse model that mice were still able to produce an antigen-specific T cell response upon administration of murine CAR T cells targeting murine CXCR5, indicating that cellular immunity in the patients will most likely not be compromised. In this experiment, CAR T cells were infused in irradiated C57BL/6N mice and after over two weeks, their efficacy was confirmed by detection of continuous CAR T cell presence and B cell depletion. Subsequently, the mice were immunized with immunogenic SV40 large T antigen expressing tumor cells. After 8 days, antigen-specific $CD8^+$ T cells could be detected (Bunse*, Pfeilschifter* et al., 2021).

As mentioned, the elimination of tumor-supportive $CXCR5^+CD4^+$ T_{FH} cells is a desirable consequence. $CXCR5^+CD8^+$ T cells were recently described as a subset with anti-tumor function in follicular lymphoma (Chu et al., 2019). $CD4^+CXCR5^+FOXP3^+$ follicular regulatory (T_{FR}) cells act as opponents to T_{FH} cells and suppress the GC reaction, activation of B cells and T_{FH} cell cytokine secretion. In diffuse large B cell lymphoma, they are most likely beneficial for the patients (Cha et al., 2018). Nevertheless, the benefit of tumor cell removal by the anti-CXCR5 CAR T cells should be of higher therapeutic significance.

A great risk factor in adoptive T cell therapy is the expression of the targeted antigen in unrelated tissue, leading to inflammation and organ damage. In order to exclude CXCR5 expression on non-hematopoietic tissue, CXCR5 expression was carefully analyzed. PCR on a cDNA library of 48 human tissues showed very restricted *Cxcr5* expression on mRNA level. A broad panel of human primary cells and cell lines was additionally analyzed on protein level. CXCR5 negativity could further be ensured for these endothelial cells, cells of the nervous system and gastro-intestinal cells. All in all, the expression pattern of CXCR5 on human tissues was restricted to lymphoid tissue. Additionally, anti-CXCR5 CAR T cells were coincubated with these non-hematopoietic primary cells and cell lines and did not mount a reaction towards them, indicating that the CAR T cells did not encounter their antigen.

In the literature, it was described that CXCR5 was upregulated on astrocytes in a murine neuropathic pain model (Jiang et al., 2016). The authors detected CXCL13 upregulation in neurons and CXCR5 activation in astrocytes upon induction of inflammation by spinal nerve ligation. CXCR5 expression in human nervous tissue would be disastrous for patients treated with CXCR5 CAR T cell therapy and had to be further evaluated. In this work, this was addressed

experimentally by inducing an inflammatory status in human primary astrocytes as well as other primary cells by interferon γ incubation. CXCR5 upregulation upon inflammation could not be confirmed for human primary cells; additionally, coculture of anti-CXCR5 CAR T cells and inflamed primary cells did not result in interferon γ release by the CAR T cells.

Also, alterations in neurogenesis of CXCR5 knockout mice have been published (Stuart et al., 2014). Fritze et al. recently had a look at the murine subventricular zone, a region of adult neurogenesis, and found proliferative differences and upregulation of CXCR5/CXCL13 signaling in aged CXCR5 knockout mice. The authors reanalyzed a previously published single cell RNA sequencing dataset of the wildtype subventricular zone, which also included neurons and astrocytes. They were able to confirm the absence of CXCR5 and CXCL13 in these cell types, indicating that the alterations in the CXCR5 knockout mice were caused by an indirect effect (Fritze et al., 2020). This throughout investigation emphasizes that it has to be considered that alterations in neuronal tissues do not necessarily have to be accredited to CXCR5 expression by neuronal cells.

As human and murine tissues express CXCR5 in a similar pattern, more information about potential CAR-mediated on-target/off-tumor toxicity can be collected in a syngeneic mouse model. In this group, the safety of anti-CXCR5 CAR T cell treatment was further analyzed in immunocompetent sublethally irradiated mice injected with murine CAR T cells targeting murine CXCR5. In these mice, the numbers of $CXCR5^+$ B cells and $CXCR5^+CD4^+$ T cells were strongly reduced, indicating potent anti-CXCR5 activity. In the treated mice, liver, lung and colon tissues were free from inflammatory infiltrates and serum markers did not indicate any organ damage (Bunse*, Pfeilschifter* et al., 2021). As the CAR T cells did not seem to have caused damage in tissues for which CXCR5 expression is not expected, this experiment further contributed to the validation of CXCR5 as a safe target.

In summary, the CXCR5 expression under homeostatic and inflammatory conditions as characterized in this thesis is limited to lymphoid tissues. Due to this restricted expression pattern, CXCR5 appears to be a safe target for CAR T cell therapy.

5.2.2 Anti-CXCR5 CAR T cells do not show off-target reactivity

Adoptive T cell transfer-mediated toxicity can be caused by off-target effects. In clinical testing of an affinity-enhanced T cell receptor product directed towards melanoma-associated antigen 3 (MAGE-A3) for treatment of myeloma and melanoma, patients died from cardiogenic shock. T cell infiltrates in the myocardium and severe tissue damage were detected; however, the heart tissue lacked MAGE-A3 expression. Exhaustive research ultimately revealed that the TCR-engineered T cells recognized a peptide derived from the protein titin, which is specific for striated muscle tissue (Linette et al., 2013). Adoptive transfer of another MAGE-A3 TCR

product caused fatal neurotoxicity in a number of patients. It was eventually found out that the TCR-engineered T cells recognized homologous peptides of other MAGE-A proteins; previously unknown MAGE-A12 expression was detected in brain tissue (Morgan et al., 2013; Zajac et al., 2017). The experiences from the MAGE-A3 trials make it clear that off-target effects can have serious consequences for the treated patients. Off-target toxicity upon recognition of cross-reactive peptides has not been detected in CAR T cell trials (Bonifant et al., 2016). Nevertheless, potential off-target effects must be considered in pre-clinical testing and addressed as extensively as possible in preparation for a clinical trial (Krackhardt et al., 2018). Off-target toxicity cannot be excluded by expression analysis on protein or mRNA level. Thus, flow cytometry applying the CXCR5 antibody or performing PCR for *Cxcr5* expression on a tissue cDNA library is insufficient; this only helps to prevent on-target/off-tumor toxicity caused by anti-CXCR5 CAR T cells targeting CXCR5 on tissues with unexpected CXCR5 expression. Several assays were therefore performed to exclude potential off-target effects of anti-CXCR5 CAR T cells. Numerous cocultures of anti-CXCR5 CAR T cells incubated with antigen-negative target cells showed that the CAR T cells did not release IFNγ in the absence of CXCR5; IFNγ was secreted exclusively in response to CXCR5. This indicates that CXCR5-targeted T cells do not recognize other unrelated structures on the target cells *in vitro*. Additionally, off-target reactivity was assessed *in vivo*. Immunodeficient NSG mice were injected with different amounts of anti-CXCR5 CAR T cells. Immunodeficient animals had to be used to prevent that the recipients mount an immune reaction towards the human T cells and deplete them. Also, the anti-CXCR5 CAR T cells target human CXCR5 and do not recognize murine CXCR5. Signs of organ damage or inflammation were not detected in the mice. In this immunodeficient mouse model, the anti-CXCR5 CAR T cells did not cause off-target effects.

The data collected in *in vivo* and *in vitro* experiments suggest that the anti-CXCR5 CAR T cells exclusively recognize CXCR5. The anti-CXCR5 CAR seems therefore suitable for clinical testing, as off-target reactivity could not be detected.

5.3 Anti-lymphoma activity of anti-CXCR5 CAR T cells

In this work, the anti-CXCR5 CAR T cells were shown to mount a robust anti-lymphoma effect i*n vitro* and *in vivo*. CAR T cells generally either kill directly or secrete cytokines to induce cell lysis upon binding to the target cell (Benmebarek et al., 2019). Direct killing is supported by the release of inflammatory cytokines, such as interferon γ and tumor necrosis factor (TNF), which act on malignant cells and immune cells. They inhibit pathways required for the tumor cell to mediate immune evasion. Deletion of key signaling genes of IFNγ signaling, TNF signaling and antigen presentation was shown to protect the malignant cells from $CD8^+$ T cell-

mediated direct killing. TNF was further shown to induce cytokine-mediated cell death and bystander killing (Kearney et al., 2018). IFNγ, mainly produced by T_H1 and cytotoxic $CD8^+$ T cells, induces MHC upregulation on target cells, which makes them more visible to the immune system; it also acts anti-proliferative and pro-apoptotic (Castro et al., 2018; Kotredes and Gamero, 2013). IFNγ was a suitable read-out for the coculture assays performed in this thesis, as cytokine production, opposed to direct cytotoxicity, is only achieved at a high activation threshold (Lanzavecchia et al., 1999). A fast-acting killing mechanism is the release of granzyme/perforin cytotoxic granules by the CAR T cells. The Fas/Fas ligand pathway, initiated upon membrane bound expression of tumor necrosis factor (TNF) family ligands by the T cell, is involved in a slow-acting killing mechanism. Both direct lysis mechanisms induce apoptosis in the targeted cell upon activation of a caspase cascade, resulting in the cleavage of cellular substrates (Benmebarek et al., 2019). Research of human cytotoxic T cells showed that the main mode of cytotoxicity is granule exocytosis (Yasukawa et al., 2000). For CAR T cells, the preferred cytotoxic killing pathway appears to be dependent on the target cell type. CAR T cells against CD5 were developed, which is expressed on most T cell leukemias/lymphomas, but also on benign T cells. The CAR T cell culture suffered to a certain extent from fratricide during expansion *in vitro*, meaning that anti-CD5 CAR T cells killed CD5 expressing CAR T cells. Inhibition experiments with pathway blockers revealed that fratricide is dependent on granzyme/perforin-mediated killing, whereas tumor cell killing was mediated to a higher degree also by Fas/Fas ligand interaction (Mamonkin et al., 2015). As CXCR5 is not only expressed on B lymphoma cells and on follicular helper T cells, but is also upregulated in T cell subsets upon activation, fratricide was also a concern during the generation of the anti-CXCR5 CAR T cells. Förster et al. first showed that a fraction of peripheral blood T cells upregulated CXCR5 on day three after onset of activation with an anti-CD3 monoclonal antibody (Förster et al., 1994) and it was later demonstrated that *in vivo* activated $CD4^+$ T cells upregulated CXCR5 (Ansel et al., 2000). Further research confirmed that CXCR5 marks activated memory $CD4^+$ T cells. CXCR5 is induced upon contact with antigen-presenting dendritic cells and downregulated upon terminal effector cell differentiation (Schaerli et al., 2001). During the generation of anti-CXCR5 CAR T cells, T cells were activated by anti-CD3/28 stimulation prior to γ-retroviral transduction in order to improve efficiency. CXCR5 upregulation on activated T cells resulting in fratricide of anti-CXCR5 CAR T cells could be the reason why total anti-CXCR5 CAR T cell numbers at the end the expansion period were reduced by around 30% compared with CAR T cell numbers of the anti-CD19 CAR product. Another reason for reduced CXCR5 CAR T cell expansion could be tonic signaling due to differences in the scFvs of the CXCR5, CD19, and SP6 constructs (Calderon et al., 2020). Tonic signaling is also dependent on the CAR surface expression levels, which in turn depend on the viral vectors and promoters used. Improvement could be achieved

by modifying the vector or using a different one (Ajina and Maher, 2018). Nevertheless, it was easily possible to generate sufficient numbers for *in vitro* and *in vivo* experiments. In this thesis, anti-CXCR5 CAR T cells achieved an expansion rate of around 15 over the course of 10 days, which was comparable to the expansion rate described for anti-CD19 CAR T cells in clinical protocols using the CliniMACS Prodigy (Jackson et al., 2020; Mock et al., 2016). In the group, first experiments using the CliniMACS Prodigy showed that high cell counts are achievable. The manufacturing process can be further optimized to obtain even higher cell numbers for clinical application.

5.3.1 Comparison between the anti-CXCR5 CAR and the anti-CD19 CAR

The aim of this thesis was to present anti-CXCR5 CAR T cell therapy as an alternative to anti-CD19 CAR T cell therapy. Relapsed and refractory patients suffering from diffuse large B-cell lymphoma treated with anti-CD19 CAR T cells (Kymriah) in the JULIET study showed overall response rates of 52%. Thus, many patients could benefit from alternative CAR T cell therapies instead of or upon failure of anti-CD19 CAR T cell therapy (Schuster et al., 2019). Anti-CXCR5 CAR T cells, but not anti-CD19 CAR T cells, could also be administered to many patients suffering from B-NHLs that lost CD19 expression. In this thesis, CAR T cells equipped with the anti-CD19 CAR were included in many experiments as a reference for anti-CXCR5 CAR T cell functionality. Anti-CD19 CAR T cells were suitable for a comparison with the anti-CXCR5 CAR T cells due to the large overlap in the expression profiles of their antigens. Many B-NHLs express both CD19 and CXCR5. The dissociation constant of the non-humanized rat anti-human CXCR5 mAb RF8B2 was 0.7 nM, whereas the value for the CD19 mAB FMC63 was 1.1 nM (Cheng et al., 2007; Emrich, 1995). Both CAR constructs were second generation CARs with a CD28 costimulatory domain and a CD3ζ activation domain (Bluhm, 2018). Most definitely, differences in the activity between the anti-CXCR5 CAR T cells and anti-CD19 CAR T cells can rather be attributed to their distinct antigens than to the affinity or structure of the CAR constructs. Due to the different functions of these tumor-associated antigens, their densities naturally differ. CD19 is a transmembrane glycoprotein of the immunoglobulin superfamily and regulates B cell signaling thresholds (Wang et al., 2012). CD19 is expressed throughout most B cell development stages, whereas CXCR5 expression on B cells is restricted to mature cells. CXCR5, as a chemokine receptor, is a G protein-coupled receptor with seven transmembrane domains. It acts in guiding B cells, but also $CXCR5^+$ T cells, such as T_{FH} cells, to the B cell zones of secondary lymphoid organs following the CXCL13 gradient. Expression levels similar to CD19 would not be physiological for a chemokine receptor. In this work, Quantibrite analysis of CXCR5 and CD19 on lymphoma cell lines revealed that CD19 expression is up to 10 times higher. Nevertheless, the reactivity of the anti-CXCR5 CAR T cells towards these cell lines, as

quantified by IFNγ ELISA, was comparable to the reactivity of the anti-CD19 CAR T cells. The mantle cell lymphoma cell line, which was used in the NSG xenotransplantation experiments, expressed on average 10940 CD19 molecules/cell, but only 1667 CXCR5 molecules/cell. However, the anti-tumor effect of the anti-CXCR5 CAR T cells was in a similar range as of the anti-CD19 CAR T cells and was not diminished due to a lower CXCR5 antigen density on the tumor cells. As antigen levels contribute to CAR T cell activation, but other factors, such as CAR expression density on the T cell, antigen localization and accessibility, play an important role as well, the observed CXCR5 expression levels are sufficient to mount functional activity in *in vitro* assays and in the xenotransplantation experiments (Arcangeli et al., 2017; Walker et al., 2017). In fact, in the assays involving the primary patient material, a stronger response of the anti-CXCR5 CAR T cells was observed for some tumor samples.

According to the different nature of the antigens, lymphoma cells benefit from expressing CXCR5, as it regulates homing to B cell follicles in secondary lymphoid organs. In a mouse model of chronic lymphocytic leukemia, it was demonstrated that leukemic cells depend on CXCR5 expression to access survival niches and lack of CXCR5 resulted in slower tumor growth kinetics (Heinig et al., 2014). Therefore, CXCR5 antigen escape upon anti-CXCR5 CAR T cell therapy would be disadvantageous for the tumor, as lymphoma cells that lack antigen expression could not enter these survival niches, whereas CD19 antigen loss does not seem to have a negative effect on tumor progression.

5.3.2 Intrinsic characteristics of CXCR5 CAR T cells

The success of CAR T cell therapy can be impaired for various reasons. Reduced CAR T cell persistence can be caused by (i) inadequate expansion of the CAR T cell product, (ii) elimination due to immunogenic CAR sequences by the host immune system, (iii) immunosuppression by the tumor, (iv) benign B cells inducing tolerance by expressing tumor-associated antigens, (v) activation-induced cell death (AICD), (vi) exhaustion upon chronic/tonic CAR/TCR triggering and (vii) T cell contraction upon lack of antigen (McLellan and Ali Hosseini Rad, 2019).

T cell exhaustion occurs upon persistent antigenic/inflammatory stimulation in cancer or chronic inflammation. Upon exhaustion, T cells experience loss of effector functions and express inhibitory receptors (Wherry and Kurachi, 2015).

The functional characteristics measured in the stress test are influenced by the effector and memory T cell subset diversification, which largely contributes to the quality and durability of the anti-tumor response (Busch et al., 2016). Effector memory T (T_{EM}) cells are able to exert immediate effector functions and home to tissues, whereas central memory T (T_{CM}) cells migrate to lymphoid organs (Sallusto et al., 1999). Despite their poor cytotoxicity, T_{CM} cells are preferred in adoptive T cell transfer due to their stem cell-like properties. T_{CM} cells renew the

memory cell pool and give rise to T_{CM} cells, but also T_{EM} cells, and differentiate into effector T cells to mount an immune response (Graef et al., 2014; McLellan and Ali Hosseini Rad, 2019). A minor memory subset, stem cell memory T (T_{SCM}) cells are very similar to central memory T cells with even more pronounced self-renewal capacities (Busch et al., 2016; Gattinoni et al., 2011). T_{SCM} cells were shown to engraft and proliferate drastically better in NSG mice and showed better anti-tumor activity compared with T_{CM} and T_{EM} cells. Especially T_{EM} cells both proliferated and functioned poorly (Gattinoni et al., 2011). Culture conditions during the T cell expansion period influence the T cell subset composition. T cells required IL7/15 to maintain their proliferative capacities *in vitro* and showed enhanced proliferation and activation in humanized mice expressing IL7/15 (Drake et al., 2016). In a lymphoma xenotransplantation model, CAR T cells expanded with IL7/15 showed superior engraftment, anti-tumor activity and improved long-term survival compared to cells expanded with IL2. IL7/15 culture drove, upon infusion in the immunodeficient mice, $CD8^+$ central memory differentiation, whereas IL2 culture generated more $CD8^+$ effector memory cells (Zhou et al., 2019). IL7/15 were shown to promote T_{SCM} cell accumulation (Cieri et al., 2013). Altogether, many publications favor IL7/15 supplementation for T cell expansion for adoptive transfer. The *in vivo* expansion of CAR T cells in the patient also benefits from these cytokines; preconditioning lymphodepletion removes cellular cytokine “sinks” and increases the levels of IL7 and IL15 in the patients, which enhances the function of adoptively transferred T cells (Klebanoff et al., 2005).

CAR T cells for the stress test and *in vivo* experiments were expanded using IL7 and IL15. At the end of the expansion period for CAR T cells used in the stress test, T cell memory subpopulations were determined by flow cytometry. The vast majority of anti-CXCR5 CAR T cells were memory T cells, with on average around 10% $CD4^+$ T_{CM} cells, 10% $CD8^+$ T_{CM} cells, 20% $CD4^+$ T_{EM} cells and 40% $CD8^+$ T_{EM} cells. IL7/15 expansion drives T_{CM} cell formation; however a major factor that influences the phenotype, persistence and expansion capacity of CAR T cells, is the choice of the costimulatory domain (Jafarzadeh et al., 2020). The anti-CXCR5 CAR harbors a CD28-based costimulatory domain, which drives T_{EM} cell formation. Possibly, switching to a 4-1BB-based CAR could have improved longevity and anti-tumor efficacy in the xenotransplantation experiments using NSG mice, as the 4-1BB costimulatory domain promotes T_{CM} cell formation, which perform better in the mice.

CD28- and 4-1BB-based costimulatory domains influence the metabolic characteristics of CAR T cells. CAR T cells with CD28 domains show enhanced glycolysis and increased effector memory T cell differentiation. CAR T cells with 4-1BB domains have increased respiratory capacity, fatty acid oxidation and mitochondrial biogenesis. Enhanced survival of 4-1BB-based CAR T cells was found to be associated with an enriched population of central memory T cells (Kawalekar et al., 2016). 4-1BB-based CAR T cells persisted up to 4 years in the patient,

whereas CD28-based CAR T cells could be detected for around 30 days, but both have similar long-term response rates (Kawalekar et al., 2016; Weinkove et al., 2019). In aggressive B-NHL, CD28-based CARs achieve a higher response rate and in B-ALL, 4-1BB-CARs induce longer progression free survival. Thus, the ideal costimulatory domain might be disease-dependent and clinical trials, which compare the two domains, are underway (Weinkove et al., 2019). As of now, there is not a clear preference for any of the signaling domains in clinical application, with the first two FDA approved anti-CD19 CAR products Kymriah harboring a 4-1BB domain and Yescarta haboring a CD28 domain and the equal usage of both these domains in clinical trials (Mchayleh et al., 2019; Weinkove et al., 2019). Therefore, for the treatment of patients, a CD28-based anti-CXCR5 CAR construct as presented in this thesis is suitable.

5.3.3 CXCR5 CAR T cell-mediated anti-tumor activity in animal models

An immunodeficient xenotransplantation model allowed growth of human-derived tumor cells *in vivo*. NSG (NOD.Cg-Prkdc^{scid} Il2rg^{tm1Wjl}/SzJ) mice harbor mutations that render them deficient in B, T and NK cells and enable the engraftment of human cells. *In vivo* imaging using bioluminescence made it possible to track and quantify the growth of luciferase-transduced lymphoma cells in the mouse over time. In this model, a striking anti-tumor effect of anti-CXCR5 CAR T cells against JEKO-1 mantle cell lymphoma cells was demonstrated. The cell line was injected intravenously; tumor growth was mostly localized in the bone marrow. Anti-CXCR5 CAR T cells were shown to reduce tumor load and control tumor growth over the course of over two weeks. A comparison between the anti-CXCR5 and the anti-CD19 CAR T cells was performed twice. One time, the anti-CD19 CAR T cells showed superior performance, and one time, the anti-CXCR5 CAR T cells performed better, indicating that they have very comparable anti-tumor efficacy.

However, the anti-CXCR5 CAR T cells did not induce complete tumor elimination and durable remission in the mice. Several mechanisms could account for this. First, tumor escape could be explained by outgrowth of CXCR5 negative loss variants; however, CXCR5 was not down-regulated on tumor cells harvested from mice in the anti-CXCR5 CAR group. Secondly, CAR T cell function could potentially be hampered by CXCR5 shedding of the anti-CXCR5 CAR-targeted epitope. Shedding was described for B-cell maturation antigen (BCMA). The enzyme γ-secretase cleaves BCMA's extracellular domain, generating soluble BCMA (sBCMA) fractions (Laurent et al., 2015). Soluble BCMA is increased in the serum of multiple myeloma patients, who experience expansion of BCMA^{+} plasma cells (Sanchez et al., 2012). CXCR5 shedding has never been reported; however, shedding of other G-protein-coupled receptors is described in the literature (Mattila et al., 2016; Tseng et al., 2018; Vallon and Essler, 2006).

CXCR5 shedding could result in reduced surface expression of anti-CXCR5 CAR targeted molecules on lymphoma/leukemic cells. As previously mentioned, downregulation of CXCR5 expression was not observed on tumor cells analyzed at the end point of experiments. Additionally, soluble CXCR5 could possibly block anti-CXCR5 CAR activity, as hypothesized for sBCMA, which was found to decrease binding of an anti-BCMA antibody *in vitro* at concentrations measured in MM patients (Chen et al., 2019). Activity reduction of CXCR5 CAR T cells upon incubation with the CXCR5 N-terminal epitope was not observed at concentrations similar to the sBCMA serum concentrations described for MM patients or higher concentrations, indicating that soluble CXCR5 is most likely not the cause for incomplete tumor removal in the NSG mice and would most likely not interfere with anti-CXCR5 CAR T cell treatment in patients. In the *in vivo* experiments, the anti-CXCR5 CAR T cells were analyzed at the time point of tumor outgrowth, but signs of exhaustion, as classified by upregulation of the exhaustion markers PD-1, LAG-3 and TIM-3, were not observed in comparison to SP6 CAR T cells. These findings excluded T cell exhaustion as a potential cause for incomplete tumor removal in the mice.

Most likely, the lack of a durable anti-tumor response of the anti-CXCR5 CAR T cells can be attributed to limitations of the NSG mouse model. Murine factors, such as growth factors and chemokines, are species-specific and do not sufficiently support the transferred human primary T cells. Signaling through the receptors for IL2, IL4, IL7, IL9, IL15 and IL21 is disturbed as a result of the mutation of the IL2 receptor γ-chain locus, which impairs T and B cell function and development and inhibits NK cell development (Shultz et al., 2007; Sugamura et al., 1996). The *scid* mutation further prevents T and B cell development and the NOD strain background harbors intrinsic deficiencies in innate immunity (Shultz et al., 2014). In these mice, lymphoid structures are not properly developed and differences in species-specific homing factors hamper trafficking of human immune cells. Another approach, in which the anti-CXCR5 CAR T cells might receive better support from the microenvironment, is provided with humanized mouse models. In humanized models, immunodeficient mice are engrafted with human primary hematopoietic cells or tissues to establish a functional human immune system (Shultz et al., 2012). Improved immune function can be achieved by expression of human transgenes or injection of human recombinant proteins (Drake et al., 2012; O'Connell et al., 2010). Also, genetically engineered mouse strains are available, which improve immunity in humanized mice by expressing human-specific factors (Shultz et al., 2012). Humanized models have been used to study anti-CD19 CAR T cells. Jin et al. generated a mouse model with a functional human immune system by administering human fetal tissues and cells and induced genetically-matched autologous primary acute B-lymphoblastic leukemia. Using this model, it was possible to observe an increase in cytokine production by the CAR T cells, but also by the host

monocytes and macrophages. The authors also registered an increase in regulatory T cells, which is known to happen in patients treated with anti-CD19 CAR T cells. Altogether, it was shown that humanized mouse models are a valuable tool to characterize the mechanisms of action of human CAR T cells *in vivo* (Jin et al., 2019).

An alternative to study the effect of CAR T cells *in vivo* are syngeneic mouse models. In syngeneic models, murine CAR T cells specific for the murine antigen are administered to immunocompetent mice. They can help to answer questions that are left unanswered in immunodeficient mouse models and, for instance, shed light on the factors influencing *in vivo* killing, such as dosage, phenotype, persistence and homing of the T cells and conditioning chemotherapy. In a B-ALL syngeneic tumor model, anti-CD19 CAR T cells were studied in greater detail. The CAR T cells were able to eliminate the tumor cells *in vivo*, cure the mice and induce B cell aplasia. The authors further showed that increased conditioning chemotherapy enhanced tumor eradication and CAR T cell persistence (Davila et al., 2013). In a similar syngeneic approach, it is possible to study the reciprocal interactions of the anti-CXCR5 CAR T cells with the microenvironment. A suitable model is the immunocompetent *Eμ-Tcl1* mouse model, which was also used in this thesis to investigate the influence of lymphoma growth on T cells. $CXCR5^+$ *Eμ-Tcl1* tumor cells are adaptively transferred into C57BL/6N mice, followed by anti-murine CXCR5 (mCXCR5) CAR T cells, which then target the tumor cells within an intact lymphoid environment. Thus, it is possible to study the distribution of anti-mCXCR5 CAR T cells within the SLOs and their interaction with the tumor cells by immunohistology or *in vivo* microscopy. The group showed that the anti-mCXCR5 CAR T cells intermingled with *Eμ-Tcl1* tumor cells in B cell areas, expanded and mediated strong anti-tumor efficacy (Bunse*, Pfeilschifter* et al., 2021). Research using the mCXCR5 CAR T cells in the *Eμ-Tcl1* mouse model is still ongoing in the lab. The model could be used in the future to study whether elimination of $CXCR5^+$ T_{FH} cells and other T cell subpopulations by the anti-mCXCR5 CAR T cells is supportive of the anti-tumor effect, for instance in comparison with the anti-mCD19 CAR T cells, which exclusively remove benign and malignant B cells.

5.4 Targeting the TME with next generation CAR T cells

Immunotherapy has revolutionized treatment for patients of numerous malignancies; monoclonal antibody (mAb)-based therapies have largely contributed to these advances. CAR T cell therapy is however an autologous approach, costly in terms of time and labor. They induce target cell lysis and cytotoxicity is triggered by low levels of antigen. Monoclonal antibodies on the other hand need high levels of antigen expression in order to induce antibody-dependent cellular cytotoxicity or the complement cascade; tumor cells with low expression levels can

escape easier in mAb-based therapy. Biodistribution also differs in CAR T cell and mAb-based therapies. They are both administered intravenously, but mAbs face greater difficulties to overcome endothelial, epithelial and interstitial barriers. CAR T cells, however, have the ability to extravasate and migrate within tissues. CAR T cells additionally show considerably better durability. Patients need multiple injections with mAbs, which have a short half-life *in vivo*, to induce remission. For instance, the anti-CD20 mAb Rituximab has a half-life of around three weeks. CAR T cells are usually only administered once and expand upon injection. They persist long-term in the patients and can be found months and years after infusion, inducing a long lasting anti-tumor response (Caruana et al., 2014).

Despite the introduction of anti-CD19 CAR T cell therapy to the clinic, which filled a previously unmet need for the treatment of patients suffering from refractory or relapsed aggressive B-cell lymphomas, durable remission is only achieved in 33%–40% of patients. In the majority of refractory or relapsed B-NHL cases after anti-CD19 CAR T cell therapy, CD19 is still expressed by the tumor cells. Treatment failure in these patients is associated with poor functional characteristics of the infused CAR T cells and unfavorable interactions of the CAR T cells with the immunosuppressive lymphoma microenvironment, resulting in immune evasion and T cell exhaustion (Abramson et al., 2019).

In a study of CLL patients treated with an anti-CD19 CAR product, the authors compared the differences in CAR T cells of responders and non-responders. CAR T cells from completely-responding patients showed increased expression of memory genes and an IL6/STAT3 signature, opposed to CAR T cells of non-responders, which upregulated genes involved in effector differentiation and glycolysis. These findings indicate that CAR T cell modifications before or after infusion could improve the anti-tumor response (Fraietta et al., 2018).

Impaired trafficking to the tumor site, T cell suppression by soluble inhibitors produced by the tumor cells or stroma cells and checkpoint-mediated immunosuppression cause major obstacles in CAR T cell treatment that can be overcome by next generation CARs, which harbor novel features (Höpken and Rehm, 2019).

Armored CAR T cells or TRUCKS (T cells redirected for universal cytokine killing) have been proposed as 4th generation CAR T cells with the ability to secrete cytokines. The released cytokines can either work in an autocrine manner to support T cell survival or in a paracrine manner to modify the immunosuppressive microenvironment (Chmielewski and Abken, 2012, 2020). TRUCK strategies were suggested for anti-CD19 CAR T cells. Boice et al. introduced CAR T cells with local and continuous HVEM (Herpes Virus Entry Mediator) production, which bound to BTLA (B and T lymphocyte attenuator) on follicular lymphoma cells and restored the inhibitory BTLA signal. HVEM is often lost in FL and loss was shown to promote lymphoma development in a mouse model. HVEM restoration improved therapeutic activity (Boice et al.,

2016). Interestingly, the HVEM/BTLA axis acted as a negative regulator in the interaction between T_{FH} cells, which strongly express BTLA, and FL cells. T_{FH} cells provided more help to HVEM-deficient than to HVEM-expressing B cells, for which the intact HVEM/BTLA axis restrained T_{FH}-mediated B cell help (Mintz et al., 2019). Thus, T_{FH} cell-mediated support for HVEM-deficient FL could be disrupted by HVEM-expressing CAR T cells.

In another approach, IL12 was secreted by anti-murine CD19 (mCD19) CAR T cells in a lymphoreplete mouse model with normal lymphocyte counts. Lymphodepletion is usually performed before CAR T cell infusion to remove host lymphoid cells, which compete for cytokines and space in lymphoid tissues with the transferred CAR T cells. It is however toxic for the patient and also destroys immune cells with anti-tumor activity. In this model, lymphodepletion was not required as the CAR T cells received autocrine IL12 stimulation, which boosted cytotoxic activity and engraftment. It was demonstrated that the IL12 secreting CAR T cells directly killed $mCD19^+$ tumor cells. IL12 secreted by the CAR T cells further seemed to lessen the tumor cell-mediated immune suppression and allowed host immune cells to contribute to an anti-tumor response in an mCD19 independent manner due to epitope spreading (Kueberuwa et al., 2018).

Impaired trafficking to the tumor site is addressed by CAR T cells expressing additional chemokine receptors. Introduced by Di Stasi et al., chemokine receptor expressing anti-CD30 CAR T cells were shown to have improved homing function and anti-tumor efficacy in a murine Hodgkin's lymphoma model. Hodgkin's tumor cells preferentially attracted $CCR4^+$ T_H2 cells and regulatory T cells, creating an immunosuppressive microenvironment. Effector $CD8^+$ T cells did not express CCR4 and were absent from the tumor site, but transgenic CCR4 induction in these cells improved migration to $CD30^+$ lymphoma cells (Di Stasi et al., 2009). On a side note, expression of CXCR5 was introduced on CAR T cells in HIV research. In chronic HIV infection, T_{FH} cells are a major reservoir of virus production in the B cell follicle. The authors developed a CAR, which targeted the viral envelope protein on cells infected with the simian immunodeficiency virus and expressed rhesus macaque CXCR5. CXCR5 expression allowed trafficking to the B cell follicle following the CXCL13 gradient *ex vivo* in rhesus macaque lymph nodes. Introduction of CXCR5 expression in CAR T cells targeting HIV infected cells could possibly achieve durable remission in HIV patients, as CXCR5 could aid to locate the CAR T cells to their target site (Haran et al., 2018).

As of today, targeting solid tumors with CAR T cells remains especially challenging. Application of CAR T cell therapy in solid tumors is often constrained by limited T cell trafficking to tumor sites, reduced functionality in an immunosuppressive microenvironment and non-homogenous antigen expression on the tumor cells (Braun et al., 1999; Craddock et al., 2010; Fargion et al., 1986; Mohammed et al., 2017). Novel CAR approaches and designs aim to improve the

therapeutic efficacy in solid tumors. Morrissey et al. first developed CAR-Ps (CARs for phagocytosis) and introduced them into macrophages (Morrissey et al., 2018). Klichinsky et al. established CAR macrophages against the solid tumor antigen HER2, which are currently being prepared for a clinical trial. With CAR macrophages, phagocytosis *in vitro* in an antigen-dependent manner and tumor reduction in a mouse model was shown. Apart from their direct anti-tumor effect, CAR macrophages succeed in modifying the tumor microenvironment. They induced pro-inflammatory pathways in macrophages, activated dendritic cells and T cells *in vitro* and enhanced T cell mediated anti-tumor activity *in vivo* (Klichinsky et al., 2020). Macrophages do not face the problems that T cells face in targeting solid tumors. Poor trafficking to tumor sites is not an issue, as tumor-associated macrophages are among the major inflammatory cells that infiltrate tumors attracted by tumor-derived chemotactic factors (Biswas et al., 2013; Green et al., 2009). Moreover, the antigenic heterogeneity of the tumor mass is overcome by the macrophage function as an antigen-presenting cell, which engages the adaptive immune system after phagocytosis. Another approach to engage the innate immune answer against solid tumors was pursued by Chmielewski et al. with IL12 TRUCKs. Upon antigen encounter, cytotoxic CAR T cells release IL12, which attracts macrophages to the tumor site and boosts their function. Upon IL12 secretion, an innate response is triggered towards malignant cells that go unrecognized by CAR T cells due to antigen loss. Additionally, immunosuppressive cells are reprogrammed (Chmielewski and Abken, 2012). The benefit of CAR-mediated IL12 release was demonstrated in tumor models of hepatocellular carcinoma and ovarian cancer (Koneru et al., 2015; Liu et al., 2019). These novel strategies have in common that they elicit an innate immune response at the tumor site and exert influence on the immunosuppressive tumor microenvironment.

5.5 Conclusion and further perspectives

5.5.1 Conclusion

In this thesis, a novel CAR directed against a chemokine receptor has been characterized that allows simultaneous targeting of lymphoma and the tumor-supportive microenvironment (Figure 40). The CAR T cells investigated in this thesis were directed against CXCR5, which is expressed on mature B cells and B non-Hodgkin lymphoma cells derived from mature B cells. CXCR5 is further expressed on subsets of T cells, most prominently the follicular helper T cells. In order to ensure the safety of the CAR product, extensive expression studies on mRNA and protein level were performed, which were able to confirm a restrictive expression of CXCR5 in the hematopoietic compartment. The presented results show that the anti-CXCR5 CAR T cells specifically target CXCR5 expressing cell lines and primary patient material, including CLL, MCL, FL and MZL, but also follicular helper T cells, which are described to support tumor progression in CLL and FL. In xenotransplantation models, it could be shown that anti-CXCR5 CAR T cells efficiently reduce CXCR5$^+$ tumor growth *in vivo*. The data support the anti-CXCR5 CAR T cell product as a valuable alterative to the anti-CD19 CAR T cell product, which is predominantly used in clinical application. Especially in CLL and FL patients, anti-CXCR5 CAR T cell therapy could be advantageous as tumor-supportive follicular helper T cells are eliminated by the CAR T cells.

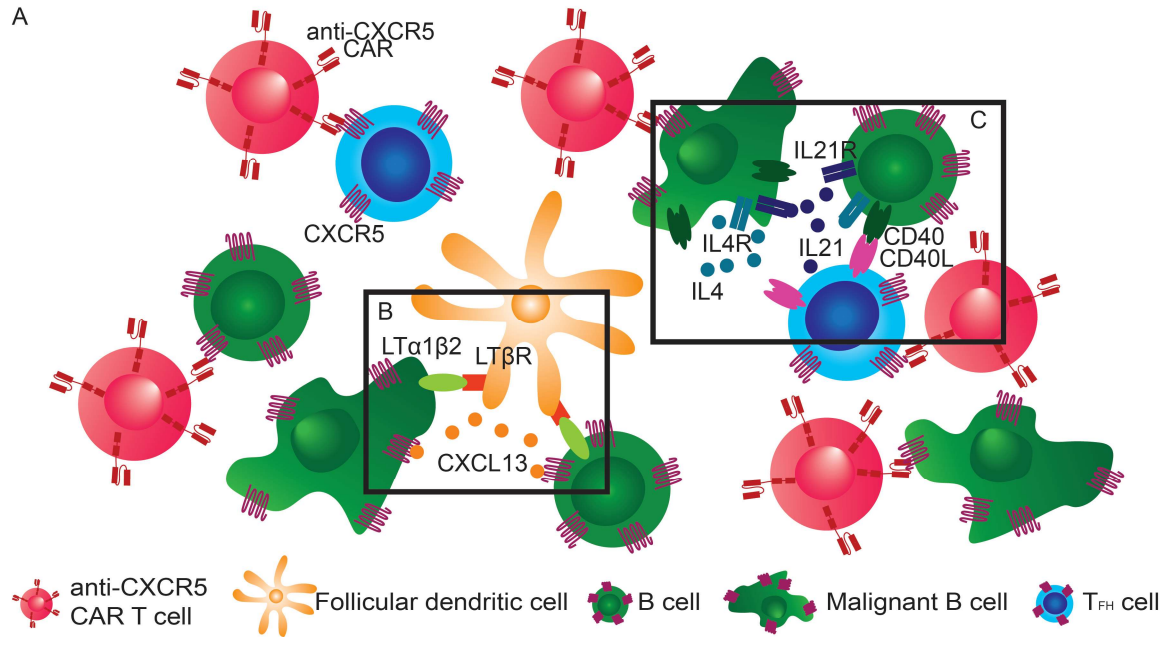

Figure 40: Anti-CXCR5 CAR T cells simultaneously target lymphoma and the tumor-supportive microenvironment. **A** CXCR5-expressing benign and malignant B cells as well as follicular helper T cells are targeted by the anti-CXCR5 CAR T cells in the B cell follicle. **B** Follicular dendritic cells secrete CXCL13, which attracts CXCR5$^+$ cells to the B cell follicle. They engage with B cells and lymphoma cells in a CXCL13/lymphotoxin positive feedback loop. **C** T_{FH} cells support the survival and expansion of B cells and lymphoma cells by IL4/21 secretion and CD40L engagement.

Additionally, using a mouse model of chronic lymphocytic leukemia, a strong influence of lymphoma growth on the CXCR5$^+$ splenic T cell compartment was shown by single cell RNA sequencing. The fractions of effector CD8$^+$ cells, follicular helper T cells and follicular regulatory T cells were enriched upon tumor challenge. With a special focus on follicular helper T cells, it was shown that profound changes were induced on transcriptional level. *Il4*, *Il21* and *Cd40lg*, which were described to stimulate CLL cells *in vitro*, were shown to be upregulated early in CLL progression in *Eμ-Tcl1* tumor-challenged T_{FH} cells. These results support the descriptions of tumor-supportive functions of T_{FH} cells in the literature and add a more detailed analysis on mRNA level to them.

5.5.2 Future perspectives

The treatment options for patients with refractory or relapsed aggressive B cell lymphomas were revolutionized by the advent of anti-CD19 CAR T cell therapy. Nevertheless, complete remission is still only achieved in less than 40% of patients, with a major fraction of treatment failures attributed to poor CAR T cell function due to disadvantageous interactions with the microenvironment (Abramson et al., 2019). In an immunosuppressive lymphoma microenvironment, CAR T cells can be functionally hampered by the engagement of immune-inhibitory checkpoints, most prominently PD-1 and CTLA-4, whose ligands are often expressed by tumor cells. Checkpoint-mediated immunosuppression is a huge obstacle in efficient adoptive T cell therapy. Checkpoint receptors engagement causes T cell exhaustion, dysfunction, suppressed effector activity and results in a reduced anti-tumor response (Alsaab et al., 2017; Gowrishankar et al., 2018). The introduction of checkpoint blockage, one of the major milestones of immunotherapy, has provided a tool to diminish CAR T cell inhibition. John et al. were able to boost CAR T cell activity by blocking PD-1-mediated immunosuppression with an anti-PD-1 monoclonal antibody. Mice treated with both CAR T cells and the antibody showed enhanced tumor regression and survival compared with the treatments administered separately (John et al., 2013). These preclinical experiments provided proof of principle and checkpoint blockage in CAR T cell therapy was further investigated in clinical trials; many trials with patients suffering from B cell malignancies treated with this combination immunotherapy are still ongoing and look promising (Grosser et al., 2019). Apart from administering checkpoint blockage agents, more sophisticated strategies were developed. CAR T cells were modified to secrete PD-1-blocking soluble single chain variable fragments (scFv) at the tumor site. Release of PD-1-blocking scFvs was shown to enhance the anti-tumor activity in a murine hematologic tumor model by two mechanisms. First, autocrine PD-1 blockage improved CAR T cell function. Secondly, paracrine blockage activated bystander tumor-specific T cells. As the secreted scFvs acted locally, side effects of systemic checkpoint inhibition could be avoided (Rafiq et al.,

2018). In cell-intrinsic approaches, CAR T cell expression of a mock-PD-1 receptor with scavenger function, which reduced ligand binding to the endogenous PD-1 receptor, or PD-1 receptor knockdown by cotransduction with PD-1 shRNAs were further shown to restore CAR T cell effector function (Cherkassky et al., 2016). Also, in order to transform the inhibitory PD-1-mediated signaling, anti-CD19 CAR T cells with a chimeric switch receptor were developed, with the extracellular domain of PD-1 and the transmembrane and cytoplasmic signaling domains of CD28. These CAR T cells showed superior proliferation, cytokine production and killing capacities *in vitro* and in the patient compared to conventional anti-CD19 CAR T cells without the switch receptor (Liu et al., 2020b).

Major difficulties are also related to the generation of autologous CAR T cells from patient-derived T cells that have been influenced by cancer-mediated immune effects and chemotherapy or other previous treatments. Also, autologous production has the disadvantages of higher costs, manufacturing time, which delays treatment, and the possibility of manufacturing failure. Allogeneic ”off-the-shelf” CAR products could overcome all these issues and provide patients with high-quality cells from selected donors. Risks in administering allogeneic CAR products, which should be kept in mind, are graft-versus-host disease (GvHD) and limited anti-tumor efficacy due to fast elimination by the host immune system (Depil et al., 2020). In administering allogeneic CAR T cells, GvHD can be reduced by T cell engineering. As GvHD can be attributed to the broad repertoire of allogeneic T cell receptors, endogenous T cell receptor deletion is an option to address this issue, for instance by permanent deletion of T cell receptor chains with designer zinc finger nucleases (Kim and Cho, 2020; Torikai et al., 2012). Results of the first allogeneic gene-edited CAR T cell study have recently been published. The authors disrupted expression of the T cell receptor and CD52 in anti-CD19 CAR T cells. CD52 disruption allowed the use of an anti-CD52 antibody to induce lymphodepletion in the host. The treatment was shown to have a manageable safety profile and had an overall response rate of 78% (Neelapu et al., 2020) (NCT03939026, clinicaltrials.gov).

Not only T cells can be equipped with a CAR, but also natural killer (NK) cells. NK cells are highly cytotoxic, but show a superior safety profile for allogeneic therapy due to lower risks of graft-versus-host disease, cytokine release syndrome and neurotoxicity (Xie et al., 2020). Most clinical trials with CAR NK cells were only initiated during the last years and results are not published yet, but the first large-scale study was recently published (Xie et al., 2020). Liu et al. engineered cord blood-derived NK cells to express an anti-CD19 CAR construct and IL15. The CAR NK cells had strong anti-tumor efficacy and great persistence in a murine xenograft lymphoma model, which was especially improved upon IL15 production (Liu et al., 2018). The authors initiated a clinical trial with this CAR and showed treatment response in a majority of patients, without severe toxicities (Liu et al., 2020a). Allogeneic CAR products can be

advantageous not only for the patients, but also considering the manufacturing process. Future research will show if they are suitable to ultimately replace autologous CAR T cell therapy.

As presented in this thesis, CXCR5 is a promising target for CAR T cell therapy of B non-Hodgkin lymphomas derived from mature B cells. The anti-CXCR5 CAR T cells targeted specifically CXCR5 expressing cells, spared CXCR5 negative cell and performed well *in vitro* and *in vivo*. Therefore, the next step is to prepare the anti-CXCR5 CAR product for clinical application with the ultimate goal to provide an alternative to anti-CD19 CAR T cell therapy to B-NHL patients. In clinical application, peripheral blood mononuclear cells are collected from the patient in leukapheresis and the apheresis product is further processed. In the next steps, for instance the CliniMACS Prodigy system can be used for clinical-grade manufacturing under good manufacturing procedure (GMP) (Wang and Rivière, 2016). It might also be interesting to investigate whether the enrichment of certain T cell subsets, for example memory stem cells might be beneficial for the final anti-CXCR5 CAR product. Upon subsequent T cell activation, which is often performed using CD3/CD28 beads, upregulation of CXCR5 is expected on a small subpopulation of activated T cells. Once the T cells are equipped with the anti-CXCR5 CAR, this subpopulation is subject to fratricide. In this thesis, it was easily possible to generate sufficient anti-CXCR5 CAR T cells and potential fratricide did not seem to be detrimental to the final product, which was shown to be highly functional in numerous *in vitro* and *in vivo* experiments. It is expected that the large-scale production for clinical application will obtain sufficient cell numbers in order to treat patients. Further, it could be interesting to explore the above-mentioned ”off-the-shelf” therapies using allogeneic T cells or NK cells with the anti-CXCR5 CAR construct.

Using the *Eμ-Tcl1* mouse model, a profound impact of lymphoma growth on $CXCR5^+$ T cells in the murine spleen was shown in this thesis by single cell RNA sequencing. In order to validate the data, splenic T_{FH} cells can be isolated from *Eμ-Tcl1* tumor-challenged mice and analyzed for the upregulated genes by quantitative PCR or, to obtain data on protein level, by flow cytometry. Further, cocultures of *Eμ-Tcl1* tumor cells with T_{FH} cells isolated from the murine spleen could be performed; the supernatant could be analyzed for cytokine secretion by ELISA and the cells could be analyzed by flow cytometry. These cocultures could also be used for antibody blockage experiments to validate the importance of the expressed genes for the reciprocal interaction between T cells and tumor cells. It remains challenging to isolate sufficient numbers of viable T_{FH} cells by fluorescence-activated cell sorting. Cells isolated by magnetic cell sorting can usually only be sorted for one antigen in addition to CD4 due to the set-up of available kits, therefore they could only be sorted for CXCR5, but not PD-1. An alternative could be cocultures with $CD3^+$ or $CD4^+CXCR5^+$ cells with tumor cells to analyze if changes are

induced in T cell subsets *in vitro*. Also, cocultures of CLL patient biopsies with human cT_{FH} cells isolated from peripheral blood could be of interest. Due to the lack of a single marker identifying T_{FH} cells, T_{FH} knock-out mice are not available. Alternatively, it might be of interest to analyze *Eμ-Tcl1* tumor progression in transgenic mice upon conditional cell ablation of cells expressing IL21, one of the main cytokines produced by T_{FH} cells. Ultimately, these experiments will shed light on the reciprocal interactions of lymphoma cells and $CXCR5^+$ T cells, in particular T_{FH} cells, in the B cell follicle. Insights in the mechanisms of tumor progression will allow to propose ways to inhibit tumor support by the microenvironment.

6 References

Abramson, J.S., Lunning, M., and Palomba, M.L. (2019). Chimeric Antigen Receptor T-Cell Therapies for Aggressive B-Cell Lymphomas: Current and Future State of the Art. American Society of Clinical Oncology Educational Book 446–453.

Adams, J.M., Harris, A.W., Pinkert, C.A., Corcoran, L.M., Alexander, W.S., Cory, S., Palmiter, R.D., and Brinster, R.L. (1985). The c-myc oncogene driven by immunoglobulin enhancers induces lymphoid malignancy in transgenic mice. Nature *318*, 533–538.

Advani, R.H., Buggy, J.J., Sharman, J.P., Smith, S.M., Boyd, T.E., Grant, B., Kolibaba, K.S., Furman, R.R., Rodriguez, S., Chang, B.Y., et al. (2013). Bruton tyrosine kinase inhibitor ibrutinib (PCI-32765) has significant activity in patients with relapsed/refractory B-cell malignancies. J. Clin. Oncol. *31*, 88–94.

Ahearne, M.J., Willimott, S., Piñon, L., Kennedy, D.B., Miall, F., Dyer, M.J.S., and Wagner, S.D. (2013). Enhancement of CD154/IL4 proliferation by the T follicular helper (Tfh) cytokine, IL21 and increased numbers of circulating cells resembling Tfh cells in chronic lymphocytic leukaemia. Br. J. Haematol. *162*, 360–370.

Ahmed, N., Owen, T.E., Rubinger, M., Williams, G., Nugent, Z., Ahmed, S., and Cooke, A. (2013). Early Stage W.H.O. Grade I and II Follicular Lymphoma Treated with Radiation Therapy Alone. PLoS ONE *8*, e65156.

Ajina, A., and Maher, J. (2018). Strategies to Address Chimeric Antigen Receptor Tonic Signaling. Mol Cancer Ther *17*, 1795–1815.

Alabanza, L., Pegues, M., Geldres, C., Shi, V., Wiltzius, J.J.W., Sievers, S.A., Yang, S., and Kochenderfer, J.N. (2017). Function of Novel Anti-CD19 Chimeric Antigen Receptors with Human Variable Regions Is Affected by Hinge and Transmembrane Domains. Mol. Ther. *25*, 2452–2465.

Alberts, Johnson, and Lewis (2002). Molecular Biology of the Cell.

Ali, N., Adil, S.N., and Shaikh, M.U. (2015). Autologous Hematopoietic Stem Cell Transplantation-10 Years of Data From a Developing Country. Stem Cells Transl Med *4*, 873–877.

Alizadeh, A.A., Eisen, M.B., Davis, R.E., Ma, C., Lossos, I.S., Rosenwald, A., Boldrick, J.C., Sabet, H., Tran, T., Yu, X., et al. (2000). Distinct types of diffuse large B-cell lymphoma identified by gene expression profiling. Nature *403*, 503–511.

Allen, C.D.C., Ansel, K.M., Low, C., Lesley, R., Tamamura, H., Fujii, N., and Cyster, J.G. (2004). Germinal center dark and light zone organization is mediated by CXCR4 and CXCR5. Nat. Immunol. *5*, 943–952.

Alsaab, H.O., Sau, S., Alzhrani, R., Tatiparti, K., Bhise, K., Kashaw, S.K., and Iyer, A.K. (2017). PD-1 and PD-L1 Checkpoint Signaling Inhibition for Cancer Immunotherapy: Mechanism, Combinations, and Clinical Outcome. Front Pharmacol *8*, 561.

Amé-Thomas, P., Le Priol, J., Yssel, H., Caron, G., Pangault, C., Jean, R., Martin, N., Marafioti, T., Gaulard, P., Lamy, T., et al. (2012). Characterization of intratumoral follicular helper T cells in follicular lymphoma: role in the survival of malignant B cells. Leukemia *26*, 1053–1063.

Ansel, K.M., Ngo, V.N., Hyman, P.L., Luther, S.A., Förster, R., Sedgwick, J.D., Browning, J.L., Lipp, M., and Cyster, J.G. (2000). A chemokine-driven positive feedback loop organizes lymphoid follicles. Nature *406*, 309–314.

Ansell, S.M., Hurvitz, S.A., Koenig, P.A., LaPlant, B.R., Kabat, B.F., Fernando, D., Habermann, T.M., Inwards, D.J., Verma, M., Yamada, R., et al. (2009). Phase I study of ipilimumab,

an anti-CTLA-4 monoclonal antibody, in patients with relapsed and refractory B-cell non-Hodgkin lymphoma. Clin. Cancer Res. *15*, 6446–6453.

Aoki, Y., Takakuwa, K., Kodama, S., Tanaka, K., Takahashi, M., Tokunaga, A., and Takahashi, T. (1991). Use of adoptive transfer of tumor-infiltrating lymphocytes alone or in combination with cisplatin-containing chemotherapy in patients with epithelial ovarian cancer. Cancer Res. *51*, 1934–1939.

Arcangeli, S., Rotiroti, M.C., Bardelli, M., Simonelli, L., Magnani, C.F., Biondi, A., Biagi, E., Tettamanti, S., and Varani, L. (2017). Balance of Anti-CD123 Chimeric Antigen Receptor Binding Affinity and Density for the Targeting of Acute Myeloid Leukemia. Mol Ther *25*, 1933–1945.

Awad, R.M., De Vlaeminck, Y., Maebe, J., Goyvaerts, C., and Breckpot, K. (2018). Turn Back the TIMe: Targeting Tumor Infiltrating Myeloid Cells to Revert Cancer Progression. Front Immunol *9*, 1977.

Bachelerie, F., Ben-Baruch, A., Burkhardt, A.M., Combadiere, C., Farber, J.M., Graham, G.J., Horuk, R., Sparre-Ulrich, A.H., Locati, M., Luster, A.D., et al. (2014). International Union of Basic and Clinical Pharmacology. [corrected]. LXXXIX. Update on the extended family of chemokine receptors and introducing a new nomenclature for atypical chemokine receptors. Pharmacol. Rev. *66*, 1–79.

Bahler, D.W., Campbell, M.J., Hart, S., Miller, R.A., Levy, S., and Levy, R. (1991). Ig VH gene expression among human follicular lymphomas. Blood *78*, 1561–1568.

Bajénoff, M., and Germain, R.N. (2009). B-cell follicle development remodels the conduit system and allows soluble antigen delivery to follicular dendritic cells. Blood *114*, 4989–4997.

Baldin, V., Lukas, J., Marcote, M.J., Pagano, M., and Draetta, G. (1993). Cyclin D1 is a nuclear protein required for cell cycle progression in G1. Genes Dev. *7*, 812–821.

Barnes, D.W.H., Corp, M.J., Loutit, J.F., and Neal, F.E. (1956). Treatment of Murine Leukaemia with X Rays and Homologous Bone Marrow. BMJ *2*, 626–627.

Below, J., and M Das, J. (2020). Vincristine. In StatPearls, (Treasure Island (FL): StatPearls Publishing), p.

Bendle, G.M., Linnemann, C., Hooijkaas, A.I., Bies, L., de Witte, M.A., Jorritsma, A., Kaiser, A.D.M., Pouw, N., Debets, R., Kieback, E., et al. (2010). Lethal graft-versus-host disease in mouse models of T cell receptor gene therapy. Nat Med *16*, 565–570.

Benmebarek, M.-R., Karches, C., Cadilha, B., Lesch, S., Endres, S., and Kobold, S. (2019). Killing Mechanisms of Chimeric Antigen Receptor (CAR) T Cells. IJMS *20*, 1283.

Bhoj, V.G., Arhontoulis, D., Wertheim, G., Capobianchi, J., Callahan, C.A., Ellebrecht, C.T., Obstfeld, A.E., Lacey, S.F., Melenhorst, J.J., Nazimuddin, F., et al. (2016). Persistence of long-lived plasma cells and humoral immunity in individuals responding to CD19-directed CAR T-cell therapy. Blood *128*, 360–370.

Bichi, R., Shinton, S.A., Martin, E.S., Koval, A., Calin, G.A., Cesari, R., Russo, G., Hardy, R.R., and Croce, C.M. (2002). Human chronic lymphocytic leukemia modeled in mouse by targeted TCL1 expression. Proceedings of the National Academy of Sciences *99*, 6955–6960.

Bird, R.E., Hardman, K.D., Jacobson, J.W., Johnson, S., Kaufman, B.M., Lee, S.M., Lee, T., Pope, S.H., Riordan, G.S., and Whitlow, M. (1988). Single-chain antigen-binding proteins. Science *242*, 423–426.

Biswas, S.K., Allavena, P., and Mantovani, A. (2013). Tumor-associated macrophages: functional diversity, clinical significance, and open questions. Semin Immunopathol *35*, 585–600.

Blank, C., Brown, I., Peterson, A.C., Spiotto, M., Iwai, Y., Honjo, T., and Gajewski, T.F. (2004). PD-L1/B7H-1 inhibits the effector phase of tumor rejection by T cell receptor (TCR) transgenic CD8+ T cells. Cancer Res. *64*, 1140–1145.

Bluhm, J. (2018). Chimeric antigen receptor T cell therapy to target lymphoid neoplasms. Humboldt-Universität zu Berlin.

Boice, M., Salloum, D., Mourcin, F., Sanghvi, V., Amin, R., Oricchio, E., Jiang, M., Mottok, A., Denis-Lagache, N., Ciriello, G., et al. (2016). Loss of the HVEM Tumor Suppressor in Lymphoma and Restoration by Modified CAR-T Cells. Cell *167*, 405-418.e13.

Bonifant, C.L., Jackson, H.J., Brentjens, R.J., and Curran, K.J. (2016). Toxicity and management in CAR T-cell therapy. Molecular Therapy - Oncolytics *3*, 16011.

Boyiadzis, M.M., Dhodapkar, M.V., Brentjens, R.J., Kochenderfer, J.N., Neelapu, S.S., Maus, M.V., Porter, D.L., Maloney, D.G., Grupp, S.A., Mackall, C.L., et al. (2018). Chimeric antigen receptor (CAR) T therapies for the treatment of hematologic malignancies: clinical perspective and significance. J Immunother Cancer *6*, 137.

Braig, F., Brandt, A., Goebeler, M., Tony, H.-P., Kurze, A.-K., Nollau, P., Bumm, T., Böttcher, S., Bargou, R.C., and Binder, M. (2017). Resistance to anti-CD19/CD3 BiTE in acute lymphoblastic leukemia may be mediated by disrupted CD19 membrane trafficking. Blood *129*, 100–104.

Braun, A., Worbs, T., Moschovakis, G.L., Halle, S., Hoffmann, K., Bölter, J., Münk, A., and Förster, R. (2011). Afferent lymph-derived T cells and DCs use different chemokine receptor CCR7-dependent routes for entry into the lymph node and intranodal migration. Nat. Immunol. *12*, 879–887.

Braun, S., Hepp, F., Sommer, H.L., and Pantel, K. (1999). Tumor-antigen heterogeneity of disseminated breast cancer cells: implications for immunotherapy of minimal residual disease. Int. J. Cancer *84*, 1–5.

Breitfeld, D., Ohl, L., Kremmer, E., Ellwart, J., Sallusto, F., Lipp, M., and Förster, R. (2000). Follicular B Helper T Cells Express Cxc Chemokine Receptor 5, Localize to B Cell Follicles, and Support Immunoglobulin Production. Journal of Experimental Medicine *192*, 1545–1552.

Bridgeman, J.S., Hawkins, R.E., Bagley, S., Blaylock, M., Holland, M., and Gilham, D.E. (2010). The optimal antigen response of chimeric antigen receptors harboring the CD3zeta transmembrane domain is dependent upon incorporation of the receptor into the endogenous TCR/CD3 complex. J. Immunol. *184*, 6938–6949.

Brudno, J.N., and Kochenderfer, J.N. (2016). Toxicities of chimeric antigen receptor T cells: recognition and management. Blood *127*, 3321–3330.

Buadi, F.K., Micallef, I.N., Ansell, S.M., Porrata, L.F., Dispenzieri, A., Elliot, M.A., Gastineau, D.A., Gertz, M.A., Lacy, M.Q., Litzow, M.R., et al. (2006). Autologous hematopoietic stem cell transplantation for older patients with relapsed non-Hodgkin's lymphoma. Bone Marrow Transplant. *37*, 1017–1022.

Bunse, M., Pfeilschifter, J., Bluhm, J., Zschummel, M., Joedicke, J.J., Wirges, A., Stark, H., Kretschmer, V., Chmielewski, M., Uckert, W., et al. (2021). CXCR5 CAR-T cells simultaneously target B cell non-Hodgkin's lymphoma and tumor-supportive follicular T helper cells. Nat Commun *12*, 240.

Burger, J.A. (2011). Nurture versus Nature: The Microenvironment in Chronic Lymphocytic Leukemia. Hematology *2011*, 96–103.

Busch, D.H., Fräßle, S.P., Sommermeyer, D., Buchholz, V.R., and Riddell, S.R. (2016). Role of memory T cell subsets for adoptive immunotherapy. Semin Immunol *28*, 28–34.

Butcher, E.C., and Picker, L.J. (1996). Lymphocyte Homing and Homeostasis. Science *272*, 60–67.

Calderon, H., Mamonkin, M., and Guedan, S. (2020). Analysis of CAR-Mediated Tonic Signaling. In Chimeric Antigen Receptor T Cells, K. Swiech, K.C.R. Malmegrim, and V. Picanço-Castro, eds. (New York, NY: Springer US), pp. 223–236.

Caruana, I., Diaconu, I., and Dotti, G. (2014). From monoclonal antibodies to chimeric antigen receptors for the treatment of human malignancies. Semin. Oncol. *41*, 661–666.

Castro, F., Cardoso, A.P., Gonçalves, R.M., Serre, K., and Oliveira, M.J. (2018). Interferon-Gamma at the Crossroads of Tumor Immune Surveillance or Evasion. Front. Immunol. *9*, 847.

Cavallaro, U., and Christofori, G. (2004). Cell adhesion and signalling by cadherins and Ig-CAMs in cancer. Nat Rev Cancer *4*, 118–132.

Cesta, M.F. (2006). Normal Structure, Function, and Histology of Mucosa-Associated Lymphoid Tissue. Toxicol Pathol *34*, 599–608.

Cha, Z., Zang, Y., Guo, H., Rechlic, J.R., Olasnova, L.M., Gu, H., Tu, X., Song, H., and Qian, B. (2013). Association of peripheral CD4+ CXCR5+ T cells with chronic lymphocytic leukemia. Tumour Biol. *34*, 3579–3585.

Cha, Z., Gu, H., Zang, Y., Wang, Z., Li, J., Huang, W., Qin, A., Zhu, L., Tu, X., Cheng, N., et al. (2018). The prevalence and function of CD4+CXCR5+Foxp3+ follicular regulatory T cells in diffuse large B cell lymphoma. Int Immunopharmacol *61*, 132–139.

Chavez, J.C., Bachmeier, C., and Kharfan-Dabaja, M.A. (2019). CAR T-cell therapy for B-cell lymphomas: clinical trial results of available products. Ther Adv Hematol *10*, 2040620719841581.

Chen, D.R., and Cohen, P.L. (2012). Living life without B cells: is repeated B-cell depletion a safe and effective long-term treatment plan for rheumatoid arthritis? Int J Clin Rheumtol *7*, 159–166.

Chen, H., Li, M., Xu, N., Ng, N., Sanchez, E., Soof, C.M., Patil, S., Udd, K., Bujarski, S., Cao, J., et al. (2019). Serum B-cell maturation antigen (BCMA) reduces binding of anti-BCMA antibody to multiple myeloma cells. Leukemia Research *81*, 62–66.

Cheng, M., and Anderson, M.S. (2018). Thymic tolerance as a key brake on autoimmunity. Nat. Immunol. *19*, 659–664.

Cheng, W.W.K., Das, D., Suresh, M., and Allen, T.M. (2007). Expression and purification of two anti-CD19 single chain Fv fragments for targeting of liposomes to CD19-expressing cells. Biochimica et Biophysica Acta (BBA) - Biomembranes *1768*, 21–29.

Cherkassky, L., Morello, A., Villena-Vargas, J., Feng, Y., Dimitrov, D.S., Jones, D.R., Sadelain, M., and Adusumilli, P.S. (2016). Human CAR T cells with cell-intrinsic PD-1 checkpoint blockade resist tumor-mediated inhibition. Journal of Clinical Investigation *126*, 3130–3144.

Cheson, B.D., Bennett, J.M., Grever, M., Kay, N., Keating, M.J., O'Brien, S., and Rai, K.R. (1996). National Cancer Institute-sponsored Working Group guidelines for chronic lymphocytic leukemia: revised guidelines for diagnosis and treatment. Blood *87*, 4990–4997.

Chmielewski, M., and Abken, H. (2012). CAR T cells transform to trucks: chimeric antigen receptor–redirected T cells engineered to deliver inducible IL-12 modulate the tumour stroma to combat cancer. Cancer Immunol Immunother *61*, 1269–1277.

Chmielewski, M., and Abken, H. (2020). TRUCKS, the fourth-generation CAR T cells: Current developments and clinical translation. Adv Cell Gene Ther *3*.

Choi, W.W.L., Weisenburger, D.D., Greiner, T.C., Piris, M.A., Banham, A.H., Delabie, J., Braziel, R.M., Geng, H., Iqbal, J., Lenz, G., et al. (2009). A new immunostain algorithm classifies diffuse large B-cell lymphoma into molecular subtypes with high accuracy. Clin. Cancer Res. *15*, 5494–5502.

Chtanova, T., Tangye, S.G., Newton, R., Frank, N., Hodge, M.R., Rolph, M.S., and Mackay, C.R. (2004). T Follicular Helper Cells Express a Distinctive Transcriptional Profile, Reflecting Their Role as Non-Th1/Th2 Effector Cells That Provide Help for B Cells. J Immunol *173*, 68–78.

Chu, F., Li, H.S., Liu, X., Cao, J., Ma, W., Ma, Y., Weng, J., Zhu, Z., Cheng, X., Wang, Z., et al. (2019). CXCR5+CD8+ T cells are a distinct functional subset with an antitumor activity. Leukemia *33*, 2640–2653.

Chung, J.B., Silverman, M., and Monroe, J.G. (2003). Transitional B cells: step by step towards immune competence. Trends in Immunology *24*, 342–348.

Cieri, N., Camisa, B., Cocchiarella, F., Forcato, M., Oliveira, G., Provasi, E., Bondanza, A., Bordignon, C., Peccatori, J., Ciceri, F., et al. (2013). IL-7 and IL-15 instruct the generation of human memory stem T cells from naive precursors. Blood *121*, 573–584.

Clay, T.M., Custer, M.C., Sachs, J., Hwu, P., Rosenberg, S.A., and Nishimura, M.I. (1999). Efficient transfer of a tumor antigen-reactive TCR to human peripheral blood lymphocytes confers anti-tumor reactivity. J. Immunol. *163*, 507–513.

clinicaltrials.gov (2020). Search of the clinicaltrials.gov database 8/20.

CLL Trialists' Collaborative Group (1999). Chemotherapeutic options in chronic lymphocytic leukemia: a meta-analysis of the randomized trials. J. Natl. Cancer Inst. *91*, 861–868.

Cocco, P., t'Mannetje, A., Fadda, D., Melis, M., Becker, N., de Sanjosé, S., Foretova, L., Mareckova, J., Staines, A., Kleefeld, S., et al. (2010). Occupational exposure to solvents and risk of lymphoma subtypes: results from the Epilymph case-control study. Occup Environ Med *67*, 341–347.

Coiffier, B., Thieblemont, C., Van Den Neste, E., Lepeu, G., Plantier, I., Castaigne, S., Lefort, S., Marit, G., Macro, M., Sebban, C., et al. (2010). Long-term outcome of patients in the LNH-98.5 trial, the first randomized study comparing rituximab-CHOP to standard CHOP chemotherapy in DLBCL patients: a study by the Groupe d'Etudes des Lymphomes de l'Adulte. Blood *116*, 2040–2045.

Corthay, A. (2009). How do Regulatory T Cells Work? Scandinavian Journal of Immunology *70*, 326–336.

Costa, L.J., Xavier, A.C., Wahlquist, A.E., and Hill, E.G. (2013). Trends in survival of patients with Burkitt lymphoma/leukemia in the USA: an analysis of 3691 cases. Blood *121*, 4861–4866.

Craddock, J.A., Lu, A., Bear, A., Pule, M., Brenner, M.K., Rooney, C.M., and Foster, A.E. (2010). Enhanced tumor trafficking of GD2 chimeric antigen receptor T cells by expression of the chemokine receptor CCR2b. J. Immunother. *33*, 780–788.

Crisci, S., Di Francia, R., Mele, S., Vitale, P., Ronga, G., De Filippi, R., Berretta, M., Rossi, P., and Pinto, A. (2019). Overview of Targeted Drugs for Mature B-Cell Non-hodgkin Lymphomas. Front Oncol *9*, 443.

Croft, M., So, T., Duan, W., and Soroosh, P. (2009). The significance of OX40 and OX40L to T-cell biology and immune disease. Immunol Rev *229*, 173–191.

Crotty, S. (2011). Follicular Helper CD4 T Cells. Annu. Rev. Immunol. *29*, 621–663.

Crotty, S. (2014). T follicular helper cell differentiation, function, and roles in disease. Immunity *41*, 529–542.

Crump, M., Neelapu, S.S., Farooq, U., Van Den Neste, E., Kuruvilla, J., Westin, J., Link, B.K., Hay, A., Cerhan, J.R., Zhu, L., et al. (2017). Outcomes in refractory diffuse large B-cell lymphoma: results from the international SCHOLAR-1 study. Blood *130*, 1800–1808.

Cyster, J.G., Ansel, K.M., Reif, K., Ekland, E.H., Hyman, P.L., Tang, H.L., Luther, S.A., and Ngo, V.N. (2000). Follicular stromal cells and lymphocyte homing to follicles. Immunol. Rev. *176*, 181–193.

Dancescu, M., Rubio-Trujillo, M., Biron, G., Bron, D., Delespesse, G., and Sarfati, M. (1992). Interleukin 4 protects chronic lymphocytic leukemic B cells from death by apoptosis and upregulates Bcl-2 expression. J Exp Med *176*, 1319–1326.

D'Apuzzo, M., Rolink, A., Loetscher, M., Hoxie, J.A., Clark-Lewis, I., Melchers, F., Baggiolini, M., and Moser, B. (1997). The chemokine SDF-1, stromal cell-derived factor 1, attracts early stage B cell precursors via the chemokine receptor CXCR4. Eur. J. Immunol. *27*, 1788–1793.

Davila, M.L., Kloss, C.C., Gunset, G., and Sadelain, M. (2013). CD19 CAR-Targeted T Cells Induce Long-Term Remission and B Cell Aplasia in an Immunocompetent Mouse Model of B Cell Acute Lymphoblastic Leukemia. PLoS ONE *8*, e61338.

De Clercq, E. (2019). Mozobil® (Plerixafor, AMD3100), 10 years after its approval by the US Food and Drug Administration. Antivir Chem Chemother *27*, 2040206619829382.

DeBenedette, M.A., Chu, N.R., Pollok, K.E., Hurtado, J., Wade, W.F., Kwon, B.S., and Watts, T.H. (1995). Role of 4-1BB ligand in costimulation of T lymphocyte growth and its upregulation on M12 B lymphomas by cAMP. J. Exp. Med. *181*, 985–992.

DeBerardinis, R.J., Lum, J.J., Hatzivassiliou, G., and Thompson, C.B. (2008). The Biology of Cancer: Metabolic Reprogramming Fuels Cell Growth and Proliferation. Cell Metabolism *7*, 11–20.

Depil, S., Duchateau, P., Grupp, S.A., Mufti, G., and Poirot, L. (2020). 'Off-the-shelf' allogeneic CAR T cells: development and challenges. Nat Rev Drug Discov *19*, 185–199.

DeVries, M.E., Kelvin, A.A., Xu, L., Ran, L., Robinson, J., and Kelvin, D.J. (2006). Defining the Origins and Evolution of the Chemokine/Chemokine Receptor System. J Immunol *176*, 401–415.

Di Stasi, A., De Angelis, B., Rooney, C.M., Zhang, L., Mahendravada, A., Foster, A.E., Heslop, H.E., Brenner, M.K., Dotti, G., and Savoldo, B. (2009). T lymphocytes coexpressing CCR4 and a chimeric antigen receptor targeting CD30 have improved homing and antitumor activity in a Hodgkin tumor model. Blood *113*, 6392–6402.

Dieu-Nosjean, M.-C., Goc, J., Giraldo, N.A., Sautès-Fridman, C., and Fridman, W.H. (2014). Tertiary lymphoid structures in cancer and beyond. Trends in Immunology *35*, 571–580.

Doan, A., and Pulsipher, M.A. (2018). Hypogammaglobulinemia due to CAR T-cell therapy. Pediatr Blood Cancer *65*, e26914.

Dobner, T., Wolf, I., Emrich, T., and Lipp, M. (1992). Differentiation-specific expression of a novel G protein-coupled receptor from Burkitt's lymphoma. Eur. J. Immunol. *22*, 2795–2799.

Donnou, S., Galand, C., Touitou, V., Sautès-Fridman, C., Fabry, Z., and Fisson, S. (2012). Murine Models of B-Cell Lymphomas: Promising Tools for Designing Cancer Therapies. Advances in Hematology *2012*, 1–13.

Drake, A., Kaur, M., Iliopoulou, B.P., Phennicie, R., Hanson, A., and Chen, J. (2016). Interleukins 7 and 15 Maintain Human T Cell Proliferative Capacity through STAT5 Signaling. PLoS ONE *11*, e0166280.

Drake, A.C., Chen, Q., and Chen, J. (2012). Engineering humanized mice for improved hematopoietic reconstitution. Cell Mol Immunol *9*, 215–224.

Du, H., Zhang, L., Li, G., Liu, W., Tang, W., Zhang, H., Luan, J., Gao, L., and Wang, X. (2019). CXCR4 and CCR7 Expression in Primary Nodal Diffuse Large B-Cell Lymphoma—A Clinical and Immunohistochemical Study. The American Journal of the Medical Sciences *357*, 302–310.

Dudley, M.E., Wunderlich, J.R., Shelton, T.E., Even, J., and Rosenberg, S.A. (2003). Generation of tumor-infiltrating lymphocyte cultures for use in adoptive transfer therapy for melanoma patients. J. Immunother. *26*, 332–342.

Dupuis, J., Boye, K., Martin, N., Copie-Bergman, C., Plonquet, A., Fabiani, B., Baglin, A.-C., Haioun, C., Delfau-Larue, M.-H., and Gaulard, P. (2006). Expression of CXCL13 by Neoplastic Cells in Angioimmunoblastic T-Cell Lymphoma (AITL): A New Diagnostic Marker Providing Evidence That AITL Derives From Follicular Helper T Cells. The American Journal of Surgical Pathology *30*, 490–494.

Dürig, J., Schmücker, U., and Dührsen, U. (2001). Differential expression of chemokine receptors in B cell malignancies. Leukemia *15*, 752–756.

Ekström Smedby, K., Vajdic, C.M., Falster, M., Engels, E.A., Martínez-Maza, O., Turner, J., Hjalgrim, H., Vineis, P., Seniori Costantini, A., Bracci, P.M., et al. (2008). Autoimmune disorders and risk of non-Hodgkin lymphoma subtypes: a pooled analysis within the InterLymph Consortium. Blood *111*, 4029–4038.

Emrich, T. (1995). Der Lymphozyten-spezifische G Protein-gekoppelte Rezeptor BLR1: Biochemische Charakterisiserung und Untersuchung des Expressionsmusters während der B- und T-Zell-Entwicklung. Ludwig-Maximilians-Universität München.

Engels, B., Cam, H., Schüler, T., Indraccolo, S., Gladow, M., Baum, C., Blankenstein, T., and Uckert, W. (2003). Retroviral Vectors for High-Level Transgene Expression in T Lymphocytes. Human Gene Therapy *14*, 1155–1168.

Epstein, M.A., Achong, B.G., and Barr, Y.M. (1964). VIRUS PARTICLES IN CULTURED LYMPHOBLASTS FROM BURKITT'S LYMPHOMA. Lancet *1*, 702–703.

Farber, D.L., Yudanin, N.A., and Restifo, N.P. (2014). Human memory T cells: generation, compartmentalization and homeostasis. Nat. Rev. Immunol. *14*, 24–35.

Fargion, S., Carney, D., Mulshine, J., Rosen, S., Bunn, P., Jewett, P., Cuttitta, F., Gazdar, A., and Minna, J. (1986). Heterogeneity of cell surface antigen expression of human small cell lung cancer detected by monoclonal antibodies. Cancer Res. *46*, 2633–2638.

Feitelson, M.A., Arzumanyan, A., Kulathinal, R.J., Blain, S.W., Holcombe, R.F., Mahajna, J., Marino, M., Martinez-Chantar, M.L., Nawroth, R., Sanchez-Garcia, I., et al. (2015). Sustained proliferation in cancer: Mechanisms and novel therapeutic targets. Semin Cancer Biol *35 Suppl*, S25–S54.

Finney, H.M., Akbar, A.N., and Lawson, A.D.G. (2004). Activation of resting human primary T cells with chimeric receptors: costimulation from CD28, inducible costimulator, CD134, and CD137 in series with signals from the TCR zeta chain. J. Immunol. *172*, 104–113.

Fitzer-Attas, C.J., Schindler, D.G., Waks, T., and Eshhar, Z. (1998). Harnessing Syk family tyrosine kinases as signaling domains for chimeric single chain of the variable domain receptors: optimal design for T cell activation. J. Immunol. *160*, 145–154.

Flynn, S., Toellner, K.-M., Raykundalia, C., Goodall, M., and Lane, P. (1998). CD4 T Cell Cytokine Differentiation: The B Cell Activation Molecule, OX40 Ligand, Instructs CD4 T Cells to Express Interleukin 4 and Upregulates Expression of the Chemokine Receptor, Blr-1. Journal of Experimental Medicine *188*, 297–304.

Förster, Davalos-Misslitz, and Rot (2008). CCR7 and its ligands: balancing immunity and tolerance. Nat Rev Immunol *8*.

Förster, R., Emrich, T., Voss, C., and Lipp, M. (1993). A general method for screening mAbs specific for G-protein coupled receptors as exemplified by using epitope tagged BLR1-transfected 293 cells and solid-phase cell ELISA. Biochem. Biophys. Res. Commun. *196*, 1496–1503.

Förster, R., Emrich, T., Kremmer, E., and Lipp, M. (1994). Expression of the G-protein--coupled receptor BLR1 defines mature, recirculating B cells and a subset of T-helper memory cells. Blood *84*, 830–840.

Förster, R., Mattis, A.E., Kremmer, E., Wolf, E., Brem, G., and Lipp, M. (1996). A putative chemokine receptor, BLR1, directs B cell migration to defined lymphoid organs and specific anatomic compartments of the spleen. Cell *87*, 1037–1047.

Förster, R., Schubel, A., Breitfeld, D., Kremmer, E., Renner-Müller, I., Wolf, E., and Lipp, M. (1999). CCR7 coordinates the primary immune response by establishing functional microenvironments in secondary lymphoid organs. Cell *99*, 23–33.

Fraietta, J.A., Lacey, S.F., Orlando, E.J., Pruteanu-Malinici, I., Gohil, M., Lundh, S., Boesteanu, A.C., Wang, Y., O'Connor, R.S., Hwang, W.-T., et al. (2018). Determinants of response and resistance to CD19 chimeric antigen receptor (CAR) T cell therapy of chronic lymphocytic leukemia. Nat Med *24*, 563–571.

Freeman, G.J., Long, A.J., Iwai, Y., Bourque, K., Chernova, T., Nishimura, H., Fitz, L.J., Malenkovich, N., Okazaki, T., Byrne, M.C., et al. (2000). Engagement of the PD-1 immunoinhibitory receptor by a novel B7 family member leads to negative regulation of lymphocyte activation. J. Exp. Med. *192*, 1027–1034.

Fritze, J., Ginisty, A., McDonald, R., Quist, E., Stamp, E., Monni, E., Dhapola, P., Lang, S., and Ahlenius, H. (2020). Loss of Cxcr5 alters neuroblast proliferation and migration in the aged brain. Stem Cells.

Garboczi, D.N., Ghosh, P., Utz, U., Fan, Q.R., Biddison, W.E., and Wiley, D.C. (1996). Structure of the complex between human T-cell receptor, viral peptide and HLA-A2. Nature *384*, 134–141.

Gattinoni, L., Lugli, E., Ji, Y., Pos, Z., Paulos, C.M., Quigley, M.F., Almeida, J.R., Gostick, E., Yu, Z., Carpenito, C., et al. (2011). A human memory T cell subset with stem cell-like properties. Nat Med *17*, 1290–1297.

Gaulard, P., and de Leval, L. (2011). Follicular helper T cells: implications in neoplastic hematopathology. Semin Diagn Pathol *28*, 202–213.

Gerber, D.E., Pruitt, S.L., and Halm, E.A. (2015). Should criteria for inclusion in cancer clinical trials be expanded? J Comp Eff Res *4*, 289–291.

Ghia, P., Strola, G., Granziero, L., Geuna, M., Guida, G., Sallusto, F., Ruffing, N., Montagna, L., Piccoli, P., Chilosi, M., et al. (2002). Chronic lymphocytic leukemia B cells are endowed with the capacity to attract CD4+, CD40L+ T cells by producing CCL22. Eur. J. Immunol. *32*, 1403–1413.

Gloger, M., Menzel, L., Grau, M., Vion, A.-C., Anagnostopoulos, I., Zapukhlyak, M., Gerlach, K., Kammertöns, T., Hehlgans, T., Zschummel, M., et al. (2020). Lymphoma Angiogenesis Is Orchestrated by Noncanonical Signaling Pathways. Cancer Res *80*, 1316–1329.

Goedert, J.J., Coté, T.R., Virgo, P., Scoppa, S.M., Kingma, D.W., Gail, M.H., Jaffe, E.S., and Biggar, R.J. (1998). Spectrum of AIDS-associated malignant disorders. Lancet *351*, 1833–1839.

Gong, M.C., Latouche, J.B., Krause, A., Heston, W.D., Bander, N.H., and Sadelain, M. (1999). Cancer patient T cells genetically targeted to prostate-specific membrane antigen specifically lyse prostate cancer cells and release cytokines in response to prostate-specific membrane antigen. Neoplasia *1*, 123–127.

Good-Jacobson, K.L., Szumilas, C.G., Chen, L., Sharpe, A.H., Tomayko, M.M., and Shlomchik, M.J. (2010). PD-1 regulates germinal center B cell survival and the formation and affinity of long-lived plasma cells. Nat. Immunol. *11*, 535–542.

Gorgun, G., Ramsay, A.G., Holderried, T.A.W., Zahrieh, D., Le Dieu, R., Liu, F., Quackenbush, J., Croce, C.M., and Gribben, J.G. (2009). E(mu)-TCL1 mice represent a model for immunotherapeutic reversal of chronic lymphocytic leukemia-induced T-cell dysfunction. Proc Natl Acad Sci U S A *106*, 6250–6255.

Gowrishankar, K., Birtwistle, L., and Micklethwaite, K. (2018). Manipulating the tumor microenvironment by adoptive cell transfer of CAR T-cells. Mamm Genome *29*, 739–756.

Graef, P., Buchholz, V.R., Stemberger, C., Flossdorf, M., Henkel, L., Schiemann, M., Drexler, I., Höfer, T., Riddell, S.R., and Busch, D.H. (2014). Serial transfer of single-cell-derived immunocompetence reveals stemness of CD8(+) central memory T cells. Immunity *41*, 116–126.

Green, C.E., Liu, T., Montel, V., Hsiao, G., Lester, R.D., Subramaniam, S., Gonias, S.L., and Klemke, R.L. (2009). Chemoattractant signaling between tumor cells and macrophages regulates cancer cell migration, metastasis and neovascularization. PLoS One *4*, e6713.

Grivennikov, S.I., Greten, F.R., and Karin, M. (2010). Immunity, inflammation, and cancer. Cell *140*, 883–899.

Grogg, K.L., Attygalle, A.D., Macon, W.R., Remstein, E.D., Kurtin, P.J., and Dogan, A. (2005). Angioimmunoblastic T-cell lymphoma: a neoplasm of germinal-center T-helper cells? Blood *106*, 1501–1502.

Gross, G., Gorochov, G., Waks, T., and Eshhar, Z. (1989). Generation of effector T cells expressing chimeric T cell receptor with antibody type-specificity. Transplant. Proc. *21*, 127–130.

Grosser, R., Cherkassky, L., Chintala, N., and Adusumilli, P.S. (2019). Combination Immunotherapy with CAR T Cells and Checkpoint Blockade for the Treatment of Solid Tumors. Cancer Cell *36*, 471–482.

Guedan, S., Chen, X., Madar, A., Carpenito, C., McGettigan, S.E., Frigault, M.J., Lee, J., Posey, A.D., Scholler, J., Scholler, N., et al. (2014). ICOS-based chimeric antigen receptors program bipolar TH17/TH1 cells. Blood *124*, 1070–1080.

Guedan, S., Posey, A.D., Shaw, C., Wing, A., Da, T., Patel, P.R., McGettigan, S.E., Casado-Medrano, V., Kawalekar, O.U., Uribe-Herranz, M., et al. (2018). Enhancing CAR T cell persistence through ICOS and 4-1BB costimulation. JCI Insight *3*.

Guest, R.D., Hawkins, R.E., Kirillova, N., Cheadle, E.J., Arnold, J., O'Neill, A., Irlam, J., Chester, K.A., Kemshead, J.T., Shaw, D.M., et al. (2005). The role of extracellular spacer regions in the optimal design of chimeric immune receptors: evaluation of four different scFvs and antigens. J. Immunother. *28*, 203–211.

Gunn, M.D., Ngo, V.N., Ansel, K.M., Ekland, E.H., Cyster, J.G., and Williams, L.T. (1998). A B-cell-homing chemokine made in lymphoid follicles activates Burkitt's lymphoma receptor-1. Nature *391*, 799–803.

Gu-Trantien, C., Loi, S., Garaud, S., Equeter, C., Libin, M., de Wind, A., Ravoet, M., Le Buanec, H., Sibille, C., Manfouo-Foutsop, G., et al. (2013). CD4+ follicular helper T cell infiltration predicts breast cancer survival. J. Clin. Invest. *123*, 2873–2892.

Habermann, T.M., Weller, E.A., Morrison, V.A., Gascoyne, R.D., Cassileth, P.A., Cohn, J.B., Dakhil, S.R., Woda, B., Fisher, R.I., Peterson, B.A., et al. (2006). Rituximab-CHOP versus CHOP alone or with maintenance rituximab in older patients with diffuse large B-cell lymphoma. J. Clin. Oncol. *24*, 3121–3127.

Hafemeister, C., and Satija, R. (2019). Normalization and variance stabilization of single-cell RNA-seq data using regularized negative binomial regression. Genome Biol *20*, 296.

Hamblin, T.J., Davis, Z., Gardiner, A., Oscier, D.G., and Stevenson, F.K. (1999). Unmutated Ig V(H) genes are associated with a more aggressive form of chronic lymphocytic leukemia. Blood *94*, 1848–1854.

Han, S., Zhuang, H., Shumyak, S., Yang, L., and Reeves, W.H. (2015). Mechanisms of autoantibody production in systemic lupus erythematosus. Front Immunol *6*, 228.

Hanahan, D., and Folkman, J. (1996). Patterns and Emerging Mechanisms of the Angiogenic Switch during Tumorigenesis. Cell *86*, 353–364.

Hanahan, D., and Weinberg, R.A. (2000). The Hallmarks of Cancer. Cell *100*, 57–70.

Hanahan, D., and Weinberg, R.A. (2011). Hallmarks of Cancer: The Next Generation. Cell *144*, 646–674.

Haran, K.P., Hajduczki, A., Pampusch, M.S., Mwakalundwa, G., Vargas-Inchaustegui, D.A., Rakasz, E.G., Connick, E., Berger, E.A., and Skinner, P.J. (2018). Simian Immunodeficiency Virus (SIV)-Specific Chimeric Antigen Receptor-T Cells Engineered to Target B Cell Follicles and Suppress SIV Replication. Front Immunol *9*, 492.

Harjunpää, A., Junnikkala, S., and Meri, S. (2000). Rituximab (anti-CD20) therapy of B-cell lymphomas: direct complement killing is superior to cellular effector mechanisms. Scand. J. Immunol. *51*, 634–641.

Harris, N., Jaffe, E., Stein, H., Banks, P., Chan, J., Cleary, M., Delsol, G., De Wolf- Peeters, C., Falini, B., and Gatter, K. (1994). A revised European-American classification of lymphoid neoplasms: a proposal from the International Lymphoma Study Group [see comments]. Blood *84*, 1361–1392.

Haso, W., Lee, D.W., Shah, N.N., Stetler-Stevenson, M., Yuan, C.M., Pastan, I.H., Dimitrov, D.S., Morgan, R.A., FitzGerald, D.J., Barrett, D.M., et al. (2013). Anti-CD22-chimeric antigen receptors targeting B-cell precursor acute lymphoblastic leukemia. Blood *121*, 1165–1174.

Heinig, K., Gätjen, M., Grau, M., Stache, V., Anagnostopoulos, I., Gerlach, K., Niesner, R.A., Cseresnyes, Z., Hauser, A.E., Lenz, P., et al. (2014). Access to follicular dendritic cells

is a pivotal step in murine chronic lymphocytic leukemia B-cell activation and proliferation. Cancer Discov *4*, 1448–1465.

Henle, G., Henle, W., and Diehl, V. (1968). Relation of Burkitt's tumor-associated herpes-ytpe virus to infectious mononucleosis. Proc. Natl. Acad. Sci. U.S.A. *59*, 94–101.

Herek, T.A., and Cutucache, C.E. (2017). Using Murine Models to Investigate Tumor-Lymphoid Interactions: Spotlight on Chronic Lymphocytic Leukemia and Angioimmunoblastic T-Cell Lymphoma. Front Oncol *7*, 86.

Herman, S.E.M., Mustafa, R.Z., Gyamfi, J.A., Pittaluga, S., Chang, S., Chang, B., Farooqui, M., and Wiestner, A. (2014). Ibrutinib inhibits BCR and NF-κB signaling and reduces tumor proliferation in tissue-resident cells of patients with CLL. Blood *123*, 3286–3295.

Hewitson, J.P., West, K.A., James, K.R., Rani, G.F., Dey, N., Romano, A., Brown, N., Teichmann, S.A., Kaye, P.M., and Lagos, D. (2020). Malat1 Suppresses Immunity to Infection through Promoting Expression of Maf and IL-10 in Th Cells. J.I. *204*, 2949–2960.

Hildinger, M., Abel, K.L., Ostertag, W., and Baum, C. (1999). Design of 5′ Untranslated Sequences in Retroviral Vectors Developed for Medical Use. J. Virol. *73*, 4083–4089.

Hofbauer, J.P., Heyder, C., Denk, U., Kocher, T., Holler, C., Trapin, D., Asslaber, D., Tinhofer, I., Greil, R., and Egle, A. (2011). Development of CLL in the TCL1 transgenic mouse model is associated with severe skewing of the T-cell compartment homologous to human CLL. Leukemia *25*, 1452–1458.

Hoffman, W., Lakkis, F.G., and Chalasani, G. (2016). B Cells, Antibodies, and More. Clin J Am Soc Nephrol *11*, 137–154.

Holmes, E.C. (1985). Immunology of tumor infiltrating lymphocytes. Ann. Surg. *201*, 158–163.

Höpken, U.E., and Rehm, A. (2019). Targeting the Tumor Microenvironment of Leukemia and Lymphoma. Trends in Cancer *5*, 351–364.

Hoster, E., Klapper, W., Hermine, O., Kluin-Nelemans, H.C., Walewski, J., van Hoof, A., Trneny, M., Geisler, C.H., Di Raimondo, F., Szymczyk, M., et al. (2014). Confirmation of the mantle-cell lymphoma International Prognostic Index in randomized trials of the European Mantle-Cell Lymphoma Network. J. Clin. Oncol. *32*, 1338–1346.

Hsu, Y.-C., Mildenstein, K., Hunter, K., Tkachenko, O., and Mullen, C.A. (2014). Acute lymphoid leukemia cells with greater stem cell antigen-1 (Ly6a/Sca-1) expression exhibit higher levels of metalloproteinase activity and are more aggressive in vivo. PLoS One *9*, e88966.

Hu, Y., Gale, M., Shields, J., Garron, C., Swistak, M., Nguyen, T.-H., Jacques, G., Fogle, R., Siders, W., and Kaplan, J. (2012). Enhancement of the anti-tumor activity of therapeutic monoclonal antibodies by CXCR4 antagonists. Leukemia & Lymphoma *53*, 130–138.

Huang, Q., Liu, F., and Shen, J. (2019). The significance of chemokines in diffuse large B-cell lymphoma: a systematic review and future insights. Future Oncology *15*, 1385–1395.

Hudecek, M., Sommermeyer, D., Kosasih, P.L., Silva-Benedict, A., Liu, L., Rader, C., Jensen, M.C., and Riddell, S.R. (2015). The nonsignaling extracellular spacer domain of chimeric antigen receptors is decisive for in vivo antitumor activity. Cancer Immunol Res *3*, 125–135.

Hughes, C.E., and Nibbs, R.J.B. (2018). A guide to chemokines and their receptors. FEBS J. *285*, 2944–2971.

Hughes, M.S., Yu, Y.Y.L., Dudley, M.E., Zheng, Z., Robbins, P.F., Li, Y., Wunderlich, J., Hawley, R.G., Moayeri, M., Rosenberg, S.A., et al. (2005). Transfer of a TCR gene derived

from a patient with a marked antitumor response conveys highly active T-cell effector functions. Hum. Gene Ther. *16*, 457–472.

Hummel, M., Tamaru, J., Kalvelage, B., and Stein, H. (1994). Mantle cell (previously centrocytic) lymphomas express VH genes with no or very little somatic mutations like the physiologic cells of the follicle mantle. Blood *84*, 403–407.

Hussain, S.P., Hofseth, L.J., and Harris, C.C. (2003). Radical causes of cancer. Nat Rev Cancer *3*, 276–285.

Iijima, J., Konno, K., and Itano, N. (2011). Inflammatory alterations of the extracellular matrix in the tumor microenvironment. Cancers (Basel) *3*, 3189–3205.

Indrasingh, I., Chandi, G., and Vettivel, S. (2002). Route of lymphocyte migration through the high endothelial venule (HEV) in human palatine tonsil. Ann. Anat. *184*, 77–84.

Irving, B.A., and Weiss, A. (1991). The cytoplasmic domain of the T cell receptor zeta chain is sufficient to couple to receptor-associated signal transduction pathways. Cell *64*, 891–901.

Jacamo, R., Chen, Y., Wang, Z., Ma, W., Zhang, M., Spaeth, E.L., Wang, Y., Battula, V.L., Mak, P.Y., Schallmoser, K., et al. (2014). Reciprocal leukemia-stroma VCAM-1/VLA-4-dependent activation of NF-κB mediates chemoresistance. Blood *123*, 2691–2702.

Jackson, Z., Roe, A., Sharma, A.A., Lopes, F.B.T.P., Talla, A., Kleinsorge-Block, S., Zamborsky, K., Schiavone, J., Manjappa, S., Schauner, R., et al. (2020). Automated Manufacture of Autologous CD19 CAR-T Cells for Treatment of Non-hodgkin Lymphoma. Front. Immunol. *11*, 1941.

Jafarzadeh, L., Masoumi, E., Fallah-Mehrjardi, K., Mirzaei, H.R., and Hadjati, J. (2020). Prolonged Persistence of Chimeric Antigen Receptor (CAR) T Cell in Adoptive Cancer Immunotherapy: Challenges and Ways Forward. Front Immunol *11*, 702.

Jaffe, E.S., Harris, N.L., Diebold, J., and Muller-Hermelink, H.K. (1999). World Health Organization classification of neoplastic diseases of the hematopoietic and lymphoid tissues. A progress report. Am. J. Clin. Pathol. *111*, S8-12.

Jain, M.D., Bachmeier, C.A., Phuoc, V.H., and Chavez, J.C. (2018). Axicabtagene ciloleucel (KTE-C19), an anti-CD19 CAR T therapy for the treatment of relapsed/refractory aggressive B-cell non-Hodgkin's lymphoma. Ther Clin Risk Manag *14*, 1007–1017.

Jeon, Y.-W., Yoon, S., Min, G.J., Park, S.-S., Park, S., Yoon, J.-H., Lee, S.-E., Cho, B.-S., Eom, K.-S., Kim, Y.-J., et al. (2019). Risk factors predicting graft-versus-host disease and relapse-free survival after allogeneic hematopoietic stem cell transplantation in relapsed or refractory non-Hodgkin's lymphoma. Ann. Hematol. *98*, 1743–1753.

Jiang, B.-C., Cao, D.-L., Zhang, X., Zhang, Z.-J., He, L.-N., Li, C.-H., Zhang, W.-W., Wu, X.-B., Berta, T., Ji, R.-R., et al. (2016). CXCL13 drives spinal astrocyte activation and neuropathic pain via CXCR5. J. Clin. Invest. *126*, 745–761.

Jiang, T., Shi, T., Zhang, H., Hu, J., Song, Y., Wei, J., Ren, S., and Zhou, C. (2019). Tumor neoantigens: from basic research to clinical applications. J Hematol Oncol *12*, 93.

Jin, C.-H., Xia, J., Rafiq, S., Huang, X., Hu, Z., Zhou, X., Brentjens, R.J., and Yang, Y.-G. (2019). Modeling anti-CD19 CAR T cell therapy in humanized mice with human immunity and autologous leukemia. EBioMedicine *39*, 173–181.

John, L.B., Kershaw, M.H., and Darcy, P.K. (2013). Blockade of PD-1 immunosuppression boosts CAR T-cell therapy. Oncoimmunology *2*, e26286.

Johnson, L.A., Morgan, R.A., Dudley, M.E., Cassard, L., Yang, J.C., Hughes, M.S., Kammula, U.S., Royal, R.E., Sherry, R.M., Wunderlich, J.R., et al. (2009). Gene therapy with

human and mouse T-cell receptors mediates cancer regression and targets normal tissues expressing cognate antigen. Blood *114*, 535–546.

Johnson-Arbor, K., and Dubey, R. (2020). Doxorubicin. In StatPearls, (Treasure Island (FL): StatPearls Publishing), p.

Kaldor, J.M., Day, N.E., Band, P., Choi, N.W., Clarke, E.A., Coleman, M.P., Hakama, M., Koch, M., Langmark, F., and Neal, F.E. (1987). Second malignancies following testicular cancer, ovarian cancer and Hodgkin's disease: an international collaborative study among cancer registries. Int. J. Cancer *39*, 571–585.

Kansal, R., Richardson, N., Neeli, I., Khawaja, S., Chamberlain, D., Ghani, M., Ghani, Q., Balazs, L., Beranova-Giorgianni, S., Giorgianni, F., et al. (2019). Sustained B cell depletion by CD19-targeted CAR T cells is a highly effective treatment for murine lupus. Sci. Transl. Med. *11*, eaav1648.

Katakai, T. (2012). Marginal reticular cells: a stromal subset directly descended from the lymphoid tissue organizer. Front. Immun. *3*.

Katakai, T., Suto, H., Sugai, M., Gonda, H., Togawa, A., Suematsu, S., Ebisuno, Y., Katagiri, K., Kinashi, T., and Shimizu, A. (2008). Organizer-Like Reticular Stromal Cell Layer Common to Adult Secondary Lymphoid Organs. J Immunol *181*, 6189–6200.

Katz, D.H., Hamaoka, T., Dorf, M.E., and Benacerraf, B. (1973). Cell interactions between histoincompatible T and B lymphocytes. The H-2 gene complex determines successful physiologic lymphocyte interactions. Proc. Natl. Acad. Sci. U.S.A. *70*, 2624–2628.

Kawalekar, O.U., O'Connor, R.S., Fraietta, J.A., Guo, L., McGettigan, S.E., Posey, A.D., Patel, P.R., Guedan, S., Scholler, J., Keith, B., et al. (2016). Distinct Signaling of Coreceptors Regulates Specific Metabolism Pathways and Impacts Memory Development in CAR T Cells. Immunity *44*, 380–390.

Kazanietz, M.G., Durando, M., and Cooke, M. (2019). CXCL13 and Its Receptor CXCR5 in Cancer: Inflammation, Immune Response, and Beyond. Front. Endocrinol. *10*, 471.

Kearney, C.J., Vervoort, S.J., Hogg, S.J., Ramsbottom, K.M., Freeman, A.J., Lalaoui, N., Pijpers, L., Michie, J., Brown, K.K., Knight, D.A., et al. (2018). Tumor immune evasion arises through loss of TNF sensitivity. Sci. Immunol. *3*, eaar3451.

Kim, D.W., and Cho, J.-Y. (2020). Recent Advances in Allogeneic CAR-T Cells. Biomolecules *10*.

Klebanoff, C., Khong, H., Antony, P., Palmer, D., and Restifo, N. (2005). Sinks, suppressors and antigen presenters: how lymphodepletion enhances T cell-mediated tumor immunotherapy. Trends in Immunology *26*, 111–117.

Klein, L., Kyewski, B., Allen, P.M., and Hogquist, K.A. (2014). Positive and negative selection of the T cell repertoire: what thymocytes see (and don't see). Nat. Rev. Immunol. *14*, 377–391.

Klein, U., Klein, G., Ehlin-Henriksson, B., Rajewsky, K., and Küppers, R. (1995). Burkitt's lymphoma is a malignancy of mature B cells expressing somatically mutated V region genes. Mol. Med. *1*, 495–505.

Klichinsky, M., Ruella, M., Shestova, O., Lu, X.M., Best, A., Zeeman, M., Schmierer, M., Gabrusiewicz, K., Anderson, N.R., Petty, N.E., et al. (2020). Human chimeric antigen receptor macrophages for cancer immunotherapy. Nat Biotechnol.

Kluin-Nelemans, H.C., Hoster, E., Hermine, O., Walewski, J., Trneny, M., Geisler, C.H., Stilgenbauer, S., Thieblemont, C., Vehling-Kaiser, U., Doorduijn, J.K., et al. (2012). Treatment of older patients with mantle-cell lymphoma. N. Engl. J. Med. *367*, 520–531.

Kolb, H.J., Mittermüller, J., Clemm, C., Holler, E., Ledderose, G., Brehm, G., Heim, M., and Wilmanns, W. (1990). Donor leukocyte transfusions for treatment of recurrent chronic myelogenous leukemia in marrow transplant patients. Blood *76*, 2462–2465.

Kolb, H.J., Schattenberg, A., Goldman, J.M., Hertenstein, B., Jacobsen, N., Arcese, W., Ljungman, P., Ferrant, A., Verdonck, L., Niederwieser, D., et al. (1995). Graft-versus-leukemia effect of donor lymphocyte transfusions in marrow grafted patients. Blood *86*, 2041–2050.

Koneru, M., Purdon, T.J., Spriggs, D., Koneru, S., and Brentjens, R.J. (2015). IL-12 secreting tumor-targeted chimeric antigen receptor T cells eradicate ovarian tumors *in vivo*. OncoImmunology *4*, e994446.

Kotredes, K.P., and Gamero, A.M. (2013). Interferons as inducers of apoptosis in malignant cells. J. Interferon Cytokine Res. *33*, 162–170.

Krackhardt, A.M., Anliker, B., Hildebrandt, M., Bachmann, M., Eichmüller, S.B., Nettelbeck, D.M., Renner, M., Uharek, L., Willimsky, G., Schmitt, M., et al. (2018). Clinical translation and regulatory aspects of CAR/TCR-based adoptive cell therapies—the German Cancer Consortium approach. Cancer Immunol Immunother *67*, 513–523.

Krangel, M.S. (2009). Mechanics of T cell receptor gene rearrangement. Current Opinion in Immunology *21*, 133–139.

Krummel, M.F., and Allison, J.P. (1995). CD28 and CTLA-4 have opposing effects on the response of T cells to stimulation. J. Exp. Med. *182*, 459–465.

Kueberuwa, G., Kalaitsidou, M., Cheadle, E., Hawkins, R.E., and Gilham, D.E. (2018). CD19 CAR T Cells Expressing IL-12 Eradicate Lymphoma in Fully Lymphoreplete Mice through Induction of Host Immunity. Mol Ther Oncolytics *8*, 41–51.

Künzli, M., Schreiner, D., Pereboom, T.C., Swarnalekha, N., Litzler, L.C., Lötscher, J., Ertuna, Y.I., Roux, J., Geier, F., Jakob, R.P., et al. (2020). Long-lived T follicular helper cells retain plasticity and help sustain humoral immunity. Sci. Immunol. *5*, eaay5552.

Küppers, R., Rajewsky, K., and Hansmann, M.L. (1997). Diffuse large cell lymphomas are derived from mature B cells carrying V region genes with a high load of somatic mutation and evidence of selection for antibody expression. Eur. J. Immunol. *27*, 1398–1405.

Küppers, R., Klein, U., Hansmann, M.-L., and Rajewsky, K. (1999). Cellular Origin of Human B-Cell Lymphomas. N Engl J Med *341*, 1520–1529.

Kuwana, Y., Asakura, Y., Utsunomiya, N., Nakanishi, M., Arata, Y., Itoh, S., Nagase, F., and Kurosawa, Y. (1987). Expression of chimeric receptor composed of immunoglobulin-derived V regions and T-cell receptor-derived C regions. Biochem. Biophys. Res. Commun. *149*, 960–968.

Lai, Y., Wei, X., Lin, S., Qin, L., Cheng, L., and Li, P. (2017). Current status and perspectives of patient-derived xenograft models in cancer research. J Hematol Oncol *10*, 106.

Lanzavecchia, A., Iezzi, G., and Viola, A. (1999). From TCR engagement to T cell activation: a kinetic view of T cell behavior. Cell *96*, 1–4.

Laurent, S.A., Hoffmann, F.S., Kuhn, P.-H., Cheng, Q., Chu, Y., Schmidt-Supprian, M., Hauck, S.M., Schuh, E., Krumbholz, M., Rübsamen, H., et al. (2015). γ-Secretase directly sheds the survival receptor BCMA from plasma cells. Nat Commun *6*, 7333.

Legler, D.F., Loetscher, M., Roos, R.S., Clark-Lewis, I., Baggiolini, M., and Moser, B. (1998). B cell-attracting chemokine 1, a human CXC chemokine expressed in lymphoid tissues, selectively attracts B lymphocytes via BLR1/CXCR5. J. Exp. Med. *187*, 655–660.

Lesokhin, A.M., Ansell, S.M., Armand, P., Scott, E.C., Halwani, A., Gutierrez, M., Millenson, M.M., Cohen, A.D., Schuster, S.J., Lebovic, D., et al. (2016). Nivolumab in Patients With Relapsed or Refractory Hematologic Malignancy: Preliminary Results of a Phase Ib Study. J. Clin. Oncol. *34*, 2698–2704.

Li, Y., Yin, Y., and Mariuzza, R.A. (2013). Structural and biophysical insights into the role of CD4 and CD8 in T cell activation. Front Immunol *4*, 206.

Linette, G.P., Stadtmauer, E.A., Maus, M.V., Rapoport, A.P., Levine, B.L., Emery, L., Litzky, L., Bagg, A., Carreno, B.M., Cimino, P.J., et al. (2013). Cardiovascular toxicity and titin cross-reactivity of affinity-enhanced T cells in myeloma and melanoma. Blood *122*, 863–871.

Linsley, P.S., Clark, E.A., and Ledbetter, J.A. (1990). T-cell antigen CD28 mediates adhesion with B cells by interacting with activation antigen B7/BB-1. Proc. Natl. Acad. Sci. U.S.A. *87*, 5031–5035.

Linterman, M.A., Rigby, R.J., Wong, Raphael.K., Yu, D., Brink, R., Cannons, J.L., Schwartzberg, P.L., Cook, M.C., Walters, G.D., and Vinuesa, C.G. (2009). Follicular helper T cells are required for systemic autoimmunity. The Journal of Experimental Medicine *206*, 561–576.

Linterman, M.A., Pierson, W., Lee, S.K., Kallies, A., Kawamoto, S., Rayner, T.F., Srivastava, M., Divekar, D.P., Beaton, L., Hogan, J.J., et al. (2011). Foxp3+ follicular regulatory T cells control the germinal center response. Nat. Med. *17*, 975–982.

Liu, E., Tong, Y., Dotti, G., Shaim, H., Savoldo, B., Mukherjee, M., Orange, J., Wan, X., Lu, X., Reynolds, A., et al. (2018). Cord blood NK cells engineered to express IL-15 and a CD19-targeted CAR show long-term persistence and potent antitumor activity. Leukemia *32*, 520–531.

Liu, E., Marin, D., Banerjee, P., Macapinlac, H.A., Thompson, P., Basar, R., Nassif Kerbauy, L., Overman, B., Thall, P., Kaplan, M., et al. (2020a). Use of CAR-Transduced Natural Killer Cells in CD19-Positive Lymphoid Tumors. N Engl J Med *382*, 545–553.

Liu, H., Lei, W., Zhang, C., Yang, C., Wei, J., Guo, Q., Guo, X., Chen, Z., Lu, Y., Young, K.H., et al. (2020b). CD19-Specific CAR-T Cells that Express a PD-1/CD28 Chimeric Switch-Receptor is Effective in Patients with PD-L1 Positive B-Cell Lymphoma. Clin Cancer Res clincanres.1457.2020.

Liu, R., Wu, Q., Su, D., Che, N., Chen, H., Geng, L., Chen, J., Chen, W., Li, X., and Sun, L. (2012). A regulatory effect of IL-21 on T follicular helper-like cell and B cell in rheumatoid arthritis. Arthritis Res Ther *14*, R255.

Liu, Y., Chen, X., Han, W., and Zhang, Y. (2017). Tisagenlecleucel, an approved anti-CD19 chimeric antigen receptor T-cell therapy for the treatment of leukemia. Drugs Today *53*, 597–608.

Liu, Y., Di, S., Shi, B., Zhang, H., Wang, Y., Wu, X., Luo, H., Wang, H., Li, Z., and Jiang, H. (2019). Armored Inducible Expression of IL-12 Enhances Antitumor Activity of Glypican-3–Targeted Chimeric Antigen Receptor–Engineered T Cells in Hepatocellular Carcinoma. J.I. *203*, 198–207.

Llinàs, L., Lázaro, A., de Salort, J., Matesanz-Isabel, J., Sintes, J., and Engel, P. (2011). Expression profiles of novel cell surface molecules on B-cell subsets and plasma cells as analyzed by flow cytometry. Immunology Letters *134*, 113–121.

Locke, F.L., Ghobadi, A., Jacobson, C.A., Miklos, D.B., Lekakis, L.J., Oluwole, O.O., Lin, Y., Braunschweig, I., Hill, B.T., Timmerman, J.M., et al. (2019). Long-term safety and

activity of axicabtagene ciloleucel in refractory large B-cell lymphoma (ZUMA-1): a single-arm, multicentre, phase 1-2 trial. Lancet Oncol. *20*, 31–42.

van Loenen, M.M., de Boer, R., Amir, A.L., Hagedoorn, R.S., Volbeda, G.L., Willemze, R., van Rood, J.J., Falkenburg, J.H.F., and Heemskerk, M.H.M. (2010). Mixed T cell receptor dimers harbor potentially harmful neoreactivity. Proceedings of the National Academy of Sciences *107*, 10972–10977.

López-Giral, S., Quintana, N.E., Cabrerizo, M., Alfonso-Pérez, M., Sala-Valdés, M., de Soria, V.G.G., Fernández-Rañada, J.M., Fernández-Ruiz, E., and Muñoz, C. (2004). Chemokine receptors that mediate B cell homing to secondary lymphoid tissues are highly expressed in B cell chronic lymphocytic leukemia and non-Hodgkin lymphomas with widespread nodular dissemination. Journal of Leukocyte Biology *76*, 462–471.

Lowe, S.W., and Lin, A.W. (2000). Apoptosis in cancer. Carcinogenesis *21*, 485–495.

Luen, S.J., Salgado, R., Dieci, M.V., Vingiani, A., Curigliano, G., Gould, R.E., Castaneda, C., D'Alfonso, T., Sanchez, J., Cheng, E., et al. (2019). Prognostic implications of residual disease tumor-infiltrating lymphocytes and residual cancer burden in triple-negative breast cancer patients after neoadjuvant chemotherapy. Annals of Oncology *30*, 236–242.

Lundin, J., Kimby, E., Bergmann, L., Karakas, T., Mellstedt, H., and Österborg, A. (2001). Interleukin 4 therapy for patients with chronic lymphocytic leukaemia: a phase I/II study: Interleukin 4 Therapy in CLL. British Journal of Haematology *112*, 155–160.

Lunning, M.A., and Vose, J.M. (2017). Angioimmunoblastic T-cell lymphoma: the many-faced lymphoma. Blood *129*, 1095–1102.

Ma, J., Zhu, C., Ma, B., Tian, J., Baidoo, S.E., Mao, C., Wu, W., Chen, J., Tong, J., Yang, M., et al. (2012). Increased Frequency of Circulating Follicular Helper T Cells in Patients with Rheumatoid Arthritis. Clinical and Developmental Immunology *2012*, 1–7.

Ma, Q., Jones, D., Borghesani, P.R., Segal, R.A., Nagasawa, T., Kishimoto, T., Bronson, R.T., and Springer, T.A. (1998). Impaired B-lymphopoiesis, myelopoiesis, and derailed cerebellar neuron migration in CXCR4- and SDF-1-deficient mice. Proc. Natl. Acad. Sci. U.S.A. *95*, 9448–9453.

Ma, W.-T., Chang, C., Gershwin, M.E., and Lian, Z.-X. (2017). Development of autoantibodies precedes clinical manifestations of autoimmune diseases: A comprehensive review. Journal of Autoimmunity *83*, 95–112.

Mackay, F., and Browning, J.L. (1998). Turning off follicular dendritic cells. Nature *395*, 26–27.

Magen, A., Nie, J., Ciucci, T., Tamoutounour, S., Zhao, Y., Mehta, M., Tran, B., McGavern, D.B., Hannenhalli, S., and Bosselut, R. (2019). Single-Cell Profiling Defines Transcriptomic Signatures Specific to Tumor-Reactive versus Virus-Responsive CD4+ T Cells. Cell Reports *29*, 3019-3032.e6.

Maher, J., Brentjens, R.J., Gunset, G., Rivière, I., and Sadelain, M. (2002). Human T-lymphocyte cytotoxicity and proliferation directed by a single chimeric TCRzeta /CD28 receptor. Nat. Biotechnol. *20*, 70–75.

Malek, T.R., Ortega, G., Chan, C., Kroczek, R.A., and Shevach, E.M. (1986). Role of Ly-6 in lymphocyte activation. II. Induction of T cell activation by monoclonal anti-Ly-6 antibodies. J Exp Med *164*, 709–722.

Mamonkin, M., Rouce, R.H., Tashiro, H., and Brenner, M.K. (2015). A T-cell-directed chimeric antigen receptor for the selective treatment of T-cell malignancies. Blood *126*, 983–992.

Manches, O., Lui, G., Chaperot, L., Gressin, R., Molens, J.-P., Jacob, M.-C., Sotto, J.-J., Leroux, D., Bensa, J.-C., and Plumas, J. (2003). In vitro mechanisms of action of rituximab on primary non-Hodgkin lymphomas. Blood *101*, 949–954.

Mangolini, M., and Ringshausen, I. (2020). Bone Marrow Stromal Cells Drive Key Hallmarks of B Cell Malignancies. Int J Mol Sci *21*.

Mangolini, M., Götte, F., Moore, A., Ammon, T., Oelsner, M., Lutzny-Geier, G., Klein-Hitpass, L., Williamson, J.C., Lehner, P.J., Dürig, J., et al. (2018). Notch2 controls non-autonomous Wnt-signalling in chronic lymphocytic leukaemia. Nat Commun *9*, 3839.

Marlein, C.R., Piddock, R.E., Mistry, J.J., Zaitseva, L., Hellmich, C., Horton, R.H., Zhou, Z., Auger, M.J., Bowles, K.M., and Rushworth, S.A. (2019). CD38-Driven Mitochondrial Trafficking Promotes Bioenergetic Plasticity in Multiple Myeloma. Cancer Res *79*, 2285–2297.

Mårtensson, I.L., and Ceredig, R. (2000). Role of the surrogate light chain and the pre-B-cell receptor in mouse B-cell development. Immunology *101*, 435–441.

Marti, G.E., Faguet, G., Bertin, P., Agee, J., Washington, G., Ruiz, S., Carter, P., Zenger, V., Vogt, R., and Noguchi, P. (1992). CD20 and CD5 expression in B-chronic lymphocytic leukemia. Ann. N. Y. Acad. Sci. *651*, 480–483.

Mattila, S.O., Tuusa, J.T., and Petäjä-Repo, U.E. (2016). The Parkinson's-disease-associated receptor GPR37 undergoes metalloproteinase-mediated N-terminal cleavage and ectodomain shedding. J Cell Sci *129*, 1366–1377.

Maude, S.L., Frey, N., Shaw, P.A., Aplenc, R., Barrett, D.M., Bunin, N.J., Chew, A., Gonzalez, V.E., Zheng, Z., Lacey, S.F., et al. (2014). Chimeric antigen receptor T cells for sustained remissions in leukemia. N. Engl. J. Med. *371*, 1507–1517.

Maziarz, R.T., Waller, E.K., Jaeger, U., Fleury, I., McGuirk, J., Holte, H., Jaglowski, S., Schuster, S.J., Bishop, M.R., Westin, J.R., et al. (2020). Patient-reported long-term quality of life after tisagenlecleucel in relapsed/refractory diffuse large B-cell lymphoma. Blood Adv *4*, 629–637.

McDonnell, T.J., Deane, N., Platt, F.M., Nunez, G., Jaeger, U., McKearn, J.P., and Korsmeyer, S.J. (1989). bcl-2-immunoglobulin transgenic mice demonstrate extended B cell survival and follicular lymphoproliferation. Cell *57*, 79–88.

McEver, R.P. (2015). Selectins: initiators of leucocyte adhesion and signalling at the vascular wall. Cardiovasc. Res. *107*, 331–339.

Mchayleh, W., Bedi, P., Sehgal, R., and Solh, M. (2019). Chimeric Antigen Receptor T-Cells: The Future is Now. J Clin Med *8*.

McInnes, L., Healy, J., and Melville, J. (2020). UMAP: Uniform Manifold Approximation and Projection for Dimension Reduction. ArXiv:1802.03426 [Cs, Stat].

McLellan, A.D., and Ali Hosseini Rad, S.M. (2019). Chimeric antigen receptor T cell persistence and memory cell formation. Immunol Cell Biol *97*, 664–674.

Mebius, R.E. (2003). Organogenesis of lymphoid tissues. Nat Rev Immunol *3*, 292–303.

Mebius, R.E., and Kraal, G. (2005). Structure and function of the spleen. Nat Rev Immunol *5*, 606–616.

Medina, D.J., Goodell, L., Glod, J., Gélinas, C., Rabson, A.B., and Strair, R.K. (2012). Mesenchymal stromal cells protect mantle cell lymphoma cells from spontaneous and drug-induced apoptosis through secretion of B-cell activating factor and activation of the canonical and non-canonical nuclear factor κB pathways. Haematologica *97*, 1255–1263.

Mezzanzanica, D., Canevari, S., Mazzoni, A., Figini, M., Colnaghi, M.I., Waks, T., Schindler, D.G., and Eshhar, Z. (1998). Transfer of chimeric receptor gene made of variable regions of tumor-specific antibody confers anticarbohydrate specificity on T cells. Cancer Gene Ther. *5*, 401–407.

Middle, S., Coupland, S.E., Taktak, A., Kidgell, V., Slupsky, J.R., Pettitt, A.R., and Till, K.J. (2015a). Immunohistochemical analysis indicates that the anatomical location of B-cell non-Hodgkin's lymphoma is determined by differentially expressed chemokine receptors, sphingosine-1-phosphate receptors and integrins. Exp Hematol Oncol *4*, 10.

Middle, S., Coupland, S.E., Taktak, A., Kidgell, V., Slupsky, J.R., Pettitt, A.R., and Till, K.J. (2015b). Immunohistochemical analysis indicates that the anatomical location of B-cell non-Hodgkin's lymphoma is determined by differentially expressed chemokine receptors, sphingosine-1-phosphate receptors and integrins. Exp Hematol Oncol *4*, 10.

Milone, M.C., Fish, J.D., Carpenito, C., Carroll, R.G., Binder, G.K., Teachey, D., Samanta, M., Lakhal, M., Gloss, B., Danet-Desnoyers, G., et al. (2009). Chimeric receptors containing CD137 signal transduction domains mediate enhanced survival of T cells and increased antileukemic efficacy in vivo. Mol. Ther. *17*, 1453–1464.

Ming, Jeffrey, Zilberstein, Moshe E., and Karimi Anderesi, Roghieh (2018). Treatment of lupus using humanized anti-cxcr5 antibodies.

Mintz, M.A., Felce, J.H., Chou, M.Y., Mayya, V., Xu, Y., Shui, J.-W., An, J., Li, Z., Marson, A., Okada, T., et al. (2019). The HVEM-BTLA Axis Restrains T Cell Help to Germinal Center B Cells and Functions as a Cell-Extrinsic Suppressor in Lymphomagenesis. Immunity *51*, 310-323.e7.

Mock, U., Nickolay, L., Philip, B., Cheung, G.W.-K., Zhan, H., Johnston, I.C.D., Kaiser, A.D., Peggs, K., Pule, M., Thrasher, A.J., et al. (2016). Automated manufacturing of chimeric antigen receptor T cells for adoptive immunotherapy using CliniMACS Prodigy. Cytotherapy *18*, 1002–1011.

Mohammed, S., Sukumaran, S., Bajgain, P., Watanabe, N., Heslop, H.E., Rooney, C.M., Brenner, M.K., Fisher, W.E., Leen, A.M., and Vera, J.F. (2017). Improving Chimeric Antigen Receptor-Modified T Cell Function by Reversing the Immunosuppressive Tumor Microenvironment of Pancreatic Cancer. Mol. Ther. *25*, 249–258.

Mollica Poeta, V., Massara, M., Capucetti, A., and Bonecchi, R. (2019). Chemokines and Chemokine Receptors: New Targets for Cancer Immunotherapy. Front Immunol *10*, 379.

Morath, A., and Schamel, W.W. (2020). αβ and γδ T cell receptors: Similar but different. J Leukoc Biol *107*, 1045–1055.

Morgan, R.A., Dudley, M.E., Wunderlich, J.R., Hughes, M.S., Yang, J.C., Sherry, R.M., Royal, R.E., Topalian, S.L., Kammula, U.S., Restifo, N.P., et al. (2006). Cancer regression in patients after transfer of genetically engineered lymphocytes. Science *314*, 126–129.

Morgan, R.A., Yang, J.C., Kitano, M., Dudley, M.E., Laurencot, C.M., and Rosenberg, S.A. (2010). Case report of a serious adverse event following the administration of T cells transduced with a chimeric antigen receptor recognizing ERBB2. Mol. Ther. *18*, 843–851.

Morgan, R.A., Chinnasamy, N., Abate-Daga, D., Gros, A., Robbins, P.F., Zheng, Z., Dudley, M.E., Feldman, S.A., Yang, J.C., Sherry, R.M., et al. (2013). Cancer Regression and Neurological Toxicity Following Anti-MAGE-A3 TCR Gene Therapy: Journal of Immunotherapy *36*, 133–151.

Mori, S., Rempel, R.E., Chang, J.T., Yao, G., Lagoo, A.S., Potti, A., Bild, A., and Nevins, J.R. (2008). Utilization of Pathway Signatures to Reveal Distinct Types of B Lymphoma in the E -myc Model and Human Diffuse Large B-Cell Lymphoma. Cancer Research *68*, 8525–8534.

Morita, R., Schmitt, N., Bentebibel, S.-E., Ranganathan, R., Bourdery, L., Zurawski, G., Foucat, E., Dullaers, M., Oh, S., Sabzghabaei, N., et al. (2011). Human blood CXCR5(+)CD4(+) T cells are counterparts of T follicular cells and contain specific subsets that differentially support antibody secretion. Immunity *34*, 108–121.

Morrissey, M.A., Williamson, A.P., Steinbach, A.M., Roberts, E.W., Kern, N., Headley, M.B., and Vale, R.D. (2018). Chimeric antigen receptors that trigger phagocytosis. Elife *7*.

Moschovakis, G.L., Bubke, A., Friedrichsen, M., Falk, C.S., Feederle, R., and Förster, R. (2017). T cell specific Cxcr5 deficiency prevents rheumatoid arthritis. Sci Rep *7*, 8933.

Muller, W.A. (2013). Getting leukocytes to the site of inflammation. Vet. Pathol. *50*, 7–22.

Mumprecht, S., Schürch, C., Schwaller, J., Solenthaler, M., and Ochsenbein, A.F. (2009). Programmed death 1 signaling on chronic myeloid leukemia–specific T cells results in T-cell exhaustion and disease progression. Blood *114*, 1528–1536.

Murphy, Travers, Paul, and Walport, Mark (2008). Janeway's Immunobiology.

Murphy, W.J., Kumar, V., and Bennett, M. (1987). Acute rejection of murine bone marrow allografts by natural killer cells and T cells. Differences in kinetics and target antigens recognized. J. Exp. Med. *166*, 1499–1509.

Mutalima, N., Molyneux, E., Jaffe, H., Kamiza, S., Borgstein, E., Mkandawire, N., Liomba, G., Batumba, M., Lagos, D., Gratrix, F., et al. (2008). Associations between Burkitt lymphoma among children in Malawi and infection with HIV, EBV and malaria: results from a case-control study. PLoS ONE *3*, e2505.

Myers, R.C., King, R.G., Carter, R.H., and Justement, L.B. (2013). Lymphotoxin α1β2 expression on B cells is required for follicular dendritic cell activation during the germinal center response: Cellular immune response. Eur. J. Immunol. *43*, 348–359.

Nagamine, K., Peterson, P., Scott, H.S., Kudoh, J., Minoshima, S., Heino, M., Krohn, K.J.E., Lalioti, M.D., Mullis, P.E., Antonarakis, S.E., et al. (1997). Positional cloning of the APECED gene. Nat Genet *17*, 393–398.

Neelapu, S.S., Munoz, J., Locke, F.L., Miklos, D.B., Brown, R., McDevitt, J.T., Mardiros, A., Demirhan, E., Konto, C., and Tees, M.T. (2020). First-in-human data of ALLO-501 and ALLO-647 in relapsed/refractory large B-cell or follicular lymphoma (R/R LBCL/FL): ALPHA study. JCO *38*, 8002–8002.

Negrini, S., Gorgoulis, V.G., and Halazonetis, T.D. (2010). Genomic instability — an evolving hallmark of cancer. Nat Rev Mol Cell Biol *11*, 220–228.

Nesbit, C.E., Tersak, J.M., and Prochownik, E.V. (1999). MYC oncogenes and human neoplastic disease. Oncogene *18*, 3004–3016.

Ngo, V.N., Korner, H., Gunn, M.D., Schmidt, K.N., Sean Riminton, D., Cooper, M.D., Browning, J.L., Sedgwick, J.D., and Cyster, J.G. (1999). Lymphotoxin α/β and Tumor Necrosis Factor Are Required for Stromal Cell Expression of Homing Chemokines in B and T Cell Areas of the Spleen. Journal of Experimental Medicine *189*, 403–412.

Nicholson, I.C., Lenton, K.A., Little, D.J., Decorso, T., Lee, F.T., Scott, A.M., Zola, H., and Hohmann, A.W. (1997). Construction and characterisation of a functional CD19 specific single chain Fv fragment for immunotherapy of B lineage leukaemia and lymphoma. Molecular Immunology *34*, 1157–1165.

Nie, Y., Waite, J., Brewer, F., Sunshine, M.-J., Littman, D.R., and Zou, Y.-R. (2004). The Role of CXCR4 in Maintaining Peripheral B Cell Compartments and Humoral Immunity. Journal of Experimental Medicine *200*, 1145–1156.

Nieuwenhuis, P., and Opstelten, D. (1984). Functional anatomy of germinal centers. Am. J. Anat. *170*, 421–435.

Nombela-Arrieta, C., and Manz, M.G. (2017). Quantification and three-dimensional microanatomical organization of the bone marrow. Blood Adv *1*, 407–416.

Nutt, S.L., Hodgkin, P.D., Tarlinton, D.M., and Corcoran, L.M. (2015). The generation of antibody-secreting plasma cells. Nat Rev Immunol *15*, 160–171.

Obenaus, M., Leitão, C., Leisegang, M., Chen, X., Gavvovidis, I., van der Bruggen, P., Uckert, W., Schendel, D.J., and Blankenstein, T. (2015). Identification of human T-cell receptors with optimal affinity to cancer antigens using antigen-negative humanized mice. Nat. Biotechnol. *33*, 402–407.

O'Connell, R.M., Balazs, A.B., Rao, D.S., Kivork, C., Yang, L., and Baltimore, D. (2010). Lentiviral Vector Delivery of Human Interleukin-7 (hIL-7) to Human Immune System (HIS) Mice Expands T Lymphocyte Populations. PLoS ONE *5*, e12009.

Ogino, M.H., and Tadi, P. (2020). Cyclophosphamide. In StatPearls, (Treasure Island (FL): StatPearls Publishing), p.

Ohl, L., Henning, G., Krautwald, S., Lipp, M., Hardtke, S., Bernhardt, G., Pabst, O., and Förster, R. (2003). Cooperating mechanisms of CXCR5 and CCR7 in development and organization of secondary lymphoid organs. J. Exp. Med. *197*, 1199–1204.

Olszewski, A.J., and Castillo, J.J. (2013). Survival of patients with marginal zone lymphoma: analysis of the Surveillance, Epidemiology, and End Results database. Cancer *119*, 629–638.

Oprea, M., and Perelson, A.S. (1997). Somatic mutation leads to efficient affinity maturation when centrocytes recycle back to centroblasts. J. Immunol. *158*, 5155–5162.

Orlando, E.J., Han, X., Tribouley, C., Wood, P.A., Leary, R.J., Riester, M., Levine, J.E., Qayed, M., Grupp, S.A., Boyer, M., et al. (2018). Genetic mechanisms of target antigen loss in CAR19 therapy of acute lymphoblastic leukemia. Nat Med *24*, 1504–1506.

Ostroumov, D., Fekete-Drimusz, N., Saborowski, M., Kühnel, F., and Woller, N. (2018). CD4 and CD8 T lymphocyte interplay in controlling tumor growth. Cell. Mol. Life Sci. *75*, 689–713.

Ott, O.J., Rödel, C., Gramatzki, M., Niedobitek, G., Sauer, R., and Grabenbauer, G.G. (2003). Radiotherapy for stage I-III nodal low-grade non-Hodgkin's lymphoma. Strahlenther Onkol *179*, 694–701.

Pagès, F., Galon, J., Dieu-Nosjean, M.-C., Tartour, E., Sautès-Fridman, C., and Fridman, W.-H. (2010). Immune infiltration in human tumors: a prognostic factor that should not be ignored. Oncogene *29*, 1093–1102.

Panayiotidis, P., Jones, D., Ganeshaguru, K., Foroni, L., and Hoffbrand, A.V. (1996). Human bone marrow stromal cells prevent apoptosis and support the survival of chronic lymphocytic leukaemia cells in vitro. Br. J. Haematol. *92*, 97–103.

Pandey, S., Mourcin, F., Marchand, T., Nayar, S., Guirriec, M., Pangault, C., Monvoisin, C., Amé-Thomas, P., Guilloton, F., Dulong, J., et al. (2017). IL-4/CXCL12 loop is a key regulator of lymphoid stroma function in follicular lymphoma. Blood *129*, 2507–2518.

Pangault, C., Amé-Thomas, P., Ruminy, P., Rossille, D., Caron, G., Baia, M., De Vos, J., Roussel, M., Monvoisin, C., Lamy, T., et al. (2010). Follicular lymphoma cell niche: identification of a preeminent IL-4-dependent TFH–B cell axis. Leukemia *24*, 2080–2089.

Panjideh, H., Müller, G., Koch, M., Wilde, F., Scheu, S., Moldenhauer, G., and Lipp, M. (2014). Immunotherapy of B-cell non-Hodgkin lymphoma by targeting the chemokine receptor CXCR5 in a preclinical mouse model: Targeting Chemokine Receptor CXCR5 by Antibodies. Int. J. Cancer *135*, 2623–2632.

Panse, J., Friedrichs, K., Marx, A., Hildebrandt, Y., Luetkens, T., Bartels, K., Horn, C., Stahl, T., Cao, Y., Milde-Langosch, K., et al. (2008). Chemokine CXCL13 is overexpressed in the tumour tissue and in the peripheral blood of breast cancer patients. Br J Cancer *99*, 930–938.

Parkhurst, M.R., Yang, J.C., Langan, R.C., Dudley, M.E., Nathan, D.-A.N., Feldman, S.A., Davis, J.L., Morgan, R.A., Merino, M.J., Sherry, R.M., et al. (2011). T Cells Targeting Carcinoembryonic Antigen Can Mediate Regression of Metastatic Colorectal Cancer but Induce Severe Transient Colitis. Molecular Therapy *19*, 620–626.

Pascutti, M.F., Jak, M., Tromp, J.M., Derks, I.A.M., Remmerswaal, E.B.M., Thijssen, R., van Attekum, M.H.A., van Bochove, G.G., Luijks, D.M., Pals, S.T., et al. (2013). IL-21 and CD40L signals from autologous T cells can induce antigen-independent proliferation of CLL cells. Blood *122*, 3010–3019.

Passos, G.A., Speck-Hernandez, C.A., Assis, A.F., and Mendes-da-Cruz, D.A. (2018). Update on Aire and thymic negative selection. Immunology *153*, 10–20.

Patten, P.E.M., Buggins, A.G.S., Richards, J., Wotherspoon, A., Salisbury, J., Mufti, G.J., Hamblin, T.J., and Devereux, S. (2008). CD38 expression in chronic lymphocytic leukemia is regulated by the tumor microenvironment. Blood *111*, 5173–5181.

Pearse, G. (2006). Normal Structure, Function and Histology of the Thymus. Toxicol Pathol *34*, 504–514.

Perera, L.P., Zhang, M., Nakagawa, M., Petrus, M.N., Maeda, M., Kadin, M.E., Waldmann, T.A., and Perera, P.-Y. (2017). Chimeric antigen receptor modified T cells that target chemokine receptor CCR4 as a therapeutic modality for T-cell malignancies. Am J Hematol *92*, 892–901.

Petersen, C.T., Hassan, M., Morris, A.B., Jeffery, J., Lee, K., Jagirdar, N., Staton, A.D., Raikar, S.S., Spencer, H.T., Sulchek, T., et al. (2018). Improving T-cell expansion and function for adoptive T-cell therapy using ex vivo treatment with PI3Kδ inhibitors and VIP antagonists. Blood Adv *2*, 210–223.

Philip, T., Guglielmi, C., Hagenbeek, A., Somers, R., Van der Lelie, H., Bron, D., Sonneveld, P., Gisselbrecht, C., Cahn, J.Y., and Harousseau, J.L. (1995). Autologous bone marrow transplantation as compared with salvage chemotherapy in relapses of chemotherapy-sensitive non-Hodgkin's lymphoma. N. Engl. J. Med. *333*, 1540–1545.

Pollok, K.E., Kim, Y.J., Zhou, Z., Hurtado, J., Kim, K.K., Pickard, R.T., and Kwon, B.S. (1993). Inducible T cell antigen 4-1BB. Analysis of expression and function. J. Immunol. *150*, 771–781.

Porter, D.L., Hwang, W.-T., Frey, N.V., Lacey, S.F., Shaw, P.A., Loren, A.W., Bagg, A., Marcucci, K.T., Shen, A., Gonzalez, V., et al. (2015). Chimeric antigen receptor T cells persist and induce sustained remissions in relapsed refractory chronic lymphocytic leukemia. Sci. Transl. Med. *7*, 303ra139-303ra139.

Prieto, J.M.B., and Felippe, M.J.B. (2017). Development, phenotype, and function of non-conventional B cells. Comparative Immunology, Microbiology and Infectious Diseases *54*, 38–44.

Puckett, Y., Gabbar, A., and Bokhari, A.A. (2020). Prednisone. In StatPearls, (Treasure Island (FL): StatPearls Publishing), p.

Pulte, D., Jansen, L., Gondos, A., Emrich, K., Holleczek, B., Katalinic, A., Brenner, H., and GEKID Cancer Survival Working Group (2013). Survival of patients with non-Hodgkin lymphoma in Germany in the early 21st century. Leuk. Lymphoma *54*, 979–985.

Rafiq, S., Yeku, O.O., Jackson, H.J., Purdon, T.J., van Leeuwen, D.G., Drakes, D.J., Song, M., Miele, M.M., Li, Z., Wang, P., et al. (2018). Targeted delivery of a PD-1-blocking scFv by CAR-T cells enhances anti-tumor efficacy in vivo. Nat. Biotechnol. *36*, 847–856.

Ramello, M.C., Benzaïd, I., Kuenzi, B.M., Lienlaf-Moreno, M., Kandell, W.M., Santiago, D.N., Pabón-Saldaña, M., Darville, L., Fang, B., Rix, U., et al. (2019). An immunoproteomic approach to characterize the CAR interactome and signalosome. Sci Signal *12*.

Rapoport, A.P., Stadtmauer, E.A., Binder-Scholl, G.K., Goloubeva, O., Vogl, D.T., Lacey, S.F., Badros, A.Z., Garfall, A., Weiss, B., Finklestein, J., et al. (2015). NY-ESO-1-specific TCR-engineered T cells mediate sustained antigen-specific antitumor effects in myeloma. Nat. Med. *21*, 914–921.

Reff, M.E., Carner, K., Chambers, K.S., Chinn, P.C., Leonard, J.E., Raab, R., Newman, R.A., Hanna, N., and Anderson, D.R. (1994). Depletion of B cells in vivo by a chimeric mouse human monoclonal antibody to CD20. Blood *83*, 435–445.

Rehm, A., Mensen, A., Schradi, K., Gerlach, K., Wittstock, S., Winter, S., Büchner, G., Dörken, B., Lipp, M., and Höpken, U.E. (2011). Cooperative function of CCR7 and lymphotoxin in the formation of a lymphoma-permissive niche within murine secondary lymphoid organs. Blood *118*, 1020–1033.

Reighard, S.D., Cranert, S.A., Rangel, K.M., Ali, A., Gyurova, I.E., de la Cruz-Lynch, A.T., Tuazon, J.A., Khodoun, M.V., Kottyan, L.C., Smith, D.F., et al. (2020). Therapeutic Targeting of Follicular T Cells with Chimeric Antigen Receptor-Expressing Natural Killer Cells. Cell Reports Medicine *1*, 100003.

Ribatti, D., Nico, B., Ranieri, G., Specchia, G., and Vacca, A. (2013). The role of angiogenesis in human non-Hodgkin lymphomas. Neoplasia *15*, 231–238.

Robbins, P.F., Morgan, R.A., Feldman, S.A., Yang, J.C., Sherry, R.M., Dudley, M.E., Wunderlich, J.R., Nahvi, A.V., Helman, L.J., Mackall, C.L., et al. (2011). Tumor regression in patients with metastatic synovial cell sarcoma and melanoma using genetically engineered lymphocytes reactive with NY-ESO-1. J. Clin. Oncol. *29*, 917–924.

Rock, K.L., Reits, E., and Neefjes, J. (2016). Present Yourself! By MHC Class I and MHC Class II Molecules. Trends Immunol. *37*, 724–737.

Rosenberg, S.A., Packard, B.S., Aebersold, P.M., Solomon, D., Topalian, S.L., Toy, S.T., Simon, P., Lotze, M.T., Yang, J.C., Seipp, C.A., et al. (1988). Use of Tumor-Infiltrating Lymphocytes and Interleukin-2 in the Immunotherapy of Patients with Metastatic Melanoma. N Engl J Med *319*, 1676–1680.

Rosenberg, S.A., Yang, J.C., Sherry, R.M., Kammula, U.S., Hughes, M.S., Phan, G.Q., Citrin, D.E., Restifo, N.P., Robbins, P.F., Wunderlich, J.R., et al. (2011). Durable complete responses in heavily pretreated patients with metastatic melanoma using T-cell transfer immunotherapy. Clin. Cancer Res. *17*, 4550–4557.

Rosenblum, M.D., Gratz, I.K., Paw, J.S., and Abbas, A.K. (2012). Treating human autoimmunity: current practice and future prospects. Sci Transl Med *4*, 125sr1.

Ruan, J., Hajjar, K., Rafii, S., and Leonard, J.P. (2009). Angiogenesis and antiangiogenic therapy in non-Hodgkin's lymphoma. Annals of Oncology *20*, 413–424.

Sakuishi, K., Apetoh, L., Sullivan, J.M., Blazar, B.R., Kuchroo, V.K., and Anderson, A.C. (2010). Targeting Tim-3 and PD-1 pathways to reverse T cell exhaustion and restore anti-tumor immunity. J. Exp. Med. *207*, 2187–2194.

Sallusto, F., Lenig, D., Förster, R., Lipp, M., and Lanzavecchia, A. (1999). Two subsets of memory T lymphocytes with distinct homing potentials and effector functions. Nature *401*, 708–712.

Samaha, H., Dumontet, C., Ketterer, N., Moullet, I., Thieblemont, C., Bouafia, F., Callet-Bauchu, E., Felman, P., Berger, F., Salles, G., et al. (1998). Mantle cell lymphoma: a retrospective study of 121 cases. Leukemia *12*, 1281–1287.

Sanchez, E., Li, M., Kitto, A., Li, J., Wang, C.S., Kirk, D.T., Yellin, O., Nichols, C.M., Dreyer, M.P., Ahles, C.P., et al. (2012). Serum B-cell maturation antigen is elevated in multiple myeloma and correlates with disease status and survival. Br J Haematol *158*, 727–738.

Savoldo, B., Ramos, C.A., Liu, E., Mims, M.P., Keating, M.J., Carrum, G., Kamble, R.T., Bollard, C.M., Gee, A.P., Mei, Z., et al. (2011). CD28 costimulation improves expansion and persistence of chimeric antigen receptor-modified T cells in lymphoma patients. J. Clin. Invest. *121*, 1822–1826.

Schaerli, P., Willimann, K., Lang, A.B., Lipp, M., Loetscher, P., and Moser, B. (2000a). Cxc Chemokine Receptor 5 Expression Defines Follicular Homing T Cells with B Cell Helper Function. Journal of Experimental Medicine *192*, 1553–1562.

Schaerli, P., Willimann, K., Lang, A.B., Lipp, M., Loetscher, P., and Moser, B. (2000b). Cxc Chemokine Receptor 5 Expression Defines Follicular Homing T Cells with B Cell Helper Function. Journal of Experimental Medicine *192*, 1553–1562.

Schaerli, P., Loetscher, P., and Moser, B. (2001). Cutting Edge: Induction of Follicular Homing Precedes Effector Th Cell Development. J Immunol *167*, 6082–6086.

Scherer, L.D., Brenner, M.K., and Mamonkin, M. (2019). Chimeric Antigen Receptors for T-Cell Malignancies. Front. Oncol. *9*, 126.

Schmidt, M., Weyer-Elberich, V., Hengstler, J.G., Heimes, A.-S., Almstedt, K., Gerhold-Ay, A., Lebrecht, A., Battista, M.J., Hasenburg, A., Sahin, U., et al. (2018). Prognostic impact of CD4-positive T cell subsets in early breast cancer: a study based on the FinHer trial patient population. Breast Cancer Res *20*, 15.

Schnoor, M., Alcaide, P., Voisin, M.-B., and van Buul, J.D. (2015). Crossing the Vascular Wall: Common and Unique Mechanisms Exploited by Different Leukocyte Subsets during Extravasation. Mediators of Inflammation *2015*, 1–23.

Schoggins, J.W. (2019). Interferon-Stimulated Genes: What Do They All Do? Annu Rev Virol *6*, 567–584.

Schuster, S.J., Bishop, M.R., Tam, C.S., Waller, E.K., Borchmann, P., McGuirk, J.P., Jäger, U., Jaglowski, S., Andreadis, C., Westin, J.R., et al. (2019). Tisagenlecleucel in Adult Relapsed or Refractory Diffuse Large B-Cell Lymphoma. N Engl J Med *380*, 45–56.

Scott, D.W., and Gascoyne, R.D. (2014). The tumour microenvironment in B cell lymphomas. Nat Rev Cancer *14*, 517–534.

Shimabukuro-Vornhagen, A., Gödel, P., Subklewe, M., Stemmler, H.J., Schlößer, H.A., Schlaak, M., Kochanek, M., Böll, B., and von Bergwelt-Baildon, M.S. (2018). Cytokine release syndrome. J Immunother Cancer *6*, 56.

Shui, R., Yang, W., Sun, M., Shi, D., and Zhu, X. (2003). [Detection of cyclin D1 protein expression and t(11;14) chromosomal translocation in paraffin-embedded tissues and its clinicopathologic significance for mantle cell lymphoma]. Zhonghua Bing Li Xue Za Zhi *32*, 337–341.

Shultz, L.D., Lyons, B.L., Burzenski, L.M., Gott, B., Chen, X., Chaleff, S., Kotb, M., Gillies, S.D., King, M., Mangada, J., et al. (2005). Human Lymphoid and Myeloid Cell Development in NOD/LtSz- scid IL2Rγnull Mice Engrafted with Mobilized Human Hemopoietic Stem Cells. J Immunol *174*, 6477–6489.

Shultz, L.D., Ishikawa, F., and Greiner, D.L. (2007). Humanized mice in translational biomedical research. Nat Rev Immunol *7*, 118–130.

Shultz, L.D., Brehm, M.A., Garcia-Martinez, J.V., and Greiner, D.L. (2012). Humanized mice for immune system investigation: progress, promise and challenges. Nat Rev Immunol *12*, 786–798.

Shultz, L.D., Goodwin, N., Ishikawa, F., Hosur, V., Lyons, B.L., and Greiner, D.L. (2014). Human Cancer Growth and Therapy in Immunodeficient Mouse Models. Cold Spring Harbor Protocols *2014*, pdb.top073585-pdb.top073585.

Simpson, N., Gatenby, P.A., Wilson, A., Malik, S., Fulcher, D.A., Tangye, S.G., Manku, H., Vyse, T.J., Roncador, G., Huttley, G.A., et al. (2010). Expansion of circulating T cells resembling follicular helper T cells is a fixed phenotype that identifies a subset of severe systemic lupus erythematosus. Arthritis Rheum *62*, 234–244.

Smith, A., Crouch, S., Lax, S., Li, J., Painter, D., Howell, D., Patmore, R., Jack, A., and Roman, E. (2015). Lymphoma incidence, survival and prevalence 2004-2014: sub-type analyses from the UK's Haematological Malignancy Research Network. Br. J. Cancer *112*, 1575–1584.

Smith, S.M., Godfrey, J., Ahn, K.W., DiGilio, A., Ahmed, S., Agrawal, V., Bachanova, V., Bacher, U., Bashey, A., Bolaños-Meade, J., et al. (2018). Autologous transplantation versus allogeneic transplantation in patients with follicular lymphoma experiencing early treatment failure. Cancer *124*, 2541–2551.

Song, D.-G., Ye, Q., Poussin, M., Harms, G.M., Figini, M., and Powell, D.J. (2012). CD27 costimulation augments the survival and antitumor activity of redirected human T cells in vivo. Blood *119*, 696–706.

Soriano, A.O., Thompson, M.A., Admirand, J.H., Fayad, L.E., Rodriguez, A.M., Romaguera, J.E., Hagemeister, F.B., and Pro, B. (2007). Follicular dendritic cell sarcoma: A report of 14 cases and a review of the literature. Am. J. Hematol. *82*, 725–728.

Sotillo, E., Barrett, D.M., Black, K.L., Bagashev, A., Oldridge, D., Wu, G., Sussman, R., Lanauze, C., Ruella, M., Gazzara, M.R., et al. (2015). Convergence of Acquired Mutations and Alternative Splicing of CD19 Enables Resistance to CART-19 Immunotherapy. Cancer Discov *5*, 1282–1295.

Starr, T.K., Jameson, S.C., and Hogquist, K.A. (2003). Positive and Negative Selection of T Cells. Annu. Rev. Immunol. *21*, 139–176.

Stein, P.H., Fraser, J.D., and Weiss, A. (1994). The cytoplasmic domain of CD28 is both necessary and sufficient for costimulation of interleukin-2 secretion and association with phosphatidylinositol 3'-kinase. Mol. Cell. Biol. *14*, 3392–3402.

Storb, R., Prentice, R.L., Thomas, E.D., Appelbaum, F.R., Deeg, H.J., Doney, K., Fefer, A., Goodell, B.W., Mickelson, E., and Stewart, P. (1983). Factors associated with graft rejection after HLA-identical marrow transplantation for aplastic anaemia. Br. J. Haematol. *55*, 573–585.

Stuart, M.J., Corrigan, F., and Baune, B.T. (2014). Knockout of CXCR5 increases the population of immature neural cells and decreases proliferation in the hippocampal dentate gyrus. J Neuroinflammation *11*, 31.

Stuart, T., Butler, A., Hoffman, P., Hafemeister, C., Papalexi, E., Mauck, W.M., Hao, Y., Stoeckius, M., Smibert, P., and Satija, R. (2019). Comprehensive Integration of Single-Cell Data. Cell *177*, 1888-1902.e21.

Subramaniam, J.M., Whiteside, G., McKeage, K., and Croxtall, J.C. (2012). Mogamulizumab: first global approval. Drugs *72*, 1293–1298.

Sugamura, K., Asao, H., Kondo, M., Tanaka, N., Ishii, N., Ohbo, K., Nakamura, M., and Takeshita, T. (1996). The interleukin-2 receptor gamma chain: its role in the multiple cytokine receptor complexes and T cell development in XSCID. Annu. Rev. Immunol. *14*, 179–205.

Swerdlow, S.H., Campo, E., Pileri, S.A., Harris, N.L., Stein, H., Siebert, R., Advani, R., Ghielmini, M., Salles, G.A., Zelenetz, A.D., et al. (2016). The 2016 revision of the World Health Organization classification of lymphoid neoplasms. Blood *127*, 2375–2390.

Szabo, K., Papp, G., Barath, S., Gyimesi, E., Szanto, A., and Zeher, M. (2013). Follicular helper T cells may play an important role in the severity of primary Sjögren's syndrome. Clinical Immunology *147*, 95–104.

Tangye, S.G., Ma, C.S., Brink, R., and Deenick, E.K. (2013). The good, the bad and the ugly — TFH cells in human health and disease. Nat Rev Immunol *13*, 412–426.

Tariq, A., Aziz, M.T., Mehmood, Y., Asghar, S.A., and Khurshid, A. (2018). Clinical Response to CHOP vs. R-CHOP in Adult Patients with Diffuse Large B-Cell Lymphomas. Asian Pac. J. Cancer Prev. *19*, 1181–1184.

Taub, R., Kirsch, I., Morton, C., Lenoir, G., Swan, D., Tronick, S., Aaronson, S., and Leder, P. (1982). Translocation of the c-myc gene into the immunoglobulin heavy chain locus in human Burkitt lymphoma and murine plasmacytoma cells. Proc. Natl. Acad. Sci. U.S.A. *79*, 7837–7841.

Ternynck, T., Dighiero, G., Follezou, J., and Binet, J.L. (1974). Comparison of normal and CLL lymphocyte surface Ig determinants using peroxidase-labeled antibodies. I. Detection and quantitation of light chain determinants. Blood *43*, 789–795.

The Non-Hodgkin's Lymphoma Classification Project (1997). A clinical evaluation of the International Lymphoma Study Group classification of non-Hodgkin's lymphoma. The Non-Hodgkin's Lymphoma Classification Project. Blood *89*, 3909–3918.

Tierens, A., Delabie, J., Pittaluga, S., Driessen, A., and DeWolf-Peeters, C. (1998). Mutation analysis of the rearranged immunoglobulin heavy chain genes of marginal zone cell lymphomas indicates an origin from different marginal zone B lymphocyte subsets. Blood *91*, 2381–2386.

Tokarew, N., Ogonek, J., Endres, S., von Bergwelt-Baildon, M., and Kobold, S. (2019). Teaching an old dog new tricks: next-generation CAR T cells. Br J Cancer *120*, 26–37.

Topalian, S.L., Solomon, D., Avis, F.P., Chang, A.E., Freerksen, D.L., Linehan, W.M., Lotze, M.T., Robertson, C.N., Seipp, C.A., and Simon, P. (1988). Immunotherapy of patients

with advanced cancer using tumor-infiltrating lymphocytes and recombinant interleukin-2: a pilot study. J. Clin. Oncol. *6*, 839–853.

Torikai, H., Reik, A., Liu, P.-Q., Zhou, Y., Zhang, L., Maiti, S., Huls, H., Miller, J.C., Kebriaei, P., Rabinovitch, B., et al. (2012). A foundation for universal T-cell based immunotherapy: T cells engineered to express a CD19-specific chimeric-antigen-receptor and eliminate expression of endogenous TCR. Blood *119*, 5697–5705.

de Totero, D., Meazza, R., Zupo, S., Cutrona, G., Matis, S., Colombo, M., Balleari, E., Pierri, I., Fabbi, M., Capaia, M., et al. (2006). Interleukin-21 receptor (IL-21R) is up-regulated by CD40 triggering and mediates proapoptotic signals in chronic lymphocytic leukemia B cells. Blood *107*, 3708–3715.

de Totero, D., Meazza, R., Capaia, M., Fabbi, M., Azzarone, B., Balleari, E., Gobbi, M., Cutrona, G., Ferrarini, M., and Ferrini, S. (2008). The opposite effects of IL-15 and IL-21 on CLL B cells correlate with differential activation of the JAK/STAT and ERK1/2 pathways. Blood *111*, 517–524.

Tseng, W.-Y., Jan Wu, Y.-J., Yang, T.-Y., Chiang, N.-Y., Tsai, W.-P., Gordon, S., Chang, G.-W., Kuo, C.-F., Luo, S.-F., and Lin, H.-H. (2018). High levels of soluble GPR56/ADGRG1 are associated with positive rheumatoid factor and elevated tumor necrosis factor in patients with rheumatoid arthritis. Journal of Microbiology, Immunology and Infection *51*, 485–491.

Tsimberidou, A.M., Wen, S., O'Brien, S., McLaughlin, P., Wierda, W.G., Ferrajoli, A., Faderl, S., Manning, J., Lerner, S., Mai, C.V., et al. (2007). Assessment of chronic lymphocytic leukemia and small lymphocytic lymphoma by absolute lymphocyte counts in 2,126 patients: 20 years of experience at the University of Texas M.D. Anderson Cancer Center. J. Clin. Oncol. *25*, 4648–4656.

Tsujimoto, Y., Gorham, J., Cossman, J., Jaffe, E., and Croce, C.M. (1985). The t(14;18) chromosome translocations involved in B-cell neoplasms result from mistakes in VDJ joining. Science *229*, 1390–1393.

Tumeh, P.C., Koya, R.C., Chodon, T., Graham, N.A., Graeber, T.G., Comin-Anduix, B., and Ribas, A. (2010). The impact of ex vivo clinical grade activation protocols on human T-cell phenotype and function for the generation of genetically modified cells for adoptive cell transfer therapy. J. Immunother. *33*, 759–768.

Turka, L.A., Ledbetter, J.A., Lee, K., June, C.H., and Thompson, C.B. (1990). CD28 is an inducible T cell surface antigen that transduces a proliferative signal in CD3+ mature thymocytes. J. Immunol. *144*, 1646–1653.

Turtle, C.J., Hay, K.A., Hanafi, L.-A., Li, D., Cherian, S., Chen, X., Wood, B., Lozanski, A., Byrd, J.C., Heimfeld, S., et al. (2017). Durable Molecular Remissions in Chronic Lymphocytic Leukemia Treated With CD19-Specific Chimeric Antigen Receptor–Modified T Cells After Failure of Ibrutinib. JCO *35*, 3010–3020.

Ueno, H. (2016). Human Circulating T Follicular Helper Cell Subsets in Health and Disease. J Clin Immunol *36*, 34–39.

Vale, A.M., and Schroeder, H.W. (2010). Clinical consequences of defects in B-cell development. J. Allergy Clin. Immunol. *125*, 778–787.

Vallon, M., and Essler, M. (2006). Proteolytically Processed Soluble Tumor Endothelial Marker (TEM) 5 Mediates Endothelial Cell Survival during Angiogenesis by Linking Integrin $\alpha_v \beta_3$ to Glycosaminoglycans. J. Biol. Chem. *281*, 34179–34188.

Vaux, D.L., Cory, S., and Adams, J.M. (1988). Bcl-2 gene promotes haemopoietic cell survival and cooperates with c-myc to immortalize pre-B cells. Nature *335*, 440–442.

Velasquez, M.P., and Gottschalk, S. (2017). Targeting CD19: the good, the bad, and CD81. Blood *129*, 9–10.

Vermi, W., Lonardi, S., Bosisio, D., Uguccioni, M., Danelon, G., Pileri, S., Fletcher, C., Sozzani, S., Zorzi, F., Arrigoni, G., et al. (2008). Identification of CXCL13 as a new marker for follicular dendritic cell sarcoma. J. Pathol. *216*, 356–364.

Verstappen, G.M., Meiners, P.M., Corneth, O.B.J., Visser, A., Arends, S., Abdulahad, W.H., Hendriks, R.W., Vissink, A., Kroese, F.G.M., and Bootsma, H. (2017). Attenuation of Follicular Helper T Cell-Dependent B Cell Hyperactivity by Abatacept Treatment in Primary Sjögren's Syndrome: ABATACEPT IN PRIMARY SJÖGREN'S SYNDROME. Arthritis & Rheumatology *69*, 1850–1861.

Victora, G.D., and Nussenzweig, M.C. (2012). Germinal centers. Annu. Rev. Immunol. *30*, 429–457.

Vidal, L., Gafter-Gvili, A., Salles, G., Bousseta, S., Oberman, B., Rubin, C., van Oers, M.H.J., Fortpied, C., Ghielmini, M., Pettengell, R., et al. (2017). Rituximab maintenance improves overall survival of patients with follicular lymphoma-Individual patient data meta-analysis. Eur. J. Cancer *76*, 216–225.

Vormittag, P., Gunn, R., Ghorashian, S., and Veraitch, F.S. (2018). A guide to manufacturing CAR T cell therapies. Curr. Opin. Biotechnol. *53*, 164–181.

Voutsadakis, I.A. (2000). Apoptosis and the Pathogenesis of Lymphoma. Acta Oncologica *39*, 151–156.

Walker, A.J., Majzner, R.G., Zhang, L., Wanhainen, K., Long, A.H., Nguyen, S.M., Lopomo, P., Vigny, M., Fry, T.J., Orentas, R.J., et al. (2017). Tumor Antigen and Receptor Densities Regulate Efficacy of a Chimeric Antigen Receptor Targeting Anaplastic Lymphoma Kinase. Mol Ther *25*, 2189–2201.

Walker, L.S.K., Gulbranson-Judge, A., Flynn, S., Brocker, T., Raykundalia, C., Goodall, M., Förster, R., Lipp, M., and Lane, P. (1999). Compromised Ox40 Function in Cd28-Deficient Mice Is Linked with Failure to Develop Cxc Chemokine Receptor 5–Positive Cd4 Cells and Germinal Centers. Journal of Experimental Medicine *190*, 1115–1122.

Wang, X., and Rivière, I. (2016). Clinical manufacturing of CAR T cells: foundation of a promising therapy. Mol Ther Oncolytics *3*, 16015.

Wang, K., Wei, G., and Liu, D. (2012). CD19: a biomarker for B cell development, lymphoma diagnosis and therapy. Exp Hematol Oncol *1*, 36.

Wang, M., Munoz, J., Goy, A., Locke, F.L., Jacobson, C.A., Hill, B.T., Timmerman, J.M., Holmes, H., Jaglowski, S., Flinn, I.W., et al. (2020). KTE-X19 CAR T-Cell Therapy in Relapsed or Refractory Mantle-Cell Lymphoma. N Engl J Med *382*, 1331–1342.

Watanabe, T., Tobinai, K., Shibata, T., Tsukasaki, K., Morishima, Y., Maseki, N., Kinoshita, T., Suzuki, T., Yamaguchi, M., Ando, K., et al. (2011). Phase II/III study of R-CHOP-21 versus R-CHOP-14 for untreated indolent B-cell non-Hodgkin's lymphoma: JCOG 0203 trial. J. Clin. Oncol. *29*, 3990–3998.

de Weerdt, I., Hofland, T., de Boer, R., Dobber, J.A., Dubois, J., van Nieuwenhuize, D., Mobasher, M., de Boer, F., Hoogendoorn, M., Velders, G.A., et al. (2019). Distinct immune composition in lymph node and peripheral blood of CLL patients is reshaped during venetoclax treatment. Blood Advances *3*, 2642–2652.

Weiden, P.L., Flournoy, N., Thomas, E.D., Prentice, R., Fefer, A., Buckner, C.D., and Storb, R. (1979). Antileukemic effect of graft-versus-host disease in human recipients of allogeneic-marrow grafts. N. Engl. J. Med. *300*, 1068–1073.

Weinkove, R., George, P., Dasyam, N., and McLellan, A.D. (2019). Selecting costimulatory domains for chimeric antigen receptors: functional and clinical considerations. Clin Transl Immunology *8*, e1049.

Wherry, E.J., and Kurachi, M. (2015). Molecular and cellular insights into T cell exhaustion. Nat Rev Immunol *15*, 486–499.

Willinger, T., Rongvaux, A., Strowig, T., Manz, M.G., and Flavell, R.A. (2011). Improving human hemato-lymphoid-system mice by cytokine knock-in gene replacement. Trends in Immunology *32*, 321–327.

Wing, J.B., Kitagawa, Y., Locci, M., Hume, H., Tay, C., Morita, T., Kidani, Y., Matsuda, K., Inoue, T., Kurosaki, T., et al. (2017). A distinct subpopulation of CD25− T-follicular regulatory cells localizes in the germinal centers. Proc Natl Acad Sci USA *114*, E6400–E6409.

Wotherspoon, A.C., Ortiz-Hidalgo, C., Falzon, M.R., and Isaacson, P.G. (1991). Helicobacter pylori-associated gastritis and primary B-cell gastric lymphoma. Lancet *338*, 1175–1176.

Wu, Y., and Zhou, B.P. (2009). Inflammation: a driving force speeds cancer metastasis. Cell Cycle *8*, 3267–3273.

Wu, X., Wang, Y., Huang, R., Gai, Q., Liu, H., Shi, M., Zhang, X., Zuo, Y., Chen, L., Zhao, Q., et al. (2020). SOSTDC1-producing follicular helper T cells promote regulatory follicular T cell differentiation. Science (New York, N.Y.) *369*, 984–988.

Xie, G., Dong, H., Liang, Y., Ham, J.D., Rizwan, R., and Chen, J. (2020). CAR-NK cells: A promising cellular immunotherapy for cancer. EBioMedicine *59*, 102975.

Xu, W., Zhao, X., Wang, X., Feng, H., Gou, M., Jin, W., Wang, X., Liu, X., and Dong, C. (2019). The Transcription Factor Tox2 Drives T Follicular Helper Cell Development via Regulating Chromatin Accessibility. Immunity *51*, 826-839.e5.

Yamamoto, R., Nishikori, M., Kitawaki, T., Sakai, T., Hishizawa, M., Tashima, M., Kondo, T., Ohmori, K., Kurata, M., Hayashi, T., et al. (2008). PD-1–PD-1 ligand interaction contributes to immunosuppressive microenvironment of Hodgkin lymphoma. Blood *111*, 3220–3224.

Yam-Puc, J.C., Zhang, L., Zhang, Y., and Toellner, K.-M. (2018). Role of B-cell receptors for B-cell development and antigen-induced differentiation. F1000Res *7*, 429.

Yang, Y., Mallampati, S., Sun, B., Zhang, J., Kim, S.-B., Lee, J.-S., Gong, Y., Cai, Z., and Sun, X. (2013). Wnt pathway contributes to the protection by bone marrow stromal cells of acute lymphoblastic leukemia cells and is a potential therapeutic target. Cancer Letters *333*, 9–17.

Yasukawa, M., Ohminami, H., Arai, J., Kasahara, Y., Ishida, Y., and Fujita, S. (2000). Granule exocytosis, and not the fas/fas ligand system, is the main pathway of cytotoxicity mediated by alloantigen-specific CD4(+) as well as CD8(+) cytotoxic T lymphocytes in humans. Blood *95*, 2352–2355.

Yi, Z., Prinzing, B.L., Cao, F., Gottschalk, S., and Krenciute, G. (2018). Optimizing EphA2-CAR T Cells for the Adoptive Immunotherapy of Glioma. Mol Ther Methods Clin Dev *9*, 70–80.

Yu, T.T.L., Gupta, P., Ronfard, V., Vertès, A.A., and Bayon, Y. (2018). Recent Progress in European Advanced Therapy Medicinal Products and Beyond. Front Bioeng Biotechnol *6*, 130.

Zajac, P., Schultz-Thater, E., Tornillo, L., Sadowski, C., Trella, E., Mengus, C., Iezzi, G., and Spagnoli, G.C. (2017). MAGE-A Antigens and Cancer Immunotherapy. Front Med (Lausanne) *4*, 18.

Zavras, P.D., Wang, Y., Gandhi, A., Lontos, K., and Delgoffe, G.M. (2019). Evaluating tisagenlecleucel and its potential in the treatment of relapsed or refractory diffuse large B cell lymphoma: evidence to date. Onco Targets Ther *12*, 4543–4554.

Zech, L., Haglund, U., Nilsson, K., and Klein, G. (1976). Characteristic chromosomal abnormalities in biopsies and lymphoid-cell lines from patients with Burkitt and non-Burkitt lymphomas. Int. J. Cancer *17*, 47–56.

Zhang, W., Trachootham, D., Liu, J., Chen, G., Pelicano, H., Garcia-Prieto, C., Lu, W., Burger, J.A., Croce, C.M., Plunkett, W., et al. (2012). Stromal control of cystine metabolism promotes cancer cell survival in chronic lymphocytic leukaemia. Nat Cell Biol *14*, 276–286.

Zhang, Y., Tech, L., George, L.A., Acs, A., Durrett, R.E., Hess, H., Walker, L.S.K., Tarlinton, D.M., Fletcher, A.L., Hauser, A.E., et al. (2018). Plasma cell output from germinal centers is regulated by signals from Tfh and stromal cells. Journal of Experimental Medicine *215*, 1227–1243.

Zhao, Z., Condomines, M., van der Stegen, S.J.C., Perna, F., Kloss, C.C., Gunset, G., Plotkin, J., and Sadelain, M. (2015). Structural Design of Engineered Costimulation Determines Tumor Rejection Kinetics and Persistence of CAR T Cells. Cancer Cell *28*, 415–428.

Zhong, X.-S., Matsushita, M., Plotkin, J., Riviere, I., and Sadelain, M. (2010). Chimeric antigen receptors combining 4-1BB and CD28 signaling domains augment PI3kinase/AKT/Bcl-XL activation and CD8+ T cell-mediated tumor eradication. Mol. Ther. *18*, 413–420.

Zhou, D.-M., Xu, Y.-X., Zhang, L.-Y., Sun, Y., Wang, Z.-Y., Yuan, Y.-Q., and Fu, J.-X. (2017). The role of follicular T helper cells in patients with malignant lymphoid disease. Hematology *22*, 412–418.

Zhou, J., Jin, L., Wang, F., Zhang, Y., Liu, B., and Zhao, T. (2019). Chimeric antigen receptor T (CAR-T) cells expanded with IL-7/IL-15 mediate superior antitumor effects. Protein Cell *10*, 764–769.

Zinkernagel, R.M., and Doherty, P.C. (1974). Restriction of in vitro T cell-mediated cytotoxicity in lymphocytic choriomeningitis within a syngeneic or semiallogeneic system. Nature *248*, 701–702.

7 Acknowledgements

An erster Stelle möchte ich mich bei PD Dr. Uta Höpken für die Möglichkeit an diesem spannenden Projekt zu arbeiten, die ausgezeichnete Betreuung und die hervorragenden Arbeitsbedingungen bedanken. Sie hatte immer ein offenes Ohr und stand mir mit praktischer Hilfe zur Seite. Ihr großes Engagement hat wesentlich zum Erfolg des Projektes beigetragen. Bei Dr. Armin Rehm möchte ich mich für die zahlreichen Anregungen in Diskussionen und Unterstützung bedanken.

Besonderer Dank geht an Dr. Mario Bunse für die langjährige Zusammenarbeit am CAR Projekt. Ich habe es sehr genossen, mit ihm zusammen im Labor zu arbeiten und bin sehr dankbar für das Fachwissen, das er mit mir geteilt hat.

Vielen Dank an Professor Thomas Sommer für die Übernahme der Betreuung der Dissertation am Institut für Biologie an der HU Berlin.

Bei Dr. Vanessa Stache und Dr. Julia Bluhm möchte ich mich für die Einführung in das Thema und Methoden am Anfang meiner Arbeit bedanken. Vielen Dank an Kerstin Krüger und Kerstin Gerlach für die ausgezeichnete Unterstützung und Tipps im Labor. Außerdem möchte ich mich bei Dr. Hans-Peter Rahn und Kirstin Rautenberg für die Unterstützung in der FACS Facility, Caroline Bräuning, Dr. Cornelius Fischer und Sarah Vicetz von der Genomics Platform und Tadhg Crowley für die Unterstützung bei der bioinformatischen Analyse bedanken.

Bei Professor Jörg Westermann möchte ich mich für das Bereitstellen der Patientenproben, die in dieser Arbeit analysiert wurden, bedanken. Ich danke außerdem allen Spendern der Blutspenden.

Allen Mitgliedern der AG Höpken und AG Rehm danke ich für die großartige Atmosphäre, die Unterstützung im Labor, Hilfe in Diskussion and die vielen, schönen Erinnerungen. Ich habe es sehr genossen, mit ihnen zusammenzuarbeiten, kann mir keine besseren Kollegen vorstellen und werde alle sehr vermissen.

Mein tiefster Dank gilt meinen Eltern, insbesondere meiner Mutter, die mich immer unterstützt hat. Besonders danken möchte ich Roman, der mich sehr unterstützt und ermutigt hat, vor allem während ich die Arbeit geschrieben habe, und der immer mit dem Essen auf mich gewartet hat, wenn ich spät nach Hause gekommen bin. Ohne sie hätte ich es nicht geschafft.

8 Publication

Parts of the data of this thesis are published in Nature Communications with me as a shared first author. I generated the following data of this publication (a) on my own or (b) in joint experiments with Dr. Bunse (shared first author and Postdoc in the group of PD Dr. Uta Höpken).
(a) Figure 1a, b, d, e; Figure 2b-d; Figure 5a-c; Figure 6a-d, Supplementary Figure 7a-c; Supplementary Figure 9a-d; Supplementary Figure 10; Supplementary Figure 11a-h;
(b) Figure 1c; Figure 2f; Figure 3a-i; Figure 4a-d; Figure 7a-d; Supplementary Figure 1a-e; Supplementary Figure 2a-e; Supplementary Figure 4a-f; Supplementary Figure 8a-e; Supplementary Figure 12a, b

Mario Bunse*, Janina Pfeilschifter*, Julia Bluhm, Maria Zschummel, Jara J. Joedicke, Anthea Wirges, Helen Stark, Vivien Kretschmer, Markus Chmielewski, Wolfgang Uckert, Hinrich Abken, Jörg Westermann, Armin Rehm, and Uta E. Höpken
"CXCR5 CAR-T cells simultaneously target B cell Non-Hodgkin's lymphoma and tumor-supportive follicular T helper cells" *equal contribution
Nat Commun 12, 240 (2021) https://doi.org/10.1038/s41467-020-20488-3

9 Declaration

Hiermit erkläre ich, die Dissertation selbstständig und nur unter Verwendung der angegebenen Hilfen und Hilfsmittel angefertigt zu haben.

Berlin, den _____ _____

Unterschrift